Formulating asymmetric liposomes using a novel cyclodextrin-lipid complexation method

A thesis submitted by

Yaqeen Nadheer Abood Al Badri

A thesis submitted in partial fulfilment of the requirements of the University of Sunderland for the degree of Doctor of Philosophy- PhD

Faculty of Health Sciences and Wellbeing

July 2025

Abstract

Liposomes have long been explored as versatile drug delivery systems. Recently, achieving and maintaining asymmetry of liposomes has been the focus of liposomal research. The maintenance of asymmetry remains a challenge due to the flip-flop of lipids within the vesicle's bilayer (inner and outer leaflets).

This research aims to provide a novel method for formulating asymmetric liposomes, focusing on the development and optimisation of asymmetric liposome formulation using a novel cyclodextrin (CD)-lipid exchange method. **In** the literature, asymmetric liposomes are generally formulated using complex methods that are time-consuming and require expensive equipment. Moreover, the simpler methods tend to have short stability (48 hours). The method used in the research enhances the stability of the liposomes while ensuring simpler formulation techniques. The method involves dissolving cyclodextrin in buffer while heating. The phospholipid is then dissolved in methanol and added to the cyclodextrin solution. The mixture is gently mixed to allow for complexation and methanol evaporation. Complexation of the lipid and cyclodextrin is confirmed by several methods. Then, large unilamellar vesicles are formulated using thin-film hydration. Finally, the cyclodextrin-lipid complex is added to the acceptor vesicle suspension and mixed to allow lipid exchange.

The novel method was tested on several liposomal formulations using bromocresol green as a model drug, and it was found that the most optimised formulation was the one with 1-palmitoyl-2-oleoyl-sn-glycero-3-phosphocholine (POPC) in the outer leaflet and POPC (30%), Dioleoyl-3-trimethylammonium propane (DOTAP) (30%), and cholesterol (40%) in the inner leaflet. Further optimisation was trialled on this method, and it was found that increasing the DOTAP to 45% has increased the entrapment efficiency from 41.11% to 44.22%, a small increase but expected considering that DOTAP increased by only 15%. The liposomes were analysed using size and zetapotential analysis, microscopy and UV/VIS spectrophotometry plus pH gradient method to calculate entrapment efficiency. The novel cyclodextrin-lipid method offers a major improvement over existing asymmetric liposome formation techniques. It simplifies the process by eliminating the need to form multilamellar vesicles (explained further in chapter 3), making it much easier to create the donor complex and separate the asymmetric liposomes from the rest of the suspension.

The final formulation containing POPC in the outer leaflet and POPC (15%), DOTAP (45%), and cholesterol (40%) was used to entrap salmon sperm DNA. Three different encapsulation techniques were trialled, and the most optimised technique was entrapping the DNA during

symmetric liposomes formation then performing the lipid exchange. The entrapment efficiency was determined using nanodrop lite machine. When 6µl of DNA is added to asymmetric liposomes (final concentration 2mM) at a ratio of 19.4:1 liposome to DNA, the entrapment efficiency was 92.5%. The liposomes were then stored at 4°C and remained stable for 1 week. In conclusion, the novel method was successful in formulating asymmetric liposomes. These liposomes were able to efficiently entrap DNA and were stable for 1 week at 4 °C. With this method, liposomes were able to stay stable much longer than those made using the conventional cyclodextrin-exchange method, which lasted only 48 hours (explained in chapter 1).

Acknowledgements

I would like to express my heartfelt gratitude to my husband and my family for their unwavering support, encouragement, and patience throughout my PhD journey. Their belief in me has been my greatest source of strength. I am deeply grateful to my supervisor, Professor Amal Elkordy, and my co-supervisor, Dr. Chaw, for their invaluable guidance, expertise, and continuous support. Their mentorship has been instrumental in shaping both my research and my academic growth. I would also like to extend my sincere appreciation to the technicians and university of Sunderland staff for their assistance and dedication, which have greatly contributed to the success of my work.

Research activity

Publication:

Al Badri, Yaqeen Nadheer, Chaw, Cheng and Elkordy, Amal (2023) Insights into Asymmetric Liposomes as a Potential Intervention for Drug Delivery Including Pulmonary Nanotherapeutics. Pharmaceutics, 15 (294). pp. 1-22. ISSN 1999-4923

Oral Presentation:

University of Sunderland Research Conference, University of Sunderland (21/06/2023) Title: Formulation and mRNA encapsulation of asymmetric liposomes that mimic the cell membrane

Award: Best presentation award

Table of Contents

List of figures

List of tables

List of equations

List of abbreviations

BCG- Bromocresol green

CD- Cyclodextrin

DOTAP- 1,2-Dioleoyl-3-trimethylammonium propane

EE- Entrapment efficiency

LUV- Large unilamellar vesicles

MLV- Multilamellar vesicle

NBD- nitrobenzodiazole

POPC- 1-palmitoyl-2-oleoyl-sn-glycero-3-phosphocholine

POPE- 1-palmitoyl-2-oleoyl-sn-glycero-3-phosphoethanolamine

SM- Sphingomyelin

ZP- zetapotential

Chapter 1

Introduction and literature review

This chapter has been published as an article

1. Brief Introduction to Liposomes

The direct delivery of drugs can lead to off-target side effects, poor distribution, and short circulation time due to the breakdown and clearance of the drug (1). Liposomes are a type of nanocarrier that are described as spherical, microscopic, bilayered vesicles. They have the ability to entrap materials due to the spontaneous assembly of phospholipid molecules when in contact with aqueous media, resulting in the formation of an aqueous inner core surrounded by a closed lipid-based bilayer. Their structure is very similar to the human cell membrane, which is a bilayer mainly consisting of phospholipids; the phospholipids consist of a hydrophilic head and two hydrophobic "tails" derived from fatty acids of different chain length and degree of saturation (2).

Liposomes provide many advantages to the delivery of materials. Liposomes' ability to entrap several drugs of different properties, having high entrapment efficacy (EE) to reduce dose and provide targeted drug delivery, are some of the main advantages (3). However, a significant issue with liposomes is the removal from the blood circulation as well as removal by the liver; this is mainly associated with size and charge of the liposomes. Therefore, reduction of size can lead to a longer circulation time (4). Moreover, the charge plays an important role in liposomal delivery as it affects attraction to tissue and materials inside the human body as well as some charged phospholipids can be cytotoxic (5).

2. Liposomal Formulation Composition

Liposomes are generally formulated using non-toxic phospholipids and cholesterol (6). The phospholipids used when formulating liposomes can be phosphatidylglycerols, phosphatidylcholines, phosphatidylserines, or phosphatidylethanolamines (7); The choice of the lipid can significantly affect the liposomal properties such as fluidity and charge of the

bilayer. Generally, unsaturated phospholipids tend to increase permeability while saturated phospholipids with long acyl chains leads to rigidity and impermeability (6). The unique structure of liposomes allows them to encapsulate hydrophobic molecules within the phospholipid bilayer and hydrophilic molecules withing the aqueous core (Figure 1.1). Moreover, liposomal drug delivery can be further enhanced by adding a targeting ligand to liposomes to recognize and bind specific receptors on cells, or by adding biocompatible inert polymers to them such as PEG to reduce phagocyte recognition and increase the liposomal blood circulation half-life (7).

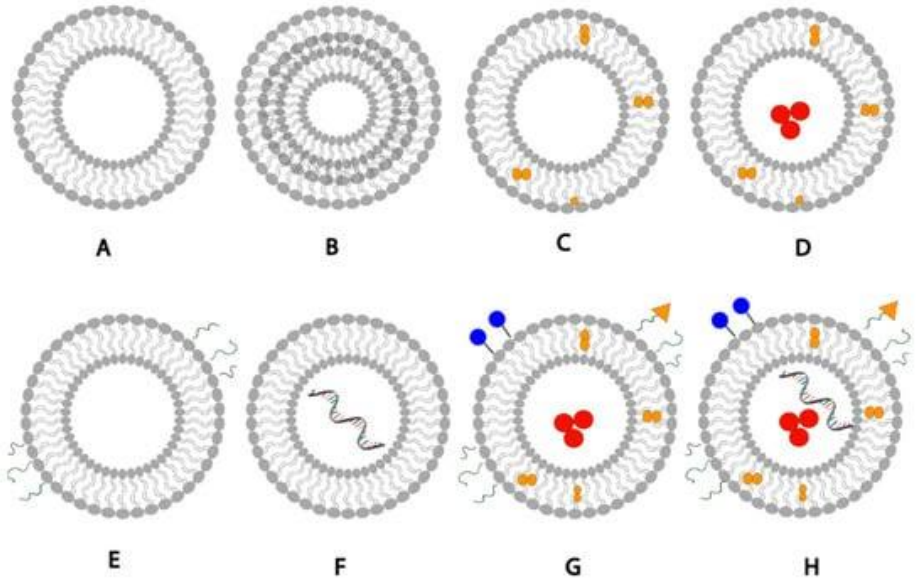

Figure 1. 1: Schematic representation of liposomal drug delivery systems: (A) unilamellar liposome, (B) multilamellar liposome, (C) liposomes loaded with hydrophobic drug, (D) liposome loaded with hydrophobic drug in the bilayer membrane and hydrophilic drug in the aqueous core, (E) PEGylated liposomes with surface PEG polymer chains, (F) liposome loaded with mRNA, (G) liposome with surface conjugated drug, targeting ligands and PEG, hydrophilic and hydrophobic drugs, (H) liposome with surface conjugated drug, targeting ligands, PEG polymer chains, hydrophilic drug, hydrophobic drugs, and mRNA loaded. (8) (Reuse permitted by MDPI).

3. Conventional Liposomal Formulation Methods

There are various methods used in the preparation of lipid-based nanocarriers such as liposomes (2). The method of preparation affects critical parameters such as size of vesicle and size distribution, permeability, lamellarity, and entrapment efficiency (9). Entrapment of compounds is performed by two main techniques; passive loading where drug entrapment occurs during the liposome formation, and active loading where drug entrapment is after the liposome formation. The three classic methods for liposome production are mechanical dispersion, solvent dispersion, and detergent removal. These methods, their advantages and

limitations have been comprehensively reviewed (6,9). The following parts provide a summary of these conventional techniques.

3.1. Thin Film Hydration

Thin film hydration (Figure 1.2) is one of the oldest and commonly used methods for formulating liposomes in small batch sizes (9). The main steps for this technique include dissolving the lipids in organic solvent (such as chloroform and ethanol) in a flask, followed by the evaporation of the organic solvent, under vacuum or by using nitrogen stream, to form a dry film of lipids on the inner wall of the flask. The thin film will then be hydrated using a suitable aqueous media while heating the lipids above the phase transition temperature (Tm) and agitating/stirring the formulation. As a result of heating and agitation, the lipid film will get hydrated, swell, and detach from the inner flask wall to form multilamellar vesicles (MLVs). These vesicles tend to be highly heterogenous in lamellarity and size (9).

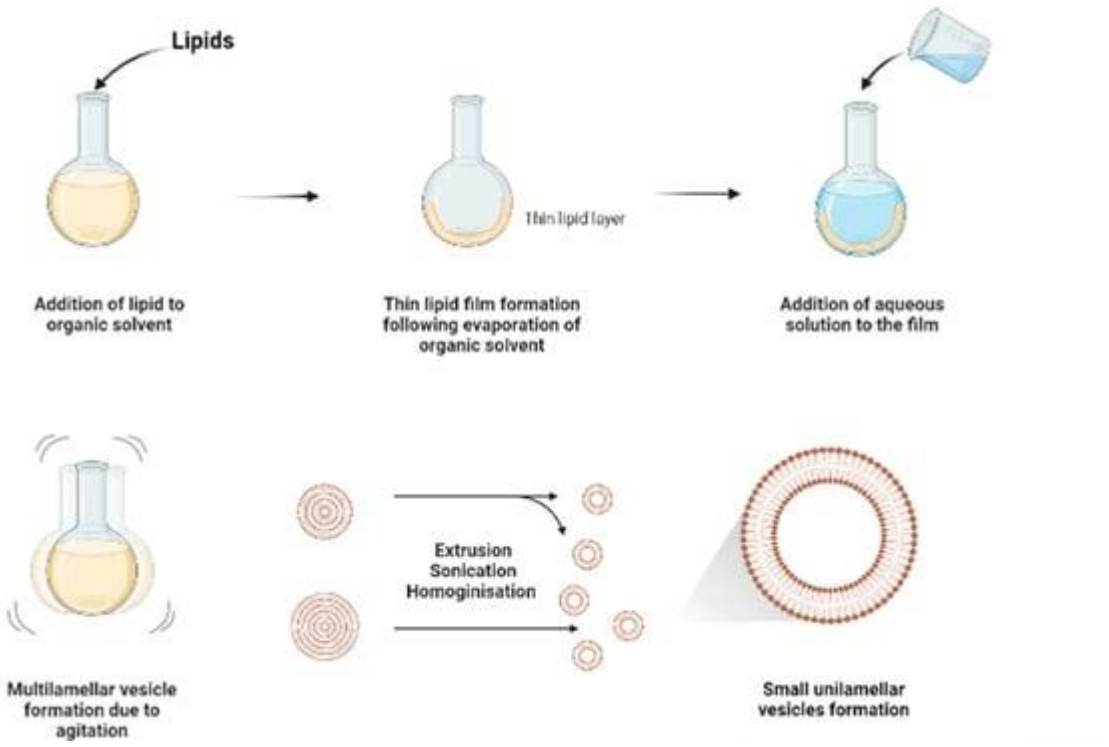

Figure 1. 2: Schematic diagram of thin film hydration method.

The MLVs can be further processed to control and reduce their size by using downsizing methods such as extrusion, sonication, or high-pressure homogenization (9). French pressure cell is a method of extrusion that involves applying high pressure and passing the material through a small orifice that transforms MLV into SUVs. It is considered a gentler size reduction technique and only allows for small volume processing (10). Membrane extrusion is a method

that uses a polycarbonate membrane with a defined pore size. Liposomes are passed through this membrane which results in the reduction of the liposome size. Product losses and difficulty to scale up are the main drawbacks. Ultrasonication can be performed by using a bath sonicator or a probe sonicator. This method provides a homogenous suspension of liposomes as well as reducing the size of liposomes by ultrasonic irradiation. However, sonication generates heat, and metal (titanium) particles may be leached off the probe tip to contaminate products and degrade sensitive actives and lipids (11). Although it reduces size of MLVs, SUVs generated tend to have wide size distribution with lower entrapment efficiency.

3.2. Ethanol and Ether Injections

This method involves dissolving the phospholipid in ethanol (Figure 1.3), and an aqueous medium is prepared and pre-heated. The ethanol solution containing the dissolved phospholipid is rapidly injected using a needle into the aqueous media containing the material to be entrapped. The mixture requires stirring at high temperature (55–65 °C) to ensure the formation of liposomes. Ethanol will evaporate (12). Ethanol injection technique is simple and can rapidly form liposomes (13). This method can form large unilamellar vesicles (LUVs) and small unilamellar vesicles (SUVs) depending on the rate of ethanol injection. Homogenous SUVs are formed when the ethanol volume does not exceed 7.5% of the total formulation volume. Otherwise, heterogenous MLVs are formed. Ethanol is a class 3 solvent which is less harmful but is volatile and flammable. The presence of residual amount of ethanol in the liposomal dispersion can risk denaturing the entrapped biologically-active macromolecules (9).

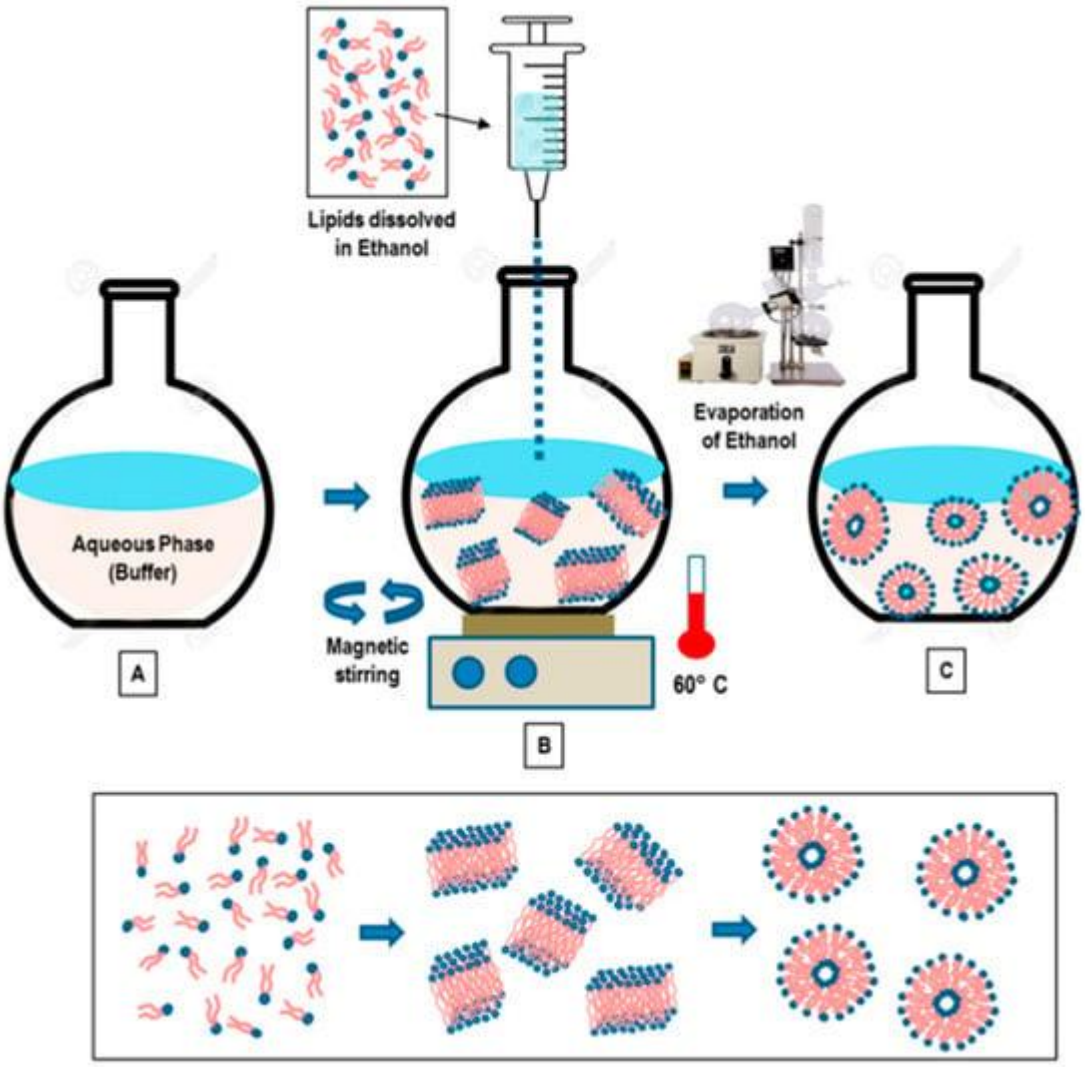

Figure 1. 3: "Schematic representation of the main stages of the ethanol injection method" (9) (Reuse permitted by MDPI).

Ether injection involves dissolving the phospholipid in ether. A solution containing phospholipids dissolved in ether is slowly injected into the aqueous media containing the desired material to be encapsulated. In order to ensure effective evaporation of ether, the mixture is heated to 55–65 °C (12). SUVs bear similar properties to those fabricated by the ethanol injection. As ether evaporates at a lower temperature than ethanol, it can be efficiently removed in a short time, forming concentrated liposome solutions with relatively good entrapment efficiency (9).

3.3. Reverse Phase Evaporation

This method involves dissolving the lipids in an organic solvent such as chloroform/methanol (2:1 *v/v*) which favours the inverted micelles formation. This is followed by the addition of aqueous buffer to create a water-in-oil microemulsion. Then, the organic solvent is evaporated using a rotary evaporator to form a viscous gel. The gel will then collapse forming liposomes (6).

The presence of large aqueous core of the microemulsions promotes entrapment of especially hydrophilic molecules where the liposomal gels showed a controlled release with a good permeation profile (14). The technique employs a large amount of organic solvent and solvent extraction process is slow and time consuming (9).

3.4. Detergent Removal

This method involves adding a detergent, such as sodium cholate and alkyl glycoside, to phospholipids to solubilise and hydrate the lipids by preventing the hydrophobic portions of the lipids from interacting with the aqueous media forming micelles containing lipid and detergent. Then, the detergent is removed progressively allowing the formation of lipid-rich micelles which spontaneously give rise to unilamellar vesicle formation (9). The easiest method to remove the detergent is by diluting the suspension using a buffer which also increases the micellar size and polydispersity. However, this technique produces low liposomal concentration and low EE of hydrophobic drugs, mainly due to the dilution step. Alternatively, dialysis technique can be used to remove the detergent. The detergent can also be removed using resin beads, centrifugation, and gel chromatography techniques (9).

3.5. Microfluidic Devices

A more recent technique involves the use of microfluidic devices for the formation of liposomes; the microfluidic device contains two inlets; the aqueous buffer is added to one inlet and phospholipids dissolved in ethanol is added to the second inlet (Figure 1.4). The two solutions are mixed through a micromixer, leading to the spontaneous self-assembly of the liposomes due to the change in polarity of the solution (15). The microfluidics device produces liposomes under ambient process temperature without heating the lipid above its transition temperature as is required in the lipid hydration technique. It also generates a laminar flow pattern for liposome formation in a controlled manner. There are different designs of the micromixers that provide an efficient mixing within short retention time in the mixing chamber, which has been extensively reviewed (16). Some drawbacks are the needs to remove residual organic solvent and cost of renewing microfluidic cartridges. This method can be made into a ‘lab-on-chip’ system and an adopted continuous flow process for potentially the large-scale liposome production.

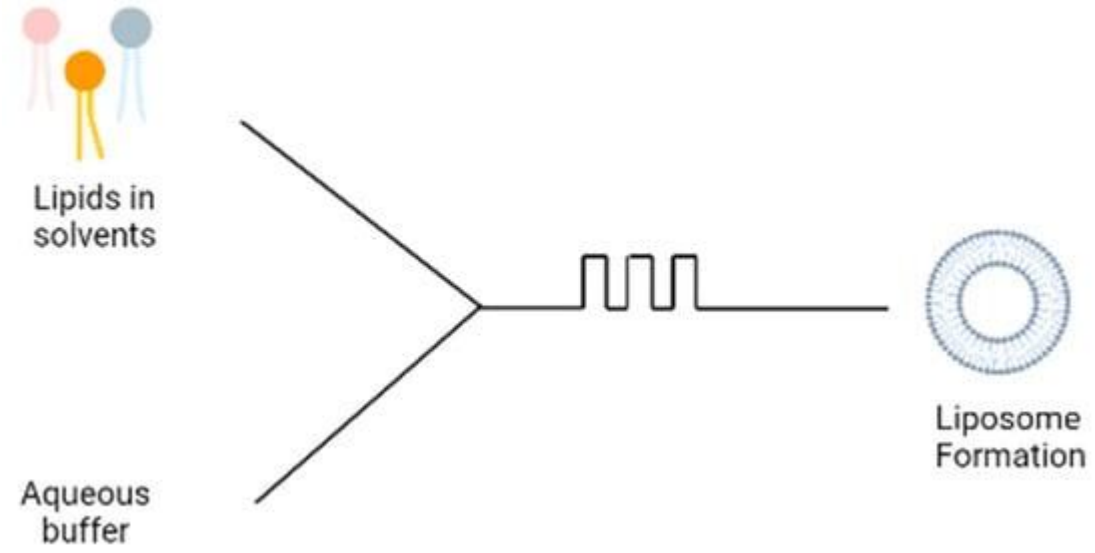

Figure 1. 4: Schematic diagram of microfluidic technique.

Although the methods described above are commonly-used methods for the effective formation of liposomes, each method has certain challenges (Table 1.1). The main drawback of these methods is that they are only able to formulate symmetrical vesicles, meaning that the liposomes contain the same lipid composition in the outer and inner leaflets (17). This is considered a limitation in the formation of liposomal carriers as artificial bilayer carriers are mostly designed for the aim of mimicking biological membranes. However, biological membranes are highly asymmetrical with different lipid compositions in each leaflet. Thus, to improve the mimicking of biological membranes, liposomes need to be formulated with an asymmetrical nature (18).

Table 1. 1: Advantages and disadvantages of symmetric liposomes formulation techniques.

Formulation Techniques	Advantages	Disadvantages
Thin film hydration	• Simple and straightforward process • Used for different kinds of lipid mixtures	• Difficult to scale up • Low entrapment efficiency for water soluble drugs • Forms large vesicles with large size range • Time-consuming
Ethanol injection	• Reproducible, rapid and simple to use.	• Difficult to remove all ethanol as it forms azeotrope with water.
Ether injection	• Results in a concentrated liposomal suspension with improved entrapment efficiency	• Inadequate mixing can result in heterogeneous liposomes

Formulation Techniques	Advantages	Disadvantages
		• Potential nozzle blockage
Reverse Phase Evaporation	• Simple process • Good encapsulation efficacy • Allows the encapsulation of small, large and macromolecules	• Requires large amount of organic solvent • Not suitable for fragile molecules like peptides • Time-consuming
Detergent removal	• Good control of particle size • Simple process • Homogenous product	• Produces low liposomal concentration • Lipophilic drugs have Low entrapment efficiency • Time consuming
Microfluidic	• Simple process • Allows particle size control	• Difficult to remove the organic solvent • Produces small amount of product

4. Nature of Biological Membranes

Biological membranes are typically formed from a phospholipid bilayer which contains hydrophilic heads facing outwards and hydrophobic acyl chains facing each other “inwards” (19). The plasma membrane contains various types of phospholipids with different properties including melting points, headgroups, intrinsic curvature, saturated/unsaturated acyl chains, and cholesterol. As shown in Figure 1.5, these phospholipids are distributed asymmetrically throughout the plasma membrane (20). The lipid layer whose headgroups are facing the outer environment form the outer leaflet (exofacial layer) and the lipid layer whose headgroups are facing the inner components of the membrane form the inner leaflet (cytofacial layer) (21).

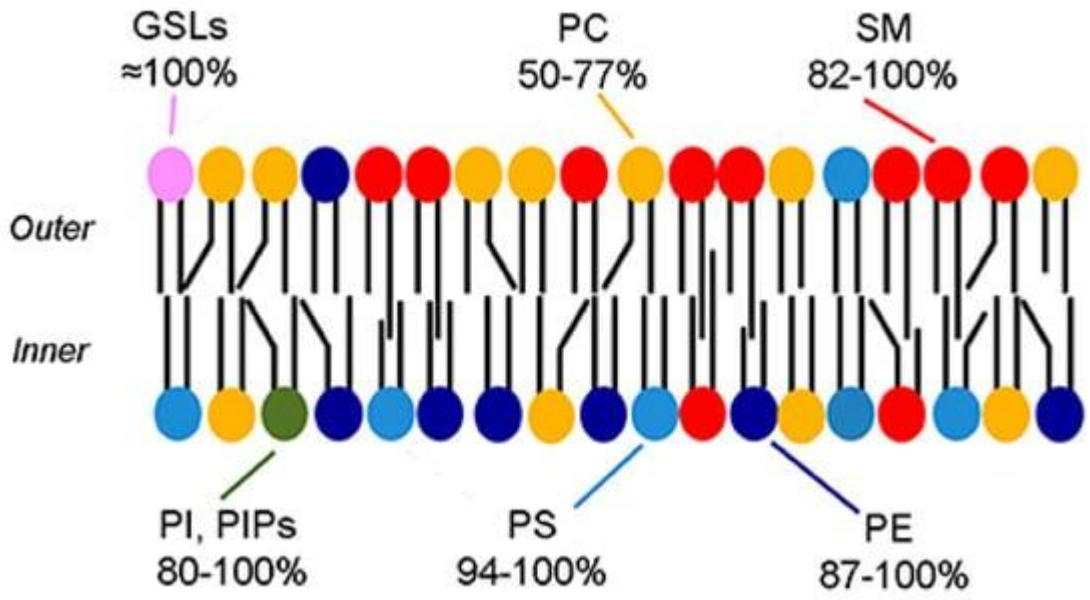

Figure 1. 5: "Phospholipid asymmetry in the erythrocyte membrane" (22) (Reuse permitted by Creative Commons Attribution License (CC BY)).

In 1972, Mark Bretscher (23), published the first report that talked about partial lipid asymmetry in biological membranes. He has found that the outer and the inner leaflets are composed of different lipids. Thus, bio-membranes have asymmetrical features (23). Eukaryotic cell membranes are bilayers of asymmetric lipids where the outer layer consists of sphingomyelin (SM) and phosphatidylcholine (PC) while phosphatidylinositol (PI), phosphatidylethanolamine (PE), and the negatively-charged phosphatidylserine (PS) are found in the inner layer (24). Additionally, cholesterol is a key lipid that is present in the phospholipid bilayer; it forms around 40 mol% of lipids in the synaptic plasma membrane and is distributed in both leaflets in an asymmetric fashion (21). Bacterial membranes were also shown to have an asymmetrical features, but with different compositions; the inner leaflet predominantly consisting of PI and PE while outer leaflet mainly consisting of phosphatidylglycerol (PG) (25,26). Lipid asymmetry is maintained by specific proteins, these proteins have a specific structure that can help in the movement of lipid molecules across the leaflets. Flip/flopases are mainly responsible for moving lipids across the leaflets, while scramblases use an energy independent and a non-selective mechanism to mediate the trans-bilayer movement (27). Moreover, other forms of asymmetry are present within the membranes as follows:

4.1. Geometric Asymmetry

A common source of asymmetry occurs due to vesicle size. As the vesicle diameter decreases, an increase in the difference between the leaflets' surface areas is noticed due to unequal number of lipid molecules that exist in bilayer leaflets (28). Moreover, lipid intrinsic curvature

leads to lateral and transverse lipid separation (29). According to the shape parameter (S) equation:

Equation 1: S=Vlcao

where V is the volume per molecule, l_c is the length of the fully-extended acyl chain, and a_o is the optimum area per molecule at the lipid/water interface. If S > 1, then an inverted cone shape will form which prefers negative curvature. While if S < 1, a cone-like shape will form with a preference to positive curvature. If S = 1, then a cylindrical shape will be adopted which corresponds to a neutral curvature (28). SM and PC were found to have regions of positive or neutral curvature, while PE and PS tend to form regions of negative to neutral curvature. Thus, this could be the explanation to the presence of PS and PE predominantly in the inner monolayer of the plasma membrane (24,30).

4.2. Cholesterol Distribution

The distribution of cholesterol within the membrane leaflets is still debated, however, some studies suggest that cholesterol molecule preferentially resides in the inner leaflet and has an asymmetric distribution within the plasma membrane (31). This speculation was based on a study by Wang et al. (32) which demonstrated that cholesterol has an affinity for areas with high curvature. It is suggested that PE, which mainly resides in the inner leaflet, has regions of high negative curvature; this could be the reason that cholesterol is preferentially drawn to the inner layer (28).

4.3. Charge

As discussed previously, the phospholipid distribution within the cell plasma membrane has an asymmetric nature. Due to this asymmetry, the charge in the outer and inner leaflets differs. Neutral lipids such as SM and zwitterionic PC are mainly located within the outer layer of the plasma membrane. While anionic phospholipids, e.g., PS, PE, and PI, tend to be present within the inner layer (33).

4.4. Exosomes

They are small, extracellular vesicles that are released from cells (34) as means of communication with other cells (35,36). Exosomes are unique vesicles which were found to contain an asymmetrical lipid membrane with similar membrane structure to eukaryotic cells (37).

The asymmetry of lipid membranes has an effect on various membrane properties, such as stability, shape, surface charge, membrane potential, and permeability (28). The loss of this

asymmetry has been associated with consequences. PS levels have a significant effect on cells, for example, during apoptosis, PS move to the outer leaflet, exposing themselves to macrophages, which signals for macrophages to degrade the cell (38). Moreover, PS acts as an important co-factor for various enzymes within the membrane, for example, protein kinase C (39) and the externalisation of PS leads to promotion of the coagulation cascade (40).

The cell membrane was found to have the ability to form platforms (rafts) which can help in cell signalling and trafficking (41). The cell membrane consists of two immiscible phases, ordered phase “Lo”, which is rich in cholesterol that is tightly bound to high-melting lipids such as SM (42,43) and disordered “Ld” phase (44) which is rich in unsaturated acyl chains (18). The lipids in the lipid disordered state are less tightly packed when compared to lipids in the ordered/gel state (45). To form platforms, the membrane segregates the constituents with the help of the two-phase immiscibility, and form compartments (rafts) which are rich in sphingolipids, cholesterol, and proteins (41).

Ordered domains formed in the outer leaflets can be isolated from cell lysates and model membranes and can be detected using fluorescence quenching (46). While the formation of ordered domains within the inner leaflet, using phospholipids that are predominant within the inner leaflet, might not be possible (47), there are speculations on the presence of ordered domains within the inner leaflet (48). Recent studies, using asymmetric model membranes, have revealed that ordered domains formation in one leaflet can lead to the formation of ordered domains in the other leaflet (49). Moreover, the tuning of lipid mixtures can induce or suppress domain formation across leaflets, suggesting interleaflet interactions (50). Interestingly, interleaflet communication can be further suggested as the formation of membrane domain in the outer leaflet can influence the inner leaflet-associated proteins organisation during the process of signal transduction (28). Additionally, the inner leaflet components can sense the outer leaflet components and respond to their physical state. However, this coupling is still not fully understood, and more studies are needed to understand this phenomenon (28). This will lead to the next sections on asymmetric liposomes as drug delivery systems, their advantages, formulation methods, formulation challenges, and their potential applications.

5. Advantages of Asymmetrical Liposomes

Asymmetric liposomes have been used for the delivery to enhance drug encapsulation as well as reducing macrophages uptake of liposomes (discussed further in the following sections). As well as drug delivery, asymmetric liposomes have been utilised for drug-free treatments. Greco et al. (51) via Anderson et al. (52), formulated asymmetric liposomes that were similar to apoptotic bodies that kill *Mycobacterium tuberculosis* bacteria free from antibiotic drugs, aiming to alleviate the incidence of antibiotic resistance in tuberculosis treatment. The asymmetric liposomes were formed from L-α-phosphatidylserine (PS) distributed at the outer membrane to mimic apoptotic bodies (hence promote uptake by macrophages) and L-α-phosphatidic acid (PA) distributed at the inner layer to improve vesicle trafficking and fusion within macrophages while reducing the inflammatory response. The asymmetric, apoptotic body-like, liposomes were effectively internalised by macrophages and led to the induction of Ca^{2+}, which was related to the inhibition of both bacterial growth and inflammatory responses.

Asymmetric liposomes are liposomes that contain different lipid composition in the outer and inner leaflets (53). Therefore, they allow for the possibility of enhancing the properties of the inner and outer leaflets independently; lipids that can maximise entrapment efficiency and reduce leakage can be used in the inner leaflet and different lipids can be used in the outer leaflet to enhance drug delivery and liposomal stability (3). In a study done by Whittenton et al. (53), inverse emulsion technique was used to formulate asymmetric liposomes that contain cationic lipids DMPC (1,2-Dimyristoyl-sn-glycero-3-phosphocholine) and DOTAP (Dioleoyl-3-trimethylammonium propane) in the inner leaflet and neutral/negatively-charged lipids DMPC/POPC (1-palmitoyl-2-oleoyl-sn-glycero-3-phosphocholine) with NBD-PC (1-oleoyl-2-(6-((7-nitro-2-1,3-benzoxadiazol-4-yl)amino)hexanoyl)-sn-glycero-3-phosphocholine)) in the outer leaflet. These liposomes were able to entrap negatively-charged polynucleotides. Moreover, the asymmetric liposomes structure can be adjusted based on the molecule used; a study done by Li and London (3) entrapped Doxorubicin, a cationic drug using different combinations of cationic lipids DOTAP, POePC (1-palmitoyl-2-oleoyl-sn-glycero-3-ethylphosphocholine)) and anionic lipids POPG (1-palmitoyl-2-oleoyl-sn-glycero-3-phospho(1'-rac-glycerol)), POPS (1-palmitoyl-2-oleoyl-snglycero-3-phospho-L-serine), and POPA (1-palmitoyl-2oleoyl-sn-glycero-3-phosphate)) in the outer and inner leaflets in different combinations. The study has shown that asymmetric liposomes containing anionic lipids in the inner leaflet, regardless of the lipid present in the outer leaflet, had the highest entrapment of doxorubicin as well as slowest leakage.

Table 1.2 compares between symmetric and asymmetric liposomes regarding their compositions, production methods, and physicochemical characteristics.

Table 1. 2: Comparison between symmetric and asymmetric liposomes.

Item	Symmetric Liposomes	Asymmetric Liposomes
Compositions	• Wide range of compositions and ratios	• Need specific ratios and compositions • Extra reagent or more than one preformed symmetric liposomes as template
Production methods and scalability	• Established for production of different sizes and lamellarity • Entrapment of small molecules and macromolecules (peptides and genes) • For small scale (thin film hydration) and large scale (microfluidic technique) • Good reproducibility in terms of characteristics and yields	• Established for production of large unilamellar vesicles • Nano-dimensions is emerging (e.g., pulse-jet flow) • Successful entrapment with small molecules; potential for entrapment of large molecules with less chance of drug leakage and greater protection to labile drug • More complex and with extra steps or reagents (for example, to enable lipid exchange) • Custom made equipment/devices; scale up opportunity remains to be established
Characteristics, routes, and Stability	• Prone to oxidation and hydrolysis related to lipid in use • Good long term storage data • Parenteral route is the main but can be adopted for all other routes • Vesicles with targeting ability (versatile surface modifications)	• Prone to lipid instability; potential interleaflet conversion • Limited long-term stability data • Targetable with different routes and better resembles to biological membranes
Physicochemical properties	size, shape, lamellarity, zeta potential and others.	Prove of asymmetry apart from standard tests.

6. Considerations Related to Formulating Asymmetrical Liposomes

There are parameters which should be taken into consideration when formulating asymmetric liposomes:

6.1. Maintenance of Asymmetry

A main challenge to formulating asymmetric liposomes is the flip/flop of the lipids and loss of asymmetry. It was suggested that the rate of flip/flop is affected by the thickness of the bilayer, where a reduced flip/flop rate was seen in bilayers with a thicker hydrocarbon region with phospholipids containing longer acyl chains. The rationale behind this link can be due to the high energy requirement to move a polar headgroup through a longer hydrophobic path of the thick membrane (28).

6.2. Interleaflet Coupling

Cheng and London (48) have studied the effect of temperature and curvature on interleaflet coupling of asymmetric large unilamellar vesicles (LUV). LUVs have reduced membrane curvature as compared to small unilamellar vesicles (SUVs) and it is a closer mimic to the plasma membranes. The study found that the properties of LUVs were similar to that of SUVs, thus, suggesting that curvature does not significantly affect interleaflet coupling. However, the interleaflet coupling was significantly affected by temperature. At ambient temperature, strong interleaflet coupling was observed as SM was exchanged into the outer leaflet and produced asymmetry. However, as temperature approaches 37 °C, interleaflet coupling became very weak. Additionally, it was observed that asymmetric LUVs showed a higher order compared to symmetric LUVs using the same lipid composition, which could also indicate interleaflet coupling (48). A considerable increase in inner leaflet order was seen due to the presence of a highly-ordered outer leaflet (48). In asymmetric vesicles containing SM on the outer leaflet, SM was able to form an ordered state; the thermal stability was significantly higher than symmetric liposomes with similar lipid composition (48).

6.3. Hydrophobic Acyl Chains

The stability of the asymmetry was found to be related to the acyl chain structure; the structure of the acyl chains influenced the transverse diffusion (flip-flop). Moreover, it was deduced that the headgroup structure of the phospholipids can influence whether the asymmetry is full or partial (54). Maintenance of asymmetry was significantly prevented when overly short or two polyunsaturated acyl chains were present; this could explain why phospholipids with these

properties are not abundant in biological membranes (55). Short acyl chains are unable to form a sufficiently stable bilayer. Moreover, two polyunsaturated acyl chains are prone to oxidation and are extremely sensitive.

6.4. Charge

Lipids with only one charge, e.g., anionic, can cross the membrane more readily in an uncharged state which can occur due to protonation or complexation with Na^+ or K^+. This gives rise to partial asymmetry. Additionally, the free energy is raised due to the repulsion between the negative charge of the neighbouring anionic lipids which exacerbated the tendency to flip between the leaflets. The presence of Phosphatidylethanolamine (PE), a zwitterionic phospholipid, can lead to more stable asymmetry. This can be due to the presence of multiple charges that can lessen this repulsion and reduce the tendency to flip. Moreover, PE has smaller headgroup size which can help in reducing steric clashing with phospholipids with larger headgroups such as PC (55).

6.5. Cholesterol Level

Cholesterol plays a significant role in modulating membrane permeability. It was found that liposomes containing 100% POPC had significantly higher permeability than those containing 60% POPC and 40% cholesterol (56). Moreover, the formation of ordered domains is more stable in vesicles containing 25 mol% cholesterol than those without cholesterol. This shows the importance of cholesterol in forming and stabilizing ordered domains (18). To control the cholesterol levels within the asymmetric vesicles, cyclodextrin-exchange method can be performed using (2-hydroxylpropyl)-α-cyclodextrin (HPαCD). HPαCD has a small ring size with little to no affinity to cholesterol and an affinity for phospholipid. This allows for cholesterol to be embedded in the acceptor vesicle, as will be explained later, before the lipid exchange process. However, the use of HPαCD can have some complications such as less affinity for certain phospholipids compared to others (57).

7. Current Formulation Techniques for Asymmetrical Liposomes

The different types of methods used to formulate asymmetric liposomes can be divided into two main categories based on the size of the formed vesicles—nano-sized and cell-sized.

7.1. Nano-Sized Asymmetric Liposomes Formulation Techniques

7.1.1. Cyclodextrin Exchange Method

Cyclodextrins (CD) are defined as cyclic oligosaccharides with two distinct regions containing a hydrophilic exterior and a hydrophobic interior (58). Cyclodextrin exchange (Figure 1.6) is a novel method, developed by Prof. London and co-workers, that leads to the formation of asymmetric liposomes with different lipids/charges in the inner and outer leaflets of the liposomes. The asymmetric liposomes can be prepared as vesicles containing lipids of different charges, e.g., zwitterionic, cationic, or anionic (3). During the preparation method, two different vesicles must be formulated, a donor and acceptor vesicles. The donor vesicle is formulated as a multi-lamellar vesicle (MLV) and added to cyclodextrin; the acceptor is formulated as a unilamellar vesicle with sucrose entrapped; sucrose is used to aid isolation during the centrifugation. This is achieved by preloading the acceptor vesicle with a high concentration of sucrose, e.g., 25% *w/w* which creates a significant density difference between the donor MLVs and the acceptor unilamellar vesicles when the vesicles are suspended in phosphate-buffered saline (PBS) (56).

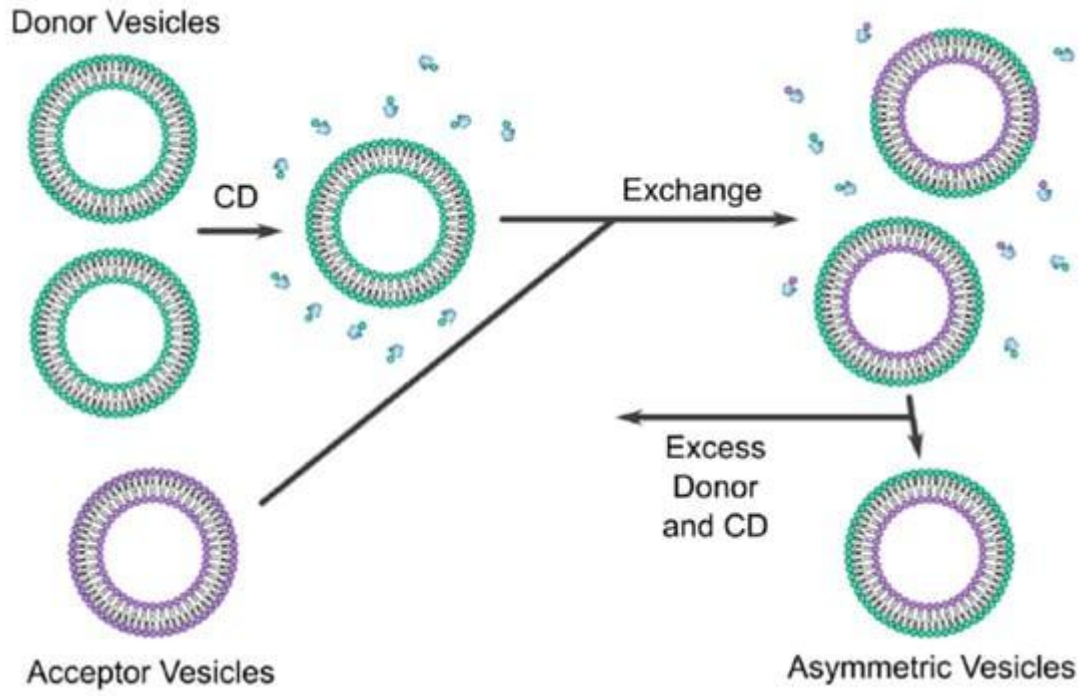

Figure 1. 6: "Schematic of the CD protocol used to prepare asymmetric vesicles" (59) (Reuse permitted by Creative Commons Attribution License (CC BY)).

The two vesicles are then added together, and with the help of CD, lipid exchange process occurs leading to the formation of asymmetric liposomes. The CD has only the ability to exchange the outer layer of the acceptor vesicle, therefore, the inner layer of the acceptor

vesicle is unaffected by the exchange process. Sucrose will help in the separation of asymmetric vesicle during the ultra-centrifugation process; the supernatant will contain all the impurities while the asymmetric liposomes will be pelleted at the bottom of the tube. The extracted vesicles are then resuspended with buffer. Once the asymmetric liposome is formulated, the outer leaflet will contain the phospholipid composition of the donor vesicle and the inner leaflet will contain that of the acceptor vesicle (3). Moreover, a concentration of 40 mol% of cholesterol was found to be the ideal concentration to get the highest yield of asymmetric liposomes obtained after centrifugation (3) which is similar to the amount of cholesterol found in synaptic plasma membrane (21).

The exchange between the donor and the acceptor vesicles must be at a 1:1 ratio i.e., for every one lipid removed from the acceptor, one lipid is added to the acceptor, otherwise, a stress will be induced between the leaflets which can lead to vesicle rupture (3). The asymmetric vesicles were able to remain stable for 48 h (3). This issue, from our point of view, can be solved by lyophilisation technique, however, stability and efficacy investigation of asymmetric liposomes after drying via lyophilisation is needed.

Although this technique provides promising results, adding a high concentration of sucrose to the acceptor vesicle can be associated with osmolarity gradient related membrane tension and potential structural perturbations due to lipid–sucrose interactions (60). To overcome this issue, Heberle et al. (60) modified the cyclodextrin-exchange method by loading the sucrose into the donor MLVs instead, this allowed for the removal of sedimented sucrose-loaded MLVs after exchange using low speed centrifugation; then the removal of the remaining cyclodextrin molecules using a centrifugal concentrator.

Further modifications were carried out by Markones et al. (61) to improve the degree of donor lipid incorporation into the final asymmetric vesicle. Instead of using donor MLVs, a donor lipid–cyclodextrin complex was used during the exchange process. ζ-potential measurement was undergone to determine the extent and stability of the asymmetry which resulted in an asymmetry stable for 14 days at 20 °C. Additionally, Markones et al. (62) was able to formulate asymmetric proteoliposomes using a five-step method which involves formulating a unilamellar vesicle with the desired lipids then adding the desired proteins (Na^+/H^+ antiporter NhaA transmembrane protein was used in this study), adding a donor lipid–cyclodextrin complex to initiate the exchange process, followed by the formation of asymmetric proteoliposomes. Finally, validation of the asymmetric proteoliposomes is achieved by measuring the ζ potential, and the protein is characterized by performing a fluorescence-based protein activity assay.

In addition to proteins incorporation into asymmetric liposomes, the addition of peptides was also tested. Doktorova et al. (63) studied the peptide-membrane interactions by looking at the effect of peptides on membrane asymmetry by using asymmetric LUVs. Gramicidin, a peptide, was used to test this effect; the results have indicated that the rate of flip-flop was increased by a factor of 3. This was further confirmed by Nguyen et al. (64) who studied the effect of gramicidin and other peptides (alamethicin, melittin, or the pH low insertion peptide (pHLIP)), and shown that the flip-flop rate with gramicidin was increased while the asymmetry was immediately destroyed when the other peptides were added to the asymmetric LUV.

7.1.2. Reverse Phase Evaporation

In a study conducted by Mokhtarieh et al. (65), using siRNA, asymmetric liposomes were formulated using a modified reverse phase evaporation method; where two inverted micelles with different phospholipid compositions were prepared separately then mixed; the inner micelle contained 1,2-dioleoyl-3-dimethylammonium-propane (DODAP) and 1,2-dioleoyl-sn-glycero-3-phosphoethanolamine (DOPE) and were dissolved in ether and citrate buffer, while the outer micelle contained 1,2-distearoyl-sn-glycero-3-phosphocholine (DSPC), DOPE, polyethylene glycol1,2-distearoyl-sn-glycero-3-phosphatidylethanolamine (PEG-PE), and cholesterol and were dissolved in ether and HEPES-buffered saline (HBS)/ethanol. Following mixing, ether evaporation and dialysis were performed to formulate the asymmetric liposomes. These liposomes were then pegylated and antibodies/peptides were conjugated. Analysis techniques involved serum stability and toxicity as well as nuclease protection assay. However, no specific analysis technique was conducted to confirm asymmetry. The result from this study showed that this method achieved more than 90% encapsulation efficiency and an average size of 200 nm, although no comparison to symmetric liposomes was done. Moreover, the liposomes were able to protect the siRNA from RNAases for up to 24 h. PEGylation lead to the prevention of aggregation as no aggregation was found in the siRNA/Asymmetric liposomes and serum mixture.

Extrusion has the ability to effectively minimize vesicle size, however, this reduces liposomes encapsulation (4). Mokhtarieh et al. (4) modified this method by adding ethanol to reduce the vesicle size. Ethanol was added immediately after the liposome formation and before the complete removal of ether. The results have shown that ethanol treatment has the ability to reduce the vesicle size to 100–200 nm without affecting the liposome's structure and properties. Moreover, the encapsulation efficacy of the liposome was not affected by the size reduction.

7.1.3. Ca^{2+} Induced Asymmetry

This method involves the use of Ca^{2+} ions to cause asymmetry. Sun et al. (66) formulated LUVs containing DPPC (1,2-dipalmitoyl-sn-glycero-3-phosphocholine) and DOPS (1,2-dioleoyl-sn-glycero-3-phospho-l-serine) then added 0.5mM of Ca^{2+} and incubated the mixture at 70 °C for about 40 h. This has driven the Ca^{2+} ions to bond to two PS molecules headgroups and forming a PS-PS-Ca^{2+} complex which favours negative curvature and leads to the migration of PS to the inner layer (66). Fluorescence quenching technique was used to confirm asymmetry and the asymmetry was stable for several days at room temperature. The parameters of this method were further explored by Guo et al. (67) who looked at the effect of temperature, lipid content, and vesicle size. It was shown that increasing mol% of PS lead to the decrease of asymmetry; asymmetry was not affected by temperature when reducing temperature from 70 °C to 50 °C; increasing the size of the vesicles lead to a reduction in asymmetry. Although this is a promising method, only negatively-charged lipids can be used to form a complex with Ca^{2+}, and furthermore, the method requires a very long incubation time (~40 h).

7.1.4. The Use of Enzymes

The asymmetry of Phosphatidylserine (PS) has the most pronounced effect on the cell, thus, keeping the levels of PS stable within the membrane is crucial. The level of PS in the outer leaflet can be between 0–3.2 mol%, while in the inner leaflet it can be as high as 20 mol% (68). A study by Drechsler et al. (68) has used a unique method to formulate asymmetric liposomes with PS content similar to that of biological membranes i.e., low PS level in the outer leaflet and a high PS level in the inner leaflet. Symmetric liposomes were formulated, then Phosphatidylserine decarboxylase (PSD) enzyme was used to decarboxylate the outer leaflet's anionic PS to neutral PE; since PSD is water soluble, it cannot penetrate the liposomal membrane. Thus, it only converts the PS on the outer leaflet while PS in the inner leaflet remains unchanged. The change in the outer leaflet was analysed by measuring ζ-potential which was dropped from −50 mV to −23 mV. Moreover, high-performance thin layer chromatography, HPTLC, was used to confirm asymmetry by measuring the content of PS after PSD treatment. The asymmetry remained unchanged for 4 days at 20 °C. Although this technique mimics the PS level in biological membranes, it converts PS to PE in the outer leaflet while PE is predominantly found in the inner layer of biological membranes

Phospholipase D was used by Takaoka et al. (69) to convert PC to PS and PE and formulate asymmetric liposomes using the same approach. Although this is an effective technique to formulate asymmetric liposomes, only lipids that interact with the enzymes can be used.

7.2. Cell-Sized Asymmetric Liposomes Formulation Techniques

7.2.1. Inverted Emulsion Technique

This method was proposed by Pautot et al. (70) to formulate asymmetric liposomes (Figure 1.7). The technique involves the assembling of each leaflet independently. First, a water-in-oil emulsion (w/o) is formed, and the lipid used to form inner leaflet of the asymmetric liposomes is used to stabilise this emulsion. The emulsion phase is then layered over an intermediate phase of the same oil but containing the outer leaflet's lipids. The intermediate phase is heavier than the emulsion phase and thus the emulsion phase will be on top. The intermediate phase will be placed over an aqueous phase. The outer leaflet's lipids found in the intermediate phase will form a monolayer between the intermediate phase and the aqueous phase. The water droplets in the w/o emulsion, that are covered with the inner leaflet's lipids, are heavier than the oil in the emulsion and intermediate phase. Thus, water droplets will sink towards the aqueous phase and pull the lipid monolayer present between the intermediate and aqueous phases to form asymmetric vesicles in the aqueous phase. Centrifugation is used to accelerate the sinking process. This method was further developed by utilizing microfluidics (71).

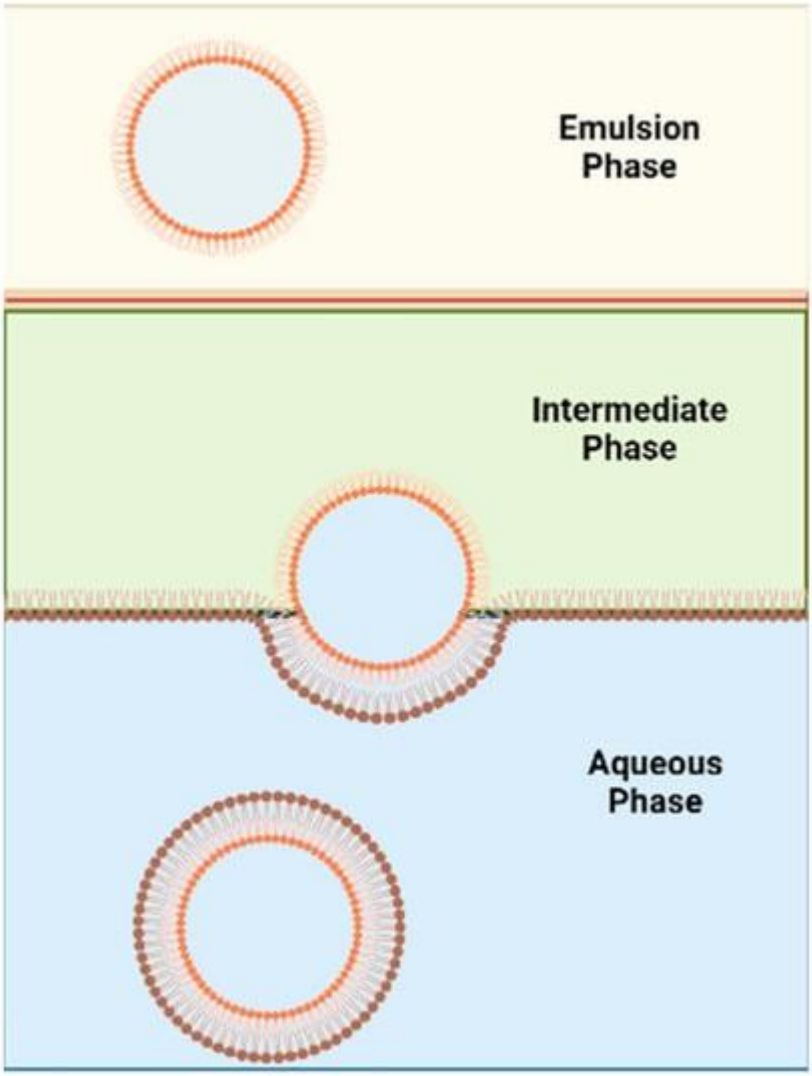

Figure 1. 7: Schematic diagram of the inverse emulsion method.

Although this method is considered less violent in terms of vesicle construction than the cyclodextrin-exchange method, the final vesicle will potentially contain organic solvent which is the main drawback of this method. According to the study done by Whittenton et al. (53), inverted emulsion technique can successfully form asymmetric liposomes. However, the inverse emulsion to liposome conversion had a low yield with this technique, especially when dodecane and mineral oil are used. The use of squalene had higher yield which could be due its higher viscosity and reduced interfacial tension (53). The asymmetry was confirmed using fluorescent NBD-labelled lipids as the fluorescent label was in the outer leaflet. For the inverted emulsion in a centrifugation field technique to be successful, the oil–water interface must be fully equilibrated (72).

7.2.2. Microfluidics

Microfluidic devices can be a useful tool for the formation of asymmetric liposomes; Hu, et al. (73) have proposed a two-step route which combines microfluidic generation with emulsion transfer to form asymmetric giant unilamellar liposomes. The formation involved two independent steps. Firstly, the microfluidic device was used to form the first monolayer; the device contained a multiphase droplet flow centrifugation which consists of a continuous oil stream which allows for the formation of water droplets; then a vessel containing a layer of oil over a layer of water is used to dispense the water droplets into. The second step involves transferring the droplets through a second oil–water interface by centrifugation. This will lead to the formation of the second monolayer, similar to the inverted emulsion technique mentioned above. Different oil phases are used to dissolve different lipids which allows for the control of the resulting lipid bilayer. Fluorescence quenching, biotin-binding assay, and annexin V assay were used to confirm asymmetry. Lu et al. (74) engineered asymmetric vesicles using combinations of novel microfluidic techniques. The method involved four main steps: (1) highly uniformed w/o emulsion formed and stabilized by the “inner-leaflet” lipid, (2) the “inner-leaflet” lipid is replaced by the “outer-leaflet” lipid surrounding the w/o emulsion, (3) this creates a w/o/w double emulsion template which encapsulates the w/o emulsion, and (4) the “outer-leaflet” lipid solution is removed from the intermediate layer of the double emulsion. The results from this study have shown that the membrane asymmetry was maintained for over 30 h; 80% of the asymmetric vesicles remained stable for at least 6 weeks, additionally this method was able to improve the size variation control.

More recently, Ghazal et al. (75) has combined a microfluidic platform based on hydrodynamic focusing on the thiol-ene chip with synchrotron small-angle X-ray scattering (SAXS) to examine the continuous production of multilamellar vesicles (MLVs) of nano-dimension. Due to an uneven distribution of the two embedded lipid molecules at the lipid interfacial-water area, formation of an asymmetric bilayer could not be ruled out and it has been suggested that the growth of asymmetric feature is a time-dependent process. Pulsed jet flow also utilising the microfluidic template has recently showed to produce a nano-dimension asymmetric liposome (37). There is an abundance of evidence supporting the production of giant-sized vesicles by microfluidic devices while production of nano-size equivalence is feasible. Further advancement in microfluidic devices is required in order to control the size of produced MLVs and bilayer asymmetry properties.

7.2.3. Hemifusion

Enoki and Feigenson (76) have formulated asymmetric giant unilamellar vesicles (GUV) using hemifusion (Figure 1.8). This technique involves formulating a giant unilamellar vesicle (GUV) by electroformation and applying a red fluorophore for visualization by confocal microscopy. A supported lipid bilayer (SLB) is formulated separately, and a green fluorophore is added. Then the GUV is put in contact with the SLB, where a fusogenic agent (Ca^{2+}), as calcium chloride, induces hemifusion; this will lead to lipid exchange between the SLB and the outer leaflet of the GUV. The GUV is then detached from the SLB by adding EDTA to chelate the calcium and stop hemifusion. A new asymmetrical GUV is formed which contains the GUV lipids in the inner leaflet and the SLB lipids in the outer leaflet. The asymmetry is confirmed by measuring the intensity of each fluorophore in the asymmetric GUV in contrast to the symmetric GUV. This method was able to approach 100% asymmetry and preserve vesicle content (76). Moreover, the line tension of domains was investigated and showed that asymmetric liposomes with DOPC-rich outer leaflet has lower line tension when compared to their symmetric counterparts (20).

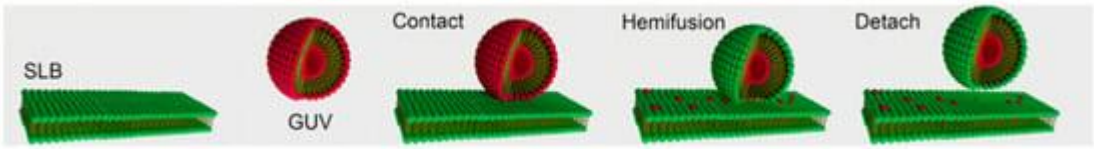

Figure 1. 8: "Hemifusion yields asymmetric GUVs (aGUVs)" (20) (Reuse permitted by Elsevier).

7.2.4. Pulsed-Jet Flow

This method involves the formation of a lipid tube which is then deformed and leads to the formation of asymmetric vesicles. Kamiya et al. (77) have used this method to formulate cell-sized giant vesicles (GVs). Microfluidic flow is applied via a jet nozzle to formulate a micro-sized lipid tube; the lipid tube contained one type of lipid in the outer layer, n-decane organic solvent in between, and a different lipid in the inner layer (DOPS and DOPC were used). Then, the tube was deformed by applying sinusoidal undulation, this in turn forms two types of asymmetric vesicles—one with a diameter of ~100–200 μm and vesicles with ~3–20 μm diameter. Confocal Raman scattering microscopy was used to study these vesicles and was shown that the latter contains only a small amount of organic solvent within the monolayers of the membrane. The 3–20 μm-sized vesicles were then used to study lipid–lipid and lipid–protein interactions. The results have shown that asymmetric vesicles containing DOPC in the inner layer and DOPS/DOPC in the outer layer has led to the increase of membrane reconstitution ratio of the proteins into lipid membranes. This method was able to overcome the remaining of residual

organic solvent issue associated with other techniques such as inverse emulsion technique. The presence of organic solvent can affect the long-term stability of vesicles and leads to vesicle rupture within few days. However, this method was able to keep vesicles stable for at least 7 days (77).

Intracellular vesicles within the cells play an important role in homeostasis and regulation of metabolism and they were found to have an asymmetric membrane that is different from the plasma membrane. Developing this system can create an in vitro model to improve the understanding of this synaptic system (78). Kamiya et al. (78) modified the pulsed-jet flow method to form a vesicle-in-a-vesicle system by using a triple-well device which mounts two separators. To generate the inner vesicles, the separator between first and second wells has an opening sized 100 μm; to generate the cell-sized vesicles, the separator between the second and third wells has an opening sized 500 μm; the inner vesicle would be inserted into the cell-sized vesicles. To confirm asymmetry, fluorescence quenching method was conducted by using phospholipid-conjugated NBD in the outer leaflet and imaging using confocal microscopy; moreover, fluorescence annexin V binding assay was used to measure the asymmetry of the inner leaflet of the cell-sized vesicle and the outer layer of the inner vesicle (78).

Further modification of this method by Kamiya et al. (37) allowed for the formation of nano-sized asymmetrical lipid vesicles using pulsed-jet flow. This was performed by using asymmetrical planar lipid bilayer with increasing the application of pressure and duration. The lipid bilayer used mimics exosomes; thus, it can provide a useful tool for exosome-like delivery systems which can improve the lipid vesicle interaction with living cells. To confirm asymmetry, the technique involved using streptavidin (biotin)-conjugated gold colloids which can bind to biotin-conjugated phospholipids on the outer leaflet.

8. Challenges Associated with Formulating Asymmetric Liposomes

Although several promising techniques have been discussed for formulating asymmetric liposomes, these methods have their own limitations (Table 1.3). Additionally, it may not be possible to compare these methods head-to-head as the published literature available does not measure the same parameters such as encapsulation efficiency, stability of asymmetry, degree of asymmetry, and asymmetric vesicle stability. Moreover, an important but overlooked parameter to consider when formulating asymmetric liposomes is differential stress. Differential stress is described as the optimal lipid packing density imbalance between the

leaflet leading to residual leaflet and it affects vesicle and asymmetry stability tension (79). Symmetric vesicles tend to have tensionless (zero tension) leaflets, while asymmetric leaflets tend to be under differential stress, in other words, have a non-zero leaflet tension (59).

Table 1. 3: Advantages and disadvantages of asymmetric liposomes formulation techniques.

Formulation Techniques	Advantages	Disadvantages
Cyclodextrin exchange	• Various types of phospholipid combinations can be used • High encapsulation efficiency • Components: lipids, cyclodextrins, sucrose	• Considered violent when constructing vesicles. Can damage liposomes. • Large amount of lipid content is lost. • The loading of sucrose within the acceptor vesicle can lead to membrane tension and structural perturbations • Requires removal of cyclodextrin and donor vesicle which could affect percentage yield of liposomes left in the formulation.
Reverse phase evaporation	• High encapsulation efficiency • Good scale-up ability • Does not require exposing the formulation to high temperature	• Requires dialysis which can be time consuming • Requires ethanol which can inactivate many biologically active macromolecules and hinder their loading to liposomes
Ca^{2+} induced asymmetry	• Has long stability of asymmetry which can last several days • Does not require forming two different vesicles to produce asymmetry. Only one form of vesicles is required • Simple techniques are used	• Only negatively charged phospholipids can be used • Long incubation time required (around 40 h)
The use of enzymes	• Has long stability of asymmetry which can last four days • Does not require forming two different vesicles to produce asymmetry. Only one form of vesicles is required • Minimally invasive • Can choose the lipids to modify without affecting other lipids within the outer leaflet of the vesicle	• The asymmetry formed is opposite of the biological membranes (PE is formed in the outer leaflet and not in the inner one) • Can only work on specific phospholipids • Enzymes can be denatured if exposed to wrong pH or temperature • Requires the removal of the enzyme after achieving

Formulation Techniques	Advantages	Disadvantages
	• Components: phosphatidylserine decarboxylase, lipids	asymmetry which can be time consuming
Inverted emulsion technique	• High degree of asymmetry • Various types of phospholipid combinations can be used • Simple techniques are used • Good scale-up ability • Components: lipids, glucose, oil, organic solvent	• Presence of organic solvent between the lipid leaflets which can affect membrane's physical and mechanical characteristics • Low liposome formation yield • Size of vesicles varies widely (polydispersity index can reach more than 20%)
Microfluidics	• Has long stability of asymmetry for at least 6 weeks when using continuous microfluidic technique • Automated method which reduces error and accelerate production of liposomes • Components: lipids, organic solvent	• Presence of organic solvent between the lipid leaflets which can affect membrane's physical and mechanical characteristics • Requires fabrication of a microfluidic device which can be time consuming and challenging
Hemifusion	• Yields near 100% asymmetry without cyclodextrin or organic solvent contamination • Yields vesicles with preserved vesicle content, with little leakage • Components: fusogenic agent, lipids	1. It requires formation and observation of the SLB which can be time consuming 2. Small amount of SLB lipid entered the inner layer of the liposome
Pulsed-jet flow	1. Has long vesicle stability for at least 7 days 2. Able to produce cell-sized and nano-sized vesicles by increasing pressure and application time of pulsed-jet flows 3. Components: lipids, organic solvent	• Presence of residual organic solvent between the lipid leaflets which can affect membrane's physical and mechanical characteristics • Lipid content is lost as vesicles with large amount of organic solvent are discarded • Requires fabrication of the pulsed microfluidic jet flow device which can be time consuming and challenging

9. General Analytical Techniques

When formulating asymmetric liposomes, it is essential to have confirmatory methods to prove the asymmetry. Measuring zeta potential is one of the methods that has the ability to detect asymmetry of ionic lipids within the liposome by measuring the charge of ionic lipids only in the outer leaflet of symmetric and asymmetric liposomes (61).

A novel method developed by London and co-workers involves using a cationic fluorescent probe to bind to the outer layer (3). DPH (diphenylhexatriene) and TMA-DPH (trimethylammonium diphenylhexatriene) fluorescence measurements are used in the confirmation of asymmetry (18). DPH can dissolve throughout the bilayer, while TMA-DPH is restricted to the outer leaflet as it does not flip rapidly between inner and outer leaflets. TMA-DPH involves the use of a fluorescence probe that has a positive charge; this probe does not cross the membranes easily and its binding is dependent on the outer-leaflet charge. When the membrane has a negative charge, the probe will have a high level of binding and as it inserts into the hydrophobic core of the liposomal bilayer; the fluorescence will significantly increase which allows for the detection of charge (3).

High-performance thin layer chromatography (HPTLC) can be used to quantify the lipid composition of the liposomes and that can be useful in monitoring the change in membrane compositions in formulating asymmetrical liposomes (80). The phospholipid composition change after lipid exchange was measured via HPTLC in a study by Li and London (3). Moreover, HPTLC was used to quantify the change of PS concentration after the application of PS decarboxylase enzyme.

Fluorescence quenching is another method that can be used to determine asymmetry by measuring the fluorescence intensity of the tagged phospholipids such as NBD-conjugated lipids (70). The use of fluorescence dye (20) is another effective method of confirming asymmetry. Fluorescently tagged annexin V is a type of fluorescence analysis that can be used to bind to PS then viewed by confocal microscopy to detect asymmetry (73,77).

Recently, neutron and X-ray scattering techniques have shown how the structural and dynamical properties of each leaflet respond to changes in lipid compositions. These analytical techniques are indispensable for the development and characterization of the complex asymmetric vesicles (81). Analysis techniques used by Heberle et al. (60) involved the use of small-angle neutron scattering (SANS) and nuclear magnetic resonance (NMR) experiments by preparing the liposomes in different buffers containing different concentrations of deuterated

water to study the influence of the fluid inner leaflet on the more ordered outer leaflet. SANS method, with subnanometer resolution, is an effective method that has the ability to determine bilayer structure (60). Furthermore, gas chromatography/mass spectroscopy was used as an exchange efficiency quantification method and the degree of asymmetry was measured using ^{1}H NMR and Pr^{3+} shift reagent which shifts resonance when binding to the choline methyl groups in the outer leaflet; this only occurs in the outer layer because Pr^{3+} does not have the ability to cross the membrane (59).

Conjugation is another useful technique used to confirm asymmetry. Conjugating certain materials with the phospholipids can help detect asymmetry. Kamiya et al. (37) used streptavidin (biotin)-conjugated gold colloids to confirm asymmetry of the vesicles. Biotin was conjugated with the lipids in the outer leaflet and the streptavidin-gold colloids were added to the solution; TEM was used to visualise the streptavidin-gold colloids (small, black spots) attached to the outer leaflet lipids and confirm asymmetry. Moreover, when the streptavidin-gold colloids were added to the biotin linked to the inner leaflet lipids, no gold colloids appeared in the TEM image, indicating that all the inner leaflet lipids were indeed in the inner leaflet.

10. Potential Benefits to Asymmetrical Liposomes in Genetic Material Delivery

Genetic material delivery into the human body requires a suitable carrier to protect the nucleic acids and allow them to be transported safely to the targeted cells; this is because naked genetic materials are significantly susceptible to degradation. Immune response sensitization, phagocytosis, serum nucleases degradation, and rapid renal clearance, in addition to low cellular uptake and target specificity, are vulnerabilities that make naked genetic material delivery highly unsuitable and ineffective and can be eliminated from the body rapidly (82). To successfully deliver genetic material to targeted cells, the carrier must form a stable complex with the encapsulated genetic material; the complex must be able to survive in the blood circulation by avoiding early recognition by macrophages and reaching the targeted cells. Opsonins are serum proteins that attach to liposomes and target them for removal by macrophages (83). Once inside the cell, the liposomal carrier must have the ability to escape the endosomal degradation “endosomal escape”. Moreover, the process of genetic material delivery should pose minimal side effects and enhanced therapeutic action (83).

Nucleic acids used in lipid carriers are generally divided into three main types, small DNA (Oligodeoxynucleotides) or chemically synthesised related molecules, large DNA molecules (Plasmid DNA), and RNAs (small interfering RNA “siRNA”, messenger RNA “mRNA”, and Ribozymes) (84). Since nucleic acids are negatively-charged, they require a positively-charged carrier to be able to bind to them. These carriers that form a complex with the nucleic material can be formed from positively-charged polymers (polyplexes) (85) or cationic lipids (lipoplexes) (86). However, the main disadvantages of the use of positively-charged carriers are the removal by the reticuloendothelial system (RES) as well as nonspecific interactions with predominantly negatively charged blood components, thus, leading to accumulation at the primary organs (87). Therefore, based on the asymmetric liposome advantages discussed, the use of asymmetric liposomes can potentially help in overcoming issues associated with the current genetic material delivery methods.

11. Recent advancement in the field of asymmetric liposomes

One of the key recent developments in the field involves the use of methyl-β-cyclodextrin to tune the lipid asymmetry by controlling the direction and the magnitude if the asymmetry formed. This allows for asymmetry formation while reducing the differential tension and net bilayer tension (88). To further improve and stabilize the asymmetry, asymmetric proteoliposomes were created by exploiting the transmembrane β-barrel outer membrane protein (OmpA) (89). the use of proteins can help to significantly stabilize asymmetric liposomes as it mimics the biological cells. Moreover, the researchers introduced a novel lipid perfusion technique, which enables them to rapidly alter the lipid environment during experiments and observe real-time changes in ion channel activity. They also developed a leaflet-specific perfusion method to independently modify the lipid composition of just one side of the bilayer (90).

In nature, cells like bacteria and immune cells show chemotaxis through complex signalling. A new active system was developed using liposomes containing enzymes. These liposomes were made asymmetric by adding pore-forming proteins (α-hemolysin), allowing substrates and products to pass through the membrane. This movement of molecules creates an imbalance that pushes the liposomes forward. The type of substrate used affects how fast and in which direction the liposomes move in a microfluidic channel. This system helps improving the understanding of how artificial and natural vesicles move and could be useful in applications like drug delivery (91).

New literature studied new analysis techniques to confirm asymmetric liposomes formation. Liposomes with DPPC in the outer leaflet and DPPS in the inner leaflet were developed and analysed Fourier-transform infrared (FTIR) spectroscopy. The application of second derivative FTIR spectra revealed distinct differences between symmetric and asymmetric liposomes in terms of lipid hydration, particularly within the glycerol backbone and choline headgroup of DPPC. Additionally, variations in hydrocarbon chain interactions during phase transitions were observed between symmetric and asymmetric systems (92).

12. Gaps in literature and contribution of this research

Despite the significant advancements in the formulation of asymmetric liposomes, current techniques remain limited by their complexity, limitation of lipids that can be used, and scalability issues. The methods often involve multistep procedures, reliance on specialized equipment, and restrictive lipid choices. Moreover, most method can create liposomes of a certain size e.g. GUV but not smaller liposomes and vice versa.

In response to these challenges, this research introduces a novel method that is simplified and more flexible for asymmetric liposome preparation. This technique minimizes the number of formulation steps and eliminates the dependency on sophisticated instrumentation, making it more accessible for routine laboratory use. Importantly, it allows for the use of a wide variety of lipids to suit different research and therapeutic applications. Additionally, this method allows for generation of liposomes with varied sizes as it does not depend in size difference for the separation of donor and acceptor liposomes. This method represents a substantial improvement over conventional asymmetric liposome preparation techniques and opens new avenues for innovation in liposomal drug delivery and biomimetic membrane studies.

13. Summary

Nano-based drug delivery systems have become an attractive approach for treating various diseases. Liposomal nanotherapeutics have many advantages for specificity and other characteristics over conventional therapies. Due to the recent advances in the formulation techniques of liposomes, the asymmetric liposomes will find their way to the clinic, they mimic the biological membranes, and hence they can enhance drug uptake to diseased cells and retain therapeutic agents in lung tissues and other tissues.

Aims and objectives

This research aims to develop a practical and novel method for formulating asymmetric liposomes using cyclodextrin-lipid complexation, with the broader goal of enhancing their use in drug and gene delivery. To support this aim, several key objectives were addressed. Several asymmetric liposomes were successfully formulated using the novel method, and their ability to encapsulate bromocresol green was tested. The formulations were also explored for their potential to encapsulate DNA, with a focus on achieving high entrapment efficiency. Stability was a main focus of this study, with both the asymmetry and overall physical stability of the liposomes evaluated and compared to values reported in the literature. To further improve performance, the impact of adding 10% Solutol HS-15 was assessed, particularly in reducing aggregation and enhancing stability. One of the most promising outcomes was the development of a liposomal formulation featuring a near-neutral outer surface, while still achieving high DNA encapsulation due to the presence of cationic lipids in the inner leaflet. Offering a useful balance between high entrapment efficiency and reduced toxicity.

Chapter 2

Materials and Methods

1. Material and Equipment

1.1. Materials

1-Palmitoyl-2-oleoyl-sn-glycero-3-phosphocholine "16:0-18:1 PC" (partly purchased from Avanti Polar Lipids via Merck (UK) and the rest was kindly given as a sample from Lipoid, Germany), *1-palmitoyl-2-oleoyl-sn-glycero-3-phosphoethanolamine* "16:0-18:1 PE" (purchased from Avanti Polar Lipids via Merck, UK), *1,2-dioleoyl-3-trimethylammonium-propane* (chloride salt) "18:1 TAP (DOTAP)" (partly purchased from Avanti Polar Lipids via Merck (UK) and the rest was kindly given as a sample from Lipoid, Germany), *Sphingomyelin* (Brain, Porcine) (purchased from Avanti Polar Lipids via Merck, UK), *1,2-distearoyl-sn-glycero-3-phosphocholine* "18:0 PC" DSPC (partly purchased from Avanti Polar Lipids via Merck (UK) and the rest was kindly given as a sample from Lipoid, Germany), *Cholesterol* (Merck, UK), *1,2-distearoyl-sn-glycero-3-phosphoethanolamine-N-(7-nitro-2-1,3-benzoxadiazol-4-yl*) (ammonium salt) "18:0 NBD PE" (purchased from Avanti Polar Lipids via Merck, UK). *Randomly methylated-α-cyclodextrin* (Cyclolab, Hungary), *Chloroform* (university of Sunderland, UK), *Methanol* (university of Sunderland, UK), *HEPES (4-(2-Hydroxyethyl)piperazine-1-ethane-sulfonic acid)* buffer (10Mm) (Merck, UK), 1X PBS *Phosphate-buffered saline* (university of Sunderland, UK), HPLC grade distilled water (university of Sunderland, UK), *Amicon® Ultra-2 Centrifugal Filter, 100 kDa MWCO* (Merck, UK), *Folded capillary disposable cuvettes DTS1070* (Malvern Panalytical, UK), *Disposable cuvettes-DLS cell and stopper DTS0012* (Malvern Panalytical, UK), *Alminium pans Pan 40 uL, Al* (Mettler Toledo, USA), *UltraPure™ Salmon Sperm DNA Solution* (ThermoFisher, UK), *Nunc F96 Microwell black polystyrene plate-96 well plates* (Black) (ThermoFisher, UK), *Sodium hydrosulfite* (Merck, UK), *Solutol HS 15* (BASF, Germany), *Sephadex G50* (G50150, Sigma Aldrich, UK). The molecular weight of the lipids and cyclodextrin are shown in table 2.1. Additionally, the transition temperatures of all the lipids are shown in table 2.2.

Table 2. 1: The molecular weights of materials required to formulate liposomes (93)

Material	MW (g/mol)
DOTAP	698.5
DSPC	790.2
POPE	718.0
SM	760.2
POPC	760.1
NBD-PE	924.2
Cholesterol	386.7
MαCD	1126.9

Table 2. 2: The phase transition temperatures (Tm) of the lipids used to formulate liposomes (94)

Lipid	Tm (°C)
DOTAP	0
DSPC	55
POPE	25
SM	37
POPC	-2
DOPE	-16

1.2. Equipment

Zetasizer ZSP (Malvern Panalyticals, UK), *Spectramax i3x* (Molecular devices LLC, USA), *Differential scanning calorimetry "DSC"* (DSC Q1000 TA Instruments, Ghent, Belgium)) with an empty cell chamber and equipped with nitrogen gas (BOC Gas, UK), *Fourier transform infrared spectroscopy "FTIR"* (Shimadzue UK LTD), *nuclear magnetic resonance "NMR"* Bruker 500 MHz NMR (Bruker UK LTD), *Thermogravimetric Analyzer "TGA"* (Mettler Toledo, USA), *Mini-Extruder* (Avanti, USA), *MIKRO 220/220R centrifuge* (Hettich UK Ltd), *Nanodrop Lite(Thermo fisher Scientifics, UK), UV-Vis Microvolume Spectrophotometer* (Thermo fisher Scientifics, UK), *UV/Vis Spectrophotometer* (Spectrasonic Camspec Ltd, Canada), Lyophilizer *VirTis BenchTop Pro* (Sp Scientific Corp., USA), *Rotavapor.R-210* (Butchi, Switzerland), *Bath sonicator* (Hilsonic, UK)

2. Methods

2.1. Preparation of buffers:

2.1.1. Phosphate buffer saline (PBS)

To prepare 2L of 1X PBS (pH 7.4), the following was added; 16g of Sodium chloride (mw:58.44g/mol), 0.4g of Potassium chloride (mw:74.55g/mol), 2.88g of Sodium phosphate dibasic (mw:141.96g/mol), and 0.49g of potassium phosphate monobasic (mw:136.09g/mol). Then, HPLC grade distilled water was added up to 2L; the pH is adjusted to 7.4 by adding NaOH or HCl.

2.1.2. 4-(2-hydroxyethyl)piperazine-1-ethanesulfonic acid (HEPES)

To formulate HEPES buffer (10mM; pH 7.4), 4.77g of HEPES powder (mw:238.3g/mol) was added. Then, HPLC grade distilled water was added up to 2L; the pH is adjusted to 7.4 by adding NaOH or HCl.

2.2. Methodology used in chapter 3

2.2.1. Formulating Symmetric liposomes:

The phospholipids were weighed (masses shown in table 2.3), then they were mixed and dissolved in the required amount of chloroform, the chloroform was dried using a rotary evaporator at high vacuum until fully dried, the drying process continued for another 30 minutes to 1 hours to further dry at 40-60 °C to ensure that no solvent is still attached to lipids. The dried thin film formed (Figure 2.1) was then hydrated with the required buffer and added to either a water bath (at a temperature above the phase transition temperature of the lipids) or to a sonicator bath for 30 minutes to 1 hour.

Figure 2. 1: Thin lipid film formation after removal of organic phase using rotary evaporator

Table 2. 3: The mass of lipids used to formulate the symmetric liposomes per 1mL of suspension

Formulation	POPC (mg)	POPE (mg)	DOTAP (mg)	CHOLESTEROL (mg)
POPC + CHOL	0.9	-	-	0.3
DOTAP + POPE + CHOL	-	0.4	0.4	0.3

2.2.2. Formulating Asymmetric liposomes

2.2.2.1. Formulating the donor lipid-cyclodextrin (CD) complex

The donor complex was formulated by first, dissolving 22.5mg of cyclodextrin in 1mL (masses in table 2.4) of HEPES buffer. The final concentration of the solution was 20mM. The solution was then heated in a water bath to 55°C. Following that, donor lipid (masses shown in table 2.4) was dissolved in 500µl methanol. The final concentration was 4mM. This solution was then added to the cyclodextrin solution in a drop-wise approach while gently shaking. The solution was then left at 55°C and 100RPM for 2 hours to allow complexation and methanol evaporation (figure 2.2). Finally, the solution was sonicated for 1 hour to allow the breaking of any small micellar formation.

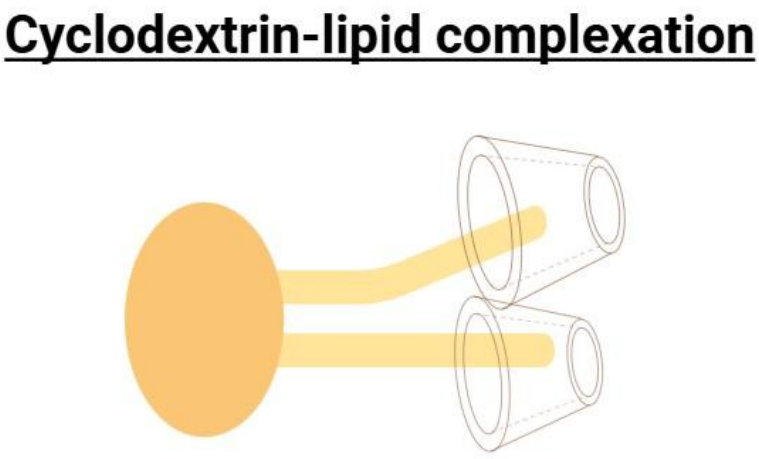

Figure 2. 2: The complexation of cyclodextrin and phospholipids

Table 2. 4: The mass of material used to formulate the lipid-cyclodextrin (CD) complex

Formulation	Mass (mg)
DOTAP-CD complex	CD: 22.5
	DOTAP: 2.8
POPC-CD complex	CD: 22.5
	POPC: 3.0
POPE-CD complex	CD: 22.5
	POPE: 2.9
SM-CD complex	CD: 22.5
	SM: 3.0

2.2.2.2. *Formulating the acceptor vesicles*

The formulation had a final concentration of 2mM of the acceptor vesicles similar to the symmetric liposomes as large unilamellar vesicles (LUVs). Masses shown in table 2.3.

2.2.2.3. *The exchange process*

To formulate asymmetric liposomes,1ml of the lipid-CD complex was added to 1ml of the acceptor vesicles and were gently shaken at 100RPM for 1 hours to allow lipid exchange (Room temperature:23°C). The asymmetric liposomes formed were separated from the rest of the solution by either centrifugal filters use or by conventional centrifugation.

2.2.2.4. *Lyophilization process*

To study the cyclodextrin-lipid complex further, the cyclodextrin-lipid complex was formulated as mentioned in section 2.2.2.1. The solution was then dried using a lyophilizer (freeze drier) to allow further analysis. The solution was frozen at -20°C for 24 hours then was covered with parafilm and the parafilm was pierced to form tiny holes. This was done to allow the water to escape. Following that, the beakers were inserted into the machine and dried under vacuum for 48-72 hours, until a white powder was formed. The powder was then stored at room temperature (Room temperature:23°C). Small quantities of the powders were taken and used for analysis.

2.2.3. Characterisation of the prepared cyclodextrin-lipid complexes and liposomal formulations

2.2.3.1. *Vesicle Size*

The Zetasizer ZSP was used to measure the vesicle size of the formulations, the process involved adding 20µl of the liposomal suspension to 980µl of HEPES buffer inside a disposable cuvette (Disposable cuvettes-DLS cell and stopper DTS0012). The size measurements were repeated 3 times at room temperature (23 °C).

The software SOP contained:

- Material → Phospholipids (Malvern) RI:1.450 Absorption:0.001
- Dispersant → HEPES Temperature: 25°C Viscosity:0.8881cP RI:1.330
- Equilibration time: 30 seconds
- Measurement type: 173° Backscatter (NIBS default)
- Number of measurements: 3 with 25 seconds delay between each measurement

2.2.3.2. Zetapotential

The Zetasizer ZSP was used to measure the zetapotential of the formulations, the process involved adding 20µl of the liposomal suspension to 980µl of PBS buffer inside a folded capillary disposable cuvettes DTS1070. The size measurements were repeated 3 times at room temperature (23 °C).

The software SOP contained:

- Material → Phospholipds (Malvern) RI:1.450 Absorption:0.001
- Dispersant → PBS Temperature: 25°C Viscosity:0.8881cP RI:1.330
- Equilibration time: 30 seconds
- Measurement type: 173° Backscatter (NIBS default)
- Number of measurements: 3 with 25 seconds delay between each measurement

2.2.3.3. Fourier transform infrared spectroscopy (FTIR)

Following lyophilization of the sample, the resulting powders were added onto the FTIR machine and readings were taken. Each powder was tested individually, the fresh cyclodextrin, the lyophilized cyclodextrin, the physical mixture of both the CD and the lipid, and the cyclodextrin-lipid mixture. A small amount of the powder was added to the crystal of the FTIR machine to cover it, the lid closed. The background spectra were measured and subtracted before each measurement. Then, the measurements were taken at the spectral range of 600-4000cm-1 at a resolution of 4cm-1.

2.2.3.4. Thermogravimetric analysis (TGA)

The process involved adding the lyophilized powders into 100µl aluminium TGA pans, masses shown in table 2.5. The pans were added to the machine and the temperature was set to increase from 0 °C to 600 °C at a rate of 10°C/min. The mass loss with increasing temperature over time was measured.

Table 2. 5: Masses used in TGA measurements

Sample	Mass (mg)
Cyclodextrin (CD)	6.0
SM	4.2
POPC	2.1
POPE	1.8
DOTAP	11.6
CD-SM PM	8.4
CD-POPC PM	7.3
CD-POPE PM	7.3
CD-DOTAP PM	5.3
CD-SM COMPLEX	2.1
CD-POPC COMPLEX	1.7
CD-POPE COMPLEX	2.0
CD-DOTAP COMPLEX	2.7

2.2.3.5. Differential scanning calorimetry (DSC)

The lyophilized powders were added to DSC 140µl aluminium pans with lids, masses shown in table 2.6. The lidded pans were added onto the DSC machine. The samples were heated from -50°C to an upper temperature that depends on the sample to be tested. The heating rate was at 5°C/minutes using 50 ml/minute of Nitrogen.

Before measuring the samples, the device was calibrated using indium as the pure metal for calibration. The calibration process involved, putting the device into calibration mode, then adding 5.314mg of indium in the aluminium pan. The sample was heated to ensure that all indium is melted, and all of the surface area is in contact with the pan (to ensure accurate results). Then, a second heating run was done which showed an endothermic peak of 157.91°C for indium (figure 2.3), this value was close to literature (156.99 °C)(95) and confirms that the device is working correctly. Measurements were repeated twice.

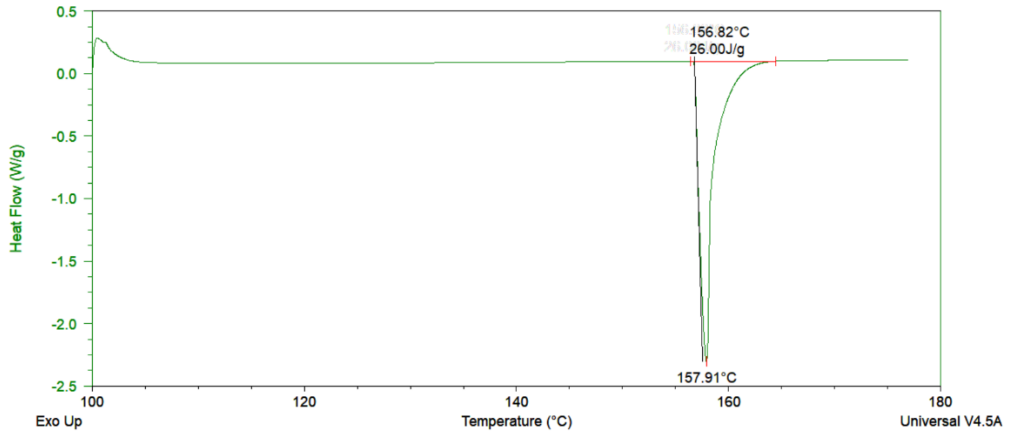

Figure 2. 3: The DSC reading for indium during calibration processes

Table 2. 6: masses used in DSC measurements

Sample	First pan sample (mg)	Second pan sample (mg)
Cyclodextrin (CD) "Fresh"	4.6	2.4
Cyclodextrin "Dried"	3.3	2.8
SM	3.0	3.5
POPC	4.5	3.6
POPE	2.2	2.5
DOTAP	6.4	5.4
CD-SM PM	6.2	6.7
CD-POPC PM	7.0	12.6
CD-POPE PM	7.4	7.4
CD-DOTAP PM	3.9	5.5
CD-SM COMPLEX	2.3	2.4
CD-POPC COMPLEX	2.2	2.2
CD-POPE COMPLEX	2.4	2.5
CD-DOTAP COMPLEX	2.0	2.9

2.2.3.6. Nuclear magnetic resonance (NMR)

The lyophilized powders were dissolved in D-methanol then put in special NMR tubes, then put into the machine for testing. The measurement was performed to identify hydrogen atoms (H1). The expected peaks for D-methanol are at 4.78 and 3.31.

2.2.3.7. Fluorescence quenching

This method involved using 7-nitro-2-1,3-benzoxadiazol-4-yl (NBD) as a fluorescent material. Sodium dithionite was used as the quenching agent for the NBD (Figure 2.4). To measure the fluorescence, a 96-well plate was used. 20µl of sample was added to 980µl of HEPES buffer. Sodium dithionite was dissolved in Trizma buffer (pH 9.23), 0.174mg was dissolved in 1ml of buffer. Then, 10µl of the sodium dithionite was added to the 1ml of each sample, after that 250µl was taken from this solution and added to the 96-well plate. The final ratio of NBD: Sodium dithionite was 0.5nmol:2µmol. The exact composition of the liposomal formulations is shown in table 2.7.

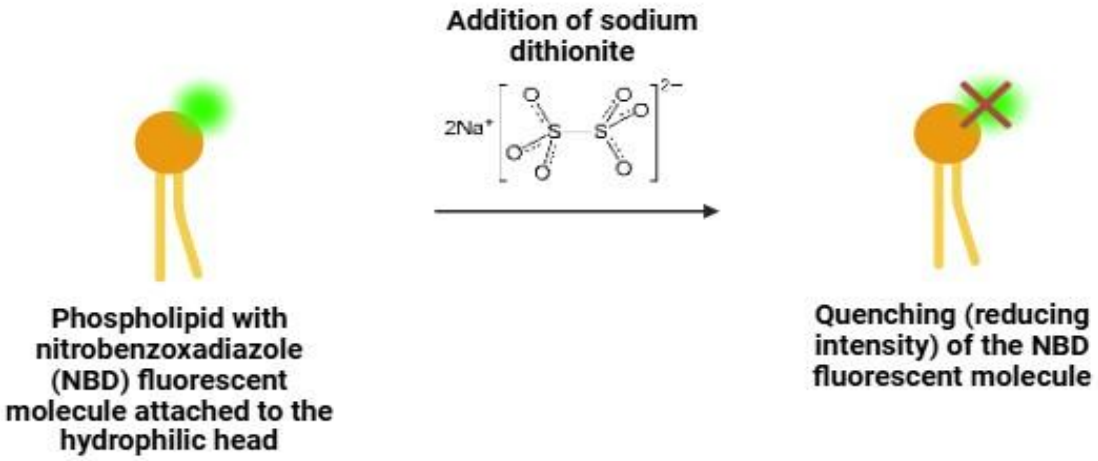

Figure 2. 4: The fluorescence quenching of NBD using sodium dithionite

Table 2. 7: The composition of the acceptor and donor used for fluorescence quenching experiment

Formulation	Composition (%)	Mass (mg)
Fluorescent Acceptor	DOTAP: 29.5%	DOTAP: 0.4
	POPE: 29.5%	POPE: 0.4
	NBD-PE: 1%	NBD-PE: 0.04
	Cholesterol: 40%	Cholesterol: 0.3
Donor	POPC: 100%	POPC: 3.0
Fluorescent donor	DOTAP: 99%	DOTAP: 2.7
	NBD-PE: 1%	NBD-PE: 0.08
Acceptor	DOTAP: 30%	DOTAP: 0.4
	POPE: 30%	POPE: 0.4
	Cholesterol: 40%	Cholesterol: 0.3

2.2.3.8. Solubility of water

This is a visual qualitative study used as a support experiment to confirm complex formation. Small amount of each lyophilized powder was taken from each sample; cyclodextrin only, phospholipids only (POPC, SM, POPE, DOTAP), cyclodextrin-lipid physical mixture, and cyclodextrin-lipid complex. 1mL of distilled water was added to each sample and waited for 5 minutes to allow the powders to dissolve at room temperature 23°C.

2.3. Chapter 4 methodology

2.3.1. The drug used

Bromocresol green (BCG): 100µl of 0.1mg/ml of BCG was added to the liposomes during the hydration stage or after the formation of liposomes.

2.3.2. Symmetric liposomes formulation technique using thin film hydration

2.3.2.1. Encapsulation of drug (BCG) during hydration process

The required phospholipids were weighed, then dissolved in chloroform (~500µl of chloroform per lipid) inside a round bottom flask. The solution was dried using a rotary evaporator at 400mbar for 10 minutes then at 200mbar for 30 minutes to 1 hour (until the film is fully dried). Once the film was formed, 900µl of HEPES buffer was added to 100µl of BCG and used to hydrate the film using a sonicator for 30 minutes. To separate the liposomes from free drug, three different separation techniques were used (refer to section 2.3.4) The masses of lipids measured are shown in table 2.8.

2.3.2.2. Encapsulation of drug (BCG) after liposomal formation

The required phospholipids were weighed (as shown in table 2.8), then dissolved in chloroform (~500µl of chloroform per lipid) inside a round bottom flask. The solution was dried using a rotary evaporator at 400mbar for 10 minutes then at 200mbar for 10 minutes and finally at 200mbar for 30 minutes. 900µl of HEPES buffer was used to form the liposomes by using a sonicator for 30 minutes. Then 100µl of BCG was added, after a wait of 15 minutes, to allow drug to enter liposomes. To separate the liposomes from free drug, three different separation techniques were used (refer to section 2.3.4). The masses of lipids measured are shown in table 2.8.

Table 2. 8: Mass of symmetric neutral lipids and cholesterol formulations per 1 mL of suspension

Lipids	Mass (mg)	Cholesterol mass (mg)
POPC	0.9	0.3
POPE	0.9	0.3
SM	0.9	0.3

2.3.3. Asymmetric liposomes formulation techniques

2.3.3.1. Drug (BCG) encapsulation during hydration process

For cyclodextrin-lipid complex, cyclodextrin was weighed and added to 1mL of HEPES buffer, the solution was heated to the required temperature. The required amount of donor lipid was dissolved in 500µl of methanol then added in a dropwise approach to the cyclodextrin solution (Table2.9). The solution is shaken at 100RPM using a water bath for 2 hours to allow methanol evaporation.

For the acceptor liposomes, the required phospholipids were weighed (Table 2.10), then dissolved in chloroform (~500µl of chloroform per lipid) inside a round bottom flask. The solution was dried using a rotary evaporator at 400mbar for 10 minutes then at 200mbar for 10 minutes and finally at 200mbar for 30 minutes. Once the film is formed, 900µl of HEPES buffer was added to 100µl of BCG and used to hydrate the film using a sonicator for 30 minutes.

The liposomes were added to the CD-lipid complex and shaken at 100RPM using a water bath for 1 hour, then to separate the free drug and the CD-Lipid complex, three different separation methods were tested (section 2.3.4). The masses of donor and acceptor lipids are shown in tables 2.9 and 2.10. The formulation in table 2.9 contained 30% main lipid, 30% DOTAP, and 40% cholesterol

2.3.3.2. Drug (BCG) encapsulation after liposomal formation

Cyclodextrin was weighed and added to 1mL of HEPES buffer, the solution was heated to the required temperature. The required amount of donor lipid was dissolved in 500µl of methanol then added in a dropwise approach to the cyclodextrin solution. The solution was shaken at 100RPM using a water bath for 2 hours to allow methanol evaporation.

The required phospholipids for the acceptor were weighed, then dissolved in chloroform (~500µl of chloroform per lipid) inside a round bottom flask. The solution was dried using a rotary evaporator at 400mbar for 10 minutes then at 200mbar for 10 minutes and finally at 200mbar for 30 minutes. Once the film is formed, 900µl of HEPES buffer was used to form the liposomes by using a sonicator for 30 minutes. Then 100µl of BCG was added, after a wait of 15 minutes, to allow drug to enter liposomes.

The liposomes were added to the CD-lipid complex and shaken at 100RPM using a water bath for 1 hour, then to separate the free drug and the CD-Lipid complex, three different separation methods were tested (refer to section 2.3.4). The masses of donor and acceptor lipids are

shown in table 2.9 and 2.10. The formulation in table 2.10 contained 30% main lipid, 30% DOTAP, and 40% cholesterol.

Table 2. 9: The mass of donor lipids and cyclodextrin per 1 ml of suspension

Lipids	Mass (mg)	Cyclodextrin mass (mg)
POPC	3.0	22.5
POPE	2.9	22.5
SM	3.0	22.5

Table 2. 10: The mass of the acceptor vesicle lipids per 1 ml of suspension (same as symmetric formulations)

Main lipid	mass (mg)	DOTAP mass (mg)	CHOL mass (mg)
POPC	0.5	0.4	0.3
POPE	0.4	0.4	0.3
SM	0.5	0.4	0.3

2.3.4. Separation of free drug techniques

2.3.4.1. Centrifugation

The suspension containing liposomes, free drug, and in some formulations, CD-lipid complex was centrifuged at 15,000 RPM for 1 hour at 4°C. the liposomes were pelleted due to its larger mass while the rest will remain floating in the supernatant (figure 2.5). The liposomal pellet was then resuspended and used for analysis. Refer to chapter 4, section 5.4 for more information.

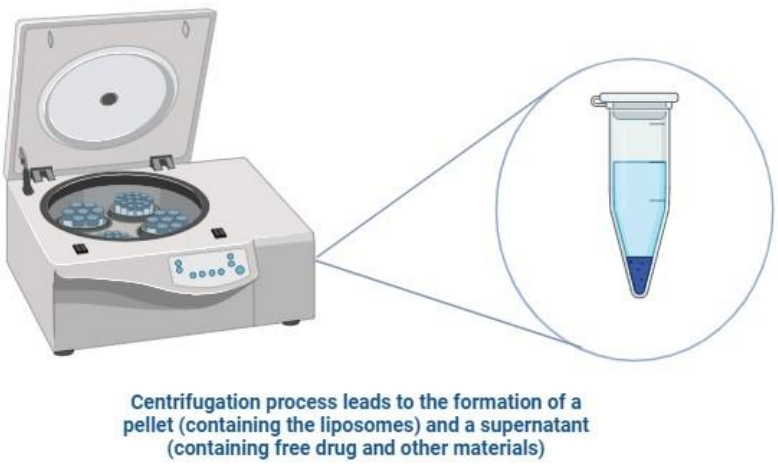

Figure 2. 5: The centrifugation process of liposomes

2.3.4.2. Centrifugal filtration

The process involves using a centrifugal filter (Figure 2.6). The suspension containing liposomes, free drug, and, in some formulations, CD-lipid complex was added to the filter, then centrifuged at 4500 RPM for 15 minutes at room temperature (23 °C). The process is repeated 4 times where each time a buffer is used to dilute the suspension. The retentate (the part that did not filter) contains the liposomes required. While the filtrate contains the filtered products to be discarded. The retentate was then diluted to required concentration and used for analysis. Refer to chapter 4, section 5.4 for more information.

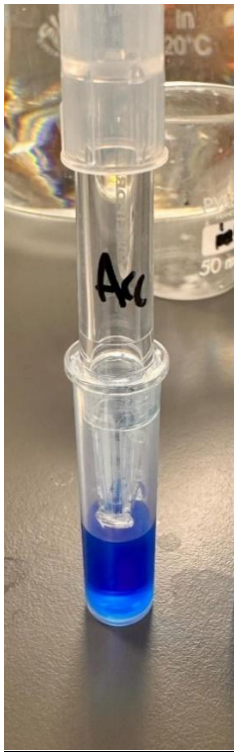

Figure 2. 6: Centrifugal filter

2.3.4.3. Gel chromatography

A Sephadex G-50 gel was added inside a narrow tube and used for gel chromatography (size exclusion chromatography) (Figure 2.7). The liposomal suspension was added, then HEPES buffer was used to push the suspension through the filter. This method can be used to separate the unentrapped smaller drug molecules from the liposomes. The liposomes would reach first, due to its larger mass, then get collected in a beaker. Following that, the rest of the suspension reaches and gets collected as free drug. This allows for the calculation of the entrapment efficiency of the drug inside the collected liposomes. Refer to chapter 4, section 5.4 for more information.

Figure 2. 7: Sephadex G-50 gel tube

2.3.5. Characterisation of the symmetric and asymmetric liposomes

2.3.5.1. Vesicle size

Same method as section 2.2.3.1

2.3.5.2. Zetapotential (ZP)

Same method as section 2.2.3.2

2.3.5.3. Optical microscope

A light microscope was used to confirm liposomal vesicle formation before the sonication step. The magnification used was 40X.

2.3.5.4. Entrapment efficiency (EE)

A UV/VIS spectrophotometer was used to measure the BCG absorbance in the solution after disruption. The process involved adding 0.5mL of the liposomal suspension to 1.5mL of isopropanol to break the liposomes and measure the absorbance at 615nm. The same process was repeated with the supernatant to measure the absorbance of the free drug. The equation below was used to measure the %EE of BCG in the liposomes. All measurements were blanked

for isopropanol and HEPES buffer. A calibration graph was used to convert absorbance values to concentration (Figure 2.8)

Equation 2: %EE = (CONC of pellet)/(CONC of total (pellet+supernatant)) x 100

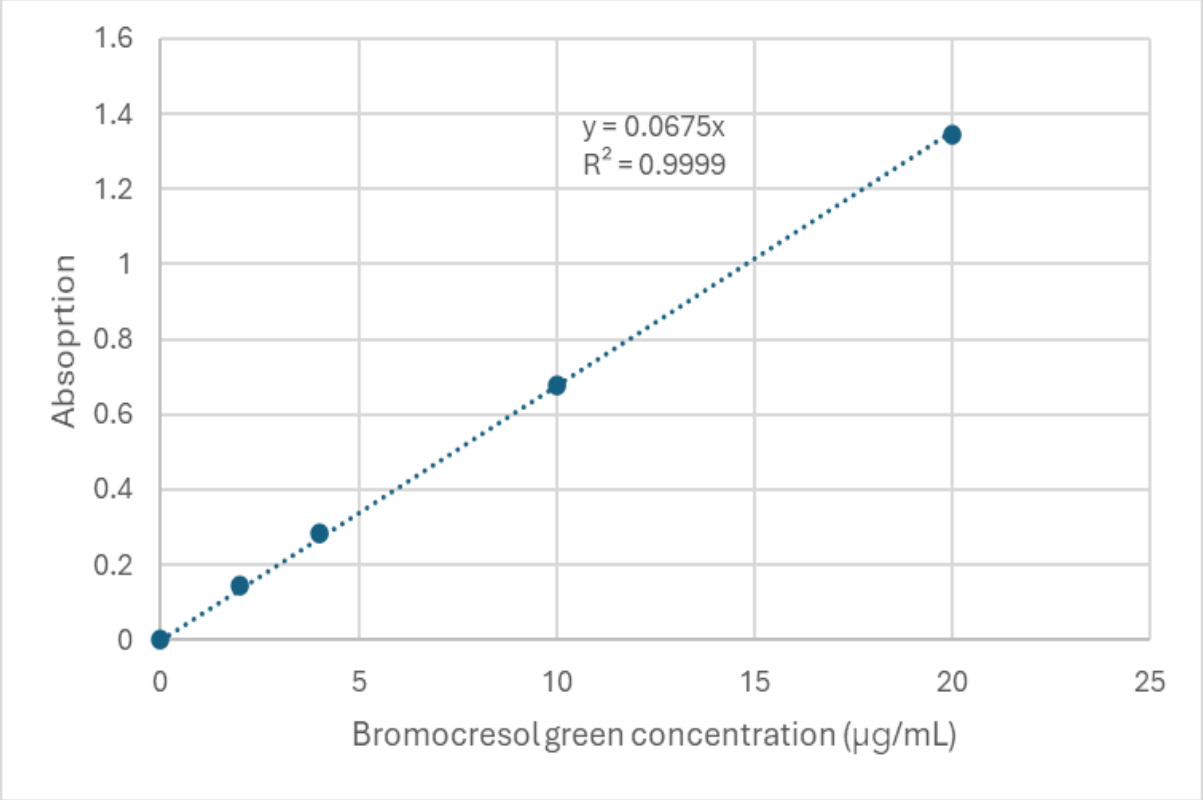

Figure 2. 8: The calibration graph of bromocresol green

2.3.5.5. pH gradient method to measure encapsulated drug inside liposomes

pH gradient was used to confirm presence of drug (bromocresol green) inside the liposomes. To test the theory, 20µl of 1M HCl was added to 0.1ml (1mg/ml) of BCG in 0.9ml HEPES buffer (10mM), this was able to turn the BCG colour to yellow. The same process was done to the liposomal suspension where 0.9ml of liposomal formulation in HEPES buffer was added to 0.1ml of BCG, then 20µl HCl was added.

If no drug is entrapped, then the suspension must turn yellow. However, if the BCG is entrapped inside the liposomes, then it will remain in its blue colour inside the liposomes, while the outside free drug will turn yellow. A combination of the blue and yellow colour should give a green colour indicating drug entrapment of the liposomes.

2.3.6. Optimisation of the chosen asymmetric liposomal formulation

The chosen asymmetric formulation contained POPC in the outer leaflet and POPC, DOTAP, and cholesterol in the inner leaflet. The donor lipid had a final concentration of 4mM while the acceptor lipids had a final concentration of 2mM. The ratio of the lipids within the acceptor vesicle contained 30% POPC, 30% DOTAP, and 40% cholesterol. Three different optimisation techniques were trialled to optimise this formulation further. the first trial involved increasing the cholesterol to 60% (masses shown in table 2.11), the second trial involved increasing the DOTAP to 45% (masses shown in table 2.12), and the third trial involved adding 10% of edge activator (span 80) to the formulation (masses shown in table 2.13). Edge activators are defined as bilayer softening component, they can be used to increase lipid bilayer flexibility and permeability (96).

Table 2. 11: Formulation optimisation by increasing cholesterol level to 60%

Donor lipid mass (mg)	Acceptor lipids mass (mg)		
3.0	POPC 0.3	DOTAP 0.2	Cholesterol 0.4

Table 2. 12: Formulation optimisation by increasing DOTAP level to 45%

Donor lipid mass (mg)	Acceptor lipids mass (mg)		
3.0	POPC 0.2	DOTAP 0.6	Cholesterol 0.3

Table 2. 13: Formulation optimisation by adding edge activator (span 80)

Donor lipid mass (mg)	Acceptor lipids mass (mg)			
3.0	POPC 0.5	DOTAP 0.4	Cholesterol 0.3	Span 80 0.04

2.4. Chapter 5 methodology

2.4.1. The drug used

Salmon sperm DNA: 10mg/ml of ultrapure salmon sperm DNA (base pairs <2000) was added to the liposomes after the formation of liposomes. Three different amounts of DNA were used, 3µl, 6µl, and 12µl.

2.4.2. Formulating asymmetric liposomes for DNA encapsulation

For the donor complex, cyclodextrin was weighed and added to 1mL of HEPES buffer, the solution was heated to the required temperature. The required amount of lipid was dissolved in 500µl of methanol then added in a dropwise approach to the cyclodextrin solution. The solution was shaken at 100RPM using a water bath for 2 hours to allow methanol evaporation. For composition refer to table 2.9.

The required phospholipids were weighed, then dissolved in chloroform (~500µl of chloroform per lipid) inside a round bottom flask. The solution was dried using a rotary evaporator at 400mbar for 10 minutes then at 200mbar for 10 minutes and finally at 200mbar for 30 minutes. Once the film is formed, the film was hydrated with 1mL HEPES buffer. Different DNA encapsulation methods were tested. For composition refer to table 2.12.

2.4.3. DNA encapsulation methods into asymmetric liposomes

2.4.3.1. DNA encapsulation of the acceptor liposomes

For the acceptor, the DNA was added to the liposomal suspension, waited 15 minutes to allow drug encapsulation, centrifuged at 15,000 RPM for 1 hour at 4°C. Then added the acceptor, resuspended pellet, liposomes to the donor CD-lipid complex and shaken at 100RPM using a water bath for 1 hour at room temperature (23°C). After that, the suspension containing liposomes, free DNA, and CD-lipid complex was centrifuged at 15,000 RPM for 1 hour at 4°C. The pellet was resuspended and used for analysis.

2.4.3.2. DNA encapsulation after exchange stage

The empty acceptor liposomes were added to the donor CD-lipid complex and shaken at 100RPM using a water bath for 1 hour at room temperature (23°C). After that, the DNA was added to the suspension, waited for 15 minutes, then the suspension containing liposomes, free DNA, and CD-lipid complex was centrifuged at 15,000 RPM for 1 hour at 4°C. The pellet was resuspended and used for analysis.

2.4.3.3. Encapsulating the asymmetric liposomes

The empty acceptor liposomes were added to the donor CD-lipid complex and shaken at 100RPM using a water bath for 1 hour at room temperature (23°C). Then, the suspension was centrifuged at 15,000 RPM for 1 hour at 4°C. the pellet was resuspended, and DNA was added, then waited for 15 minutes. After that, the suspension was centrifuged at 15,000 RPM for 1 hour at 4°C. The pellet was resuspended and used for analysis.

2.4.4. Characterisation of the symmetric and asymmetric liposomal formulations

2.4.4.1. Vesicle size and

Same method as section 2.2.3.1

2.4.4.2. Zetapotential (ZP)

Same method as section 2.2.3.2

2.4.4.3. DNA entrapment efficiency (EE) using nanodrop lite

The DNA EE was measured using the nanodrop lite. The settings were chosen for dsDNA at a ratio of 260/280. All measurements were blanked. 2µl of sample was added to the machine (nanodrop lite) and measured. All measurements were repeated 3 times. The process involved using 1.5X isopropanol to break the liposomes in the suspension (before centrifugation) then measuring the total amount of DNA in suspension. After that, the same process was repeated for the supernatant and the amount of DNA was measured. %EE was measured using the following equation:

Equation 3: %EE

Step 1: (Free DNA concentration (Supernatant))/(Total DNA concentration) X 100

Step 2: 100 – Step 1

2.4.4.4. Liposomes stability

The stability of liposomes was measured by incubating the liposomal suspension at 4°C. Measurements were performed at 24 hours, 72 hours, 1 week, 2 weeks, 3 weeks, 4 weeks. Formulations that aggregated were excluded at the time of aggregation occurring.

2.4.5. Statistical analysis

Statistical analysis was undertaken for the liposomal formulations to confirm significance in vesicle size and zetapotential values overtime. A two-tailed t-test was used to measure the p-value. P-value of <0.05 was considered significant.

Chapter 3

Novel cyclodextrin-lipid complexation method for manufacturing asymmetric liposomes as a potential carrier for genetic materials

1. Overview

Cyclodextrins (CD) are defined as cyclic oligosaccharides with two distinct regions containing a hydrophilic exterior and a hydrophobic interior (58). One of their many advantages is their use in formulating asymmetric liposomes. Cyclodextrin exchange is a novel method, developed by Prof. London and co-workers where they have created a novel method utilising cyclodextrin known as the "cyclodextrin-exchange method". Asymmetric liposomes are defined as liposomes with different lipids/charges in the inner and outer leaflets of the liposome. The cyclodextrin exchange method involves the preparation of, two different vesicles, a donor and acceptor vesicles. The donor vesicle is formulated as a multi-lamellar vesicle (MLV) then cyclodextrin is added. Next, the acceptor is formulated as a unilamellar vesicle with sucrose entrapped; sucrose is used to aid isolation during the centrifugation. A high concentration of sucrose, e.g., 25% w/w is prepared and encapsulated into the acceptor vesicle to increase the density of the vesicle and create a significant density difference between the donor MLVs and the acceptor unilamellar vesicles when the vesicles are suspended in phosphate-buffered saline (PBS). The two vesicles are then mixed with gentle stirring, to initiate the lipid exchange process with the aid of CD. The CD has only the ability to exchange the outer layer of the vesicles, therefore, the inner layer of the vesicles is unaffected by the exchange process. Following exchange, ultra-centrifugation is used to separate the two vesicles. The supernatant will contain all the impurities while the acceptor vesicles which have now formed the asymmetric liposomes will be pelleted at the bottom of the tube.

The extracted vesicles are then resuspended with buffer. The formulated asymmetric liposomes contain the phospholipid composition of the donor vesicle in the outer leaflet and the inner leaflet will contain that of the acceptor vesicle (3). Moreover, a concentration of 40 mol% of cholesterol was found to be the ideal concentration to get the highest yield of asymmetric

liposomes obtained after centrifugation (3) which is similar to the amount of cholesterol found in synaptic plasma membrane (21).

The exchange between the donor and the acceptor vesicles must be at a 1:1 ratio i.e., for every one lipid removed from the acceptor, one lipid is added to the acceptor, otherwise, a stress will be induced between the leaflets which can lead to vesicle rupture (3). Using the described process, the asymmetric vesicles were able to remain stable for 48 h (3).

Although this technique provides promising results, it relies on using a high concentration of sucrose to entrap within the acceptor vesicle which can be associated with osmolarity gradient that leads to membrane tension and potential structural perturbations due to lipid–sucrose interactions (3). To overcome this issue, Heberle *et al* (2016) (60) modified the cyclodextrin-exchange method by loading the sucrose into the donor MLVs instead, this allowed for the removal of sedimented sucrose-loaded MLVs after exchange using low speed centrifugation; then the removal of the remaining cyclodextrin molecules using a centrifugal concentrator. This also overcame the issue of having to ultra-centrifugation as conventional centrifugation can be used to achieve a good separation (60).

Further modifications were carried out by Markones *et al* (2018) (61) to improve the degree of donor lipid incorporation into the final asymmetric vesicle. Instead of using donor MLVs, a donor lipid–cyclodextrin complex was used during the exchange process which has shown a better exchange compared to the usual method. ζ-potential measurement was undergone to determine the extent and stability of the asymmetry which resulted in an asymmetry stable for 14 days at 20 °C (5). Different lipids were used to the lipids used in this research; this could indicate that some lipids are less likely to flip-flop than other lipids. Markones *et al* (2020) (62) was able to formulate a lipid-cyclodextrin complex by initially formulating MLVs, then cyclodextrin was incubated with the MLV to allow complexation (62). Finally, using a thermomixer to breakdown the MLVs and release the lipid-cyclodextrin complex. Although this method has shown promising results, it still required the formation and breaking of MLV which can be time consuming as well as having the risk of solution contamination by the non-broken MLVs. To overcome some of these challenges, a novel method was created in this research to formulate asymmetric liposomes using a phospholipid-cyclodextrin complex. The complex formation method that is widely used to complex a hydrophobic drug e.g. curcumin with cyclodextrin to allow the loading of the hydrophobic drugs (97). This occurs by dissolving the drug in an organic medium while dissolving the cyclodextrin in an aqueous medium, the drug containing organic solution is then added in a

dropwise approach to the cyclodextrin solution with continuous stirring at high temperatures. This allows the evaporation of the organic media which in turn leads to the incorporation of the hydrophobic drug inside the cyclodextrin cavity (97).

2. Aim

This chapter focuses on optimising the cyclodextrin-exchange method by providing novel changes. Solvent evaporation method was used to formulate a lipid-cyclodextrin complex that can be the mixed with the acceptor vesicle to formulate asymmetric liposomes. Centrifugal filtration can then be used to filter the lipid-cyclodextrin complex and retain the formulated asymmetric liposomes. This novel method can overcome challenges associated with the literature methods. It allows for the formation of liposomes using most lipids, and it is especially useful when using lipids that cannot form a liposome on their own e.g. DOTAP. Moreover, this method eliminates the risk of MLV contamination as no MLV formation is required. Since the only vesicle formation required is for the acceptor vesicle, this allows for the formation of any size or type of vesicles e.g. Multilamellar vesicles, giant unilamellar vesicles, and small unilamellar vesicles.

3. Novel modified cyclodextrin-lipid complexation method for the preparation of asymmetric liposomes

A modified solvent evaporation method was used to formulate asymmetric liposomes. This method consists of three steps; formulating the donor CD-lipid complex, formulating acceptor vesicles, then lipid exchange between donor and acceptor.

4. Results and discussion

To prove that the cyclodextrin-lipid complex was formed, several analysis techniques were used. To analyse the complex formation freeze-drying technique was used to dry the solution overnight and form a powder.

4.1. Fourier transform infrared spectroscopy (FTIR)

Fourier transform infrared spectroscopy was used to study and characterise the Lipid-cyclodextrin interactions and to identify any changes in the spectrum that could indicate complexation as different chemical structures produce different spectra and fingerprints (98). The different IR spectra is generated when the IR radiation is either passed through or absorbed by the sample, therefore the spectrum will represent the molecular structure of the sample (98).

The measurements were taken at the spectral range of 600-4000cm^{-1} at a resolution of 4cm^{-1}. The region between 600cm^{-1} to 1450cm^{-1} is known as the fingerprint region due to the unique patterns and complexity of infrared spectra found in this region (99). Figure (3.1) shows the IR spectra for all four lipids. Sphingomyelin has several characteristic absorption bands due to the hydrophobic regions, amide I band , and phosphate vibrations (100). The hydrophobic regions lead to C—H bond stretching at 2800-3000 cm^{-1} (100). These bands are present in the measured IR in figure (3.1) as sharp bands at 2916.37cm^{-1} and 2850.79 cm^{-1}. Moreover, CH2 scissoring vibrations are present at 1455-1485cm^{-1} (100). This is shown in fig (3.1) at 1465.90cm^{-1}. The amide I band is located generally between 1600-1689 cm^{-1} (100). This is seen as a peak at 1643.35 cm^{-1} (figure 3.1). Additionally phosphate vibrations are usually located between 1000-1110cm^{-1} (100) which is shown at 1058.99 cm^{-1} and1087.85 cm^{-1} in figure (3.1). POPC IR has peaks related to the hydrophobic regions due to C—H bond stretching at 3010.2cm^{-1} (range of 2800-3050 cm^{-1}) and C=C stretching at 1651.4cm^{-1} (101). These peaks are shown in the measured IR of POPC in figure (3.1) at 2920.23cm^{-1} and 1735.93cm^{-1}. The CH2 stretching was located at 2850.3 cm^{-1} for the symmetric stretching (101). These peaks are shown in figure (3.1) at 2850.79cm^{-1}. Phosphate group vibrations are generally located in the lower wavelengths around 1240.5 cm^{-1} for the antisymmetric stretching and 1091.3 cm^{-1} for the symmetric stretching (101). These peaks are visible at 1238.30 cm^{-1} and 1087.85 cm^{-1} in the measured IR (figure 3.1). Additionally, the C-N-C symmetric stretching is usually located at 919.4 cm^{-1} which can be seen in figure (3.1) at 925.83 cm^{-1}. As for POPE, the peaks related to the

asymmetric and symmetric CH2 stretching were located at 2924 cm^{-1} and 2854 cm^{-1} (102). This is visible in fig (3.1) at 2920.23 cm^{-1} and 2850.79 cm^{-1}. In regards to the phosphate groups with peaks related to the PO2 symmetric stretching (1073 cm^{-1}) and asymmetric stretching (1226 cm^{-1}) (102). These peaks are shown in the measured IR spectrum (figure 3.1) at 1080.14 cm^{-1} and 1222.87 cm^{-1}. Furthermore, the N-H bond stretching at 1541 cm^{-1} (102). Which was visible in figure (3.1) at 1558.48 cm^{-1}. DOTAP has two main peaks at 2924 cm^{-1} and 2854 cm^{-1} due to asymmetric and symmetric C-H bond stretching (103). This is shown in figure (3.1) at 2924.09 cm^{-1} and 2854.65 cm^{-1}. Additionally, the presence of ester gives rise to the carbonyl stretching at 1739 cm^{-1}(103). This is visible in figure (3.1) at 1739.79 cm^{-1}. The C-N bond stretching leads to a peak at 1489 cm^{-1} (103). This peak is shown in fig (3.1) at 1458.18 cm^{-1}.

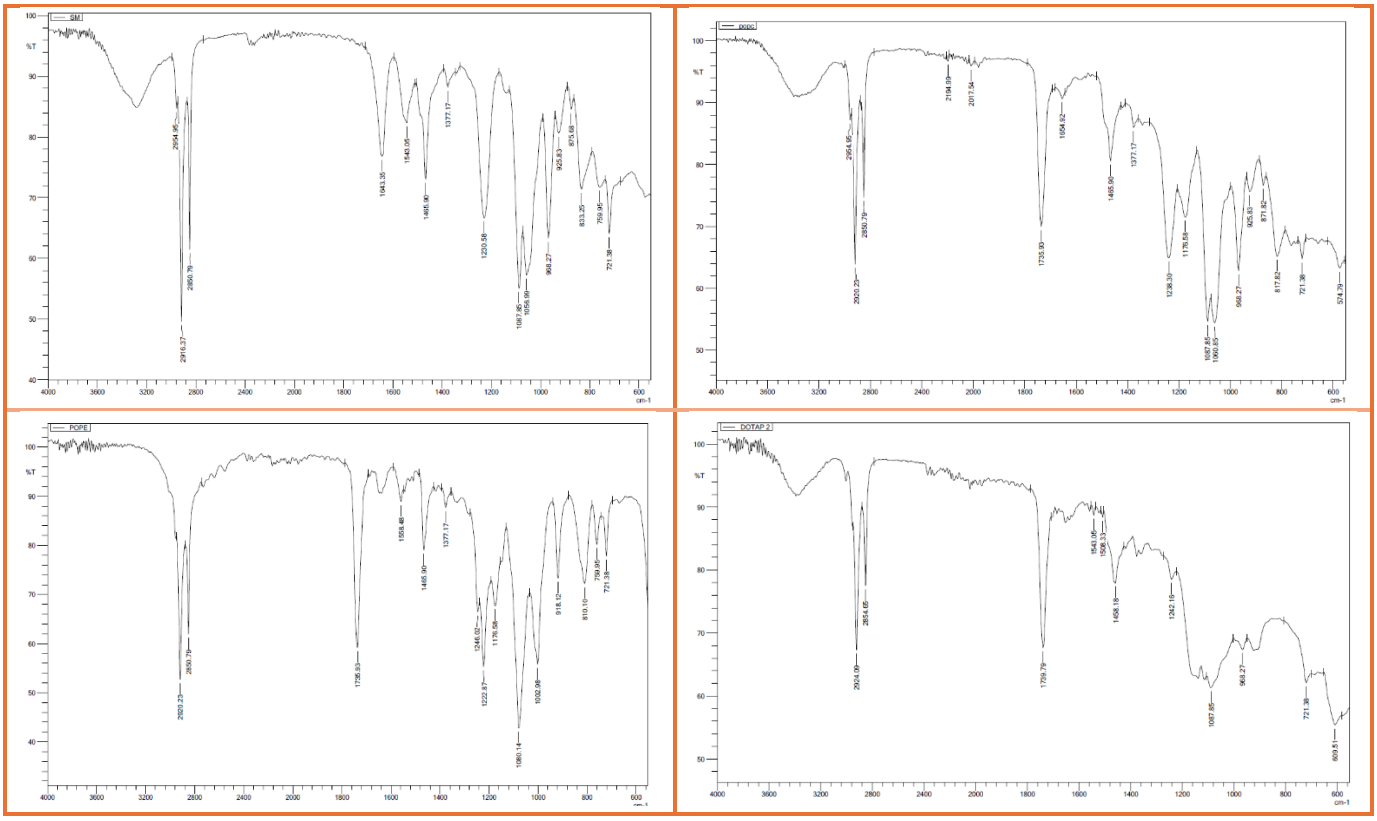

Figure 3. 1: The IR spectra of SM, POPC, POPE, & DOTAP

To eliminate the effect of the complexation method on the cyclodextrin, the same method was applied to cyclodextrin alone, figure (3.2) shows the IR spectrum of fresh cyclodextrin, while figure (3.3) shows the IR spectrum of the lyophilized (freeze dried) cyclodextrin. As shown in figure (3.2) and figure (3.3), there is no noticeable difference between the two IR spectra which indicates no effect of the processing on the cyclodextrin. The IR spectrum of cyclodextrin is characterised by the broad peak at 3426 cm^{-1} due to O-H stretching, 2932 cm^{-1} due to C-H bond stretching, 1638 cm^{-1} due to O-H bond bending, and the peaks from 1046-1158 cm^{-1} indicate C-

O stretching (104).The measured IR of cyclodextrin as shown in figure (3.3) indicates the presence of all the peaks mentioned in the literature. An O-H stretching bond was seen at 3406.29 cm^{-1} and an O-H bond bending at 1639.49 cm^{-1}, while showing a peak at 2927.94 cm^{-1} indicating C-H stretching and from 1083.99-1149.57 cm^{-1} indicating C-O bond stretching.

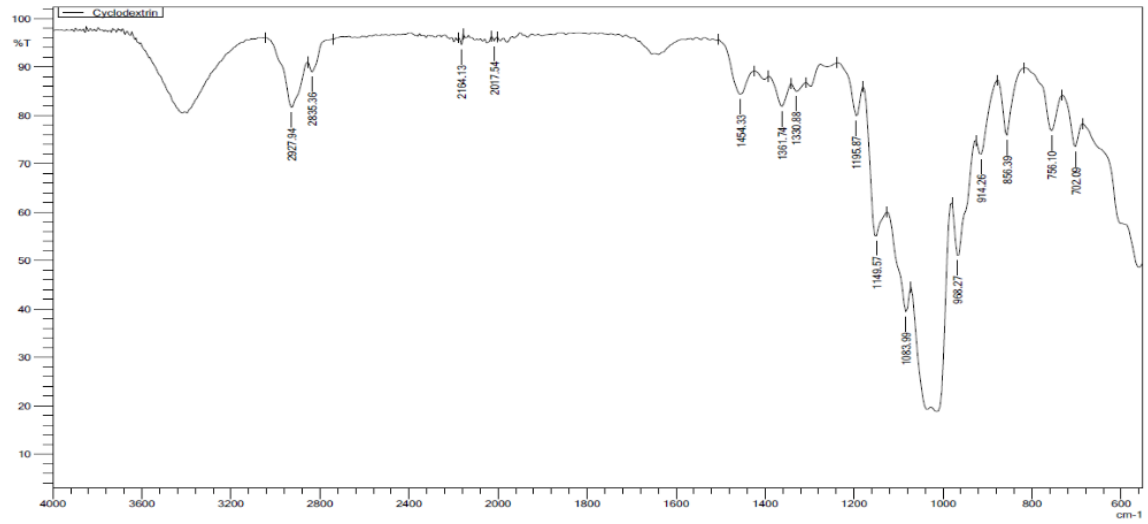

Figure 3. 2: Fresh Cyclodextrin

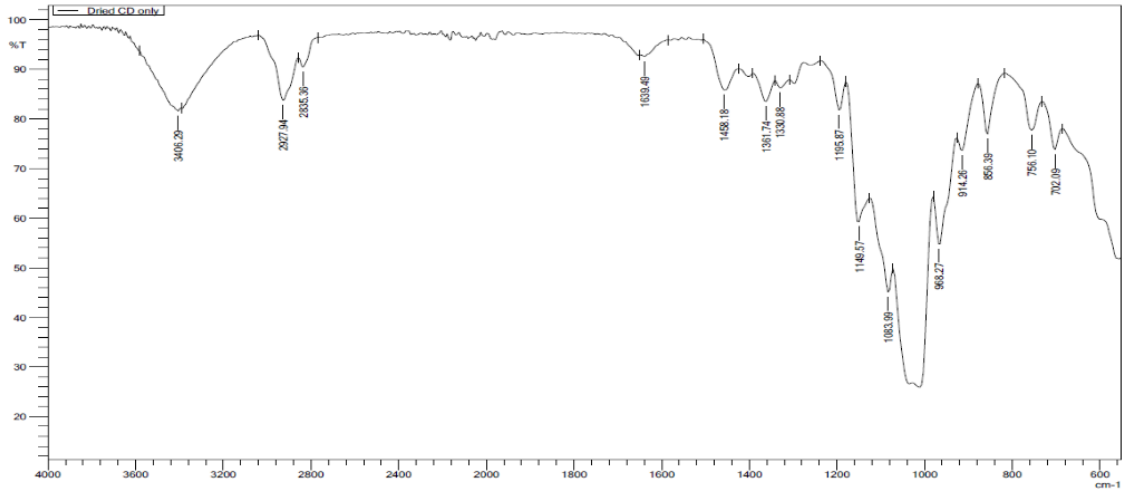

Figure 3. 3: Lyophilized Cyclodextrin

To identify complexation, the lipids (POPC, POPE, SM, & DOTAP) were mixed with the cyclodextrin to form a physical mixture (PM) and measured, then the freeze-dried lipid-cyclodextrin complex is measured to compare the spectra. As shown in figure (3.4), DOTAP and cyclodextrin physical mixture's spectrum has a peak at 2850 cm^{-1}, which indicates symmetric stretching of C-H bond, that is not present in the complex's spectrum (figure 3.5). Moreover, a small peak appeared at 1404 cm^{-1} in the complex's spectrum which was absent from the PM's

spectrum. The presence of this peak is related aliphatic (α)-CH2 bending (scissoring) vibrations (99). This difference can be negligible due to the weak intensity of the peak.

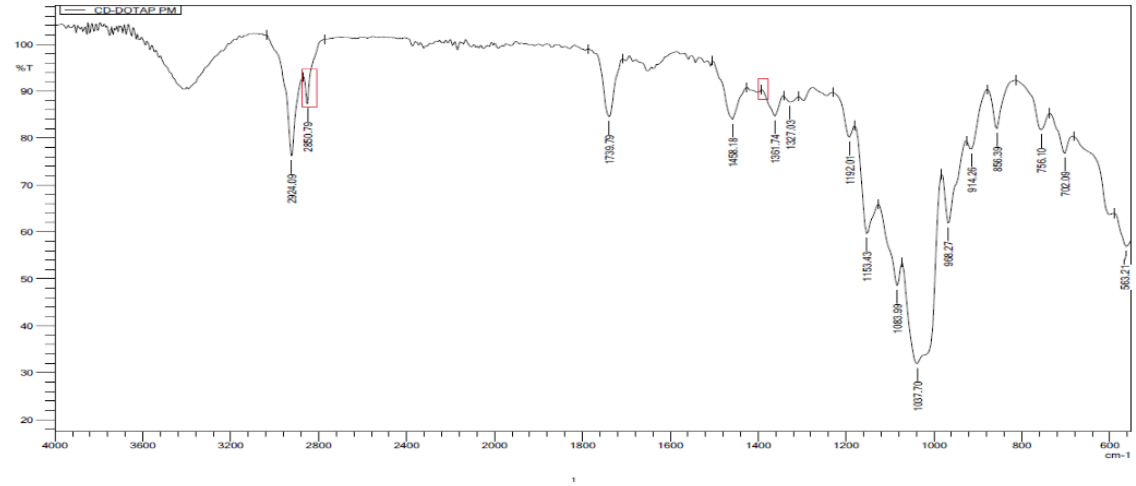

Figure 3. 4: IR spectrum of CD-DOTAP physical mixture

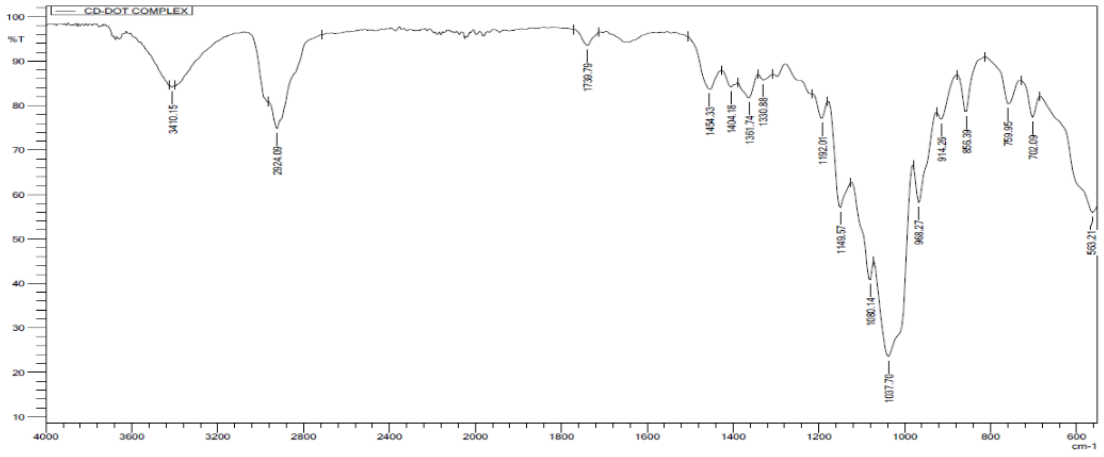

Figure 3. 5: The IR spectrum of the CD-DOTAP complex

The IR spectrum of the physical mixture of POPC and cyclodextrin has differences when compared to the CD-POPC complex's. As shown in figure (3.6) and (3.7) two main peaks at 2850 cm^{-1} and 1450.90 cm^{-1} were present in the IR spectrum of the PM while absent from the complex's. the peak at 1450 cm^{-1} is related to α-CH2 bending (scissoring) vibrations while the peak at 2850 cm^{-1} indicates symmetric stretching of C-H bond which were absent in the complex's spectrum.

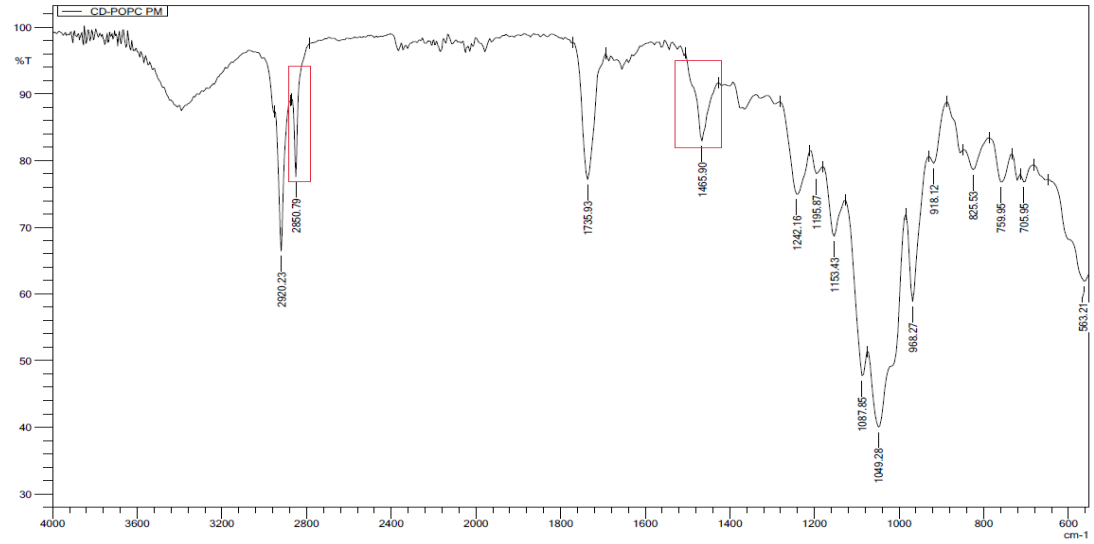

Figure 3. 6: IR spectrum of CD-POPC physical mixture

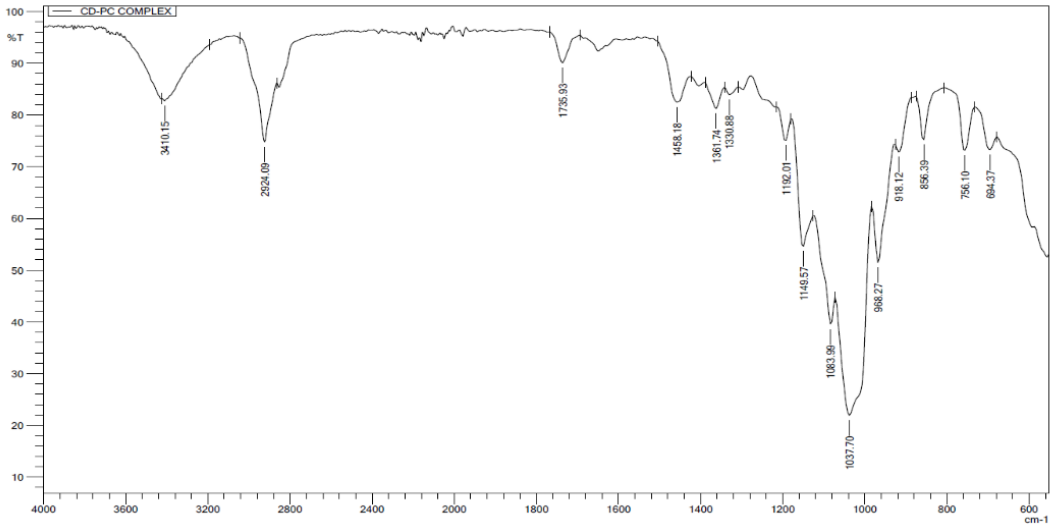

Figure 3. 7: IR spectrum of CD-POPC complex

The IR spectra of CD and SM was measured when mixed as a physical mixture (figure 3.8) and as a complex (figure 3.9). The main observation was the absence of the 2850 cm^{-1} and the 1226.73 cm^{-1} peaks from the CD-SM complex's IR spectrum while present in the PM's spectrum. As mentioned previously the peak at 2850 cm^{-1} is related to symmetric stretching of the C-H bond. The peak at 1226.73 cm^{-1} indicates PO2 asymmetric stretching.

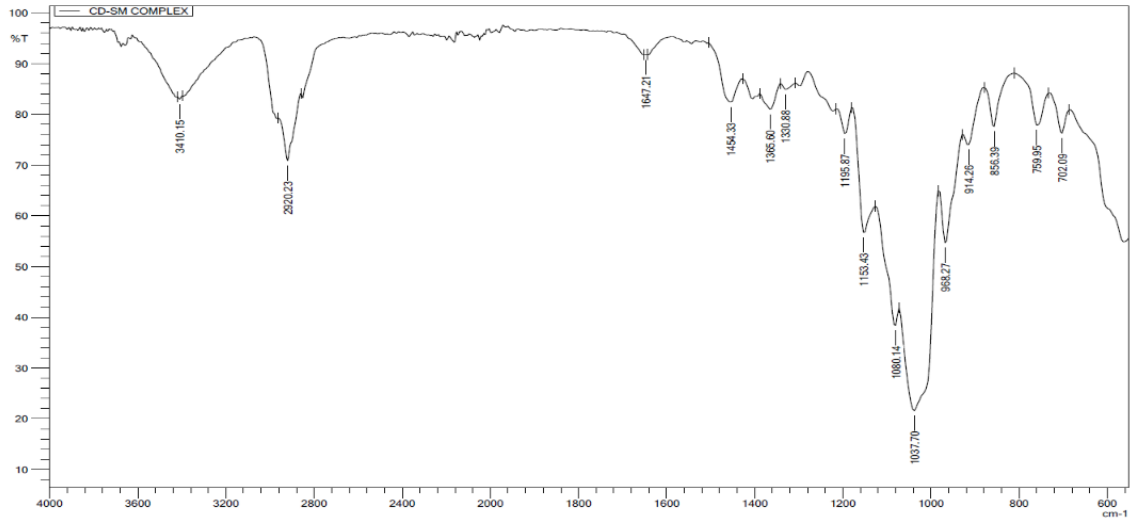

Figure 3. 8: IR spectrum of CD-SM Complex

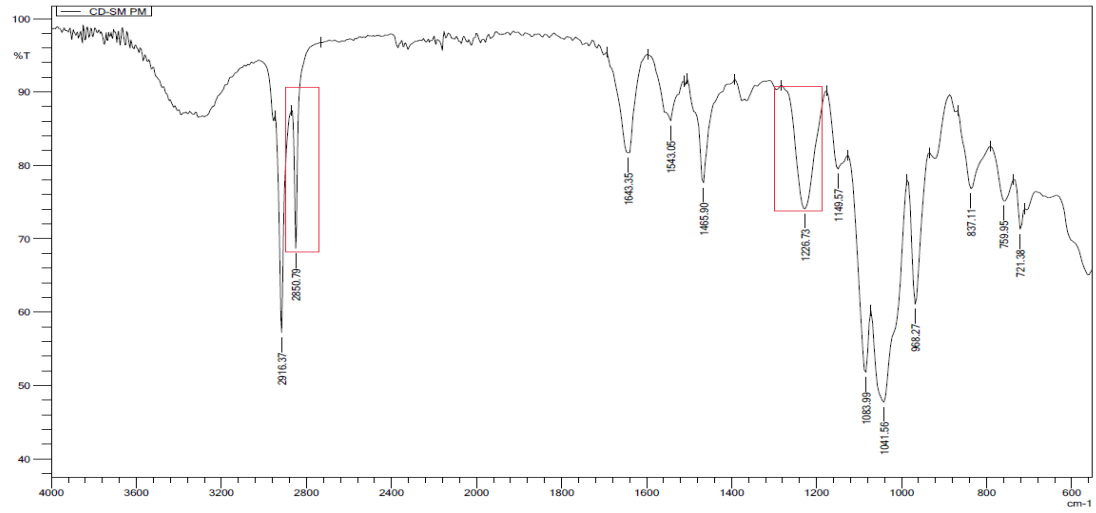

Figure 3. 9: IR spectrum of CD-SM physical mixture

The IR spectra for POPE as a PM (figure 3.10) and as a complex (figure 3.11) was measured. A similar behaviour was identified in terms of the 2850 cm^{-1} peak absence from the complex's spectrum while present in the PM's which is related to the symmetric stretching of the C-H bond. Additionally, the 1735.93 cm^{-1} peak was absent in the complex's IR spectrum compared to the PM's which indicates carbonyl (C=O) group stretching (103). The broad peak at 3410.15 cm^{-1} was absent in the PM's IR spectrum while present in the complex's. This peak is associated with O-H bond stretching (104).

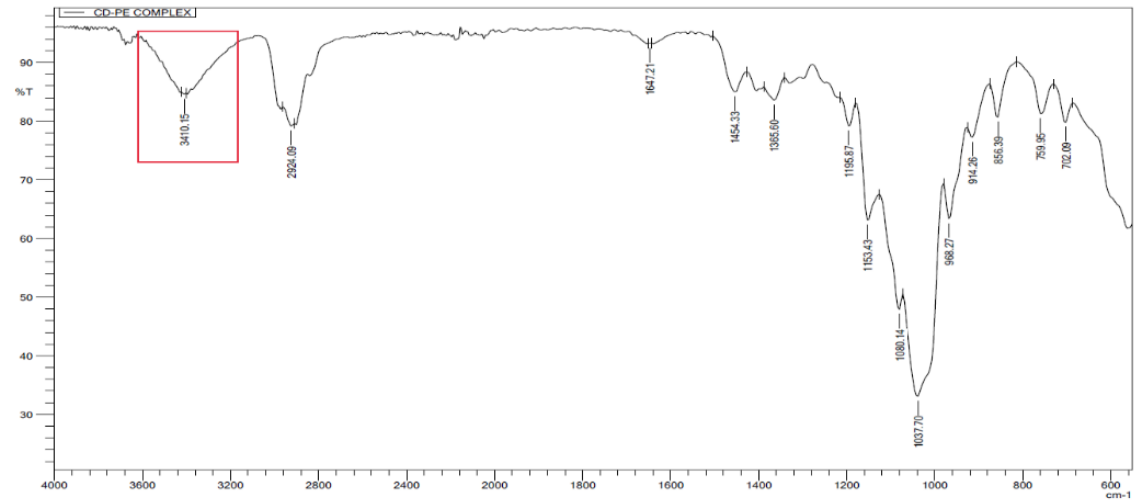

Figure 3. 10: IR spectrum of CD-PE Complex

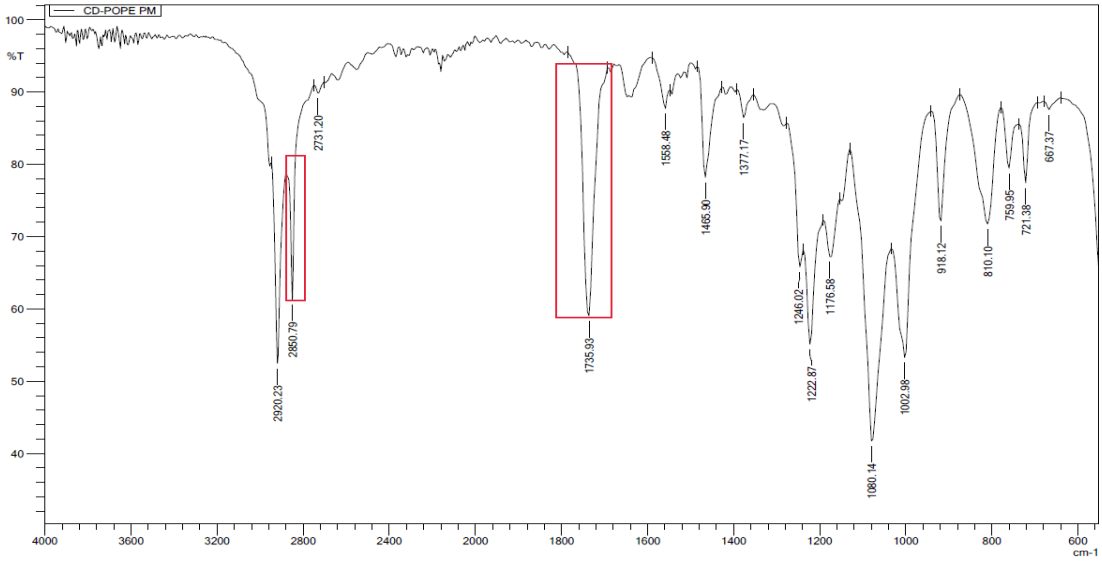

Figure 3. 11: IR spectrum of CD-PE physical mixture

Forming intermolecular hydrogen bonding can lead to significant changes in stretching vibrations (105) as well as changes in relative intensities of peaks which could be explained by the masking of functional groups when included within the CD cavity (105). Therefore, the peak at 2850 cm^{-1} was visible in the spectra of all lipids as well as the PMs while being absent from the complex's spectra. This peak is associated with symmetric stretching of C-H bond of the lipids. This change could be due to formation of inclusion complexes between phospholipids and cyclodextrins which altered the symmetry of phospholipid molecules, affecting their vibrational modes. Moreover, cyclodextrins can encapsulate parts of phospholipid molecules, such as the hydrocarbon tails, within their hydrophobic cavities. This inclusion can alter the

vibrational environment of the phospholipid's hydrophobic regions, leading to the attenuation or disappearance of certain IR absorption bands, including symmetric stretching peaks. With SM, the PO2 stretching peak was absent, this could be due to cyclodextrin's ability to encapsulate the hydrophobic portions of SM (such as its lipid tail), altering the conformation of the molecule. This conformational change might reduce the vibrational activity of the PO_2^- group due to the masking of the CD. The carbonyl group (C=O) in POPE could have been masked by the CD complexation. Similar behaviour can be seen with POPC and DOTAP where the intensity of the peak has reduced dramatically. The complexation with POPC lead to aliphatic-CH2 scissoring vibrations absence which could be due to complexation with CD. The lack of the broad O-H stretching peak when POPE was added to cyclodextrin, although an unusual behaviour, the measurement was repeated several times with the same results.

These spectral modifications are consistent with prior reports where CD complexation alters lipid vibrational modes through encapsulation, hydrogen bonding, and functional group masking. Overall, FTIR data strongly indicate successful complexation, providing molecular-level evidence of interactions that impact both the hydrophobic and polar regions of the lipid molecules.

4.2. Thermogravimetric analysis (TGA)

Thermogravimetric analysis involves measuring the mass changes of the sample overtime and with varied temperatures (106). In this experiment, TGA was used to study the degradation behaviour of the materials to confirm complexation.

The thermal curve of cyclodextrin (figure 3.12) shows an initial descent in the curve indicating weight loss starting from 28.33°C to 72.33°C with an average loss of 4.13%, then a second curve reduction starts from 325.50°C to 406.17°C where the weight reduced by 87.44%. The temperature was increased to 600°C, which is the maximum temperature an aluminium pan can tolerate (100), where 89.76% of the cyclodextrin weight was lost indicating that there was still some residual cyclodextrin left. These finding are supported by literature where a general trend was found for cyclodextrins. They tend to lose <10% of their weight below 100°C due to loss of adsorbed water and water of crystallisation (107). The second stage involves a weight loss of 70-80% mostly between 250-400°C, this stage is also associated with the formation of residue (char). The last stage >400°C involves a relatively slow thermal degradation of the char (107).

The results show that methyl-α-cyclodextrin (MαCD) requires temperatures higher than 600°C to reduce the mass to zero. No literature was found where the temperature was increased above 600°C using MαCD. However, a study was done on β-cyclodextrin where the temperature was increased to ~900°C and there was still residual cyclodextrin (108).

The curve for DOTAP (figure 3.12) had an initial weight reduction from 171.83°C to 209.67°C (10.37% reduction) followed by a second descent from 310.83°C- 407.17°C which has led to average weight loss of 98.09%. The temperature was increased to 600°C which reduced the weight by 99.85%. No literature was found containing the TGA curve for DOTAP.

To study the effect of mixing cyclodextrin with DOTAP, the two materials were mixed as a physical mixture and tested. The PM underwent an initial weight reduction of 7.41% at 175.83-209.83°C. A more dramatic weight reduction happened at 274.50-412.17°C which led to a reduction of 93.73%. The final % weight reduction was 95.45 at 600°C (figure 3.12). The behaviour of the physical mixture was somewhat similar to the DOTAP in terms of the curve descent, however, there was residue left similar to the cyclodextrin curve.

The CD-DOTAP complex was freeze-dried and tested. As shown in figure (3.12), an initial decent is apparent at 25.33-62.83°C with an average weight loss of 5.65%. This was followed by a second curve reduction from 236.50°C to 367.67°C which led to an 81.2% weight loss. The temperature reached a maximum value of 600°C with a weight loss of 89.39%. The CD-DOTAP curve (blue) has a dramatically different slope reduction values compared to the PM. Moreover, the final residue in the PM was much lower than the complex's residue, in addition to that, the final weight loss % of the complex was similar to the cyclodextrin. This could indicate that less amount of the DOTAP was degraded due to its complexation with the cyclodextrin.

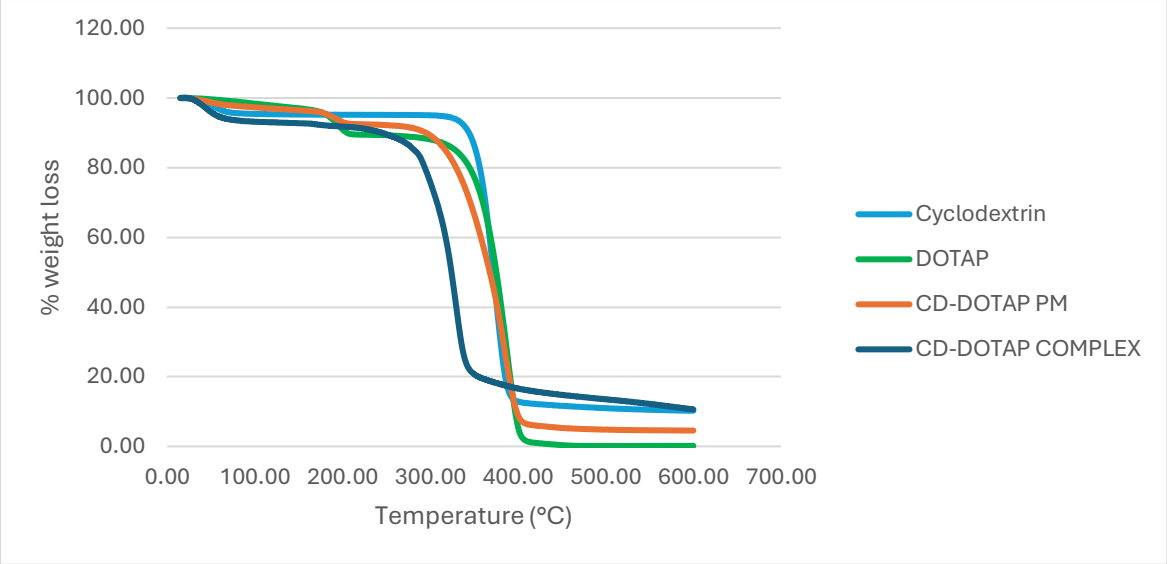

Figure 3. 12: The TGA of Cyclodextrin, DOTAP, CD-DOTAP physical mixture, and CD-DOTAP complex

The thermal curve for POPC had 4 curve reductions (Figure 3.13), the largest and most dramatic was from 283.83°C to 351.17°C with an average weight loss of 87.16%. The other three curves were, initially, at 30.50- 91.17°C (5.24% reduction), then at 226.17- 242.00°C (7.74% reduction), and the last descent was at 388.17- 438.17°C (91.47%). The temperature was increased to a maximum of 600°C (94.02% loss). A study was done to measure the mass loss of POPC and POPE, however, the study only used a maximum temperature of 250°C (109). It was shown that there was no significant reduction in mass below 100°C while mass loss became significantly higher between 100-175°C (109). Additionally, the mass loss for PE was significantly smaller than PC, this could be due to hydrogen bonding by the PE's headgroup which enhanced intermolecular interactions and led to increased stability of PE (109).

POPC was mixed with cyclodextrin to produce a physical mixture (PM) (Figure 3.13). The PM had an initial curve reduction at 38.67- 86.33°C (3.09% reduction). This was followed by a second, more noticeable descent from 253.00°C to 352.33°C (73.11% reduction). The final temperature reached 600°C with a weight loss of 80.06%. The physical mixture had a similar initial curve reduction to POPC. However, a larger amount of residue remained and a very different curve shape.

The CD-POPC complex (Figure 3.13) has a more initial reduction compared to the other three curves. The initial curve descent was from 28.50°C to 69.17°C (7.15% reduction). It was followed by a more dramatic reduction at 242.00- 372.33°C with a weight loss of 74.13%. The temperature reached a maximum of 600°C that led to a weight loss of 90.87%. As shown in figure (3.13), the curve shape of the complex is highly different compared to the other three

curves. The curve had a sharper and faster weight loss compared to the other curves. Moreover, the slope reduction was dramatically different from the PM's and the POPC's. This could indicate complexation

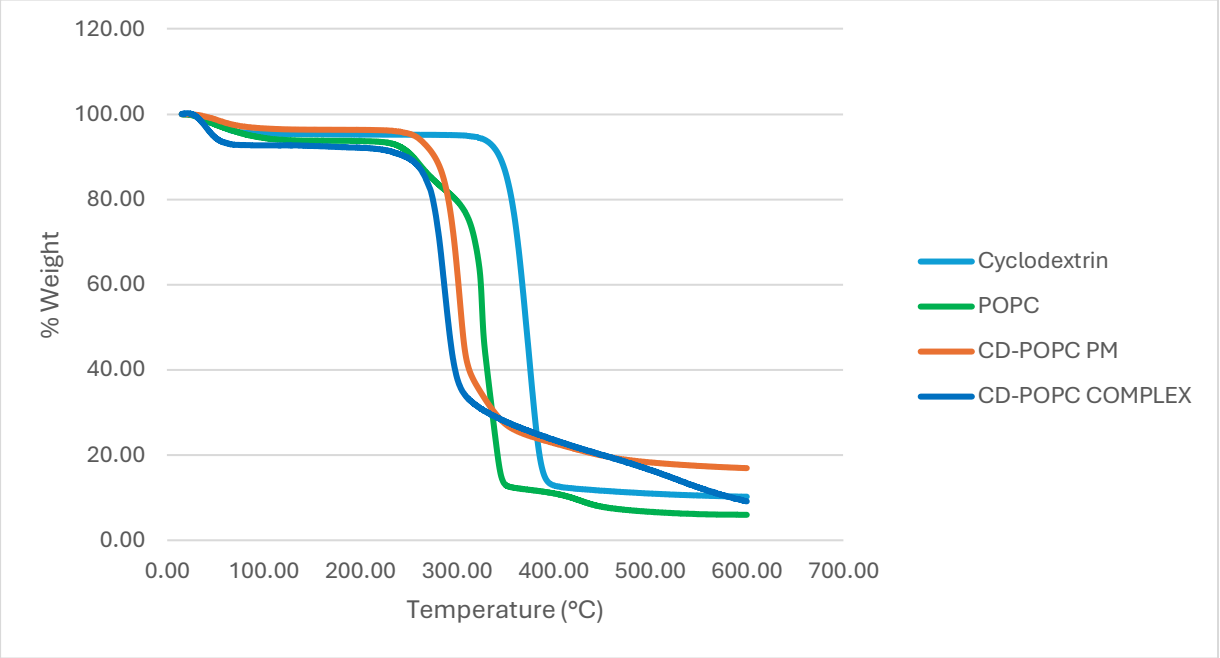

Figure 3. 13: The TGA of Cyclodextrin, POPC, CD-POPC physical mixture, and CD-POPC complex

As shown in figure (3.14), the thermal curve for SM has a markedly different shape compared to the other three curves. The curve has an initial descent at 37.00- 94.17°C (4.48% reduction). This is followed by two more large curves with a quicker and shaper decline at 230.00-325.50°C and at 355.83- 456.00°C with a total weight loss of 88.4%. The temperature was increased to 600°C where the total weight loss was 90.98%. in literature, the SM has lost around 5% of its weight at 115°C which is likely to moisture evaporation (110).

SM was mixed with cyclodextrin as a physical mixture and tested. The curve became noticeably different when compared to the SM curve. this could indicate some form of complexation in the PM. The curve had an initial reduction at 50.83- 79.17°C (2.88% reduction) followed by a larger reduction at 295.17- 347.17°C (71.55% reduction). The temperature was increased to a maximum of 600°C with a total weight loss of 83.98%.

The CD-SM complex showed a curve descent (figure 3.14) at 31.00- 67.50°C with a weight reduction of 6.09%. This was followed by a more dramatic curve reduction from 254.17°C to 322.83°C (69.87% reduction). The temperature continued increasing reaching a maximum of 600°C and yielding a total weight loss of 82.91%. Although the complex's curve has a similar

shape to the PM's curve, the curve has shifted massively which could mean that the complex has formed.

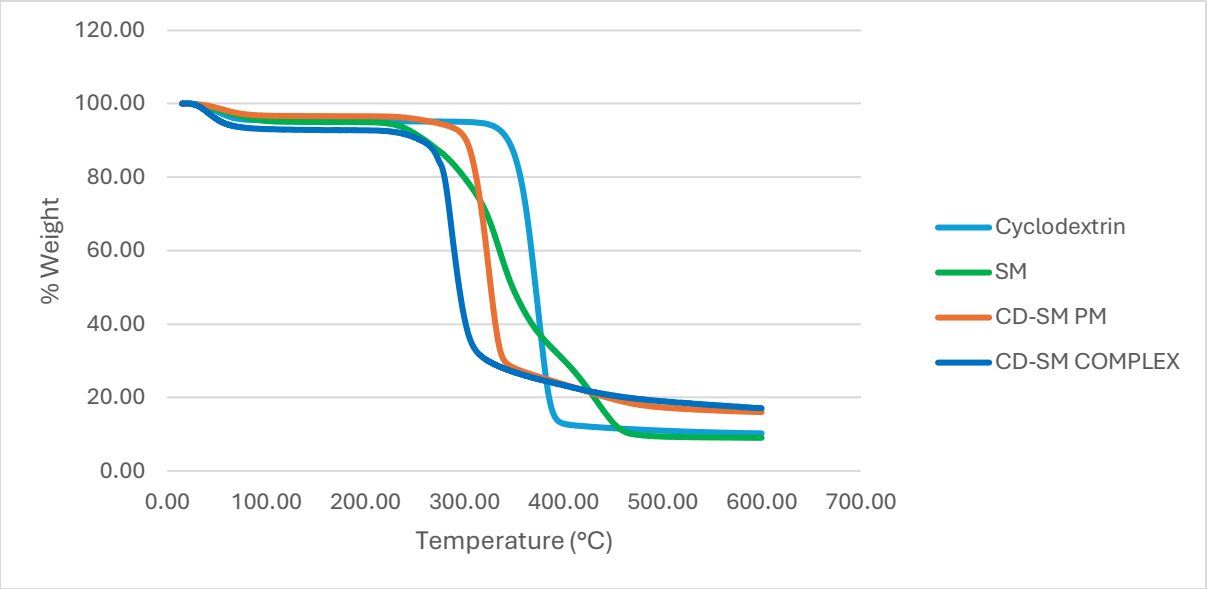

Figure 3. 14: The TGA of Cyclodextrin, SM, CD-SM physical mixture, and CD-SM complex

POPE's thermal curve was measured (figure 3.15). The thermal curve undergoes a dramatic reduction at 231.17-353.83°C with a weight reduction of 71.04%. This is followed by another curve descent starting from 353.83°C to 449.33°C with a weight reduction of 87.17%. The temperature continued to increase reaching a maximum of 600°C with a total weight loss of 89.81%. The presence of hydrogen bonding in the headgroup of PE leads to a more stable molecule due to intermolecular forces (109).

POPE was mixed with cyclodextrin as a physical mixture and tested. The thermal curve underwent a descent at 33.17-66.50°C (2.14% reduction). This was followed by a more dramatic reduction from 233.00°C to 301.33°C which plateaued briefly then continued reducing to 349.50°C with a weight loss of 86.20%. the temperature continued to increase to a maximum of 600°C leading to a total weight loss of 78.54%.

CD-POPE complex has shown two main thermal curves (figure 3.15). First a curve reduction was evident at 32.00- 57.00°C with a reduction of 5.41%. this was followed by a second, more curve descent starting from 278.00 to 361.17°C which has led to a weight loss of 79.98%. The temperature continued to increase to a maximum of 600°C and led to a total weight loss of 86.95%.

The PM curve and the complex's curve have shown a noticeably different shape to the POPE curve. The PM curve (figure 3.15) has shifted considerably when compared to the POPE and the CD's curves, this indicates some degree of complexation. In regard to the complex, the curve was also much different and has shifted from the POPE and CD curves as well as the second curve in the POPE has disappeared in the complex's curve. This potentially indicates complex formation.

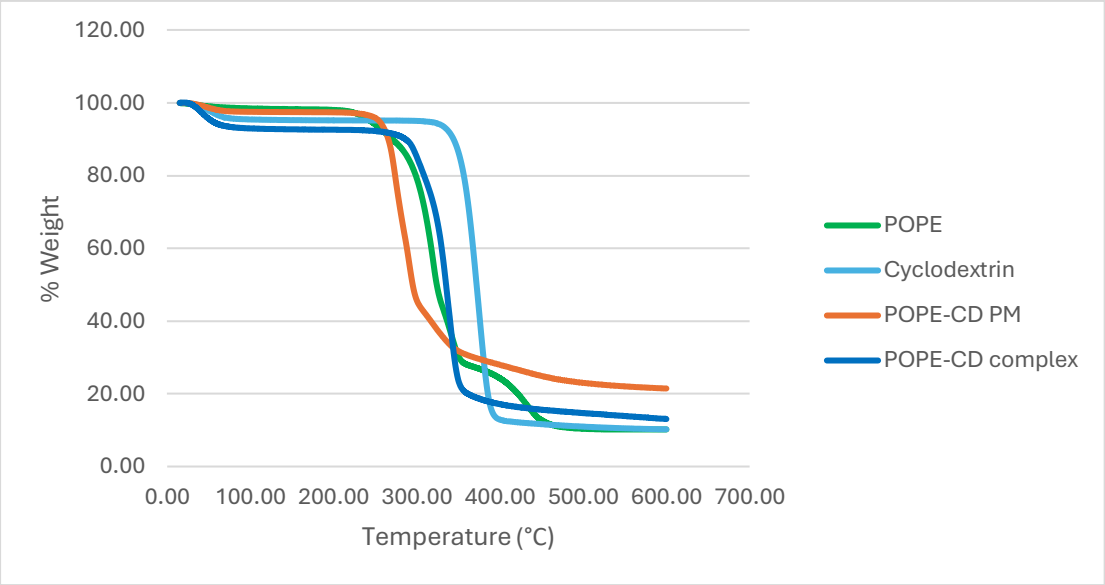

Figure 3. 15: The TGA of Cyclodextrin, POPE, CD-POPE physical mixture, and CD-POPE complex

TGA results confirm successful complexation between cyclodextrin and the lipids, as evidenced by shifted degradation temperatures, altered thermal profiles, and increased residue compared to physical mixtures and pure components, indicating enhanced thermal stability and structural interactions.

4.3. Differential scanning calorimetry (DSC)

Differential scanning calorimetry (DSC) is a thermo-analytical technique that measures the heat changes in a sample relative to a reference. The heat changes occur due to a phase transition when the sample is heated or cooled (111). The samples were heated from -50°C to an upper temperature that depends on the sample to be tested. The heating rate was at 5°C/minutes using 50ml/minute of Nitrogen. A study was performed on α-CD showed the endothermic peak at 99.8°C (112) while other sources showed endothermic peak at 57.20°C and 85.50°C (113). No existing literature was found regarding the exothermic peaks that indicate crystallization.

The initial step was to study the effect of the processing on the cyclodextrin's DSC curve. A comparison was made between fresh cyclodextrin and lyophilized cyclodextrin. As shown in figure (3.16), the broad endothermic peak at 89.51°C has shifted to 75.61°C. Moreover, the exothermic peak at 192.54°C has shifted slightly to 198.01°C. This could indicate a slight change in properties when the cyclodextrin is lyophilized. Table 3.1 shows the average value of each peak.

Table 3. 1: The peaks values in DSC readings for cyclodextrin

Sample	Peaks (°C)		Average (°C)	
Fresh cyclodextrin	84.71, 89.51	192.54, 191.91	87.11 ±3.40	192.23 ±0.45
Lyophilized cyclodextrin	75.60, 75.54, 75.61	198.01, 198.00	75.60 ±0.004	198.01 ±0.01

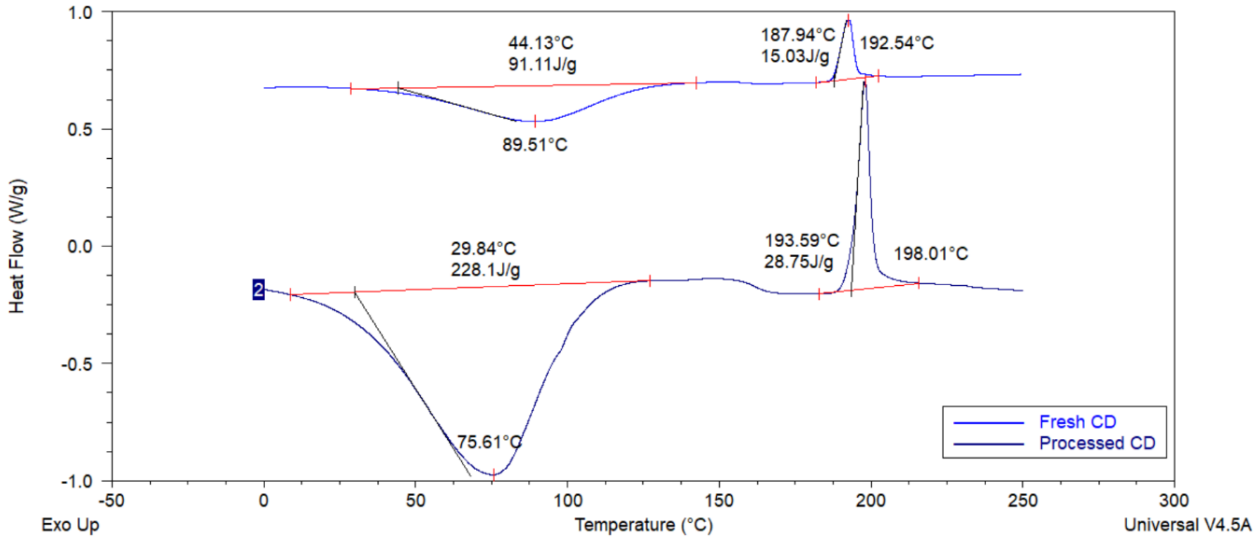

Figure 3. 16: The DSC of fresh cyclodextrin and lyophilized (processed) cyclodextrin

The DSC curve for POPC, POPC physical mixture and POPC complex were compared (Figure 3.17). The curve for POPC was measured from -50°C to 100°C, the endothermic peak at 31.79°C represents presence of POPC. Using a higher temperature did not show any events as well as it was not preferable as it could breakdown the lipids, therefore, 100°C was chosen as the optimal maximum temperature. In literature, the endothermic peak measurement varied

between 10-20°C (114). This variation could be due to different manufacturing, purity, water content and other factors affecting the lipid.

The PM's curve had the same POPC endo peak at 28.73°C which indicates POPC presence. Moreover, the PM's had a broad peak at 129.36°C which indicates presence of cyclodextrin, however the peak is markedly shifted when compared to CD on its own, this could indicate a degree of complexation between POPC and cyclodextrin. The endo peak was followed by an exothermic peak at 187.72°C which has also massively shifted when compared to the exothermic peak of CD on its own.

The CD-POPC complex curve (figure 3.17) has a noticeable difference where the POPC curve was absent, this could indicate that all of the POPC has been complexed. The complexation led to a noticeable shift in the cyclodextrin's endo peak (140.17°C) as well as the absence of the exothermic peak. The temperature was increased to a maximum of 200°C, this is due to the presence of cyclodextrin where the peaks become visible later than the POPC's peaks. Table 3.2 shows the average value for all the peaks.

Table 3. 2: The peaks values in DSC readings for POPC

Sample	Peaks (°C)			Average (°C)		
POPC	31.95, 31.79			31.87 ±0.11		
POPC-CD PM	27.59, 28.73	124.24,129.36	187.72, 185,79	28.16 ±0.81	126.3 ±4.33	186.76 ±1.36
POPC-CD complex	139.25, 140.17			139.71 ±0.65		

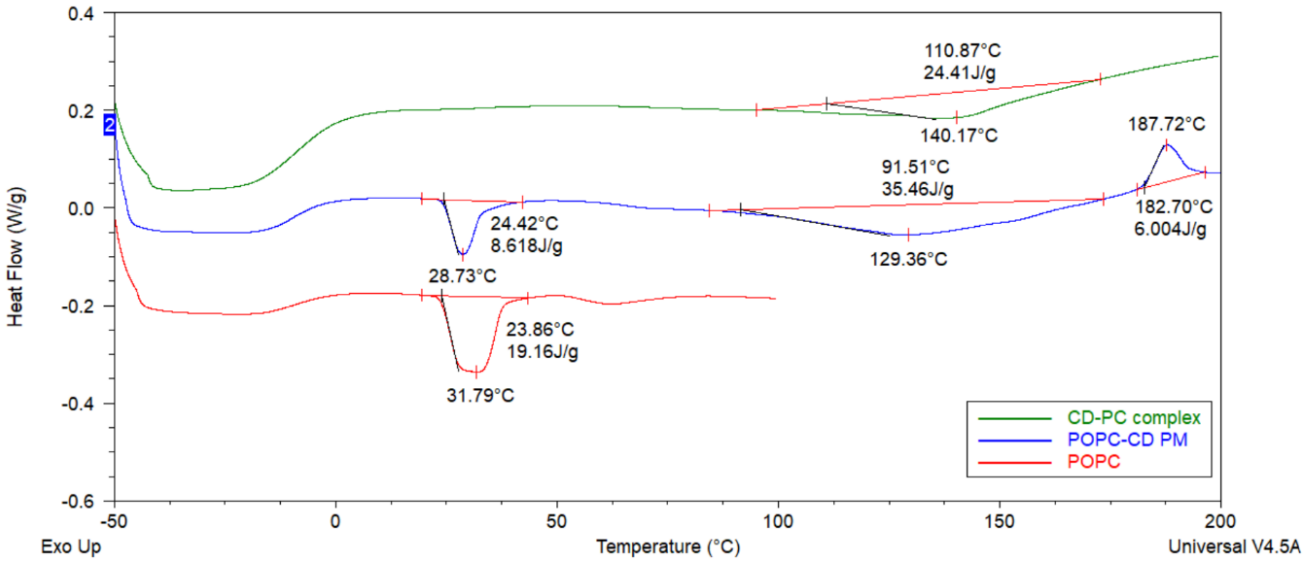

Figure 3. 17: The DSC of CD-PC complex, POPC-CD physical mixture, and POPC

POPE was tested to determine its DSC curve (Figure 3.18). The endothermic peak at 48.07°C indicates the presence of POPE in the sample. The temperature was increased to a maximum of 100°C as no more events were seen in addition to preventing the degradation of the lipid sample. The literature has shown a different value for the endothermic curve around 25.5°C (115). However, in literature the lipids used in the form of aqueous dispersions in PBS (115) which could affect the measurements. The PM's curve shows a distinct endo peak at 47.38°C which indicates the presence of POPE in the sample. However, the broad cyclodextrin endothermic peak was absent while the exothermic peak was shifted to 150.33°C. This indicates a degree of complexation between POPE and CD in the PM which has led to this shift. A similar behaviour was seen in the CD-POPE complex's curve where the broad endo peak was missing, and the exothermic peak was shifted to 152.38°C. the absence of the POPE peak in the complex's curve could indicate the effect of complexation on the sample. Moreover, the exothermic peak shift could also indicate complexation. The temperature was increased to a maximum of ~180°C as no more events have occurred after this temperature. Table 3.3 shows the average value for each peak.

Table 3. 3: The peaks values in DSC readings for POPE

Sample	**Peaks (°C)**		**Average (°C)**	
POPE	48.07, 47.06		47.57 ±0.71	
POPE-CD PM	47.38, 47.90	150.33, 150.45	47.64 ±0.37	150.39 ±0.85
POPE-CD complex	152.34, 152.38		152.36 ±0.03	

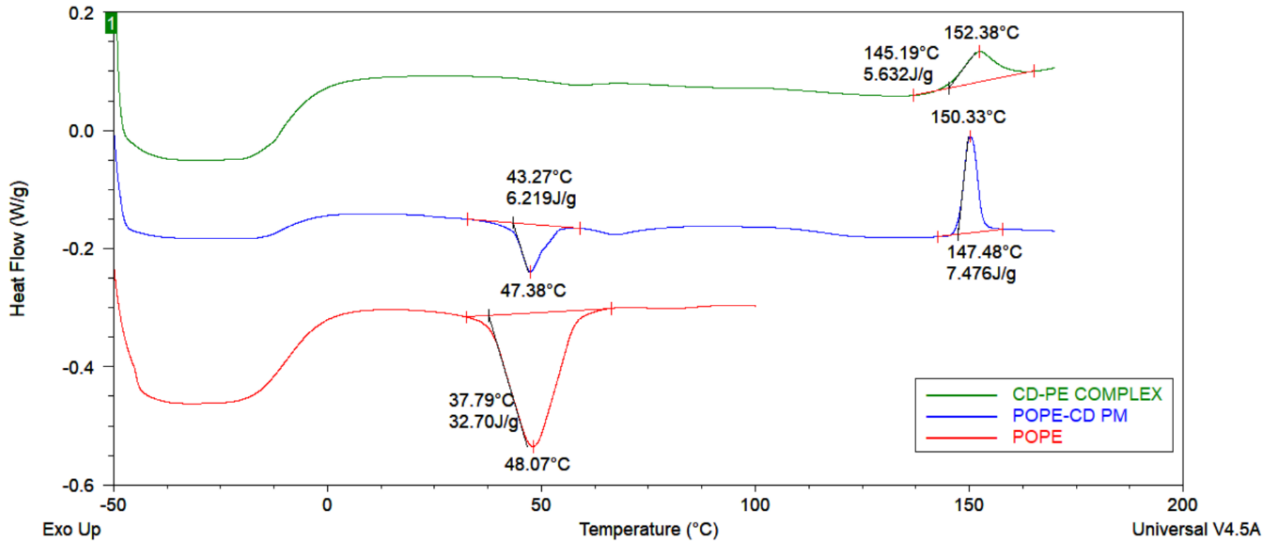

Figure 3. 18: The DSC of CD-PE complex, POPE-CD physical mixture, and POPE

DOTAP's curve has shown a distinctive endothermic peak at 6.57°C which indicates the presence of DOTAP in the sample (Figure 3.19). The temperature was increased to a maximum of 120°C as no more events were seen above this limit and this was the optimum temperature to prevent lipid degradation. Literature showed an endothermic curve value of 11.51-13.65°C (116), this difference in values could be due to literature heating the sample at a higher rate (10°C/min) which can shift the peaks.

When tested as a PM, the peak at 5.20°C indicates the presence of DOTAP in the sample. This was followed by a broad peak at 95.30°C which indicates the presence of cyclodextrin. The temperature increased to a maximum of 160°C as no more events were seen above this limit.

The CD-DOTAP complex had marked differences where the DOTAP peak was absent as well as the broad CD peak was shifted to 146.20°C indicating the possible complexation of DOTAP with the cyclodextrin. The temperature was increased to a maximum of 200°C. Table 3.4 shows the average value for each peak.

Table 3. 4: The peaks values in DSC readings for DOTAP

Sample	Peaks (°C)		Average (°C)	
DOTAP	6.87, 6.57		6.72 ±0.21	
DOTAP-CD PM	5.30, 5.20	95.30, 95.69	5.25 ±0.07	95.50 ±0.28
DOTAP-CD complex	146.20, 149.59		147.90 ±2.40	

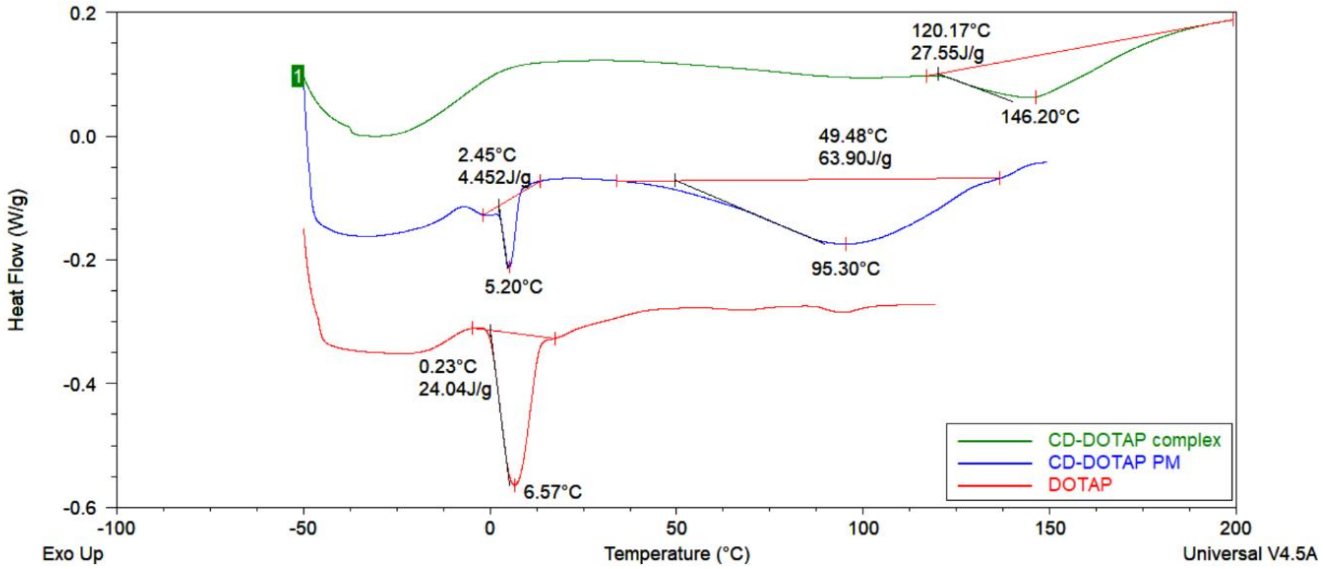

Figure 3. 19: The DSC of CD-DOTAP complex, DOTAP-CD physical mixture, and DOTAP

SM's DSC curve has shown an endothermic peak at 81.20°C which indicates the presence of SM in the sample (Figure 3.20). The temperature was increased to a maximum of 150°C as no more events were seen above this limit and this was the optimum temperature to prevent lipid degradation. Literature values show an average value of 39.5°C for the SM endothermic peak (117). However, this shift in value can be related to the use of egg SM (brain SM was used in this study) and the use of different heating rate at 0.5°C /min (117). When the physical mixture was tested, the SM peak was evident at 81.62°C which indicates the presence of SM while the broad cyclodextrin peak was absent. The exothermic peak at 154.62°C was highly shifted which indicates some degree of complexation between SM and CD. The temperature was increased to a maximum of 180°C as no more events were seen above this limit. The SM-CD complex had a

completely different curve where the SM peak was absent while the CD broad peak was present at 102.28°C where it has undergone a massive shift which indicates the potential complexation of SM with cyclodextrin. The temperature was increased to a maximum of 150°C as no more events were seen above this limit. Table 3.5 shows the average value for each peak.

Table 3. 5: The peaks values in DSC readings for SM

Sample	Peaks (°C)		Average (°C)	
SM	81.34, 81.20		81.27 ±0.10	
SM-CD PM	81.47, 81.62	154.62,154.63	81.85 ±0.11	154.63 ±0.01
SM-CD complex	102.28, 105.00		103.64 ±1.92	

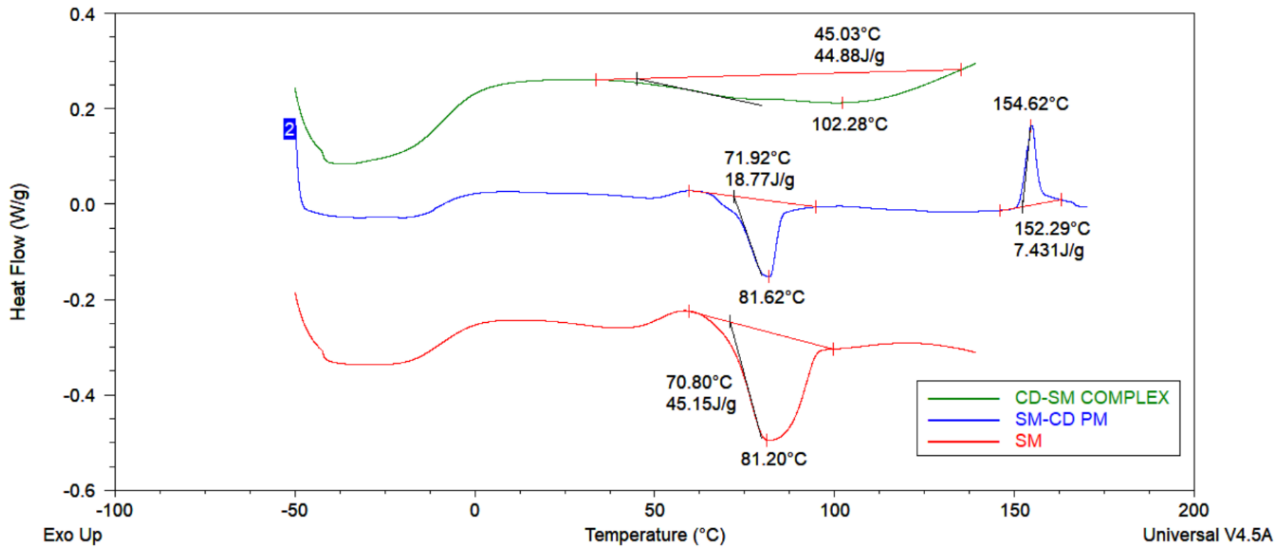

Figure 3. 20: The DSC of CD-SM complex, SM-CD physical mixture, and SM

DSC analysis confirmed the formation of lipid–cyclodextrin inclusion complexes by revealing clear alterations in thermal transitions. In the physical mixtures, lipid-specific endothermic

peaks—such as those for POPC (~31°C), POPE (~48°C), DOTAP (~6°C), and SM (~81°C) remained detectable, indicating the lipids retained their native structure. However, in the freeze-dried complexes, these peaks were either significantly shifted or completely absent, suggesting the lipids were no longer in their free form. Simultaneously, the characteristic endo- and exothermic peaks of cyclodextrin were also shifted or suppressed. These changes imply that the lipids were encapsulated within the hydrophobic cavity of cyclodextrin, which altered their phase transition behaviour. Disappearance of lipid melting peaks is particularly significant, as it indicates molecular-level interactions that restrict thermal motion, a well-established marker of successful complexation. Overall, the DSC data supports the conclusion that the inclusion of lipids into the cyclodextrin cavity disrupted their crystallinity and thermal properties, consistent with literature describing host–guest complex formation.

4.4. Nuclear magnetic resonance (NMR)

Nuclear magnetic resonance (NMR) is used to determine the content of a sample as well as measuring purity. Additionally, it can be used to identify the molecular structure of a molecule (118). In this method NMR was used to compare the spectra of different samples and identify whether complexation has occurred between the lipids and cyclodextrin. D-methanol was used for all readings to allow head-to-head comparison. The expected peaks for D-methanol are at 4.78 and 3.31(119). NMR was used in literature to confirm inclusion complex formation of cyclodextrin (97). The confirmation of cyclodextrin-curcumin inclusion complex formation was confirmed by chemical shifts as well as reduction in intensity of the hydrogens (^{1}H) (97).

The NMR spectrum was measured for cyclodextrin. As shown in figure 3.21, the main peaks of cyclodextrin were visible between 3 and 4 ppm, this indicates the presence of HC—O bonding which is very abundant in the structure of methyl-α-cyclodextrin structure which is a cyclic ring of methylated hydroxyl groups i.e. CH3 is added to OH groups within the molecule. The large peak at 4.7787 ppm indicates the presence of the D-methanol solvent. Moreover, the peaks at 4.9399 and 4.9751 ppm indicate the presence of O-H bonds. The small peaks from ~0-3ppm are considered impurities. The presence of impurities was confirmed as the NMR done by the company manufacturing the cyclodextrin does not contain any peaks (figure 3.22) (120).

The DOTAP NMR spectrum shown in figure 3.23 shows peaks between 0-2ppm that indicate the presence of R-CH bonds, which are found in the hydrophobic tail of DOTAP. The peaks at 5.2701 and 5.5475 ppm indicate the presence of C=C bond within the molecule. This bond is also present in the hydrophobic tail of DOTAP. The peaks at 2-3ppm represent the HC—C=OR

structure present in the hydrophilic head. Additionally, the peaks between 3-5ppm are likely due to the presence of HC—O bond within the link between the head and tail of the phospholipid as shown in figure (3.24) (121).

The of cyclodextrin and DOTAP are both fully visible in the CD-DOTAP physical mixture NMR as shown in figure 3.25. However, in figure 3.26, the complex's NMR show a marked reduction in the intensity of the peaks from 0-2ppm which is likely due to the masking of the hydrophobic tails bonds by the complexation/inclusion within the cyclodextrin's cavity. The peaks present in the CD's spectrum were also visible in the lipid-CD PMs and the lipid-CD complexes. The NMR spectra ware compared between the physical mixture and the complex to identify differences that can indicate complex formation. This is further confirmed by the absence of the peaks at 5.2701 ppm which is linked to the presence of C=C bond that is also present within the hydrophobic tail of DOTAP.

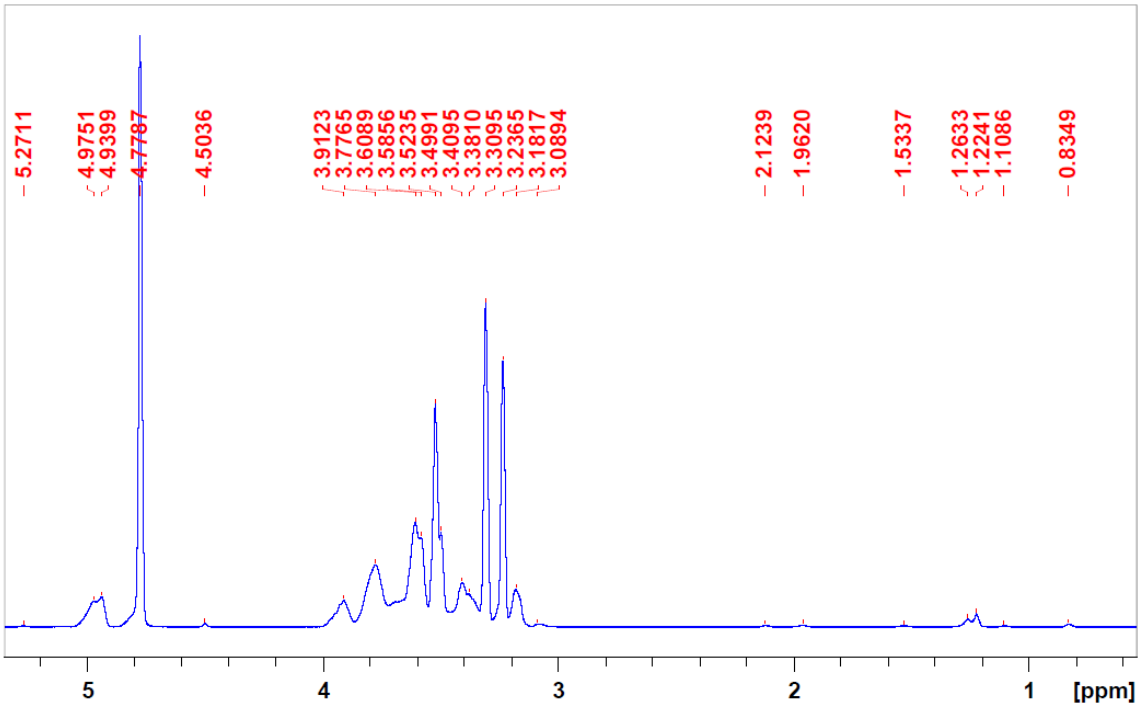

Figure 3. 21: The NMR spectrum for cyclodextrin

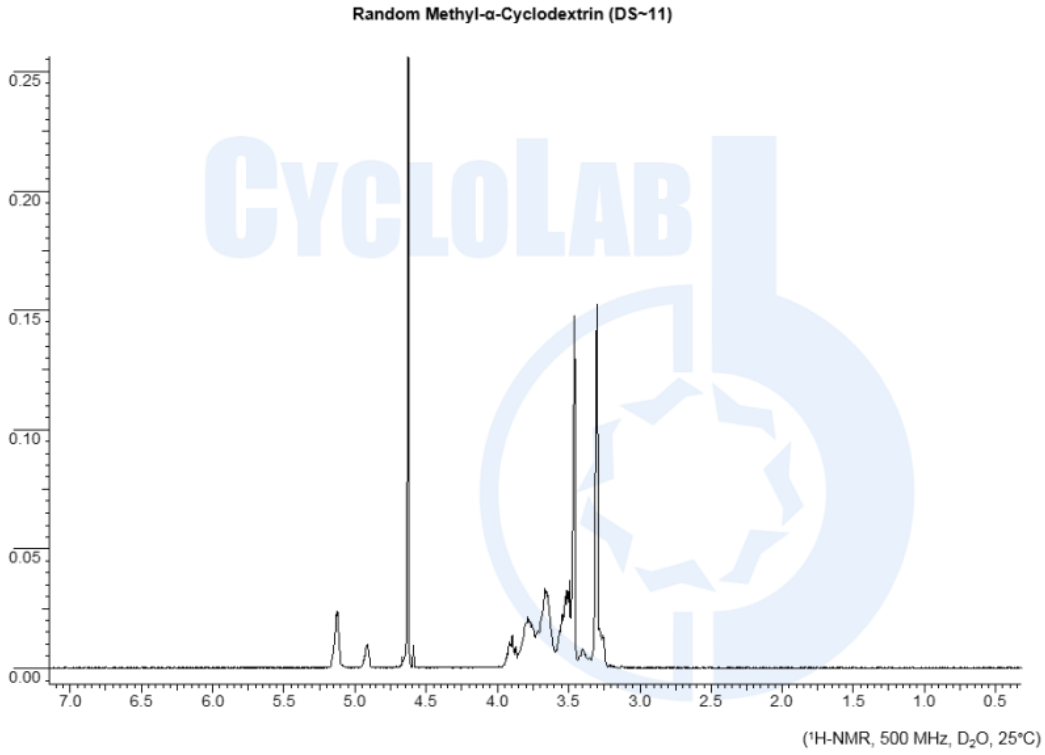

Figure 3. 22: The ¹H-NMR of methyl-α-cyclodextrin (120)

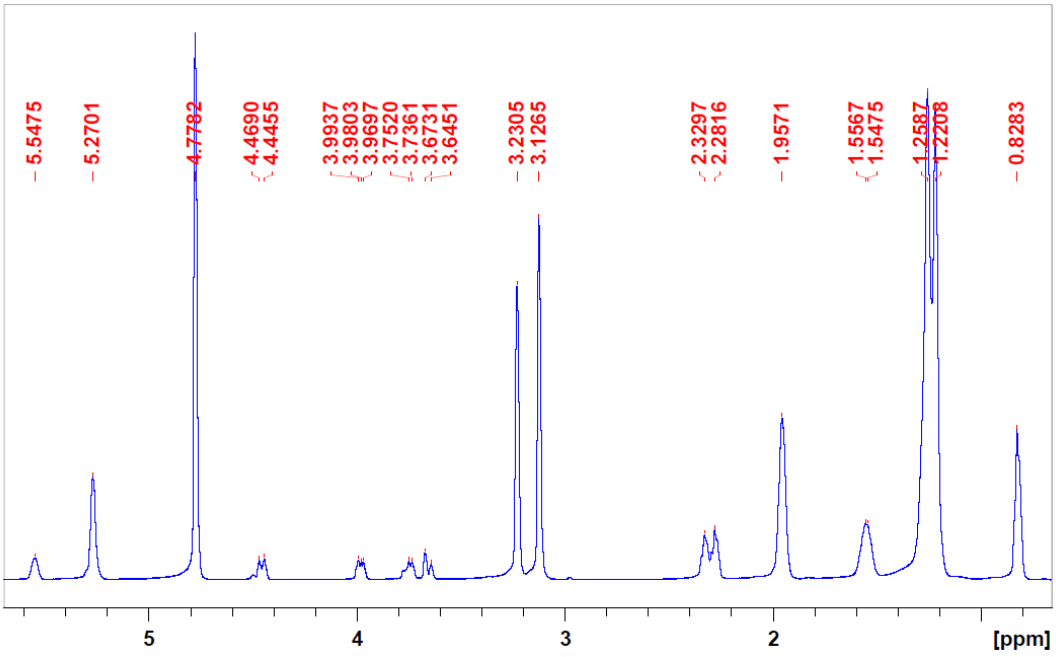

Figure 3. 23: NMR spectrum of DOTAP

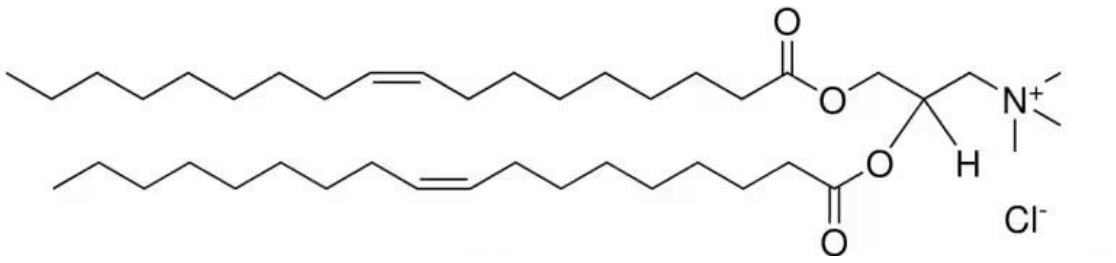

Figure 3. 24: The molecular structure of DOTAP (121)

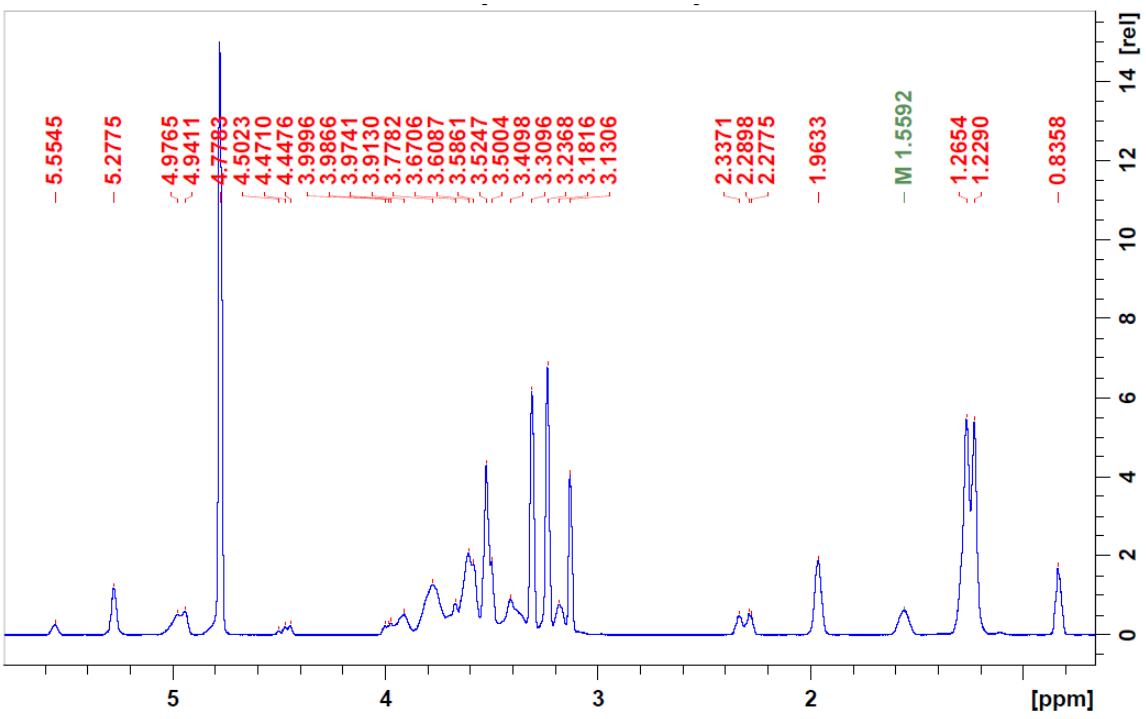

Figure 3. 25: NMR spectrum of CD-DOTAP PM

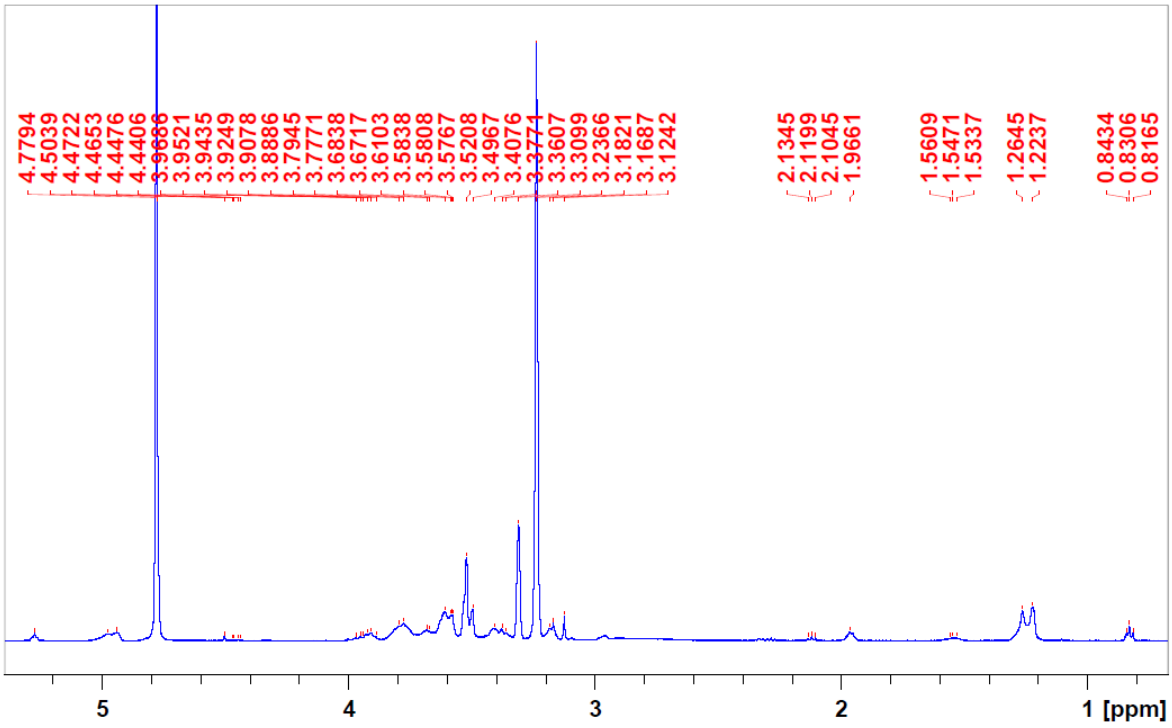

Figure 3. 26: NMR spectrum of CD-DOTAP Complex

The NMR spectrum for POPC was measured (figure 3.27). Similar to DOTAP, the peaks present between 0-2ppm represent the R—CH bond of the hydrophobic tail. Additionally, the two peaks at 5.1655 and 5.2698ppm represent C=C bond within the tail as shown in figure 3.28 (122). The link between the tail and the hydrophilic head contains HC—C=OR bond, this bond is visible in the NMR spectrum as the peaks between 2-3ppm. The HC—O present within the head is indicated by the peaks present between 3.2-4.4ppm. To confirm complexation, the NMR was measured for the CD-POPC physical mixture in figure 3.29, which shows that all the peaks for the cyclodextrin and the POPC are visible. However, the complex's spectrum (figure 3.30) has hugely reduced intensity peaks between 0-3ppm which indicates hydrophobic tail bond masking by the cyclodextrin. Furthermore, the peak at 5.2698ppm was reduced as well as the peak at 5.1655ppm being full disappeared.

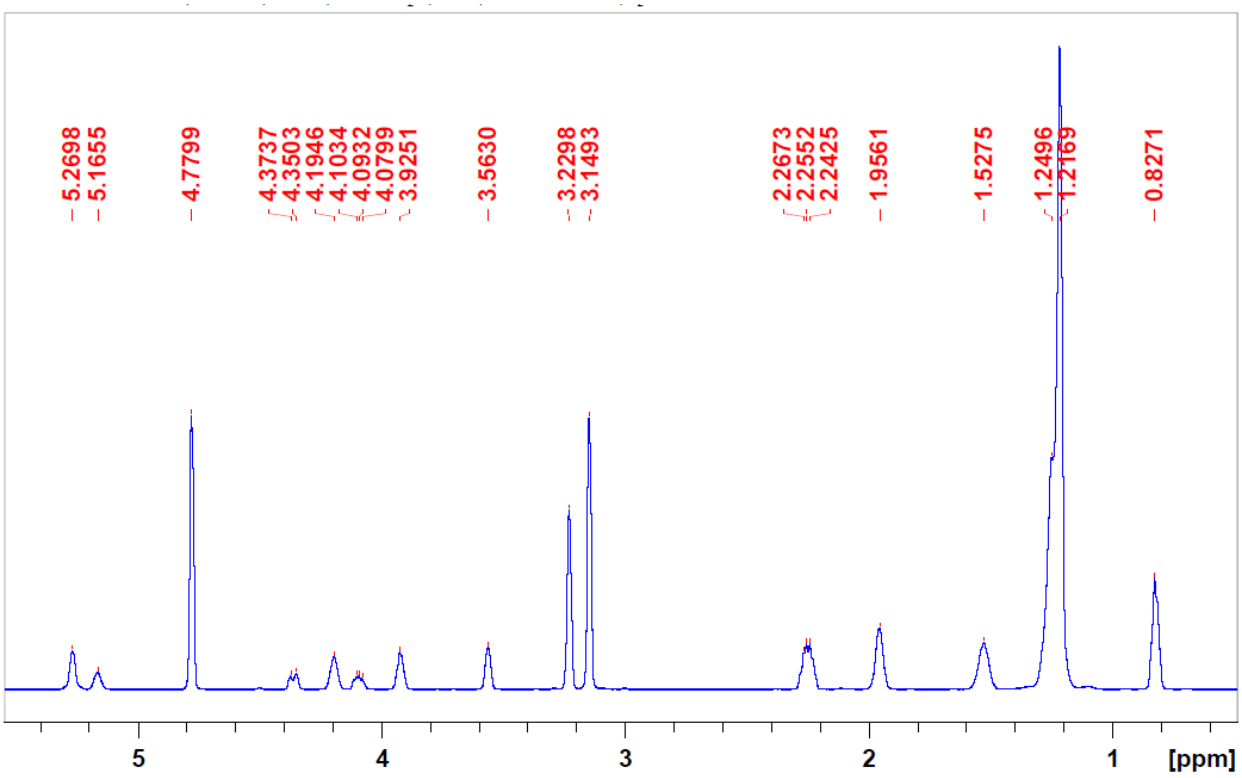

Figure 3. 27: the NMR spectrum for POPC

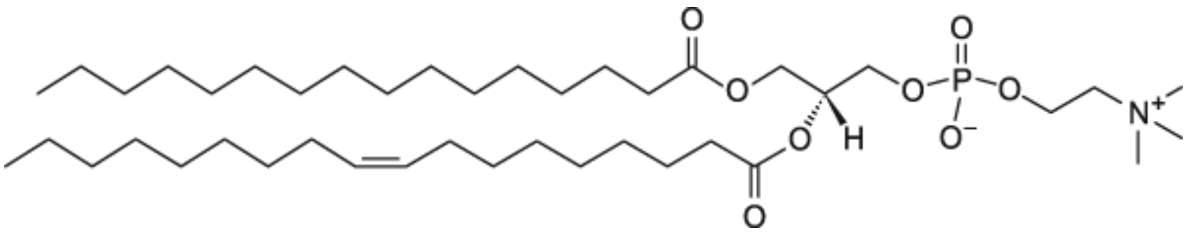

Figure 3. 28: The molecular structure of POPC (122)

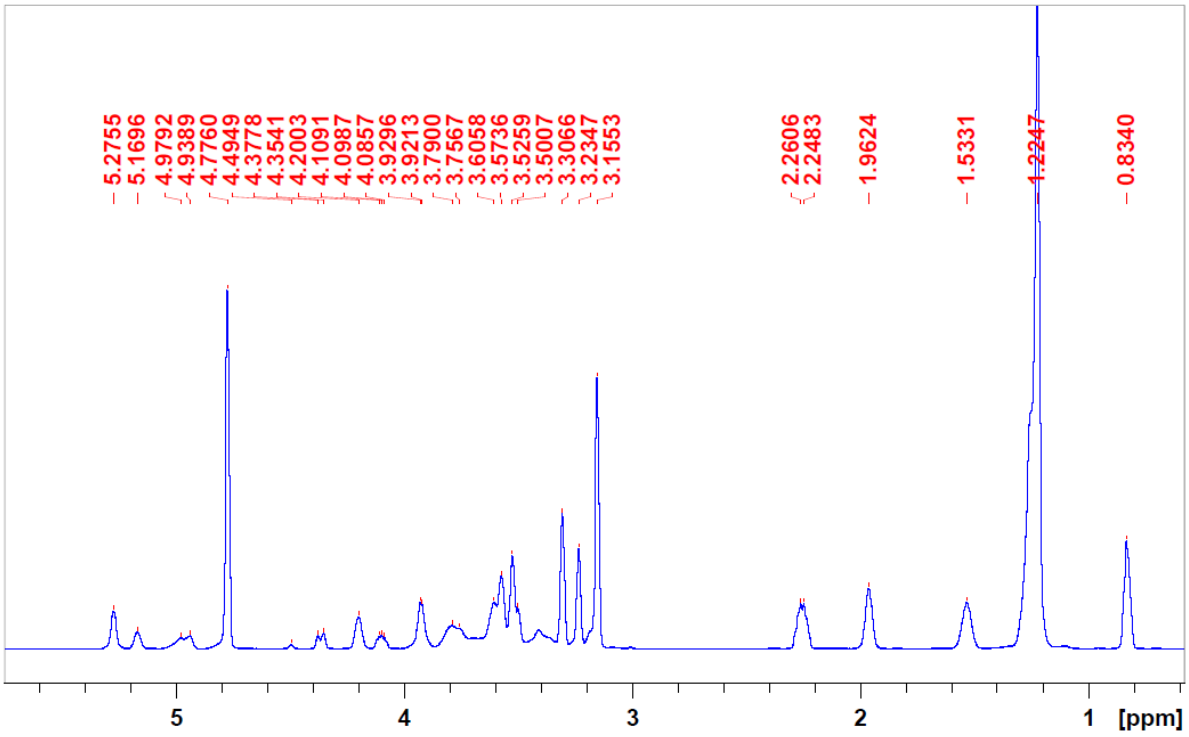

Figure 3. 29: the NMR spectrum for CD-POPC PM

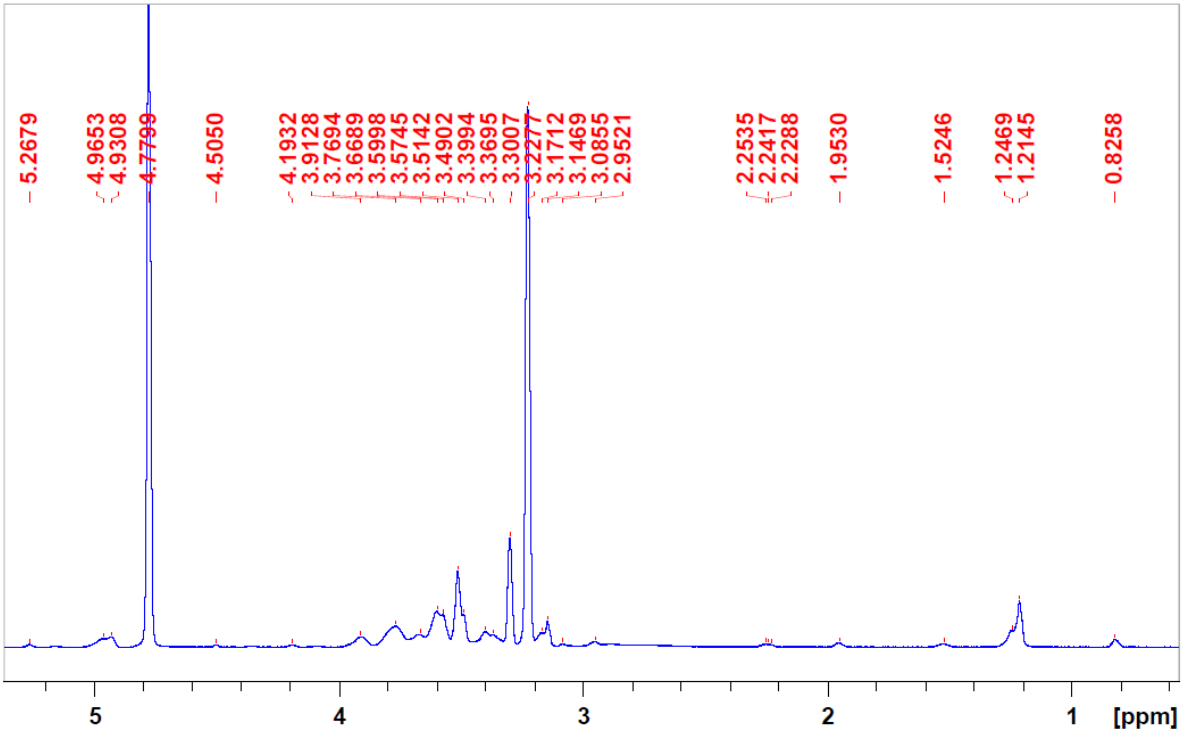

Figure 3. 30: the NMR spectrum for CD-POPC complex

The NMR spectrum for SM was measured (figure 3.31). From 0-2ppm the peaks likely indicate the presence of R—CH bond within the hydrophobic tail of SM (shown in figure 3.32) (123). The peaks after 5ppm are likely associated with C=C in the linker between the head and tail as well as the C=ONH bond within the hydrophilic tail. The peaks between 3-4ppm likely associated with the HC—O bonds as well as the N-H bond within the head structure. Figure 3.33 shows the presence of all the SM and CD peaks; this is expected as the physical mixture contains both molecules without complexation. On the other hand, figure 3.34 shows the NMR spectrum for the complex. The spectrum shows the absence of most of the peaks located after 5ppm, which could be due to the masking of the C=C within the phospholipid. Moreover, the intensity between the peaks have reduced markedly between 0-3ppm which is likely due to R—CH bond inclusion within the cyclodextrin.

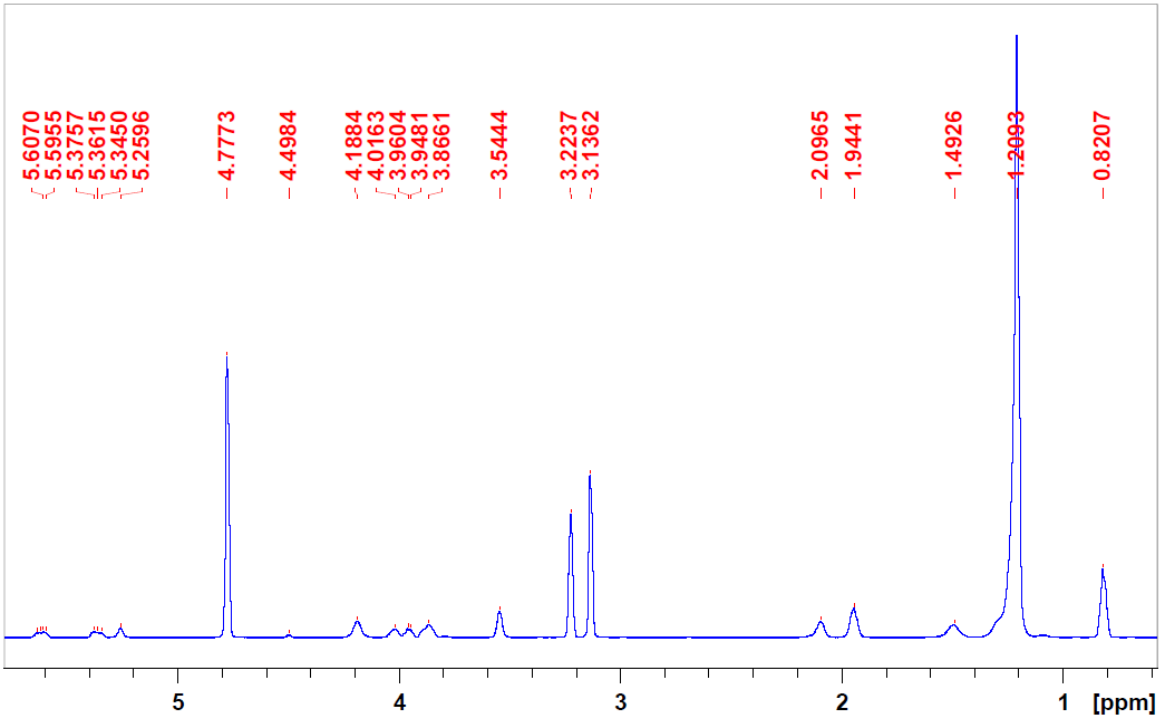

Figure 3. 31: The NMR spectrum for SM

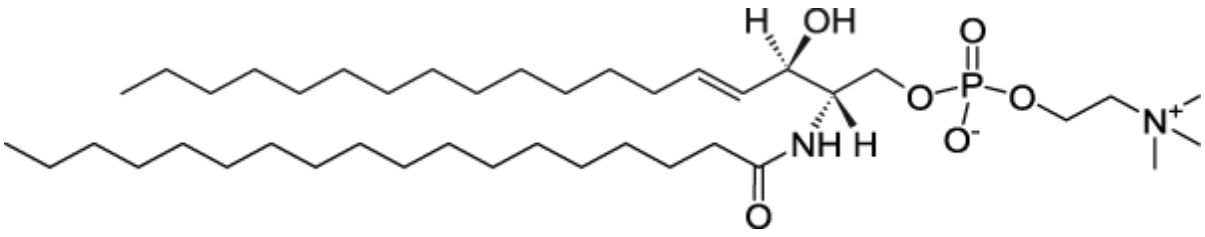

Figure 3. 32: The molecular structure for sphingomyelin (SM) (123)

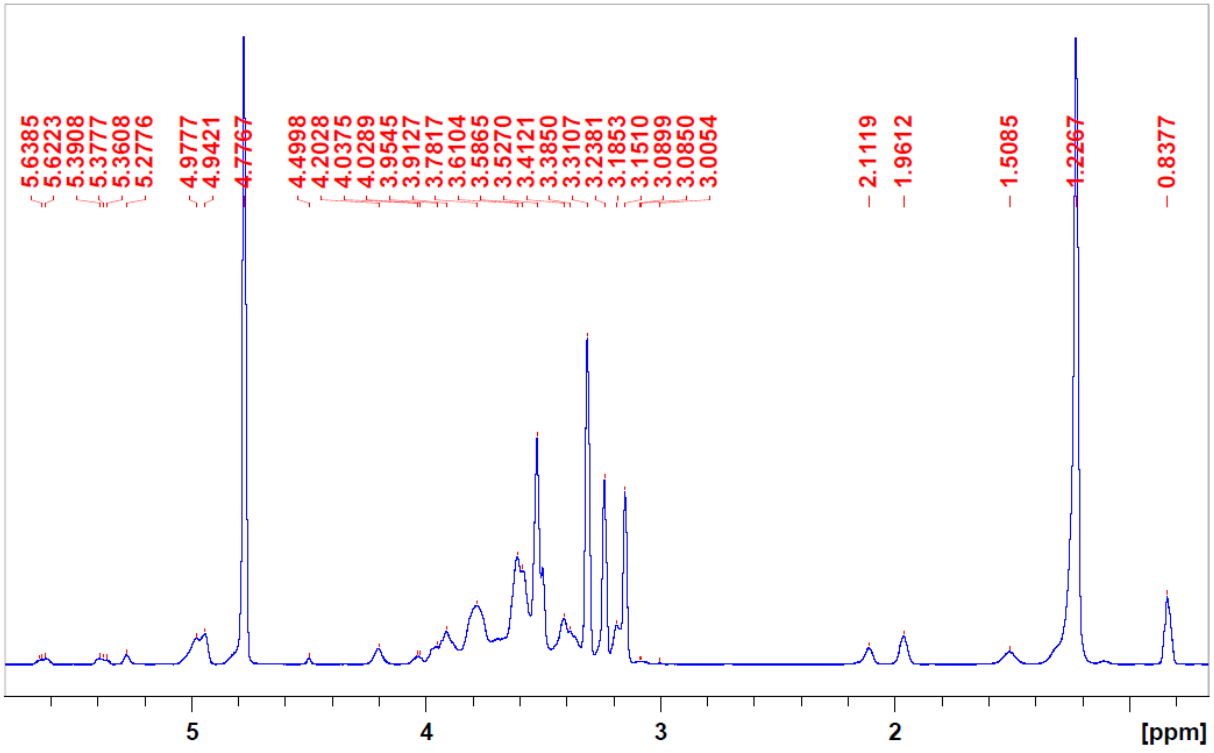

Figure 3. 33: The NMR spectrum for CD-SM PM

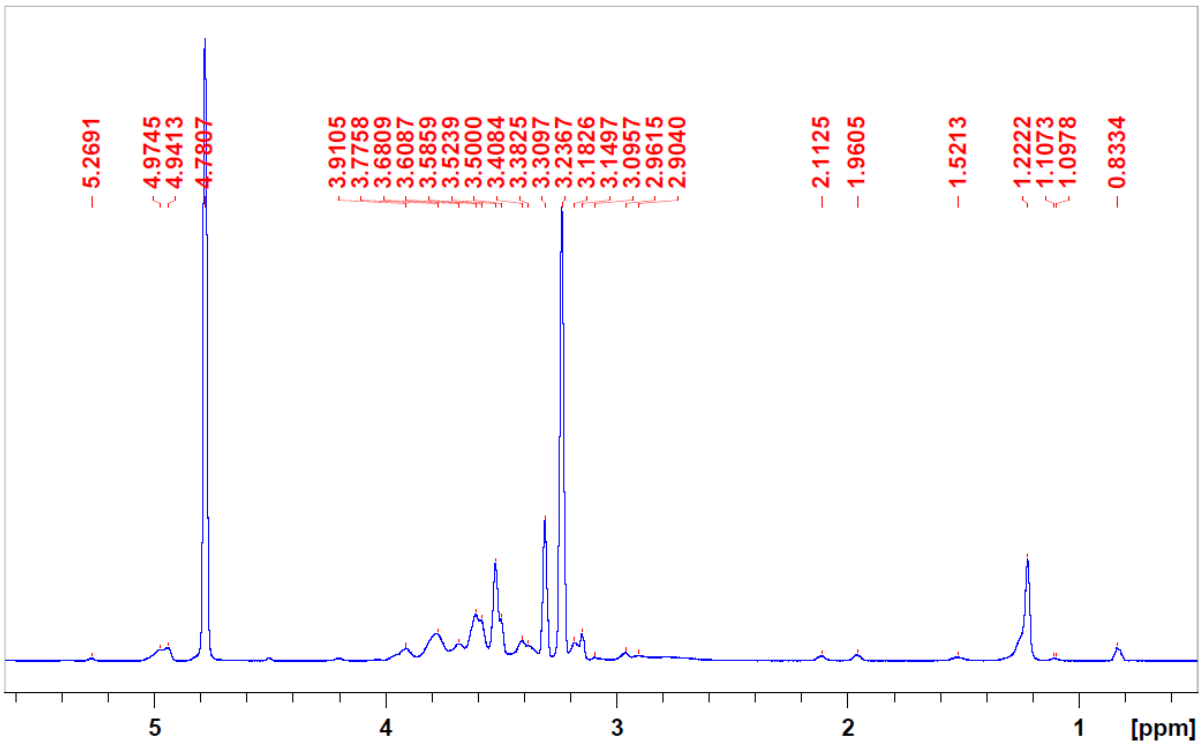

Figure 3. 34: The NMR spectrum for CD-SM complex

As shown in figure 3.35, the NMR spectrum for POPE was measured. Similar behaviour to the other lipids can be seen. The peaks between 0-2ppm indicating presence of R—CH bond within the hydrophobic tails. Moreover, the peaks at 5.1438 and 5.2583ppm indicate the presence of C=C which present within the hydrophobic tail as well as shown in figure 3.36 (124). The clear peak at 2.2373ppm is linked to the HC—C=OR bond present at the start of the hydrophobic tails. Additionally, the peaks between 3-4ppm are linked to the presence of HC—O which are located within the hydrophilic head of the molecule. The CD-POPE PM spectrum in figure 3.37 shows the peaks present in the POPE and cyclodextrin molecules, this is due to the two molecules being present separately within the solution. Meanwhile, the complex's spectrum shown in figure 3.38 shows clear lack of peaks between 0-3ppm which is likely due to masking of the peaks by the cyclodextrin as these peaks are linked to the bonds within the hydrophobic tails that is being complexed within the inner cavity of the cyclodextrin. Moreover, the peaks after 5ppm have disappeared which are linked to the C=C bond within the hydrophobic tail.

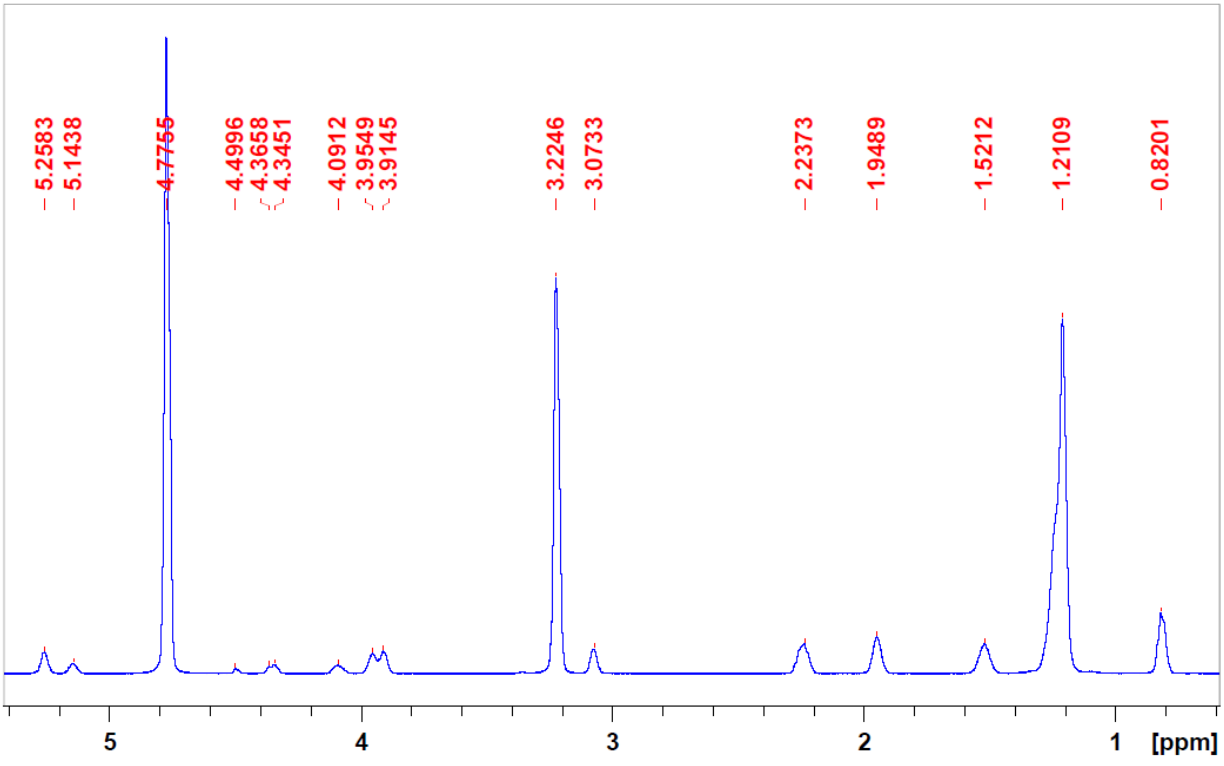

Figure 3. 35: The NMR spectrum for POPE

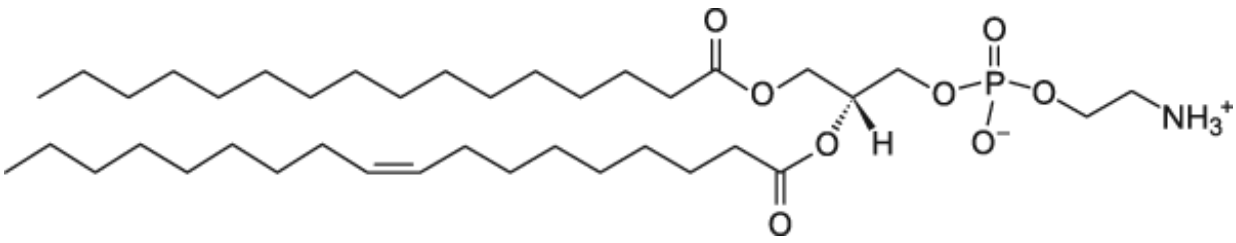

Figure 3. 36: The molecular structure of POPE (124)

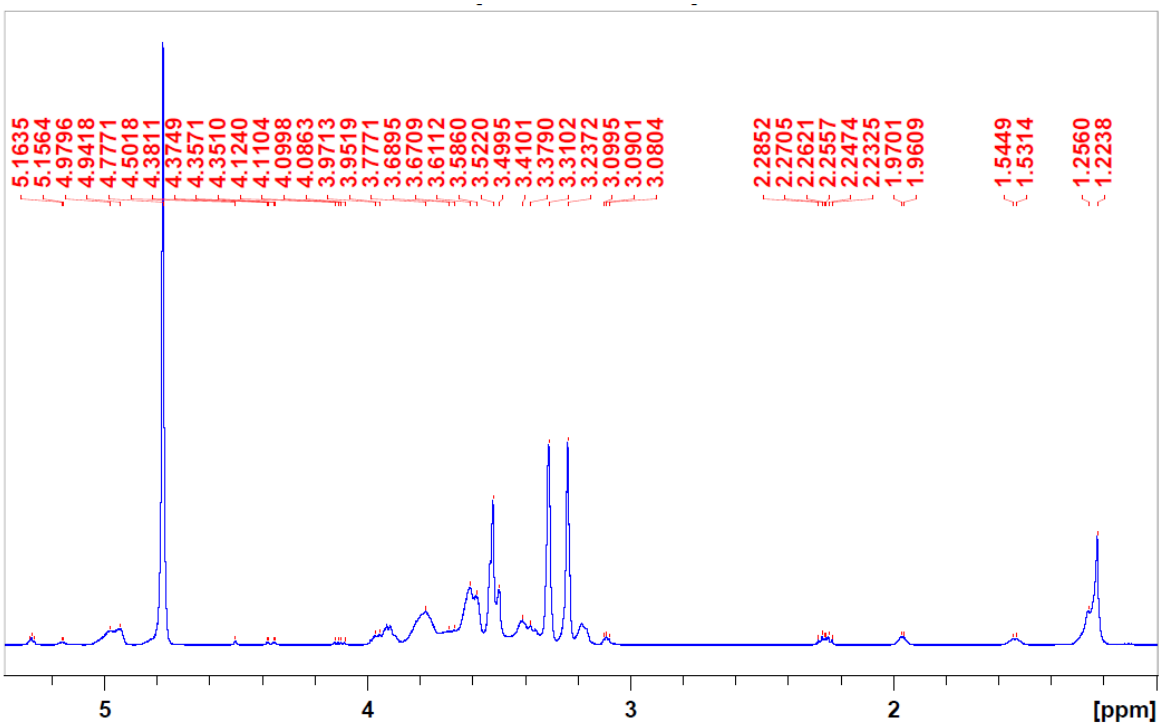

Figure 3. 37: The NMR spectrum for POPE-CD PM

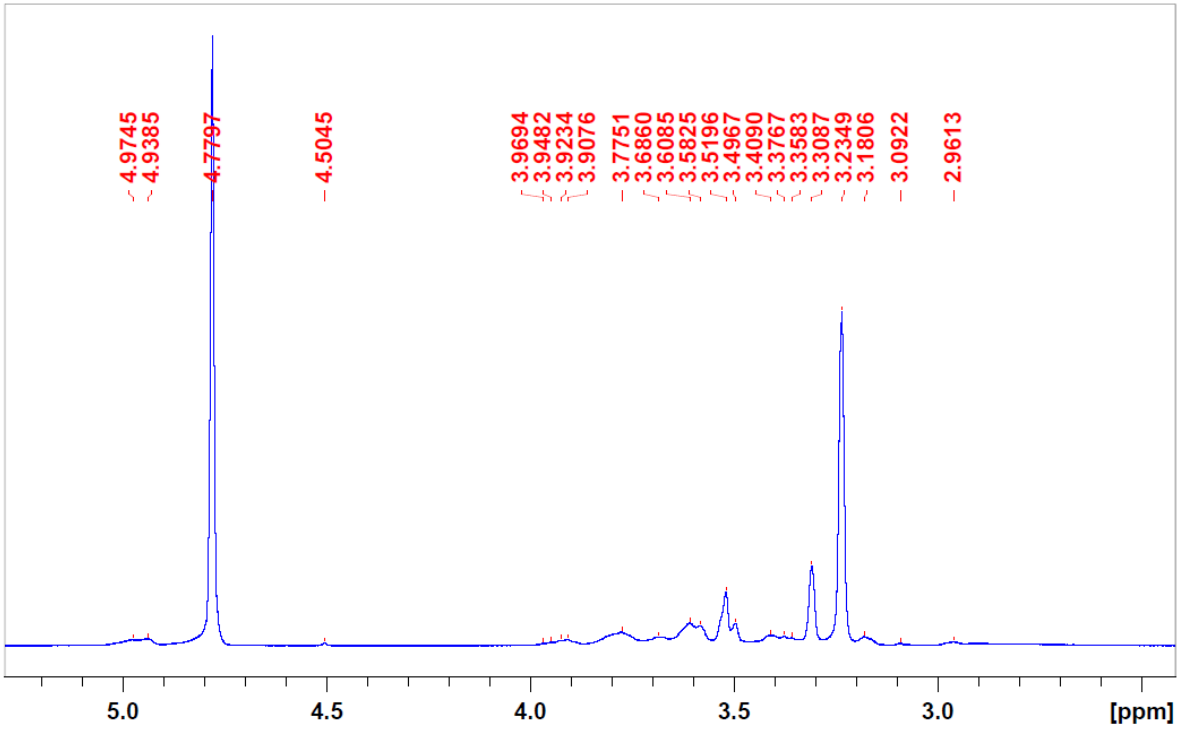

Figure 3. 38: The NMR spectrum for POPE-CD complex

NMR spectroscopy provided clear evidence of complexation between cyclodextrin and each lipid by revealing consistent changes in the chemical environments of key protons. In the physical mixtures, spectra showed distinct peaks corresponding to both lipid and cyclodextrin protons, indicating no interaction at the molecular level. However, in the complexes, notable reductions or disappearances of peaks between 0–3 ppm (R–CH protons of lipid tails) and >5 ppm (C=C bonds) were observed. These changes suggest that the hydrophobic regions of the lipids were encapsulated within the non-polar cavity of cyclodextrin, shielding them from the NMR field. This masking effect is consistent with literature findings, where such signal attenuation or shift is a hallmark of inclusion complex formation. The reproducible disappearance or reduction of key lipid peaks across all four lipids further confirms successful host–guest interactions.

4.5. Solubility in water

As a simple proof of concept to assess complexation, solubility testing was performed using distilled water (DW) as the solvent. Pure cyclodextrin (CD) powder dissolved completely in DW, as expected due to its hydrophilic outer surface. In contrast, the phospholipids on their own as well as the cyclodextrin-lipid physical mixture exhibited poor solubility, with visible undissolved particles suspended in the solution. This incomplete dissolution indicates that the lipid component remained largely insoluble, forming aggregates or precipitates due to its

hydrophobic character. Although CD was present in the physical mixture, the lack of molecular interaction between the lipid and CD prevented effective dispersion, and the hydrophobic lipid tails remained exposed to the aqueous environment, leading to phase separation. However, the freeze-dried cyclodextrin-lipid complex powder dissolved fully in DW, forming a clear solution without visible particulates. This difference in solubility supports the occurrence of complexation, whereby the hydrophobic regions of the lipid molecules, particularly the acyl chains, were encapsulated within the nonpolar cavity of cyclodextrin. By shielding the hydrophobic moieties from the aqueous environment, the inclusion complex enhances overall water compatibility and dispersibility. This behavior is well-documented in the literature, where the formation of cyclodextrin inclusion complexes significantly improves the solubility and stability of hydrophobic guest molecules (97). Therefore, the enhanced solubility of the complex, in contrast to both the pure lipid and the physical mixture, provides indirect yet compelling evidence of successful host–guest interactions.

5. Proof of formation of asymmetric liposomes

5.1. Zetapotential

The zeta potential (ZP), measured by a Zetasizer, is an essential test that gives information on the charge of nanoparticles. When particles are in a solution, they are surrounded by a liquid layer that exists in two parts; an inner region where ions are strongly attached to the particles (Stern layer) and the surface of this layer is called “stern potential”. The second outer layer known as “diffuse layer” is a region with ions loosely bound to the particles. These ions within this notional boundary move as the particles move (125). The surface of this layer is called “zeta potential” (125). The value of ZP is an indicator to the stability of the particles, higher value means there is a high repulsion, thus less chance of aggregation. On the other hand, a lower ZP value means less force between particles and a higher chance of flocculation. (125). Moreover, this parameter can be used to study the aggregation of the particles; normally, particles with values above +30 mV or −30 mV are considered stable (125).

Zetapotential is considered an ideal parameter for confirming the asymmetry of ionic lipids withing the liposomal membrane as it can exclusively measure the outer leaflet (61). The low dielectric core of the membrane acts as an “insulator” and renders the inner leaflets’ charge invisible to the measurement of ZP. Moreover, the lipid-CD complex within the solution would not affect the reading as the ZP measurements work on the basis of light scattering where the light’s intensity is proportional to the sixth power of size. Thus the small size of the complex would not be detected (61). As shown in figure (3.39), anionic POPG was added to a neutral POPC LUV at different mole fractions, then a calibration curve was created using the values of ZP from different LUV formulations as shown in part (a), at point 0.4 X_{PG}^{Out}, the ZP value was -36mV. When POPG was exchanged to the outer leaflet, the ZP value of -36mV was reached at around 0.2 X_{PG}^{Out}, indicating more POPG is on the outer leaflet in spite of the PG mole fraction, thus asymmetry formation (61).

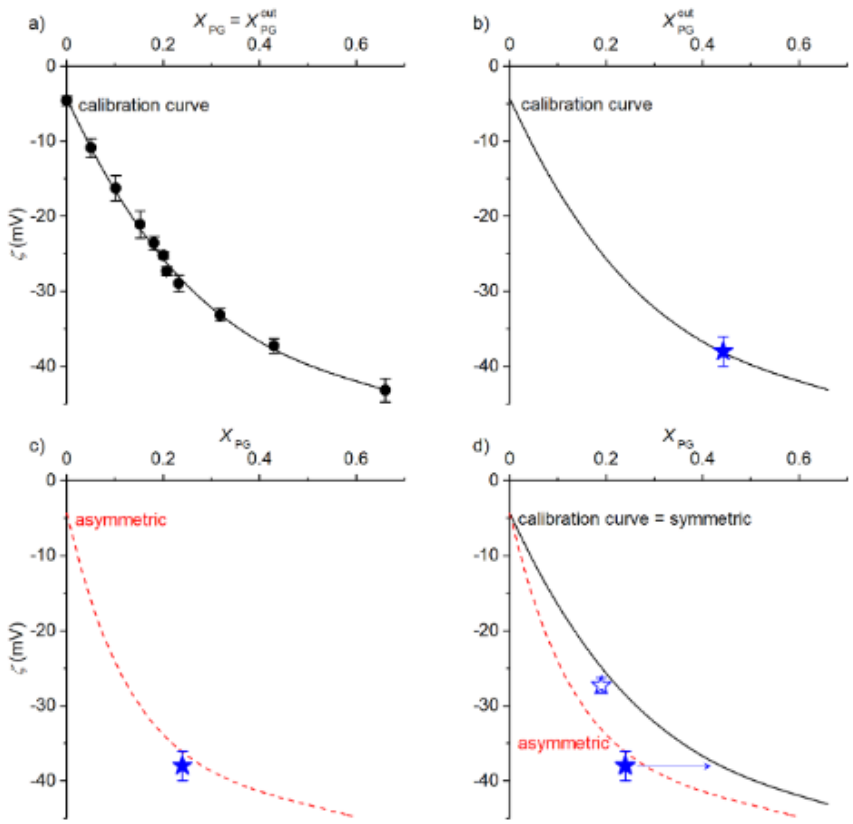

Figure 3. 39: The calibration curves for symmetric and asymmetric liposomes' zetapotential "Reprinted with permission from Markones et al. Copyright {2018} American Chemical Society." (61)

In our experiment, the zetapotential has been used as a method to determine vesicles asymmetry. The ZP is measured for the donor and the acceptor separately before exchange. Then ZP was measured for the asymmetric vesicle after exchange. This semi-quantitative method allows for the confirmation of asymmetry as well as the stability of the asymmetry by studying the charge differences between the vesicles as well as the stability of the charge.

As a proof of concept, the zwitterionic (neutral) lipid POPC has been used as an acceptor LUV and DOTAP was formulated as a CD-LIPID complex donor. Since POPC has no charge, any charge added to the liposomes is coming from the positive DOTAP (For composition refer to methods section). As shown in table (3.10), the zetapotential for POPC was -7.1 when formulated in HEPES buffer and PBS used as a dispersant. A slightly negative charge is predicted as PBS contains different salts which can lead to a slightly negative solution (126). The size of the liposomes had an average of 114.6nm with an average PDI of 0.109. The size of the complex could not be measured because the Zetasizer device was unable to measure the complex size, as it is too small. Instead, the device measured the other particles present in the

solution. However, the ZP of the donor complex was 40.6mV (Table 3.11). To confirm asymmetry, the ZP was measured for the formulated asymmetric liposome where the value has increased from an average of -7.1mV to an average of 33.9mV (table 3.12) which indicates the transfer of DOTAP from the donor to the acceptor, since ZP cannot measure the inner layer's charge, this means that the transfer was done only to the outer leaflet of the acceptor. Moreover, the size of the asymmetric liposome has reduced to 108.2nm when compared to the size of the acceptor; this is likely due to the presence of DOTAP, which causes repulsion between the vesicles and reduces aggregation.

Table 3. 6: The zetapotential and vesicle size for acceptor (Neutral POPC)

Name	Zetapotential readings (mV)	Vesicle size readings (nm)	PDI readings
Acceptor (Neutral POPC)	-7.1 ±0.75	114.6 ±0.42	0.109 ±0.02

Table 3. 7: The zetapotential and size for donor (Positively charged DOTAP)

Name	Zetapotential readings (mV)	Vesicle size readings (nm)	PDI readings
Donor (Positively charged DOTAP)	40.6 ±2.01	NA	NA

Table 3. 8: The zetapotential and vesicle size for asymmetric liposome

Name	Zetapotential readings (mV)	Vesicle size readings (nm)	PDI readings
Asymmetric liposome	33.9 ±2.08	108.2 ±0.95	0.193 ±0.02

A second trial was done where the charges were exchanged. The donor complex had a neutral charge, and the acceptor vesicle had a positive charge (For composition refer to methods section). POPC-CD complex was formed as the donor and DOTAP was formulated as the acceptor vesicle (POPE was used as a helper lipid). The ZP for the donor had an average of -3.68mV (Table 3.13) and for the acceptor was 23.5mV (table 3.14). The ZP of the asymmetric liposome was reduced to 16.2mV (table 3.15) which indicates a reduction in the ZP compared

to the acceptor. This is likely due to the transfer of POPC from the donor complex to the outer leaflet of the acceptor vesicle. Moreover, the size of the acceptor vesicle was 273.0nm which was reduced to 83.62nm when the asymmetric liposome was formulated. When the transfer of POPC occurred, a breakage of the liposomes might have occurred which has led to reduced vesicle size due to asymmetric method preparation.

Table 3. 9: The zetapotential and vesicle size for donor (Neutral POPC)

Name	Zetapotential readings (mV)	Vesicle size readings (nm)	PDI readings
Donor (Neutral POPC)	-3.68 ±0.17	NA	NA

Table 3. 10: The zetapotential and vesicle size for acceptor (Positively charged DOTAP)

Name	Zetapotential readings (mV)	Vesicle size readings (nm)	PDI readings
Acceptor (Positively charged DOTAP)	23.5 ±0.49	273.0 ±4.83	0.202 ±0.01

Table 3. 11: The zetapotential and vesicle size for asymmetric liposome

Name	Zetapotential readings (mV)	Vesicle size readings (nm)	PDI readings
Asymmetric liposome	16.2 ±0.06	83.62 ±0.55	0.176 ±0.01

Additionally, the vesicles were studied overtime to monitor changes. They were stored at 4°C. As shown in table (3.16), a marked difference can be seen in the zetapotential readings. The asymmetric liposomes with a positive outer leaflet had a decrease in the positivity from 33.9mV to 29.0mV within 24 hours which indicates a flip flop in the bilayers where the neutral POPC is leaving from the inner leaflet to the outer leaflet. For the asymmetric liposomes with a neutral outer leaflet, a noticeable reduction in the zeta potential is observed, with the value decreasing

from 16.2 to 10.6 within 24 hours. This reduction can also be attributed to the flip-flop of lipids. These findings could be due to the lipids having flip flop until they find an equilibrium where there is less stress on the vesicle (59), lipids flip-flop means that the lipids within the bilayer like to switch between the outer and inner leaflet until equilibrium is reached. This could be evident by the fact that after a dramatic change in the asymmetry after 24 hours, the values remained somewhat similar until 2 weeks.

Table 3. 12: The zetapotential readings overtime for asymmetric liposomes with positive and neutral outer leaflet

	Asymmetric (Positive outer leaflet) readings	**Asymmetric (Neutral outer leaflet) readings**
24 hours	29.0 ±0.93 mV	10.6 ±0.44 mV
48 hours	26.3 ±0.66 mV	12.1 ±0.15 mV
72 hours	28.0 ±0.85 mV	9.53 ±0.34 mV
1 week	25.97 ±1.46 mV	10.4 ±0.15 mV
2 weeks	20.5 ±0.92 mV	6.46 ±0.44 mV

In regard to the size (Table 3.17), the asymmetric liposomes with a positive outer leaflet had a continuous increase in size reaching to almost double the initial size after 2 weeks. This could be due to aggregation of the liposomes. Moreover, the asymmetric liposomes with a neutral outer leaflet had a continuous decrease in size which could be due to vesicle breakage.

Table 3. 13: The vesicle size readings overtime for asymmetric liposomes with positive and neutral outer leaflet

	Asymmetric (Positive outer leaflet) readings		**Asymmetric (Neutral outer leaflet) readings**	
24 hours	SIZE (nm)	139.1 ±2.57	SIZE (nm)	80.40 ±0.67
	PDI	0.189 ±0.01	PDI	0.118 ±0.01
48 hours	SIZE (nm)	162.0 ±2.68	SIZE (nm)	83.76 ±0.38
	PDI	0.157 ±0.01	PDI	0.181 ±0.01

72 hours	SIZE (nm)	197.0 ±1.76	SIZE (nm)	79.46 ±0.21
	PDI	0.200 ±0.003	PDI	0.092 ±0.01
1 Week	SIZE (nm)	NA	SIZE (nm)	78.43 ±0.65
	PDI	NA	PDI	0.116 ±0.01
2 Weeks	SIZE (nm)	NA	SIZE (nm)	76.75 ±0.10
	PDI	NA	PDI	0.107 ±0.03

5.2. Fluorescence quenching

In addition to zetapotential, fluorescence quenching technique was used to confirm asymmetry. This method is commonly used to determine asymmetry (66,127–129). A study was undertaken to determine asymmetry by using an nitrobenzodiazole (NBD)-labelled lipid quenching (53). As shown in figure (3.40), liposomes were formulated asymmetrically where the NBD-lipid was incorporated into the outer leaflet of the liposomes and the fluorescence was measured, then sodium hydrosulphite (dithionite) was used to quench the fluorescence. The fluorescence intensity was reduced by almost 80%. This was followed by the addition of triton-X100 to break the liposomes and measure the amount of NBD-lipid within the inner leaflet (53).

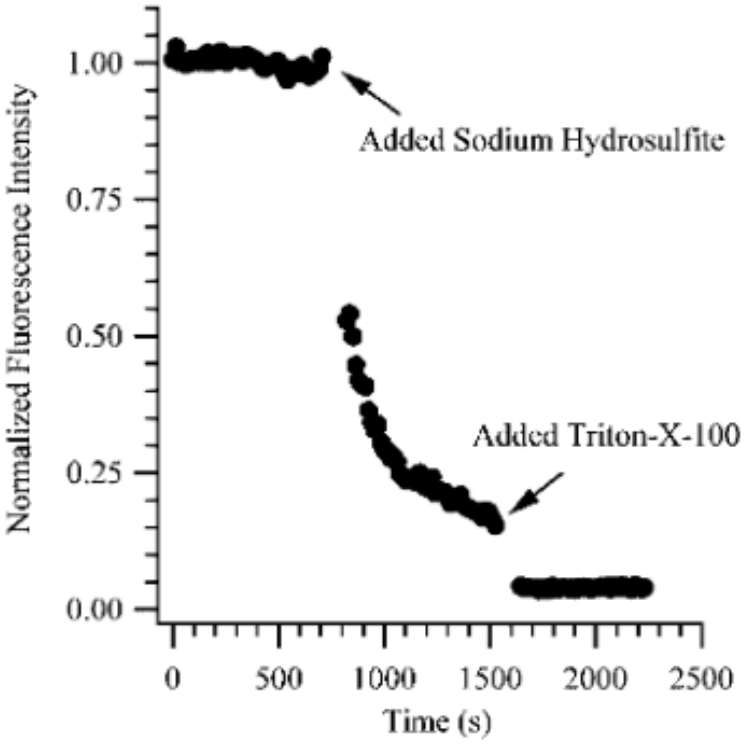

Figure 3. 40: Fluorescence quenching of NBD-lipid in asymmetric liposomes "Reprinted (adapted) with permission from Whittenton et al. Copyright {2008} American Chemical Society."

Our study involved using 7-nitro-2-1,3-benzoxadiazol-4-yl (NBD) as the fluorescent material. This material is attached to the phosphate group (head) of the phospholipid, leading to the formation of an NBD-lipid. Using 1% of the NBD-lipid within a formulation is highly beneficial for fluorescence quenching methods. Sodium dithionite was used as the quenching agent for the NBD (For composition, refer to the methods section).

First, the NBD-lipid was used when formulating the acceptor vesicle. When the acceptor vesicle is quenched, a 50% reduction in the fluorescence intensity should occur as the NBD-lipid is currently distributed between the two leaflets (symmetric vesicle). Once lipid exchange occurs and asymmetric liposome is formed. The NBD-lipid will be, by theory, only in the inner layer. Therefore, when fluorescence quenching occurs, the fluorescence intensity should not reduce massively as the NBD-lipid is within the inner leaflet and the sodium dithionite cannot enter the phospholipid bilayer.

Additionally, when the NBD-lipid is formulated as part of the lipid-CD complex and quenching occurs, the fluorescence intensity should reduce to near 0% as all of the NBD-lipid is exposed as part of the complex. The phospholipid only inserts its tail within the cyclodextrin cavity, while

the head remains in the outer environment. This means that the NBD molecule attached to the phospholipid head is still exposed and the sodium dithionite will quench all of it. Once lipid exchange occurs, the NBD-lipid will, in theory, be transferred to the outer leaflet of the vesicle only. Therefore, when fluorescence quenching occurs, the fluorescence intensity should reduce to almost near 0% as the NBD-lipid is only in the outer leaflet and nothing was transferred to the inner leaflet.

This research was done in two different methods. First, the NBD fluorescent lipid was added to the donor complex, and the acceptor vesicle was formulated as normal. Then, the donor complex was formulated as usual, and the NBD fluorescence lipid was added to the acceptor vesicle. After that, asymmetric liposomes were formulated using the two formulations. All of the above undergone a fluorescence quenching procedure to identify the location of the lipid.

The fluorescent acceptor was tested before and after quenching for 5 minutes. The acceptor was formulated as 29.5% DOTAP, 29.5% POPE, 1% NBD-PE and 40% cholesterol. As shown in figure (3.41), before quenching the average value of the fluorescence intensity (FI) was 3,186,893 however, after quenching the value has reduced to an average of 463,255 which is ~85.5% reduction in fluorescence. This result was unexpected, as the expected reduction should have been around 50% due to the presence of the fluorescent NBD-lipid in both layers. A theory was made that since sodium dithionite has a negative charge, there is a potential that it is interacting with the positive DOTAP within the formulation and breaking down the liposome or making the liposomes permeable to sodium dithionite. To prove this theory, another formulation was formulated without DOTAP using 59% DSPC, 1% NBD-PE and 40% cholesterol. DSPC was used instead of POPE because POPE alone was not able to formulate liposomes. As shown in figure (3.42), the average FI before quenching was 2,305,524 which has reduced to 1,235,259. This shows a reduction of ~46.5% which is expected as when formulating liposomes using the conventional methods, the lipids usually distribute equally within the two leaflets, hence the reduction in the acceptor (symmetric vesicle).

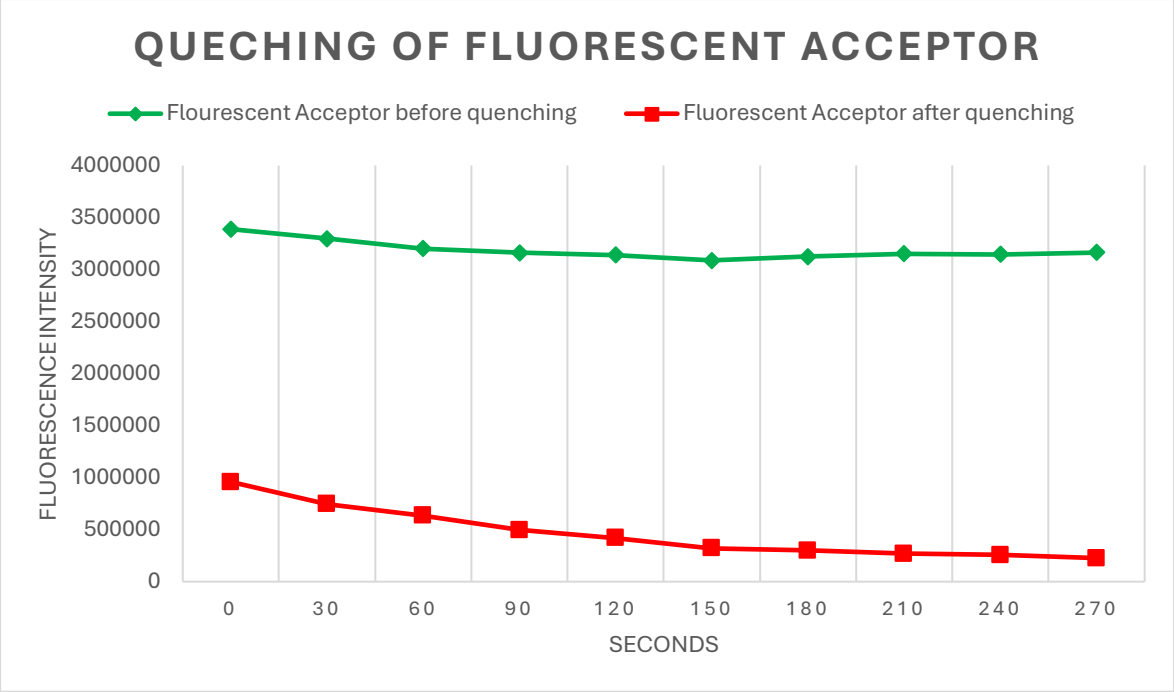

Figure 3. 41: Quenching of fluorescent acceptor

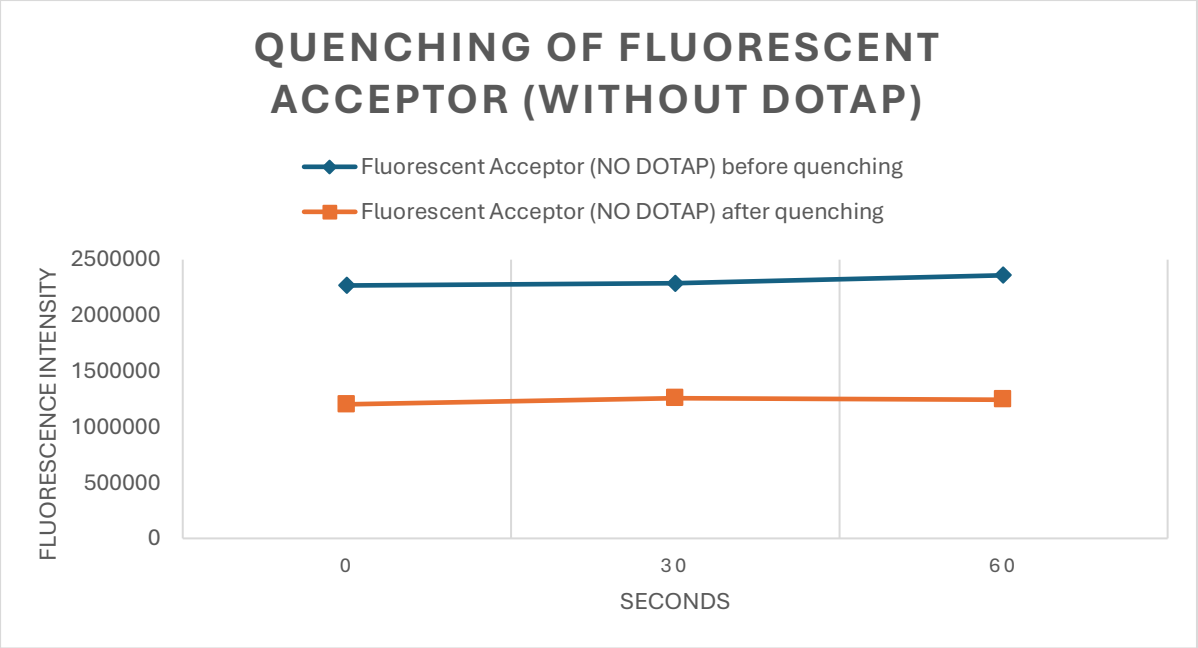

Figure 3. 42: Quenching of fluorescent acceptor (without DOTAP)

The fluorescent donor was formulated as a CD-lipid complex using 99% POPC and 1% NBD-PE, since the NBD is attached to the headgroup of the lipid, and when complexation occurs, only the tails of the lipid are complexed and inserted into the hydrophobic cyclodextrin cavity; the sodium dithionite will quench the NBD markedly and quickly. This is evident by figure (3.43)

where the fluorescence reading was reduced from an average of 2577371.1 to 487282 which is ~81.1% reduction in fluorescence intensity.

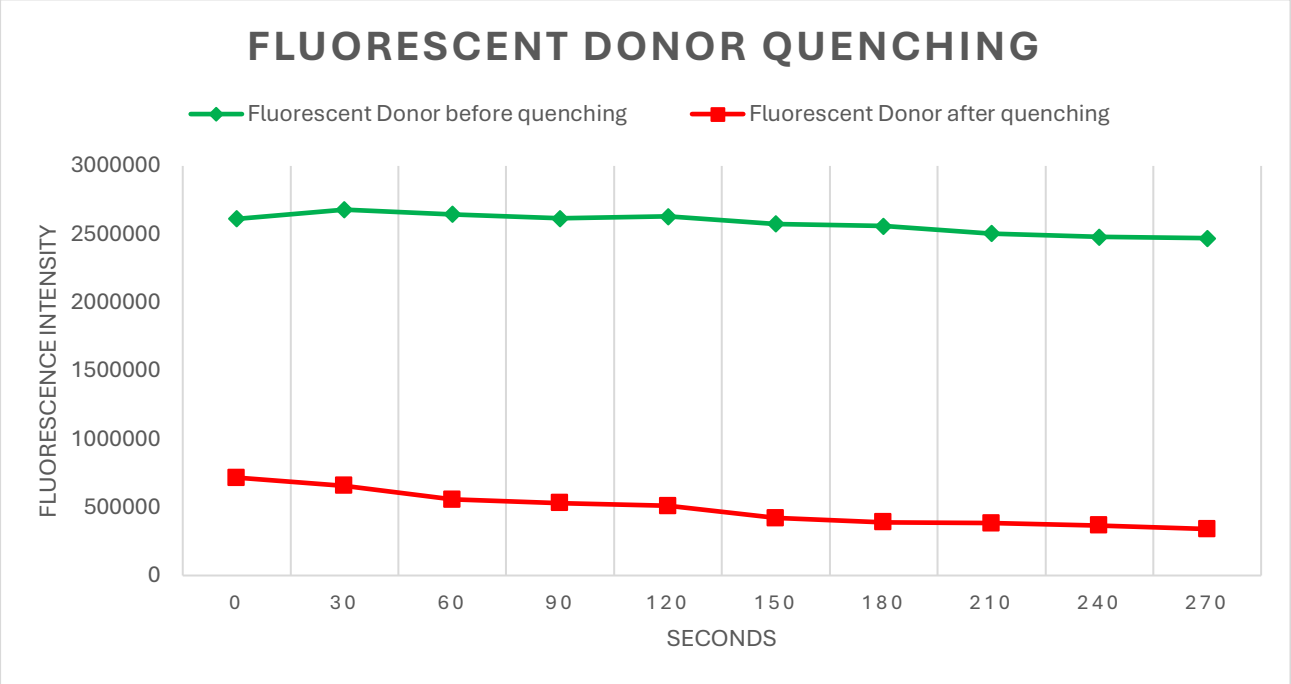

Figure 3. 43: Quenching of fluorescent donor

Next, the two asymmetric formulations were tested. First the asymmetric liposome with an outer leaflet containing NBD lipid is tested. The formulation consisted of 30% DOTAP, 30% POPE and 40% cholesterol in the inner leaflet (from the acceptor) and POPC + NBD-PE in the outer leaflet. A large decrease in fluorescence is evident in figure (3.44), the FI reduced from an average of 2274212 to 729814 which is ~67.9% reduction. This indicates that most of the lipid has transferred to the outer layer. However, since the reduction was not near 100%, this indicates the presence of some NBD-lipid within the inner leaflet, likely due to lipid flip-flop.

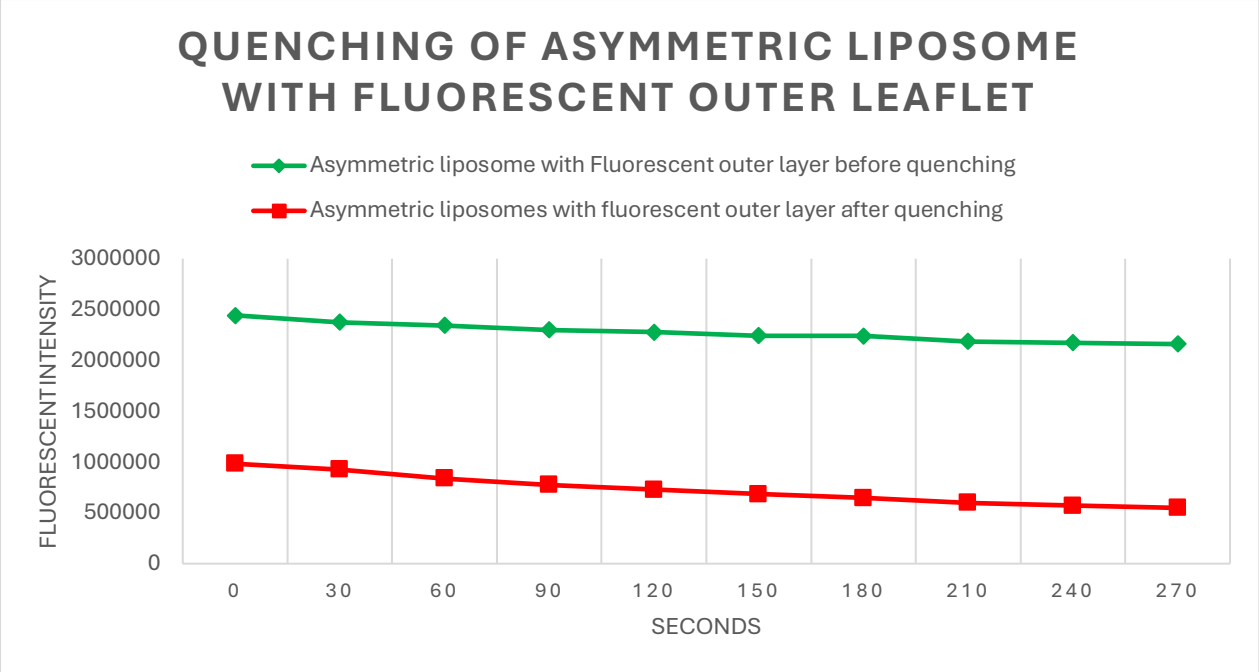

Figure 3. 44: Quenching of fluorescent asymmetric liposomes with fluorescent outer leaflet

To test the same theory, another formulation was made where the NBD-lipid was located in the inner leaflet. As shown in figure (3.45), the FI did not reduce after the addition of sodium dithionite as the NBD is mainly present in the inner leaflet. The FI before quenching had an average value of 2705392 which was reduced to 2418800 that yields ~10.6% reduction which is negligible and indicates that most of the NBD is present in the inner leaflet.

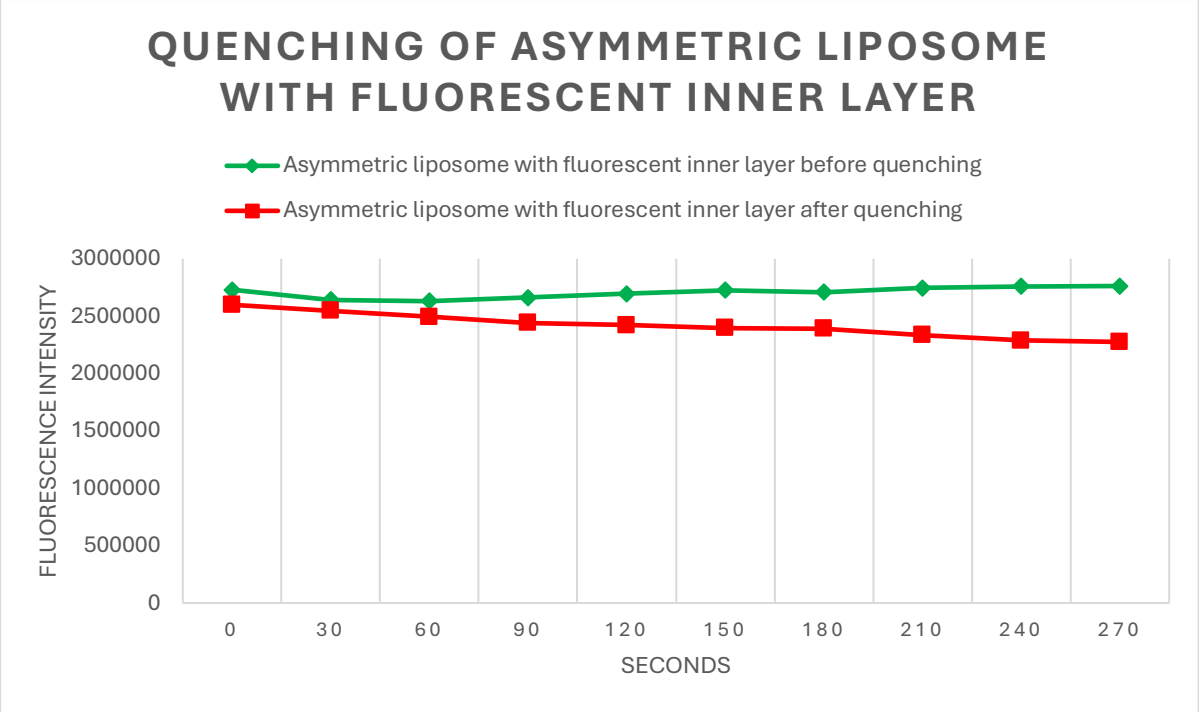

Figure 3. 45: Quenching of fluorescent asymmetric liposomes with fluorescent inner layer

6. The advantage and limitation of the novel method used to complex lipid within cyclodextrin

This novel method has the ability to overcome issues associated with current literature methods. The method created by E. London group (3) is very useful in terms of the variety of lipids that can be used. However, if a certain lipid is needed as a donor (in the outer leaflet) and this lipid cannot form a vesicle on its own e.g. DOTAP, then the conventional cyclodextrin-exchange cannot be used as it requires the formation of an MLV as a donor. This issue is resolved by our modified method as no vesicle formation is required and the donor is created as a complex only. Therefore, lipids that cannot form a liposome on its own e.g. DOTAP can be formulated as a donor lipid-CD complex.

The method created by Markones *et al* (61,62) to formulate a donor complex involves formation of an MLV donor vesicle, addition of the cyclodextrin to the MLV to allow complexation, then breaking down the MLV to release the lipid-CD complexes. Although this method involves complex formation, it does not overcome the issue using lipids that do not form a vesicle on their own. Moreover, this method has a risk of MLV contamination even after breaking down the MLVs as it cannot be guaranteed that all the MLVs will be broken down. In this modified

method, a complex if formed without the need to form an MLV, this reduces the risk of contamination as the complex will be filtered out of the centrifugal filter.

As this modified method does not require vesicle formation for the donor, the acceptor can be formulated in any size e.g. GUV, LUV, MLV, & SUV. This is because the separation method does not relay on size or weight of the vesicle to separate the donor and acceptor as the complex will be filtered out of the centrifugal filter regardless of the vesicle size. Additionally, in this method, the vesicles formed are more stable as no high concentrations of sucrose is needed. In E.London's method, sucrose is added to the acceptor vesicle which can introduce vesicle instability due to osmolarity. However, in Heberle *et al* method, a high concentration is added to the donor vesicle which is then mixed with the acceptor vesicle where the presence of sucrose can introduce instability due to the osmolarity imbalance which could affect the acceptor vesicle. Moreover, in order to separate the asymmetric liposome formed from the MLV, ultracentrifugation is needed. While in this method, required very low centrifugation speeds.

Although this method has several advantages, it has some challenges. This method has a risk of micelles formation during the complexation method, however, this can be reduced by sonicating the suspension in a bath sonicator for an 30minutes to an hour. Moreover, some lipids may not complex with the cyclodextrin as not all lipids have been studied in this research.

7. Summary

As novel method was created using the solvent evaporation method modified by the use of cyclodextrin to formulate asymmetric liposomes. This method does not require MLV formation as the donor is formulated as a lipid-cyclodextrin complex. This modification overcomes many issues associated with current literature methods to formulate asymmetric liposomes.

Chapter 4

Formulating asymmetric liposomes with bromocresol green as a model drug using the novel cyclodextrin-lipid complex method

1. Overview

A novel cyclodextrin-lipid complex method was used to formulate asymmetric liposomes. Thus, the liposomes formulated using this method require analysis to determine their properties and characteristics; different liposomal formulations were used to compare and identify which formulation is most optimised using this novel method.

Negatively charged drugs, e.g. genetic materials, methotrexate, and some anticancer drugs, are significantly susceptible to degradation. Immune response sensitisation, phagocytosis, serum nucleases degradation, and rapid renal clearance, in addition to low cellular uptake and target specificity, are vulnerabilities that make the delivery of negatively charged drugs unsuitable and ineffective, allowing them to be eliminated from the body rapidly and leading to low bioavailability. To successfully deliver the drug to targeted cells, a carrier must be present to form a stable complex with the encapsulated drug; the complex must be able to survive in the blood circulation by avoiding early recognition by macrophages and reaching the targeted cells (130).

To test the efficiency of asymmetric liposomes in loading and maintaining negatively charged drugs, bromocresol green (BCG) was used as a model drug. BCG is a pH indicator that is negatively charged at pH 3.8-5.4; it changes colour from yellow to blue-green, and it is used widely in medical and biological experiments (131). BCG was used in this study to test the liposomes' characteristics, as BCG can mimic negatively charged drugs due to its charge, and is readily available and easy to use for analysis.

2. Aim

This chapter aims to test the properties of different lipids in various liposomal formulations to identify the most optimised lipids for formulating a stable asymmetric liposome that can efficiently load negatively charged drugs.

3. Formulation of symmetric and asymmetric liposomes

The symmetric and asymmetric liposomes were formulated as mentioned in the methodology section. To check entrapment efficiency, two different loading methods were trialled. The drug was added during the hydration process and then tested. The drug was added after the liposomes were formed and then the liposomes were tested. For each formulation, the experiment was repeated twice and tested three times.

4. Results and discussion

4.1. Formulation of symmetric neutral liposomes

Phospholipids, the main component in formulating liposomes, consist of two main types according to the alcohols in their structure. Glycerophospholipids are the primary occurring type in eukaryotic cells; they all contain a glycerol in the backbone, while they differ in headgroups, hydrophobic chain saturation and the bonding type between aliphatic moieties and glycerol backbone. The other type are sphingomyelins; they differ from glycerophospholipids by having a sphingosine backbone, and they tend to form powerful interactions with cholesterol (132). Phosphatidylcholine (PC), phosphatidylethanolamine (PE), phosphatidylserine (PS) and sphingomyelin (SM) make up most of the cell bilayer membrane (133).

The main advantage of using zwitterionic (neutral) phospholipids to formulate liposomes is that their charge-neutral nature allows them to transport through the bloodstream without interactions or adsorption of proteins and negatively charged blood components (134,135). Moreover, neutral charged liposomes were shown to have the least toxicity when compared with net negative and net positive charged liposomes (136). A study done by Adams and colleagues in 1977 (137) has shown that adding 9 mol% of charged phospholipids and making the liposomes charged negatively or positively has increased toxicity, where net negative charge caused epileptic seizures and rapid death in animals; net positive charge, on the other hand, caused widespread brain damage and respiratory failure. The neutral charge formulation had the lowest reactions and morphological changes (137).

Alternatively, neutral liposomes have some disadvantages, the main one being that their encapsulation efficiency is lower compared to charged liposomes, which are capable of achieving very high encapsulation efficiencies due to electrostatic interactions (138,139).

Another challenge with neutral liposomes is stability. Due to the lack of repulsive forces, neutral liposomes have a higher tendency to aggregate when compared to charged liposomes; therefore, they have a low physical stability (140).

To identify which neutral phospholipids are most stable when formulating liposomes, three different neutral phospholipids were tested; 1-palmitoyl-2-oleoyl-glycero-3-phosphocholine (POPC), 1-palmitoyl-2-oleoyl phosphatidylethanolamine (POPE), and brain sphingomyelin (SM). The process involved formulating the phospholipids using thin film hydration at a ratio of 60% phospholipids to 40% cholesterol. To compare the behaviour of different formulations, the size and zetapotential were measured.

Sonication involves the use of acoustic energy from the bath, which induces pressure on the vesicles, leading to breakage. This process results in the formation of smaller unilamellar or multilamellar vesicles, where the size is directly affected by the time of sonication (141). Although sonication is a widely used process in size reduction, the main challenge with it includes less reproducibility of liposomal diameter and bath-to-batch differences (141). As shown in table 4.1, the size of the formulations was very large before sonication and was reduced after 30 minutes of sonication. This suggests that sonication can be an effective method for reducing particle size.

Based on literature, POPC was formulated using thin film hydration, the process involved formulating the POPC liposomes, then sonication for 10minutes at 25°C, followed by passing the liposomes fifteen times through 100 nm polycarbonate membranes (142). This resulted in liposomes with an average size of 127nm, PDI of 0.11, and a zetapotential of -5.1±0.9mV (142). The use of the polycarbonate membrane ensured a small and consistent particle size. However, the storage stability of size and zetapotential was not studied. In different studies, the size of POPC liposomes was shown to be between 8000-80,000nm (concentration of 0.5mM) due to the lack of sonication and extrusion (143). This highlights the significance of sonication and extrusion in achieving size reduction.

POPC + CHOLESTEROL (PCC) (Figure 4.1) represents a formulation containing POPC and cholesterol only; the size before sonication was extremely large (1370.63nm ±201.49), which was reduced to 179.17nm ±41.16 after sonication (Table 4.1). Moreover, the PDI reduced from 0.90 ±0.12 to 0.46 ±0.06, which indicates that the formulation became less polydisperse. The large unilamellar vesicles (LUVs) formed after sonication had a ZP value of -2.92mV ±0.43 which is expected in formulations containing zwitterionic lipids.

Figure 4. 1: POPC + CHOLESTEROL (PCC) under the optical microscope before sonication (40X magnification)

Liposomes formulated using POPE only were not found in the literature. However, a study measured the size of POPE with the addition of 10% α-TOS, and the results have shown that a size of 140nm was measured for POPE liposomes (144). The liposomes were formulated using thin film hydration and polycarbonate membrane extrusion (144). Hence, the size was small.

POPE + CHOLESTEROL (PEC) (Figure 4.2) represents a formulation that contains POPE and cholesterol where the size before sonication was 1358.14 ±332.02 which reduced to 574.81 ±75.01 (table 4.1), although there was a large reduction in the size, the liposomes were still too big to be considered LUVs; the inability of PEC to form LUVs could be due to the formulation being unstable. The PDI was also largely reduced from 0.70 ±0.17 to 0.44 ±0.06, indicating the formulation is less polydisperse. Additionally, a ZP value of -5.39 ±0.32 confirms the presence of neutral lipids in the formulation.

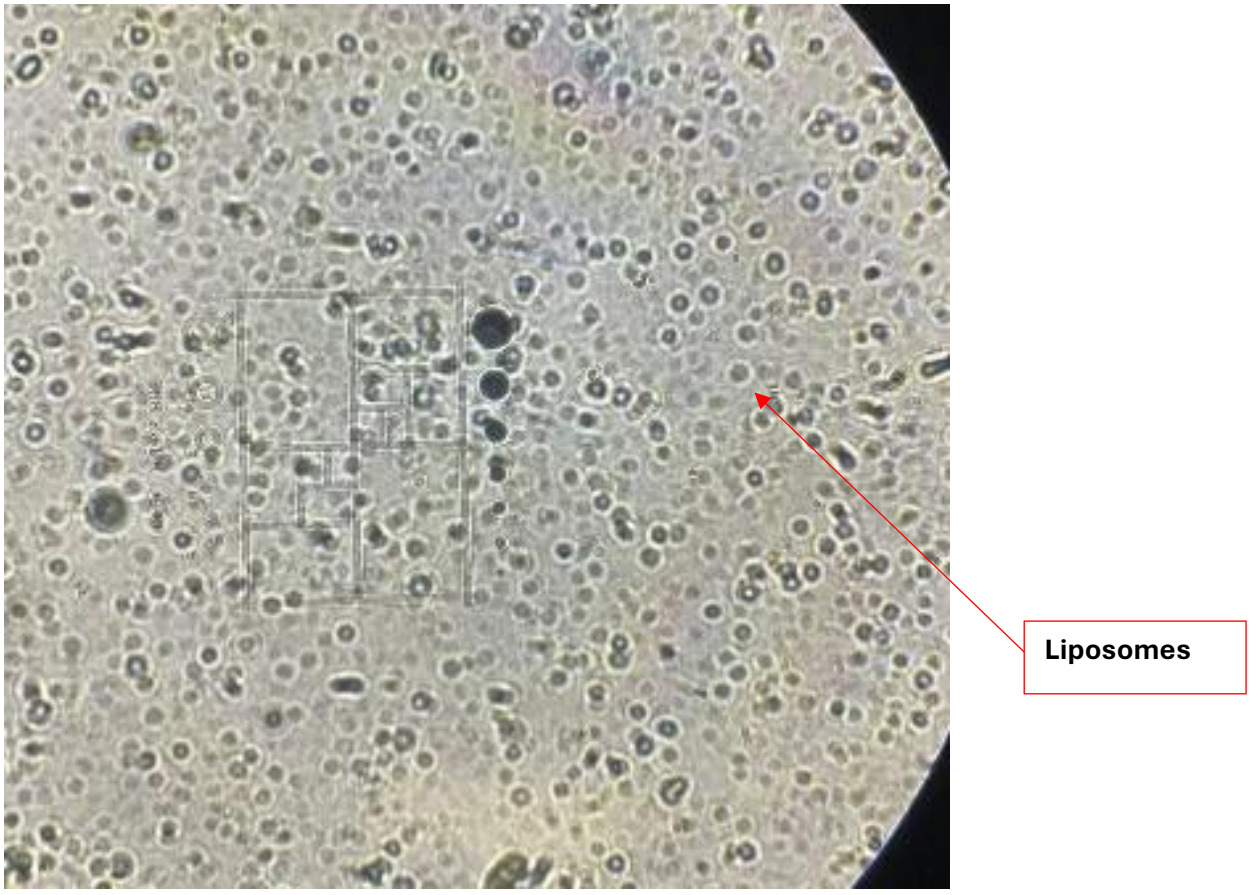

Figure 4. 2: POPE + CHOLESTEROL (PEC) under the optical microscope before sonication (40X magnification)

In literature, sphingomyelin liposomes were able to form by using the thin film hydration plus freeze-thawing method and polycarbonate membrane extrusion (145). Different-sized liposomes were created, ranging from 100-240nm, and the storage stability was measured in PBS smaller sized liposomes were able to maintain a stable size up to 7 days after formulation (110 and 190nm), while larger liposomes (up to 240nm) had a size increase over the 7 days (145). This suggests that freeze-thawing and membrane extrusion could be an important step in formulating sphingomyelin liposomes. The SM + CHOLESTEROL (SMC) formulation was unable to form liposomes using the thin film hydration method (Figure 4.3). It resulted in large aggregates that were separated from the solution, leading to phase separation, and the solution remained clear and not turbid. The sonication process did not break down these aggregates, which indicates that the formulation is too unstable to form liposomes.

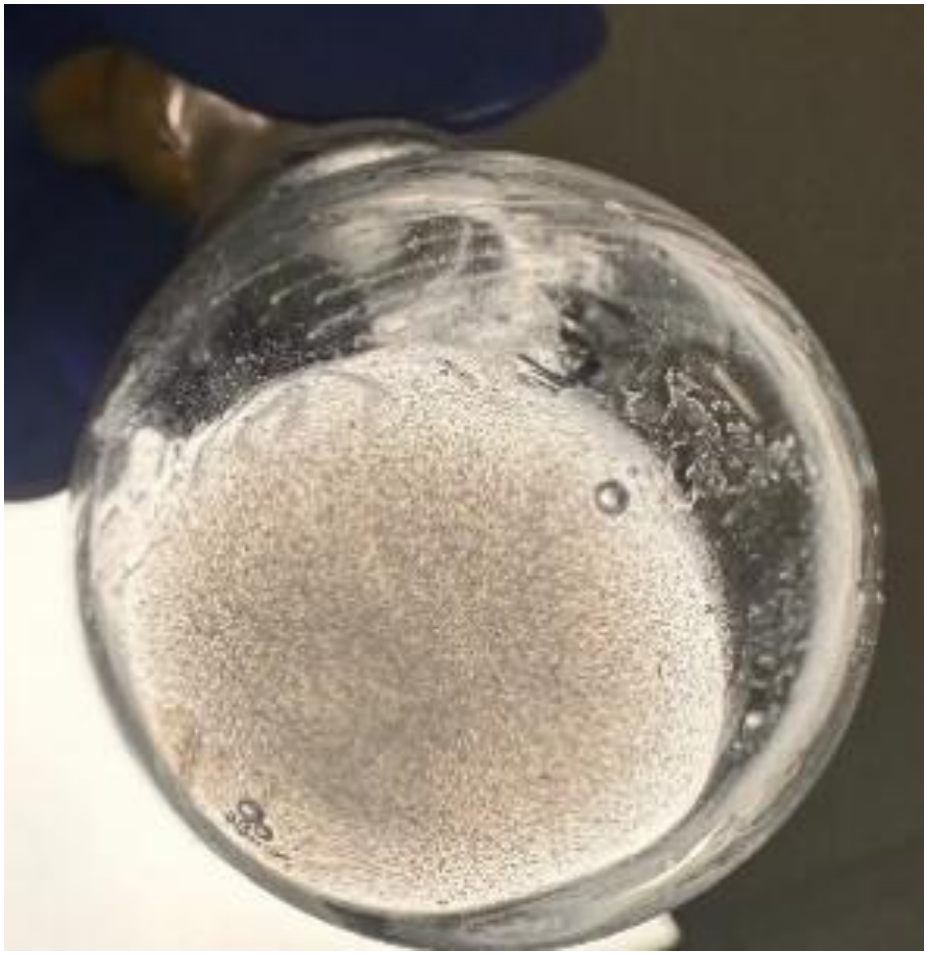

Figure 4. 3: SM + CHOLESTEROL (SMC) was not able to form liposomes after rehydration of the lipid film (phase separation of solution)

Table 4. 1: The results for size and ZP of the formulations with no drug (for formulation composition refer to table 2.8)

Formulation	Size before sonication (nm)	PDI	Size after sonication (nm)	PDI	Zeta potential (ZP) (mV)
POPC + CHOLESTEROL (PCC)	1370.63 ±201.49	0.90 ±0.12	179.17 ±41.16	0.46 ±0.06	-2.92 ±0.43
POPE + CHOLESTEROL (PEC)	1358.14 ±332.02	0.70 ±0.17	574.81 ±75.01	0.44 ±0.06	-5.39 ±0.32
SM + CHOLESTEROL (SMC)	NA		NA		NA

Neutral liposomes have a higher degree of aggregation and lower physical stability due to the lack of repulsive forces (140). In the study, after 24 hours (at 4°C), the liposomal formulations were visualised to determine stability.

POPC + CHOLESTEROL (PCC) (Figure 4.4) had a small amount of aggregates precipitating on the wall of the tube, which is expected as neutral liposomes tend to aggregate due to the lack of

repelling force by charged lipids. Additionally, the suspension remained less turbid when compared to the POPE + CHOLESTEROL (PEC) suspension (Figure 4.5). PEC (Figure 4.5) shows aggregation at the bottom of the tube, as well as a turbid suspension, which indicates a large amount of aggregation occurring within the 24 hours.

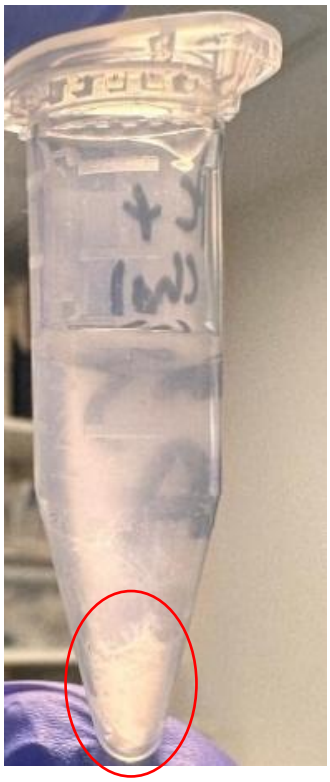

Figure 4. 4: POPC + CHOLESTEROL (PCC) after 24 hours at 4℃

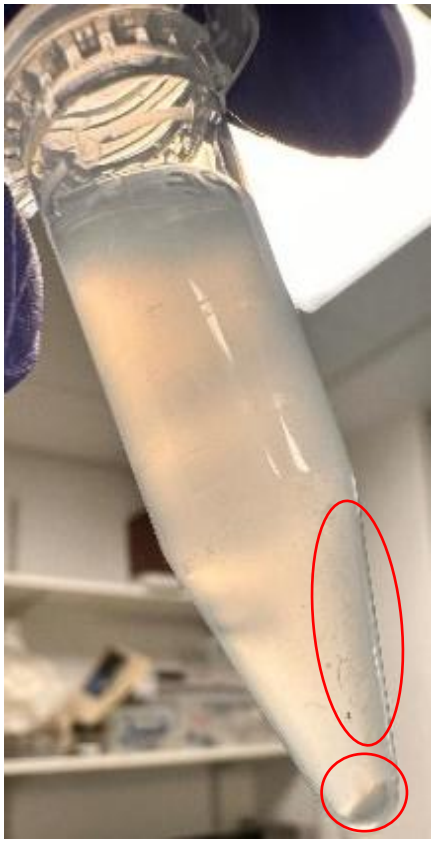

Figure 4. 5: POPE + CHOLESTEROL (PEC) after 24 hours at 4℃

The formulations were prepared using bromocresol green (BCG) as the drug to study the effect of BCG on the formulations. BCG is a negatively charged dye; in this instance, it was used to act similarly to negatively charged drugs inside the liposomes.

The characterisation involved measuring the size and zetapotential of the formulations with entrapped drug as shown in table (4.2).

Table 4. 2: The results of size and ZP of the formulations with bromocresol green (drug)

Formulation + Drug (D)	Size before sonication (nm)	PDI	Size after sonication (nm)	PDI	Zeta potential (ZP) (mV)
POPC + CHOLESTEROL (PCCD)	1442.63 ±325.95	0.81± 0.10	295.72 ±37.64	0.45 ±0.06	-2.19 ±0.37
POPE + CHOLESTEROL (PECD)	1124.56 ±243.66	0.73 ±0.14	340.03 ±68.17	0.37 ±0.04	-4.08 ±1.36
SM + CHOLESTEROL (SMCD)	4613.17 ±1288.25	0.95 ±0.11	347.15 ±24.36	0.51 ±0.05	-4.11 ±0.84

As shown in table 4.2, POPC + CHOLESTEROL+ DRUG (PCCD) with entrapped BCG during the liposomal hydration had an average size of 1442.63nm ±325.95 before sonication which reduced dramatically to 295.72nm ±37.64 with a reduced PDI from 0.81± 0.10 to 0.45 ±0.06. Although the formulation had a reduction in size, the size is still larger than the size of the liposome when formulated empty of drug. This indicates that adding the drug could lead to an increase in the size of liposomes.

POPC + CHOLESTEROL+ DRUG (PECD) had undergone improvement in size when formulated with entrapped BCG. The size reduced from 1124.56nm ±243.66 (PDI 0.73 ±0.14) to 340.03nm ±68.17 (PDI 0.37 ±0.04). This value is markedly smaller than the size of empty liposomes. This could indicate that formulating this formula with drug entrapped leads to better stability.

SM + CHOLESTEROL+ DRUG (SMCD) had a significant difference in results when formulated with drug entrapped; when formulated as empty liposomes, this formulation did not have the ability to formulate a liposome, while when the drug was added, it was able to formulate liposomes. As shown in figure 4.6, although liposomes were formed, large aggregates can be seen due to unstable formulations. Initially, the size of the liposomes was 4613.17nm ±1288.25 with a PDI of 0.95 ±0.11, this was reduced to 347.15nm ±24.36 (PDI 0.51 ±0.05) after sonication. These results indicate the formation of liposomes using SM as the main lipid when the drug is entrapped. This could mean that BCG interacts favourably with the lipid bilayer of SM, providing additional structural support and enhancing stability.

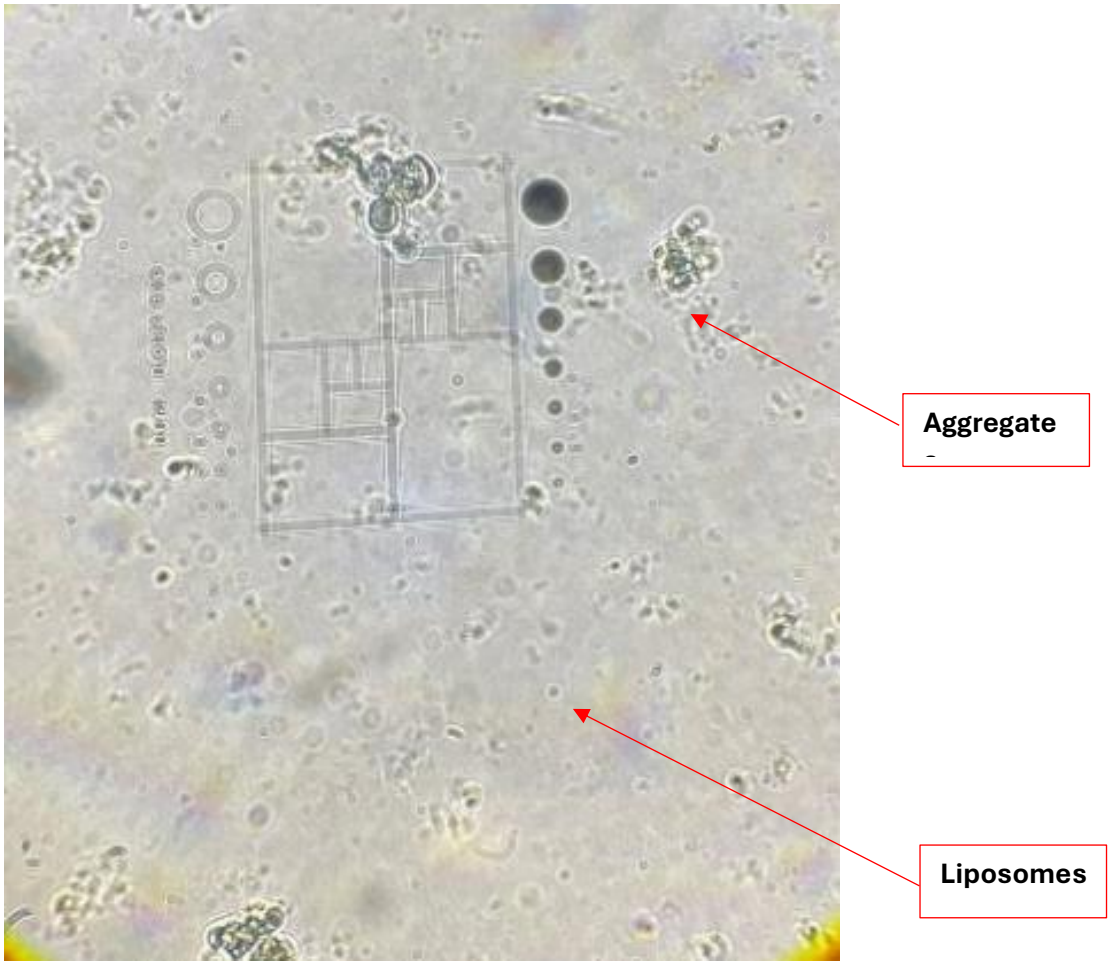

Figure 4. 6: SM + CHOLESTEROL+ DRUG (SMCD) under the microscope before sonication (40X magnification)

After 24 hours (at 4°C), the liposomal formulation was visualised to determine stability. PCCD (Figure 4.7), did not have any visual precipitates. Alternatively, PECD (Figure 4.8) and SMCD (Figure 4.9) had clear precipitation, indicating the formulations are less stable and tend to aggregate more than PCCD. Additionally, SMCD had larger amounts of aggregates compared to PECD, indicating that SMCD is the least stable formula, while PCCD is the most stable formula.

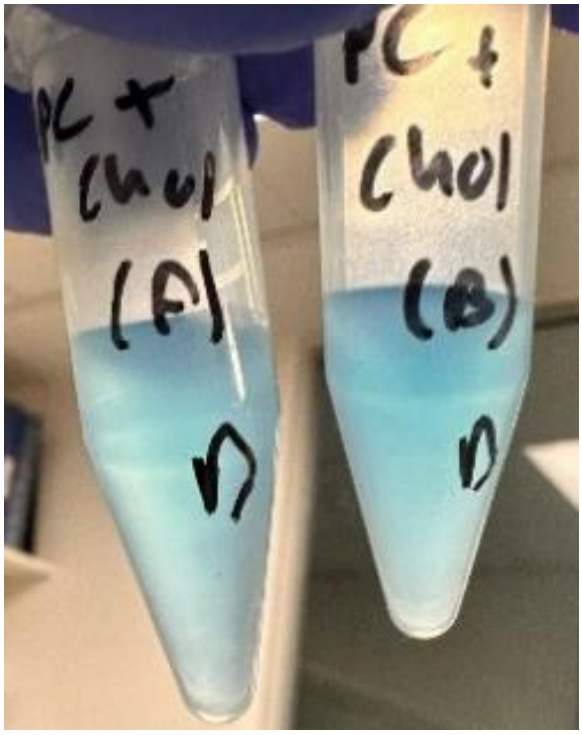

Figure 4. 7: POPC + CHOLESTEROL+ DRUG (PCCD) after 24 hours at 4℃

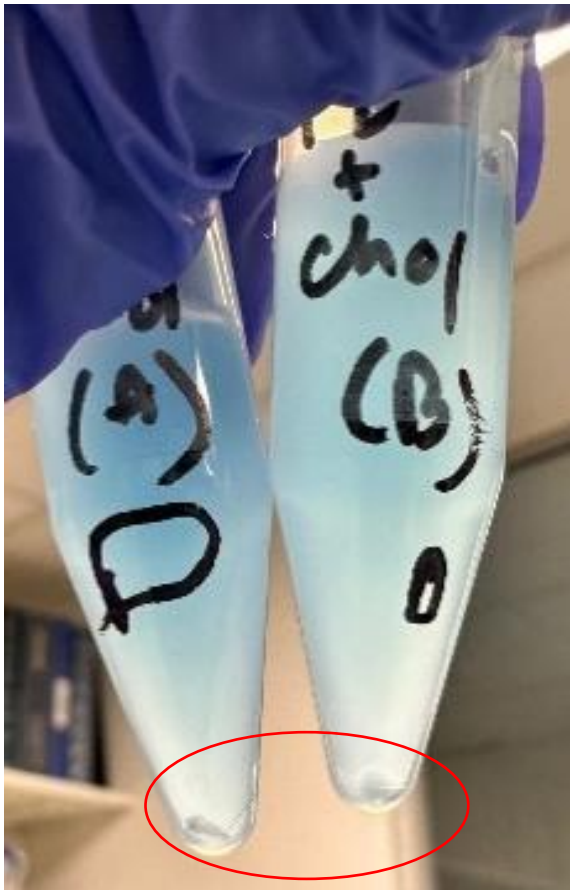

Figure 4. 8: POPE + CHOLESTEROL+ DRUG (PECD) after 24 hours at 4℃

Figure 4. 9: SM + CHOLESTEROL+ DRUG (SMCD) after 24 hours at 4℃

5.2. Effect of adding a charged phospholipid to liposomal formulations

Based on the results from the previous section, SM phospholipid had the least stability when compared to POPC and POPE; therefore, it was discarded. Thus, further modifications were trialled on POPC and POPE only. In this section, the effect of adding DOTAP, a positively charged phospholipid, will be studied to determine the best formula.

The use of charged phospholipids has certain advantages and challenges. Charged liposomes have a negative or positive headgroup, which makes the liposomal surface charged (146). The charged surfaces enable electrostatic repulsion between the liposomes, thereby reducing

aggregation (147). Moreover, the presence of charge allows for electrostatic interaction between the charged drug and the charged liposomes when opposite charges are used. This enhances the encapsulation efficiency of the liposomes, as the drug is attracted to them (148). This is evident in a study by Alhariri and others on the loading of gentamicin, where neutral and negatively charged liposomes were used. The results showed that increasing the negative charge of the liposomes increased the encapsulation efficiency of gentamicin, as gentamicin is a positively charged drug (149). When DPPC (neutral lipid) was used to formulate liposomes, the %EE had an average of 1.8 ± 0.15. However, when DMPG (negative) was added to DPPC liposomes, the %EE increased to an average of 37.2±0.46-43.6±0.65 at different ratios. This significant increase proves the importance of adding charged liposomes in terms of %EE (149). Similarly, cationic liposomes increase the entrapment of negatively charged molecules, nucleic materials such as DNA and RNA, which have a negative charge. Thus, the use of cationic liposomes was found to be the most optimised in encapsulating nucleic materials (5). Furthermore, it was demonstrated that the complexation of nucleic acids with positively charged phospholipids increased the stability of the nucleic acids, as well as enhancing their resistance to nuclease degradation (7). To study the effect of liposomes' charge on entrapment efficiency, ovalbumin, a negatively charged glycoprotein, was entrapped in cationic and anionic liposomes (150). Cationic liposomes entrapment was greatly affected by the buffer used; in phosphate buffer (PB), the entrapment efficiency ranged between 43.5% when a high amount of ovalbumin was used (7.5mg), while it increased up to 78.3% when a lower amount of ovalbumin was used (1mg). When 10% sucrose was added, the entrapment efficiency increased to 47.6% (7.5 mg ovalbumin used) and 87.2% (1 mg ovalbumin used) (150). However, when NaCl was added to the solution, the EE decreased, and as the concentration of NaCl increased in PB, the entrapment efficiency also reduced (150). On the other hand, using anionic liposomes to entrap ovalbumin led to a very low EE, reaching as low as 27-28% (150). This shows the importance of adding a charge in the entrapment of molecules within liposomes.

However, the presence of a charge increases the toxicity of liposomes. Cationic liposomes were found to have higher degree of toxicity when compared to negatively charged liposomes (151). Moreover, cationic liposomes were found to be highly toxic to macrophages and monocyte-like U937 cells, while not toxic to resting T-lymphocytes. Additionally, the higher the positive zetapotential of the cationic liposomes, the higher the cytotoxicity (136).

The size and zetapotential were measured to compare the formulations as shown in table (4.3). POPC + DOTAP +CHOLESTEROL (PCDC) formulation had an average size of 346.29nm ±79.48 before sonication which reduced to 215.20nm ±25.09 after sonication. Although marked

changes can be seen in the size of the liposomes, the PDI was not greatly affected. Moreover, to confirm the presence of DOTAP, ZP was measured which gave a value of 19.90mV ±2.17 indicating presence of a positive charge.

POPE + DOTAP +CHOLESTEROL (PEDC) formulation containing POPE as the neutral lipid had a larger average size before sonication (when compared to PCDC) of 622.86nm ±88.35 which reduced drastically to 148.06nm ±53.97 after sonication. Furthermore, the PDI had a large decrease from 0.61 ±0.14 to 0.31 ±0.14 indicating the formation of a less polydisperse formulation. The presence of DOTAP was confirmed by having a ZP value of 24.69mV ±1.42.

Table 4. 3: The size and ZP of the formulations as empty liposomes

Formulation	Size before sonication (nm)	PDI	Size after sonication (nm)	PDI	Zeta potential (ZP) (mV)
POPC + DOTAP +CHOLESTEROL (PCDC)	346.29 ±79.48	0.41 ± 0.05	215.20 ±25.09	0.41 ± 0.02	19.90 ±2.17
POPE + DOTAP +CHOLESTEROL (PEDC)	622.86 ±88.35	0.61 ±0.14	148.06 ±53.97	0.31 ±0.14	24.69 ±1.42

The exact formulations were tested when BCG, a negatively charged drug, was entrapped during the lipid hydration stage. As shown in table (4.4), the size of both formulations, with drug, after sonication has reduced when compared to the formulation without drug. This could indicate improved stability when the drug is added. Additionally, the PDI was reduced to a dramatically lower value, indicating the liposomes are more monodispersed after sonication and when adding the drug. The ZP remained at a similar value as the drug is entrapped inside the liposomes and will not affect the ZP value.

Table 4. 4: The size and ZP of the formulations with drug (bromocresol green) during film hydration stage

Formulation	Size before sonication (nm)	PDI	Size after sonication (nm)	PDI	Zeta potential (ZP) (mV)
POPC + DOTAP +CHOLESTEROL (PCDCD)	279.01 ±10.32	0.42 ±0.02	126.54 ±1.04	0.21 ± 0.02	23.90 ±0.88
POPE + DOTAP +CHOLESTEROL (PEDCD)	504.35 ± 14.80	0.47 ±0.08	111.25 ±0.59	0.22 ±0.01	24.36 ±0.09

To further study the effect of drug on size and zetapotential, the liposomal formulations were formulated as empty, then the drug was added later, incubated at room temperature (23°C) for 15 minutes, then measured size and ZP. As shown in table (4.5), POPC + DOTAP +CHOLESTEROL +DRUG (PCDCD) formulation remained somewhat of a similar size to empty liposomes (215.20nm, 199.27nm). POPE + DOTAP +CHOLESTEROL +DRUG (PEDCD) on the other hand, had a huge size increase compared to empty liposomes (148.06nm, 246.96nm). these results could suggest that when formulating PEDCD, adding the negative drug during the lipid film hydration has a better effect on the size. However, the size of PCDCD has the ability to remain stable when formulating using different methods.

Table 4. 5: The size and ZP of the formulations with drug (bromocresol green) after liposomal formulation

Formulation	Size (nm)	PDI
POPC + DOTAP +CHOLESTEROL +DRUG (PCDCD)	199.27 ±33.85	0.35 ±0.06
POPE + DOTAP +CHOLESTEROL +DRUG (PEDCD)	246.96 ±22.41	0.43 ±0.06

The primary benefit of adding a positive charge to liposomes is to enhance the entrapment efficiency (EE) of the liposomes; the drug was added to the liposomes during the lipid hydration stage. To study the effect of charge on EE, the entrapment was measured using UV light. The method involved separating the liposomes from free drug using centrifugation, then measuring the UV absorption of the pellet and supernatant separately. After that, adding the values of pellet and supernatant to get the "total" value, then dividing the pellet value by the total value. Absorbance was converted to concentration values using the calibration graph provided in the methodology section.

Equation 4: $\%EE = \frac{CONC\ of\ pellet}{CONC\ of\ total\ (pellet+supernatant)} \times 100$

As shown in table (4.6), when looking at the formulations containing only neutral lipids, POPC was found to have the highest EE compared to POPE and SM. This indicates that the PCC formulation is the most stable neutral formulation.

When DOTAP was added to increase the EE, it is visible that with PCDC, an increase in EE was seen, which is expected due to the presence of a positively charged lipid. On the other hand, the EE of PEDC did not increase; this is likely due to the formulation being unstable and leading to drug release.

However, in table (4.7), the results have differed. The entrapment efficiency of neutral liposomes was near zero, with SM not forming liposomes. On the other hand, when DOTAP was added, the %EE increased in both PCDCD and PEDCD formulations. This could indicate that entrapping BCG after the formation of liposomes is a better technique for encapsulating BCG.

Table 4. 6: Entrapment efficiency of different formulations when drug (bromocresol green) is added during hydration

Formulation	% EE
POPC + CHOLESTEROL (PCC)	17.17 ±4.78
POPE + CHOLESTEROL (PEC)	6.81 ±1.86
SM + CHOLESTEROL (SMC)	8.10 ±0.92
POPC + DOTAP + CHOLESTEROL (PCDC)	30.44 ±4.45
POPE + DOTAP + CHOLESTEROL (PEDC)	8.10 ±1.51

Table 4. 7: Entrapment efficiency of different formulations when drug (bromocresol green) is added after liposomal formulation

Formulation	% EE
POPC + CHOLESTEROL (PCCD)	1.49 ±0.10
POPE + CHOLESTEROL (PECD)	1.39 ±0.007
SM + CHOLESTEROL (SMCD)	NA
POPC + DOTAP + CHOLESTEROL (PCDCD)	62.84 ±7.84
POPE + DOTAP + CHOLESTEROL (PEDCD)	74.25 ±4.41

5.3. Comparison between symmetric and asymmetric liposomes

The main distinction between the two types is that symmetric liposomes contain the same phospholipid types and distribution across both leaflets of the liposomal bilayer, while asymmetric liposomes contain different phospholipid composition in each leaflet (53). This property of asymmetric liposomes gives them an advantage over symmetric liposomes, as it allows for the independent enhancement of inner and outer leaflet properties. This can lead to benefits, including using lipids that enhance entrapment efficiency in the inner leaflet, e.g. using cationic phospholipids when entrapping negatively charged drugs. While using phospholipids that reduce toxicity and to improve drug delivery in the outer leaflet e.g. using neutral phospholipids to minimise the toxicity liposomes (3,53). On the other hand, there are some challenges associated with asymmetric liposomes, the main one being the maintenance of asymmetry. Due to the known phenomenon of phospholipids flip/flop, the lipids exchange

their location between the inner and outer leaflets, leading to loss of asymmetry (28). Moreover, differential stress can occur between the leaflets; differential stress is defined as the imbalance in optimal lipid packing density between the leaflets, leading to residual leaflet deformation, and it affects vesicle and asymmetry stability tension (79). This issue is not present with symmetric liposomes as they have tensionless leaflets (59).

Based on the previous analysis, POPC was determined to be the best phospholipid for use. Additionally, POPE could be a potentially useful lipid in the formulation of asymmetric liposomes.

POPC was used as the donor lipid to formulate asymmetric liposomes. The choice of this phospholipid was made based on the fact that it is usually present in the outer leaflet of the cell bilayer, so using POPC as the donor will mimic the cell bilayer (28). Moreover, previous data have shown that POPC is a stable lipid suitable for use. The acceptor vesicle was made using two different phospholipids, POPC and POPE. The choice of POPC was made based on the results from previous tests, aiming to mimic the cell bilayer where PE is present in the inner leaflet.

The size and ZP were measured for the first asymmetric formulation, which had POPC in the outer leaflet and POPE + DOTAP + CHOLESTEROL in the inner leaflet. As shown in table (4.8), the size difference between the symmetric (acceptor) and asymmetric liposomes remained close which indicates the processing technique has a negligible effect on size. However, the PDI has decreased between the acceptor (0.41 ± 0.02) and the asymmetric liposomes (0.21 ± 0.05), which indicates that the asymmetric liposomes are more monodisperse.

To confirm asymmetry, the zetapotential method was used. As shown in table (4.9), the zetapotential of the donor was -2.41mV and the acceptor was 24.69mV. The final asymmetric liposomes had a value of 9.18 mV, which indicates that the outer leaflet became more neutral due to the addition of POPC and the removal of DOTAP.

Table 4. 8: The size data for POPC (OUT) / POPE + DOTAP+CHOLESTEROL (IN)

Formulation	Size Acceptor (nm)	PDI	Size Asymmetric (nm)	PDI
POPC (OUT) / POPE + DOTAP+CHOLESTEROL (IN)	148.06 ±53.97	0.41 ±0.02	166.12 ±24.39	0.21 ±0.05

Table 4. 9: The ZP data for POPC (OUT) / POPE + DOTAP+CHOLESTEROL (IN)

Formulation	ZP Donor (mV)	ZP Acceptor (mV)	ZP Asymmetric (mV)
POPC (OUT) / POPE + DOTAP+CHOLESTEROL (IN)	-2.14 ±0.31	24.69 ±1.42	9.18 ±1.63

The formulation containing POPC as the donor and POPC + DOTAP + CHOLESTEROL as the acceptor was tested. As shown in table (4.10), there was some size reduction in the asymmetric liposomes when compared to the acceptor, the reduction could be as a result of the removal of phospholipids by the cyclodextrin which can lead to breaking of some liposomes. Moreover, the PDI has reduced from 0.41 to 0.27, which indicates that the asymmetric liposomes are more monodisperse.

To confirm asymmetry formation, the zetapotential method was used. As shown in table (4.11), the ZP for the donor was -2.83mV and the acceptor was 19.90mV. The value was reduced to 7.65 mV when the asymmetric liposomes were formed, which indicates that most of the DOTAP was removed from the outer leaflet and POPC was added.

Table 4. 10: The size data for POPC (OUT) / POPC + DOTAP+CHOLESTEROL (IN)

Formulation	Size Acceptor (nm)	PDI	Size Asymmetric (nm)	PDI
POPC (OUT) / POPC + DOTAP+CHOLESTEROL (IN)	215.20 ±25.09	0.41 ±0.02	126.07 ±5.65	0.27 ±0.06

Table 4. 11: The ZP data for POPC (OUT) / POPC + DOTAP+CHOLESTEROL (IN)

Formulation	ZP Donor (mV)	ZP Acceptor (mV)	ZP Asymmetric (mV)
POPC (OUT) / POPC + DOTAP+CHOLESTEROL (IN)	-2.83 ±0.72	19.90 ±2.17	7.65 ±1.95

The size and ZP results for both asymmetric formulations were similar. To identify which formulation is the most optimised, the entrapment was measured using UV light. The drug was added to the liposomes after the liposomal formation, then they were incubated at room temperature (23°C) for 15 minutes before doing the measurements. The method involved separating the liposomes from free drug using centrifugation, then measuring the UV of the

pellet and supernatant separately. After that, adding the concentration of the pellet and supernatant to get the "total" value, and then dividing the pellet value by the total value.

As shown in table (4.12), the EE of the symmetric liposomes varies from the asymmetric liposomes. The symmetric formulation containing POPE had a better EE when compared to the POPC formulation. However, when the formulations were made into asymmetric liposomes, the formulation containing POPE lost a large amount of drug, reducing the EE from 74.25% to 29.72% which indicates that this formulation is leakier compared to the POPC containing formulation, where the EE reduced from 62.84% to 41.11%. The formulation containing POPC lipids is considered the most optimised formula as it has higher EE and less drug leakage when converting from symmetric to asymmetric.

Table 4. 12: The %EE of asymmetric liposomes for BCG

	Formulation	%EE
Symmetric liposomes	POPC + DOTAP + CHOLESTEROL	62.84 ±7.84
	POPE + DOTAP + CHOLESTEROL	74.25 ±4.41
Asymmetric liposomes	POPC (OUT) / POPC + DOTAP+CHOLESTEROL (IN)	41.11 ±4.40
	POPC (OUT) / POPE + DOTAP+CHOLESTEROL (IN)	29.72 ±0.36

5.4. Effectiveness of different separation methods to separate encapsulated liposomes

When formulating liposomes, it is important to be able to separate the free drug from the liposomes. To determine which separation method is more effective, three methods were compared: centrifugation, centrifugal filtration, and gel chromatography.

5.4.1. Centrifugation

Centrifugation is a well-established method widely used for separation. Density differences lead to liposomes being pulled by gravitational force to the bottom of the tube and accumulating as a "pellet," while the free drug, with a lower density, remains in the solution (30). Although centrifugation is a well-known method for separation, the main challenge is the

deformation or aggregation that can occur in liposomes when pelleted. Moreover, small particles (<100 nm) cannot be pelleted; therefore, it is only suitable for large particles (152). In literature, it was found that centrifugation is able to retain around 45.4% of liposomes while the rest would remain in the supernatant (153). Moreover, centrifugation can likely disrupt the liposomes and break them into smaller vesicles. Liposomes were centrifuged at 20,000g for 3 hours (153). The breakage in liposomes could lead to smaller molecules and liposomal fragments staying in the supernatant. A long centrifugation time could potentially increase the likelihood of liposomal breakage, as indicated by the results provided in the literature above.

In this study, the CD-lipid complex and the drug both have a minimal density compared to the liposomes. Therefore, when centrifugating the suspension for 1 hour at 15,000 RPM at 4°C, the liposomes form a pellet.

Some of the formulations were able to maintain their size after pelleting. However, others did not. Moreover, the formulation containing POPC in the outer leaflet and POPC+DOTAP+CHOLESTEROL in the inner leaflet was tested when the drug was added after liposomal formulation and when the drug was added during the lipid film hydration. As shown in table (4.13), The liposomes were able to maintain their size more effectively when the drug was added after liposomal formation and not during lipid film hydration.

Table 4. 13: Liposomal size change after centrifugation

Formulation	Size before centrifugation (nm)	Size after centrifugation (nm)
Drug added during hydration	126.54 ±1.04	420.26 ±75.60
Drug added after liposomal formation	215.20 ±25.09	126.07 ±5.65

Although this is a suitable separation method, it has its own set of challenges. Centrifugation can be considered a vicious process that leads to liposomes breaking down and releasing the drug, thus reducing the overall EE (153). Moreover, it cannot be used when the density difference between the materials is small, as a pellet may not form (154). The size of some formulations may increase due to aggregation (152). This method was shown to be the most effective when compared to the other two separation methods (described below).

5.4.2. Centrifugal filtration

Centrifugal filtration is a process that involves using the filter in figure (4.10). The material filtered through the filter is called filtrate, and it contains the free drug and the CD-lipid complex. The material remaining in the upper compartment is called the retentate, and it contains the concentrated asymmetric liposomes. This method can be used when low concentrations of material are used and when conventional centrifugation does not generate a pellet (155). Moreover, it only requires low centrifugation power of up to 4500 RPM, which can be less damaging to the liposomes. Membranes with 100K MWCO were able to retain liposomes within the retentate and remove the cyclodextrins and lipid-CD complexes to the filtrate (60). Moreover, this method was proven very effective in retaining liposomes and removing other smaller material from the suspension; when empty liposomes were tested, 89-99% of liposomes were recovered into the retentate (156), indicating high recovery.

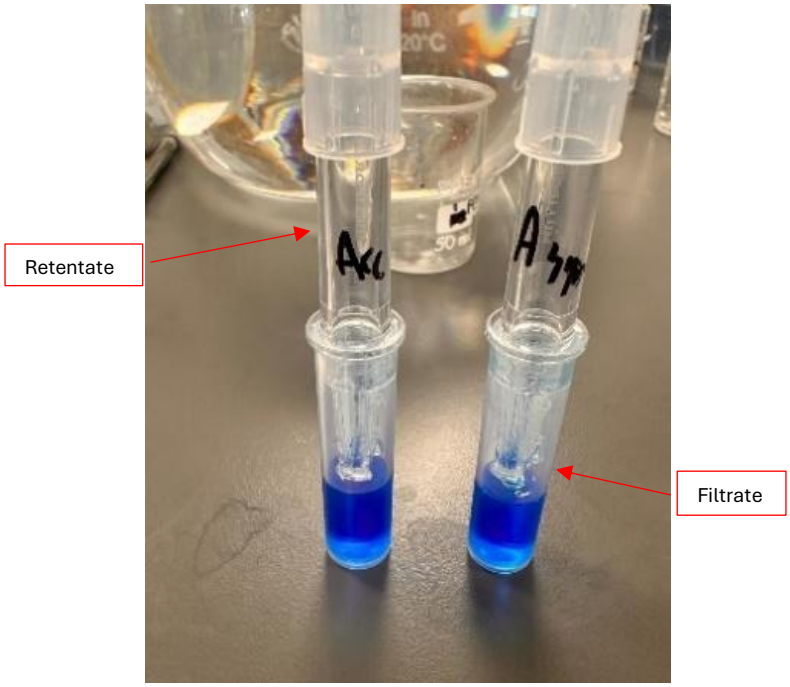

Figure 4. 10: Centrifugal filter with retentate of liposomes and filtrate of free drug

In this study, several issues appeared with this type of separation method, including the filter getting clogged easily, which reduces the filtration efficiency. When using BCG, the drug adhered to the filter during the filtration process, thereby affecting the entrapment efficiency value and leading to false results (Figure 4.11). Therefore, this method can be a useful approach for concentrating empty liposomes; however, it causes an issue when the separation of BCG is required.

Figure 4. 11: The drug (bromocresol green) sticking to the filter

5.4.3. Gel chromatography

This method involves using a Sephadex G-50 gel inside a narrow tube, followed by the application of the required buffer through the gel. After that, the required material can be added to the gel and pushed through the gel using the buffer. The material will separate based on density. Therefore, the liposomes should travel through the gel much faster than the free drug, leading to the separation of the liposomes from the free drug (157).

The biggest issue with this method is that the formulations containing the positively charged lipid, DOTAP, adhered to the gel and did not travel through it. This could be due to the structure of the gel, which consists of dextran and epichlorohydrin (158). As shown in figure (4.12), the formulation is stuck to the gel, a clear solution keeps coming out of the tube but no blue solution, indicating that the material is stuck to the gel.

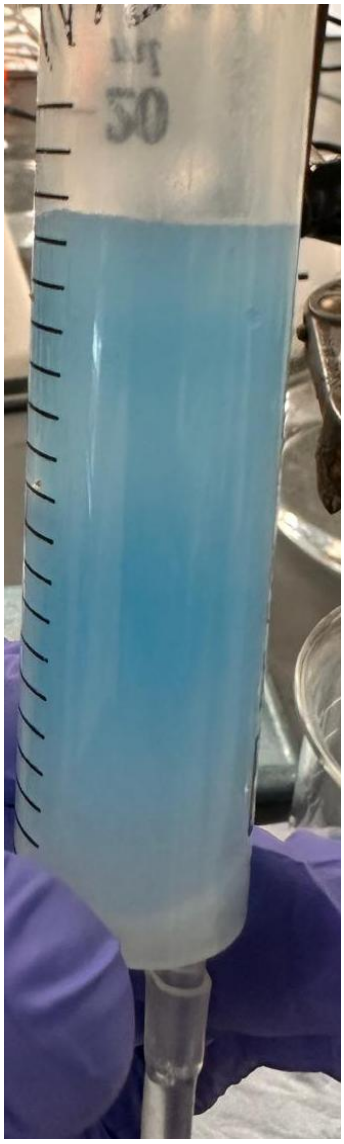

Figure 4. 12: The formulation is stuck to the gel

Moreover, this method was unsuccessful as a separation method for this method of formulation, as no separation occurred between the formulation containing only neutral lipids. This could be due to either very low entrapment efficiency, where only the free drug is collected, or to the density ratio of the formulation not being large enough to cause separation. As shown in figure (4.13), no separation occurred.

Figure 4. 13: No separation occurred between the liposomes and the free drug

5.5. Encapsulation of drug (bromocresol green) during hydration

The encapsulation of the drug during hydration, also called “passive loading”, is the process of hydrating the lipid film with buffer containing the drug. This approach has some limitations, including that it can only be used in water-soluble drugs and usually has a low entrapment efficiency (159). Moreover, passive loading can lead to undesirable membrane incorporation, thus lowering liposomal stability (159).

To study the drug entrapment of the liposomes, the drug was entrapped during the lipid film hydration. This process involves weighing the lipids, dissolving them in chloroform, then drying the solution using a rotary evaporator. This creates a thin film of the dried lipids. To entrap the drug, 0.1 mL of BCG is added to 0.9 mL of buffer, and this solution is used to hydrate the lipid.

This method allows the lipid film to swell and form a vesicle around the drug, thereby entrapping the drug.

This method is useful in entrapping hydrophilic drugs and can lead to high entrapment of some drugs. However, the main disadvantage of this method is that the processing of liposomes, including hydration at high temperatures, sonication, or extrusion, as well as any other additional processing, can damage the drug and lead to the breakdown of both the drug and the liposomes.

As shown in table (4.14), the EE efficiency reached a maximum of 30.44%, this EE is not very high, and this could be due to the processing techniques that lead to the loss of drug as the drug was entrapped during lipid film hydration. Moreover, the centrifugation could have led to breaking of some liposomes and releasing the drug.

Table 4. 14: The entrapment efficiency of BCG in different formulations

Formulation	% Entrapment efficiency
Symmetric- POPC + CHOLESTEROL	17.17 ±4.78
Symmetric- POPE + CHOLESTEROL	6.81 ±1.86
Symmetric- SM + CHOLESTEROL	8.10 ±0.92
Symmetric- POPC + DOTAP + CHOLESTEROL	30.44 ±4.45
Symmetric- POPE + DOTAP + CHOLESTEROL	8.10 ±1.51
Asymmetric- POPC (OUT) / POPC + DOTAP+CHOLESTEROL (IN)	14.51 ±7.80
Asymmetric- POPC (OUT) / POPE + DOTAP+CHOLESTEROL (IN)	17.57 ±0.32

This method has shown that entrapping medicines using passive loading (during hydration) significantly reduces the entrapment efficiency. This is likely due to liposomes being damaged during the multi-step formulation technique, which leads to drug leakage.

5.6. Encapsulation of drug (bromocresol green) after hydration

Entrapment of drugs inside the liposomes can also be done after the liposomes are formulated. This technique involves formulating the liposomes, taking 0.9 mL of the liposomes, and adding 0.1 mL of the drug to the liposomal suspension. After incubating the suspension for 15 minutes, the suspension undergoes centrifugation to separate the free drug from the entrapped drug.

This method can be a good method in entrapping the drug as the drug does not undergo any processing, which reduces the risk of the drug breaking down. However, this method may be unsuitable for certain types of liposomal formulations, as the drug may not enter the formed liposomes efficiently.

As shown in table (4.15), the maximum EE reached up to 74.25% which is the formulation containing POPE and DOTAP. The entrapment efficiency of positively charged formulations is higher than that of neutral formulations due to the presence of DOTAP, which attracts the negatively charged drug. As for the asymmetric liposomes, the formulation containing POPC as the main lipid was able to encapsulate more drug (%EE= 41.11) while the formulation containing POPE in the inner leaflet had lower entrapment (29.72%) (Table 4.15).

Table 4. 15: The entrapment efficiency of BCG in different formulations

Formulation	% Entrapment efficiency
Symmetric- POPC + CHOLESTEROL	1.49 ±0.10
Symmetric- POPE + CHOLESTEROL	1.39 ±0.007
Symmetric- SM + CHOLESTEROL	NA
Symmetric- POPC + DOTAP + CHOLESTEROL	62.84 ±7.84
Symmetric- POPE + DOTAP + CHOLESTEROL	74.25 ±4.41
Asymmetric- POPC (OUT) / POPC + DOTAP+CHOLESTEROL (IN)	41.11 ±4.05
Asymmetric- POPC (OUT) / POPE + DOTAP+CHOLESTEROL (IN)	29.72 ±0.36

5.7. pH gradient to determine drug entrapment

In literature, a pH gradient is mainly used to enhance the encapsulation efficiency of drugs inside liposomes, a process known as remote loading. The process involves a transmembrane pH gradient, where the inner cavity of liposomes contains a different pH than the outer environment. In the outer environment, the drugs are unionised and have high permeability, allowing them to diffuse across the liposomal membrane quickly. Once inside the liposomes, the different pH leads to ionisation of the drug, which reduces its permeability across the membrane. Thus, the drugs remain inside the liposomes (160). However, in this study, a modified pH gradient technique was used to confirm that the drug is entrapped inside the liposomes.

Bromocresol green is a negatively charged pH indicator that changes colour upon the change of pH. BCG turns yellow in acidic media and is blue in neutral to basic media (131). To test the theory, 20µl of 1M HCl was added to 0.1ml (1mg/ml) of BCG in 0.9ml HEPES buffer (10mM), which was able to turn the BCG colour to yellow. Therefore, when adding 0.9ml of liposomal formulation in HEPES buffer to 0.1ml of BCG, then add HCl, if no drug is entrapped, then the suspension must turn yellow. However, if the BCG is entrapped inside the liposomes, it will remain blue in colour within the liposomes, while the free drug outside will turn yellow. A

combination of blue and yellow colours should produce a green colour, indicating drug entrapment in the liposomes.

This test was performed on the formulations containing POPE and POPC only with cholesterol. As shown in figure (4.14), the formulation containing POPC and Cholesterol only turned yellow after adding the HCl, this indicates that there was no drug entrapment when drug was added to the liposomal formulation and incubated for 15 minutes.

Figure 4. 14: pH gradient of the symmetric- POPC + CHOLESTEROL formulation

The same test was done using POPE and cholesterol, as shown in figure (4.15), the same result was seen as the POPC and cholesterol indicating low EE.

Figure 4. 15: pH gradient of the symmetric- POPE + CHOLESTEROL formulation

The same formulations above were repeated with the addition of DOTAP. The results have differed hugely as shown in figure (4.16) and figure (4.17), the colour turned green indicating drug is entrapped inside the liposomes.

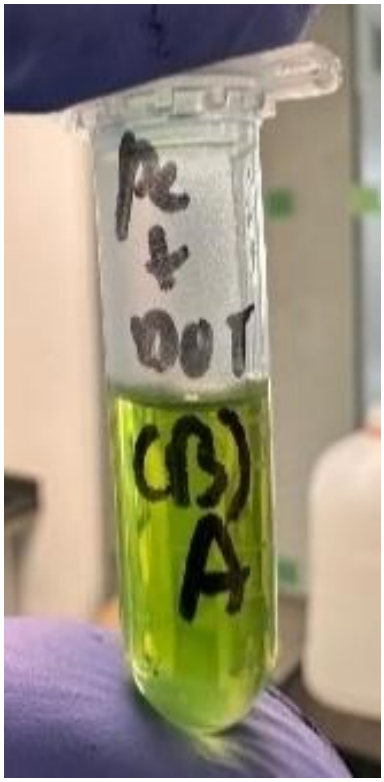

Figure 4. 16: pH gradient of the symmetric- POPC + DOTAP + CHOLESTEROL formulation

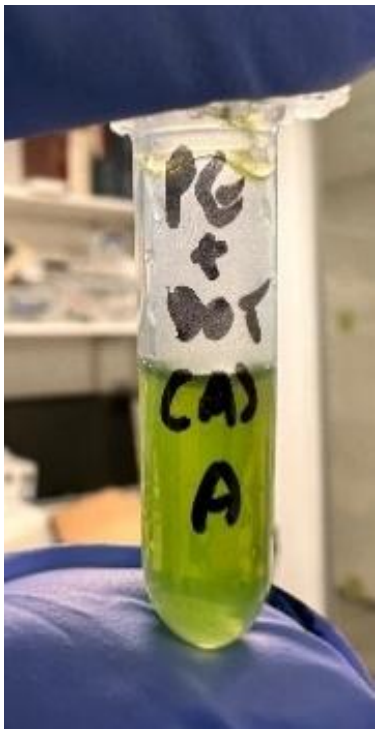

Figure 4. 17: pH gradient of the symmetric- POPE + DOTAP + CHOLESTEROL formulation

This technique was repeated with the asymmetric formulations. As shown in figure (4.18) and figure (4.19), the asymmetric liposomal formulations were able to keep the drug entrapped even after conversion to asymmetric liposomes.

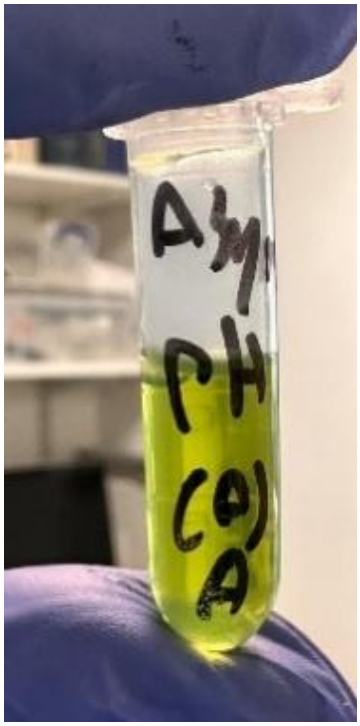

Figure 4. 18: pH gradient of the asymmetric formulation- POPC (OUT) / POPC + DOTAP + CHOLESTEROL (IN)

Figure 4. 19: pH gradient of the asymmetric formulation- POPC (OUT) / POPE + DOTAP + CHOLESTEROL (IN)

This method offers a quick and straightforward technique for qualitatively measuring the entrapment efficiency of pH-dependent, coloured drugs, particularly in the context of pH gradient-dependent liposomal entrapment.

5.8. Optimising the formulation by changing the composition of the liposomes

As mentioned previously, the most optimised asymmetric formulation was POPC (OUT) and POPC-DOTAP-CHOLESTEROL (IN). Therefore, this formulation was chosen, and further modifications were made to it to improve the entrapment efficiency.

The first modification was the trial of increasing the cholesterol %mol from 40% to 60% to potentially increase the stability of the formulation. This formulation had an increase in size from an average of 196.175nm in the acceptor vesicle to 350.05nm in the final asymmetric liposomes formed. This indicates aggregation, which could be due to the processing of liposomes, e.g. centrifugation. Moreover, to confirm asymmetry, the ZP was shown to reduce from 13.30mV to 2.724 mV (Table 4.16).

This modification had a negative effect on the formulation as it reduced the entrapment efficiency to 19.54%. This reduction in EE could be due to the cholesterol level being too high, which makes the liposomes leakier and reduces the EE. Therefore, this modification was not adopted as it did not improve the EE.

Table 4. 16: Characterisation of the new formulation with 60% cholesterol

Formulation	Size (nm)	ZP (mV)
Acceptor	196.175 ± 4.63	13.30 ±0.56
Asymmetric	350.05 ±7.34	2.724 ±0.77

The second modification involved increasing the DOTAP level to 45% to make the formulation more positive. In theory, a more positive inner leaflet will lead to more entrapment of the negatively charged dye. The EE increased to 44.22% indicating that adding more positive charge increased the EE. Moreover, the formulation remained of a stable size after the processing of the acceptor vesicle as shown in table (4.17). Asymmetry was confirmed by the reduction of ZP from 31.08mV to 10.36mV.

Table 4. 17: Characterisation of the new formulation with 45% DOTAP

Formulation	Size (nm)	ZP (mV)
Acceptor	123.78 ±1.09	31.08 ±1.93
Asymmetric	143.88 ±2.30	10.36 ±2.58

The third modification technique involved adding 5% span 80 to turn the formulation to a deformable liposome. Deformable liposomes have different types based on the agent added. Transferosomes are the first-generation deformable vesicles. They are identified by having a surfactant (edge activator) as part of the liposomal formulation (161). The addition of an edge activator leads to a destabilisation of the membrane, which provides flexible liposomes that can squeeze through passages and reach deeper (161). The main advantage of these liposomes is that they have high elasticity and stress adaptability; therefore, this can lead to reduced aggregation and higher entrapment efficiency (162).

The aim of this study is to determine if it will help make the liposomes less leaky and retain the entrapped drug. The size of this formulation remained relatively stable, with the ZP reducing from 15.12 mV to 7.23 mV (Table 4.18).

The average EE was 31.86%%, which reduced after adding the edge activator. Therefore, this modification technique was not adopted.

Table 4. 18: Characterisation of the new formulation with 5% Span 80

Formulation	Size (nm)	ZP (mV)
Acceptor	190.78 ±63.30	15.12 ±3.38
Asymmetric	145.47 ±9.88	7.23 ±0.56

These findings align with and add to existing literature on liposomal optimisation strategies. The detrimental effect of increasing cholesterol content to 60% on entrapment efficiency (EE) is consistent with previous studies, indicating that while moderate cholesterol levels (30–45%) enhance membrane rigidity and stability, excessive amounts can disrupt bilayer packing, increase permeability, and promote aggregation (163,164). Conversely, increasing DOTAP content to 45% improved EE, supporting the well-documented role of cationic lipids in enhancing encapsulation of negatively charged molecules through electrostatic interactions (165). The addition of Span 80 as an edge activator was intended to confer deformability, as observed in transferosomes, which have shown improved drug delivery in some contexts (166), but in this case, it reduced EE, likely due to excessive membrane destabilisation that facilitated leakage. This contradiction highlights that the benefits of edge activators are formulation and cargo dependent (167). Overall, these results reinforce the importance of carefully balancing lipid components to achieve optimal stability, encapsulation, and functional performance in asymmetric liposomal systems.

Summary

This research chapter involved formulating neutral symmetric liposomes to test the stability of the neutral lipids used. This was followed by the addition of a charge to test the encapsulation efficiency of the charged cationic liposomes to the negatively charged bromocresol green. After that, asymmetric liposomes were formulated from the lipids tested previously, and the most optimised formulation was chosen. The optimised formulation contained POPC lipid in the outer leaflet and POPC (30%), DOTAP (30%), and cholesterol (40%) in the inner leaflet. This formulation was further modified by increasing the DOTAP percentage to 45%. The encapsulation of bromocresol green was tested using UV/VIS spectrophotometry and a novel pH gradient method.

Chapter 5

Characterisation and entrapment of DNA in asymmetric liposomes using the novel cyclodextrin-lipid complex method

1. Overview

Nucleic materials such as DNA are susceptible to degradation inside the human body. This is due to the immune response sensitisation, phagocytosis, serum nucleases degradation, and rapid renal clearance, in addition to low cellular uptake and target specificity, which are vulnerabilities that make naked genetic material delivery highly unsuitable and ineffective and can be eliminated from the body rapidly (82). Therefore, they require a suitable carrier to deliver them to the target sites. Since DNA is negatively charged, it requires a positively charged carrier to enhance entrapment by forming a complex with the DNA (85). However, cationic liposomes are removed by the RE system as well as having non-specific interaction with negatively charged blood components, leading to accumulation at the primary organs (87). Moreover, although positive charge increases DNA entrapment, the toxicity of liposomes also increases as cationic lipids such as DOTAP were found to have increased toxicity with increased amount (168).

The use of asymmetric liposomes provides a great advantage to nucleic acid delivery as they contain different lipids in the outer and inner leaflets (53). Thus, allowing the enhancement of each leaflet independently, lipids that can maximise entrapment efficiency and reduce leakage can be used in the inner leaflet; in this case, cationic phospholipids are suitable. Different lipids can be used in the outer leaflet to enhance drug delivery and liposomal stability (3).

2. Aim

This work aims to formulate asymmetric liposomes that contain neutral phospholipids in the outer leaflet and positive phospholipids in the inner leaflet. Then, measure the stability and the entrapment efficiency of DNA inside the asymmetric liposomes.

3. Results

5.1. The formulation

The formulation used consisted of 15% POPC, 45% DOTAP, and 40% cholesterol, as this formulation was shown to have the highest entrapment efficiency of the hydrophilic dye, bromocresol green. Refer to chapter 4 for the formulation-related data.

5.2. Determination of the suitable DNA amount to be encapsulated

To identify which DNA content is suitable for the formulation, three different masses were used. The liposomal formulation used was the formulation mentioned in part 5.1; it contained lipids with a final concentration of 2mM, which had 1.164mg/ml of lipids. The DNA concentration of 10ng/µl (0.01mg/ml), 3µl, 6µl, and 12µl of DNA was used and added to the liposomal formulation. This results in mass ratios of DNA: Liposomes of 1:38.8 (3 µl), 1:19.4 (6 µl), and 1:9.7 (12 µl).

The 3µl of DNA in the formulation had a good entrapment efficiency of 84%. As shown in table (5.1), in regard to the size, a slight increase in size occurred after adding DNA; moreover, the size further increased when the liposomes were centrifuged to pellet the liposomes and discard the supernatant containing the free DNA. The PDI remained similar. The zetapotential decreased slightly after the DNA was added. This could be due to small amounts of free DNA becoming attached to the positive outer leaflet of the liposomes.

Table 5. 1: The characteristics of the asymmetric formulation encapsulating 3µl of DNA

%Entrapment efficiency	Size before adding DNA (nm)	PDI	Size after adding DNA (nm)	PDI	Size after centrifugation (nm)	PDI	Zetapotential before adding DNA (mV)	Zetapotential after adding DNA (mV)
84.2 ±0.66	125.38 ±6.28	0.279 ±0.02	169.34 ±9.42	0.270 ±0.03	227.16 ±23.5	0.215 ±0.06	29.9 ±1.35	22.6 ±1.83

The same method was repeated, but with the encapsulation of 6µl of DNA in the formulation. As shown in table (5.2), the entrapment efficiency increased by 8.3% when the DNA content was increased to 60ng/µl. The average size increased when DNA was added, indicating the presence of DNA inside the liposomes. However, the size increased more in the 6µl formulation

than in the 3µl formulation, which could be due to more DNA being encapsulated inside the vesicle. As expected, the size further increased after pelleting of the liposomes. Regarding the zetapotential, the value is slightly reduced, which could be due to the small amount of DNA attached to the surface.

Table 5. 2: The characteristics of the asymmetric formulation encapsulating 6µl of DNA

%Entrapment efficiency	Size before adding DNA (nm)	PDI	Size after adding DNA (nm)	PDI	Size after centrifugation (nm)	PDI	Zetapotential before adding DNA (mV)	Zetapotential after adding DNA (mV)
92.5 ±1.47	125.38 ±6.28	0.279 ±0.02	198.48 ±23.66	0.212 ±0.03	246.12 ±25.96	0.195 ±0.08	29.9 ±1.35	26.4 ±2.26

On the other hand, increasing the encapsulated DNA content to 12µl in the asymmetric liposomal formulation led to unstable and non-repeatable formulations. When the formulations were made, some exhibited a size increase after adding DNA, from 125.38 ± 6.28 to 369 ± 80.69 nm, while others aggregated, resulting in large particles. The formulation became more unstable when the liposomes were pelleted, resulting in large particles and large particle sizes due to the presence of large lipid aggregates.

Therefore, encapsulating 6µl of DNA was chosen to be the ideal content as it had the highest entrapment efficiency, >90%, while the size remained acceptable. This result is in agreement with the literature, where a ratio of 20:1 symmetric liposomes to DNA was used to encapsulate plasmid DNA and resulted in an average EE of ~89.6% (169).

In this study, it was crucial to ensure that DNA was entrapped inside the liposomes and not adsorbed onto their surface. Centrifugation is an effective method to remove complexed materials, e.g. proteins from liposomes; higher centrifugation speeds lead to more effective separation (170). Moreover, when DNA is added to liposomes, some of the DNA is immobilised on the surface of the liposomes. This leads to an increase in the liposomes' negative charge as the concentration of the DNA increases (171).

Therefore, the degree of reduction in ZP after adding DNA and centrifugating the suspension can be considered an indicative method for qualitatively determining the amount of DNA adsorbed onto the liposomal surface.

The results of this study align with existing literature on DNA encapsulation into cationic liposomes, particularly regarding the importance of lipid-to-DNA ratios for achieving high entrapment efficiency (EE) and formulation stability. The optimal ratio of ~20:1 (6 µL DNA) produced >90% EE with acceptable size and stability, which is consistent with previous reports using symmetric liposomes for plasmid delivery (172,173). The observed size increase after DNA addition and further enlargement upon centrifugation is due to the aggregation of liposomes. In contrast, the 12 µL DNA formulation was unstable, likely due to charge neutralisation and aggregation, a known issue at high nucleic acid loading (174). These findings reinforce the need to balance DNA content with liposome capacity and suggest that zeta potential measurements can serve as a qualitative indicator of surface-bound DNA. Overall, the 6 µL DNA loading represents the most effective and reproducible formulation in this system.

5.3. Reducing aggregation of symmetric and asymmetric liposomes by adding solutol HS-15

Solutol HS 15 is a non-ionic surfactant that consists of polyglycol mono- and diester of 12-hydroxysteric acid (70% lipophilic molecules) and 30% hydrophilic molecules of polyethylene glycol (175). It is a commonly used solubiliser (176) As it was shown to have low toxicity in animal studies (177). Moreover, it is commonly used in noisome as a co-surfactant to aid in the encapsulation of hydrophobic drugs as well as enhancing the stability of the drug delivery system, improving drug bioavailability, and allowing for targeted drug delivery (178). Therefore, in our study, the effect of solutol-HS 15 on liposomes was investigated to determine whether it would provide the same effect as on niosomes.

Solutol HS 15 was added to the liposomal formulation to investigate whether it can enhance liposomal size stability and reduce aggregation. Solutol HS-15 (10%) was added to the formulation. This percentage was chosen because it is the commonly used percentage of solutol HS-15 in noisome formulations as a co-surfactant (178). First, the effect of this was investigated on empty liposomes. As shown in table (5.3), the liposomal formulation containing solutol HS-15 had an average size of 110.96nm, the size remained relatively stable over 2 weeks, as it only increased up to 125.52nm. However, a more dramatic change can be seen with the zetapotential values as it reduced overtime, initially the value was 19.32mV which reduced 2.85mV after 2 weeks (Table 5.4). This indicates that solutol was able to maintain the size of symmetric liposomes.

Table 5. 3: The size of symmetric liposomes containing solutol

Size (nm)	PDI	24 hours size (nm)	PDI	72 hours size (nm)	PDI	1 week size (nm)	PDI	2 weeks size (nm)	PDI
110.96 ±6.08	0.300 ±0.04	115.47 ±5.74	0.300 ±0.04	121.20 ±9.12	0.270 ±0.03	119.07 ±5.48	0.33 ±0.05	125.52 ±8.90	0.29 ±0.05

Table 5. 4: The zetapotential (ZP) of symmetric liposomes containing solutol

ZP (mV)	24 hours ZP (mV)	72 hours ZP (mV)	1 week ZP (mV)	2 weeks ZP (mV)
19.32 ±1.99	18.10 ±1.65	14.72 ±0.86	4.96 ±2.07	2.85 ±1.03

The process was repeated but with asymmetric liposomes. As shown in table (5.5), the initial size was 204.38nm which remained somewhat stable up to 72 hours then increased more dramatically after 1 week. The same thing can be observed with the zetapotential values as they reduced after 1 week stability (Table 5.6). Differently from symmetric liposomes, the ability of Solutol to reduce aggregation has reduced from over 2 weeks to only 72 hours.

Table 5. 5: The size stability of asymmetric liposomes containing solutol over 2 weeks period

Size (nm)	PDI	24 hours size (nm)	PDI	72 hours size (nm)	PDI	1 week size (nm)	PDI	2 weeks size (nm)	PDI
204.38 ± 14.25	0.360 ±0.03	258.26 ±31.05	0.360 ±0,03	246.27 ±18.91	0.340 ±0.02	309.34 ±36.80	0.400 ±0.05	417.14 ±85.73	0.440 ±0.04

Table 5. 6: The zetapotential (ZP) stability of asymmetric liposomes containing solutol over 2 weeks period

ZP (mV)	24 hours ZP (mV)	72 hours ZP (mV)	1 week ZP (mV)	2 weeks ZP (mV)
10.50 ±0.14	8.22 ±1.40	7.03 ±1.40	-2.94 ±1.40	-1.46 ±2.00

Although solutol was able to form liposomes with acceptable sizes, it aggregated and led to large lipid aggregates when DNA was added to the formulation. This indicates that adding solutol with the presence of DNA leads to formulation instability and aggregation. However, solutol is known as agent that helps in enhancing stability and reducing aggregation, therefore, this formulation can be trialled with other negatively charged drugs and study the stability.

The use of Solutol HS 15 in this study aligns with existing literature that highlights its role as a non-ionic surfactant with solubilising and stabilising properties due to its amphiphilic structure. Previous studies have demonstrated its ability to enhance drug solubility and maintain micellar stability with low toxicity (179). In agreement with these findings, Solutol maintained the size stability of symmetric liposomes over two weeks, although a gradual reduction in zeta potential was observed, likely due to steric effects on surface charge. However, its stabilising effect was less pronounced in asymmetric liposomes, with a significant increase in size and reduction in zeta potential observed after 72 hours. Furthermore, the addition of DNA led to aggregation, suggesting that while Solutol HS 15 is effective in simple liposomal systems, it may not prevent electrostatic destabilisation in the presence of negatively charged macromolecules.

5.4. Asymmetric liposomes formulation compared to symmetric liposomes formulation for DNA encapsulation

Symmetric vesicles with cationic lipids were ~100 times better at entrapping nucleic acids than vesicles with only neutral lipids or negatively charged lipids (180). To compare the EE of liposomes, asymmetric liposomes were formulated, and nucleic acids were entrapped (180). It was shown that regardless of whether the outer leaflet contained neutral or negatively charged lipids, as long as the inner leaflet had a cationic lipid, the entrapment efficiency remained high. However, the nucleic acid-to-lipid ratio was reduced by 40 % relative to symmetric vesicles with cationic lipids but the EE remained higher than liposomes with neutral or anionic lipids (180).

The asymmetric formulation contained POPC as the lipid in the outer leaflet (Donor) and POPC, DOTAP, and cholesterol in the inner leaflet (Acceptor). According to literature, one of the main benefits of the asymmetric liposomes is that the outer leaflet works independently of the inner leaflet (53). Therefore, the aim was to increase the entrapment efficiency of the DNA due to the attraction of the positively charged DOTAP to the DNA while still having a near-neutral outer leaflet.

To allow comparison between the symmetric and asymmetric liposomes, three different formulations were made; asymmetric liposomes (POPC "out" and POPC/DOTAP/CHOL "in"), symmetric liposomes (POPC + Cholesterol) to mimic the outer leaflet alone, and symmetric liposomes (POPC + DOTAP + Cholesterol) to mimic the inner leaflet alone. As shown in table (5.7), the size and zetapotential were compared as empty liposomes. The symmetric formulation containing DOTAP had a good low size distribution of 125.38nm with a PDI of 0.279, this size is maintained due to the presence of a high concentration of DOTAP which causes repulsion between the liposomes and reduces aggregation. The high positive charge is evident by the ZP reading of 29.9mV. The asymmetric formulation on the other hand had a size of 302.8nm which is almost twice the size of the symmetric liposomes, this could be due to aggregation occurring as the liposomes became more neutral and less repulsive forces allowed for more aggregation. The ZP has been reduced to 10.8mV which means much lower amount of DOTAP is present in the outer leaflet. Moreover, symmetric liposomes only containing POPC and cholesterol only had an average size of 406.20nm, which is higher than the other two formulations. This is mainly due to aggregation as a result of a lack of repulsive forces where the ZP was near-neutral (-5.36mV).

Table 5. 7: Comparison between empty liposomal formulations

Formulation	**Size (nm)**	**PDI**	**Zetapotential (mV)**
Asymmetric- POPC "out" and POPC/DOTAP/CHOL "in"	302.8 ±30.29	0.379 ±0.14	10.8 ±0.69
Symmetric- POPC + Cholesterol	406.20 ±40.98	0.477 ±0.04	-5.36 ±0.494
Symmetric- POPC + DOTAP + Cholesterol	125.38 ±6.28	0.279 ±0.02	29.9 ±1.35

Different encapsulation methods were tested to compare which method has the best entrapment efficiency. Method (**A**) involved encapsulating the DNA after the formation of the

symmetric liposomes, followed by a 15-minute wait before centrifugation of the suspension to separate the free drug. The main benefit of this method is the presence of high concentrations of DOTAP, which will help in attracting DNA inside the liposomes and increasing the entrapment efficiency. As shown in table (5.8), this method was proven to be effective as it achieved an EE of 91.2% as well as having an average size of 293.2nm and a ZP reading of 13.3mV.

Table 5. 8: Method A characteristics (the size, PDI and zetapotential of the asymmetric formulation" refer to section 5.1" containing DNA)

%EE	Size (nm)	PDI	ZP (mV)
91.2 ±0.38	293.22 ±46.59	0.259 ±0.06	13.3 ±1.6

Method (**B**) involved adding the DNA during the lipid exchange stage between the donor and the acceptor. The theory was that as the cyclodextrin replaces the lipids, more empty spaces become present within the liposomes, allowing the DNA to be attracted to the inner leaflet's DOTAP and enhancing the EE. As shown in table (5.9), the entrapment efficiency has increased with this method compared to the previous method which is likely due to the presence of high concentrations of DOTAP as well as the removal and addition of the lipids which can allow more of the DNA to escape into the liposomes. Although this method had a good entrapment efficiency, the main issue with it is that it led to aggregation and formed very large particles with an average diameter of 933 nm. The exact cause of aggregation is not known.

Table 5. 9: Method B characteristics (the size, PDI and zetapotential of the asymmetric formulation" refer to section 5.1" containing DNA)

%EE	Size (nm)	PDI	ZP (mV)
94.9 ±1.53	933.4 ±250.33	0.572 ±0.04	11.84 ±0.82

Method (**C**) involves formulating empty asymmetric liposomes first, then adding the DNA, and then centrifuging to separate the free drug (Table 5.10). This method had a very low EE of 7.5% which is likely due to the outer leaflet being near-neutral, which reduces the entrapment of the DNA; moreover, the liposomes in this method undergo many vicious processes, including sonication, exchange, and two rounds of centrifugation. This could lead to damage and breakage of the liposomes, resulting in the release of the drug and a low entrapment efficiency. Moreover, this method exhibited a marked aggregation, resulting in an average size of 1324.13 nm. Furthermore, the ZP was reduced to -11.13 mV, which also indicated the formation of aggregates between the DNA and the liposomes.

Table 5. 10: Method C characteristics (the size, PDI and zetapotential of the asymmetric formulation" refer to section 5.1" containing DNA)

%EE	Size (nm)	PDI	ZP (mV)
7.5 ±6.54	1324.13 ±479.23	0.830 ±0.19	-11.13 ±1.50

Thus, the best encapsulation method to achieve good liposomes with high entrapment efficiency is method A.

As mentioned previously, the main benefit of having asymmetric liposomes is that the properties of two different symmetric formulations can be merged into one asymmetric liposome.

DNA was added to symmetric liposomes containing DOTAP/POPC/CHOL, to mimic the inner leaflet. The characteristics achieved are shown in table (5.11), the entrapment efficiency was 90.6% which is very high, and this is mainly due to the presence of DOTAP as 45% of the formulation. Moreover, the size has increased from 125.38nm to 309.75nm which could be due to presence of DNA inside the liposomes, hence increasing the size. The PDI remained somewhat similar while the ZP reduced from 29.88 to 24.65mV. This slight decrease could be due to the attachment of some of the DNA to the outside DOTAP as a result of the negative and positive charge attraction. Therefore, this formulation is great in achieving high entrapment efficiency, however, this formulation contains a high positive charge in the outer leaflet (ZP= 24.65mV) which can potentially lead to cytotoxicity and challenges when delivered to the human body.

Table 5. 11: Characteristics of symmetric formulation POPC+DOTAP+CHOL

%EE	Size (nm)	PDI	ZP (mV)
90.6 ±0.89	309.75 ±5.50	0.285 ±0.06	24.65 ±0.93

When DNA is added to symmetric liposomes containing only POPC and cholesterol, to mimic the outer leaflet, the following results are observed. As shown in table (5.12), the entrapment reduced to 36.4% when the DOTAP was not added, moreover the size of the liposomes had an average of 509.94nm which could indicate there is some aggregation due to the lack of charge. This is evident by the ZP of -7.69mV. Thus, it can be deduced that this formulation has a low EE due to the neutral charge. However, having asymmetric liposomes can provide a similar outer leaflet composition while having a high entrapment efficiency.

Table 5. 12: Characteristics of symmetric formulation POPC+CHOL

%EE	Size (nm)	PDI	ZP (mV)
36.4 ±2.39	509.94 ±21.13	0.380 ±0.06	-7.69 ±1.59

Therefore, this indicates that the liposomes mimicking the acceptor have a very high entrapment efficiency of 90.6% as well as a good size of 309.75nm. However, due to the presence of DOTAP at 45%, this formulation can be toxic when administered due to the high concentration of positive charge. On the other hand, the liposomal formulation, which mimics the outer leaflet and contains only POPC, has low toxicity due to the presence of only neutral lipids. However, the lack of a positive charge led to a low EE of 36.5% and a higher average size of 509.94nm due to an increased chance of aggregation as a result of the lack of charge.

The asymmetric formulation was able to overcome the challenges of both of the symmetric formulations. As shown in table (5.13), due to the presence of DOTAP in the inner leaflet, the entrapment efficiency of the DNA remained high at 91.2%. While the size remained small, with an average of 293.22 nm. The PDI showed a value of 0.259, which indicates that the formulation is less polydisperse. Finally, the zetapotential had an average value of 13.35mV, which is lower than the value of the symmetric liposomes, 29.88mV. This makes the formulation less positive and reduces the toxicity of the formulation while having a high entrapment of the drug. Similar behaviour is seen in literature when the negatively charged doxorubicin was entrapped within the asymmetric liposomes containing neutral lipids in the outer leaflet and a cationic lipid in the inner leaflet (3).

Table 5. 13: Characteristics of the asymmetric formulation

%EE	Size (nm)	PDI	ZP (mV)
91.2 ±0.38	293.22 ±46.59	0.259 ±0.06	13.35 ±1.62

5.5. Storage stability of the symmetric and asymmetric liposomal formulations

Different formulation techniques are currently available to formulate asymmetric liposomes. Several studies have been conducted to assess the stability of asymmetric liposomes. For asymmetric vesicles created by the cyclodextrin-exchange method, the asymmetric vesicles remained stable for 48 hours (3). Methods involving enzyme use, e.g. Phosphatidylserine decarboxylase, to exchange the outer leaflet of liposomes and create asymmetry, led to more stable asymmetric vesicles lasting for 4 days at 20 °C (68). Similarly, methods involving Ca^{2+} ions to cause asymmetry created liposomes where the asymmetry was stable for several days at room temperature (66). Microfluidic devices can be a valuable tool for the formation of asymmetric liposomes and vesicles formulated using this technique; the results from this study have shown that the membrane asymmetry was maintained for over 30 h; 80% of the asymmetric vesicles remained stable for at least 6 weeks, additionally this method was able to improve the size variation control (74). Pulsed jet flow method involves a lipid tube, which is then deformed and leads to the formation of asymmetric vesicles (77). This method was able to form asymmetric vesicles with stability lasting at least 7 days (77).

To test the stability of the liposomes, the size, PDI, and zetapotential were measured at 4°C until the liposomes aggregated or the zetapotential value changed over time. The empty symmetric formulation containing POPC/DOTAP/CHOL was compared to the empty asymmetric formulation containing POPC “out” and POPC/DOTAP/CHOL “in” at 4°C.

As shown in the tables below (Table 5.14), the size of symmetric liposomes with no DNA had an initial value of 125.38nm. This size has remained relatively constant over a 2-week storage period and reached a value of 128.16 nm. There was no significant difference in size over the 2-week period as the p-value calculated was non-significant (P-value =0.52). The stability of the size is primarily due to the presence of DOTAP in the outer leaflet, which causes repulsion. Moreover, the PDI also remained stable. As expected, the zetapotential value was high (29.88 mV); however, the value of ZP reduced by more than half after 1 week, reaching 12.47 mV. This trend is also seen in literature (181,182). The p-value calculations indicate a significant difference in ZP values after 24 hours (p-value= 0.013).

Table 5. 14: The storage stability of empty symmetric liposomes over 2 weeks period

Empty Symmetric formulation		
Initial values (fresh samples)		
Size (nm)	**PDI**	**ZP (mV)**
125.38 ±6.28	0.279 ±0.02	29.88 ±1.35
24 hours		
Size (nm)	**PDI**	**ZP (mV)**
124.46 ±10.90	0.277 ±0.04	24.93 ±1.76
72 hours		
Size (nm)	**PDI**	**ZP (mV)**
126.75 ±9.15	0.309 ±0.03	22.33 ±4.05
1 week		
Size (nm)	**PDI**	**ZP (mV)**
123.98 ±9.28	0.283 ±0.02	12.47 ±5.58
2 weeks		
Size (nm)	**PDI**	**ZP (mV)**
128.16 ±6.83	0.288 ±0.06	7.81 ±1.074

The exact measurements were performed for the empty asymmetric liposomes (Table 5.15). To test the stability of the liposomes, the size was measured. The initial size was 302.83nm, which increased dramatically after 72 hours to 568.70nm. This indicates that the liposomes started to aggregate. The change was deemed to be significant as it had a p-value of >0.05. Additionally,

the PDI increased from 0.379 to 0.481. To test the stability of asymmetry, ZP was used. The zetapotential readings showed a significant reduction in after 24 hours (p-value= 0.002). However, the value remained stable up to 72hours with no significant change (p-value= 0.83). Then, it was significantly reduced again after 1 week (p-value < 0.05).

Table 5. 15: The storage stability of empty asymmetric liposomes over 1 week period

Empty Asymmetric formulation		
Initial values (fresh samples)		
Size (nm)	**PDI**	**ZP (mV)**
302.83 ±30.29	0.379 ±0.14	10.86 ±0.69
24 hours		
Size (nm)	**PDI**	**ZP (mV)**
397.55± 37.05	0.449 ±0.05	7.70 ±0.60
72 hours		
Size (nm)	**PDI**	**ZP (mV)**
568.70 ±50.51	0.481 ±0.05	7.66 ±0.39
1 week		
Size (nm)	**PDI**	**ZP (mV)**
583.06 ±36.04	0.385 ±0.04	-2.89 ±1.22

The same investigations were carried out for liposomes with DNA to test whether DNA has any effect on the liposomes' stability (Table 5.16). As shown in the tables below, the size was maintained for 2 weeks, with only small changes observed, increasing from 309.75 nm to 323.35 nm. The same trend was seen with the PDI. The difference in vesicle size overtime did not change significantly as it measured a p-value of 0.15. However, a dramatic change in zetapotential occurred after 1 week where the value reduced from 24.65mV to 7.57mV. Moreover, a significant p-value of 0.0001was calculated for the ZP after only 24 hours. This indicates that the ZP has significantly changed for the symmetric liposomes over 24 hours.

Table 5. 16: The storage stability of symmetric liposomes containing encapsulated DNA over 2 weeks period

Symmetric formulation + DNA		
Initial values		
Size (nm)	**PDI**	**ZP (mV)**
309.750 ±5.50	0.285 ±0.06	24.65 ±0.93
24 hours		
Size (nm)	**PDI**	**ZP (mV)**
283.50 ±34.42	0.258 ±0.04	18.65 ±0.64
72 hours		
Size (nm)	**PDI**	**ZP (mV)**
304.75 ±7.61	0.246 ±0.05	16.0 ±2.23
1 week		
Size (nm)	**PDI**	**ZP (mV)**
292.00 ±4.52	0.302 ±0.03	7.57 ±1.56

2 weeks		
Size (nm)	**PDI**	**ZP (mV)**
323.35 ±3.61	0.249 ±0.06	6.63 ±1.75

The stability of asymmetric liposomes with DNA encapsulated has differed dramatically from empty asymmetric liposomes (Table 5.17). The presence of DNA was able to stabilise the liposomes. The size had an initial value of 293.23, which showed a small, gradual increase up to 2 weeks (380.65 nm). The PDI was more consistent and remained similar for over 3 weeks. The asymmetry stability was measured. The ZP value has indicated that the asymmetry remained somewhat stable up to 72 hours, with a reduction from 13.35mV to 11.30mV. After that, the ZP continued to decrease, reaching a final value of 6.67 mV after two weeks. Although the ZP value has decreased, when compared to the size, the reduction in ZP may be considered acceptable in this instance, indicating increased stability of asymmetric liposomes when DNA was added (refer to Section 6 for more information). The statistical analysis revealed that the size values showed a significant difference (P-value < 0.05, 0.034) after 2 weeks. However, for the ZP results, a significant difference was observed after 1 week (P-value = 0.0002).

Table 5. 17: The storage stability of asymmetric liposomes containing encapsulated DNA over 4 4-week period

Asymmetric formulation + DNA		
Initial values		
Size (nm)	**PDI**	**ZP (mV)**
293.23 ±46.59	0.259 ±0.06	13.35 ±1.62
24 hours		
Size (nm)	**PDI**	**ZP (mV)**
265.95± 83.86	0.243 ±0.07	10.62 ±2.35
72 hours		
Size (nm)	**PDI**	**ZP (mV)**
305.78 ±48.27	0.290 ±0.06	11.30 ±0.56
1 week		
Size (nm)	**PDI**	**ZP (mV)**
311.42 ±39.31	0.252 ±0.03	7.35 ±0.89
2 weeks		
Size (nm)	**PDI**	**ZP (mV)**
380.65 ±59.98	0.285 ±0.05	6.67 ±0.18
3 weeks		
Size (nm)	**PDI**	**ZP (mV)**

620.57 ±56.71	0.280 ±0.02	8.35 ±1.192
4 weeks		
Size (nm)	**PDI**	**ZP (mV)**
640.13 ±16.82	0.406 ±0.11	6.99 ±2.87

Based on the results above, it can be concluded that the novel CD-lipid complex method successfully maintained the stability of asymmetric liposomes containing DNA for 1 week. The presence of DNA was shown to increase the stability of asymmetric liposomes significantly.

As mentioned previously, in the literature, the asymmetric stability, using the cyclodextrin exchange method, remained stable for only 48 hours. Therefore, asymmetric liposomes formulated using the novel cyclodextrin-lipid complex method improved the stability. Moreover, other methods stated the vesicles' stability duration; however, they did not measure important parameters such as zeta potential, which could have been affected over time.

6. Asymmetric liposomes for the treatment of genetic diseases

The optimal asymmetric liposomal formulation developed in this study yields promising results for the treatment of genetic diseases. DNA and RNA-based therapy has been widely exploited for the treatment of genetic diseases. They work by targeting the genes responsible for the specific disease. Thus, opening infinite possibilities for the treatment of genetic disorders (183). Nucleic acid therapeutics work in several ways to treat gene-related diseases. One way can be by restoring the function of faulty or deficient proteins. Another way involves targeting specific deleterious proteins and halting their production, as well as increasing the synthesis of desired proteins (183). The study aims to formulate the most optimised asymmetric formulation to deliver DNA to cells for the treatment of genetic diseases. The benefits of having asymmetric liposomes are that the outer leaflet of the liposomes is near-neutral, therefore, providing less

toxicity to the body. Moreover, the inner leaflet is positively charged, thereby increasing the encapsulation of DNA.

Summary

In this research chapter, the most optimised asymmetric formulation containing POPC in the outer leaflet and POPC (30%), DOTAP (30%), and cholesterol (40%) in the inner leaflet was used to encapsulate salmon sperm DNA. Different DNA contents were investigated, and 60ng/µl was deemed the best amount. Entrapment efficiency was measured using the NanoDrop Lite machine. Moreover, the storage stability of symmetric and asymmetric liposomes, as empty or DNA loaded, was investigated and measured until formulation aggregation. An additional study on the effect of solutol HS-15 on the aggregation potential of liposomes was undertaken, providing novel findings.

Chapter 6

Conclusion and further work

1. Conclusion

This thesis presented the successful development, optimisation, and evaluation of a novel method for formulating asymmetric liposomes using a cyclodextrin (CD)-lipid exchange technique. This work forms a comprehensive exploration of asymmetric liposome formulation and application. The research first established a completely new formulation technique where lipids were first complexed with cyclodextrin using a modified solvent evaporation strategy. Complexation was confirmed via analytical techniques including FTIR, TGA, DSC, NMR, and aqueous solubility testing. These CD-lipid complexes were then successfully used to exchange outer leaflet lipids in large unilamellar vesicles (LUVs), enabling the formation of asymmetric liposomes. A key advancement was the ability to isolate the final asymmetric liposomes from excess CD-lipid complexes through conventional centrifugation, greatly simplifying the process compared to conventional methods. The asymmetry of the resulting vesicles was verified using zeta potential analysis and a fluorescence quenching assay, confirming the structural integrity of the asymmetrically distributed lipid bilayer.

This novel method was then used to formulate and compare various asymmetric liposome compositions. Bromocresol green was employed as a model anionic drug to assess encapsulation efficiency, and a novel qualitative pH-gradient method was applied to confirm drug entrapment qualitatively. Among several tested formulations, the most efficient formulation had POPC in the outer leaflet and POPC, DOTAP, and cholesterol in the inner leaflet (at 15:45:40 mol%). This configuration provided high EE for negatively charged molecules and achieved an entrapment efficiency of 44.22%. Notably, this formulation maintained a near-neutral zeta potential (outer leaflet) while containing a positively charged inner leaflet. leading to improved entrapment and reduced systemic toxicity. The developed method allows for fine-tuning lipid composition to achieve desirable physicochemical properties and encapsulation outcomes. Therefore, further optimisation techniques were trialled.

The work was expanded by investigating the encapsulation of salmon sperm DNA into the optimised asymmetric liposomes. The study revealed that incorporating DNA during the symmetric liposome formation stage, before lipid exchange, resulted in the most efficient

encapsulation, reaching a DNA entrapment efficiency of 92.5% at a 19.4:1 liposome-to-DNA ratio. This confirmed the potential of the system to encapsulate large, negatively charged biomolecules while retaining a neutral external surface, an important advancement in gene delivery technologies. Furthermore, a detailed stability study demonstrated that the DNA-loaded asymmetric liposomes remained structurally stable for up to one week at 4 °C. To further improve physical stability and reduce aggregation, the effect of adding 10% Solutol HS-15 was also explored. While Solutol showed promise in improving size retention in symmetric liposomes, its stabilising effect was reduced in asymmetric and DNA-loaded systems, indicating that its utility may depend on formulation context. Nevertheless, this investigation was a novel exploration into the compatibility of surfactant additives with structurally asymmetric systems.

This thesis collectively demonstrate the feasibility, versatility, and practicality of a new asymmetric liposome production method. The system has the ability to fine-tune inner and outer leaflet compositions independently, encapsulate both small and large molecules with high efficiency, and maintain stability over time. These findings highlight the strong potential of this platform for future biomedical applications, particularly in areas like targeted drug delivery and gene therapy, where precise control over liposome structure and cargo is essential. The results represent a significant advancement in liposome technology, particularly in achieving structural asymmetry and functional performance with minimal processing complexity. The development of a formulation that combines a near-neutral surface charge with high encapsulation of negatively charged DNA represents a major achievement in balancing delivery efficiency with safety, two critical criteria. Overall, this thesis provides both a theoretical and practical framework for future research in the field of liposomal drug and gene delivery, with a formulation approach that is adaptable, reproducible, and capable of meeting the demands of advanced nanomedicine.

FLOW CHART CHAPTER 3

STEP 1:

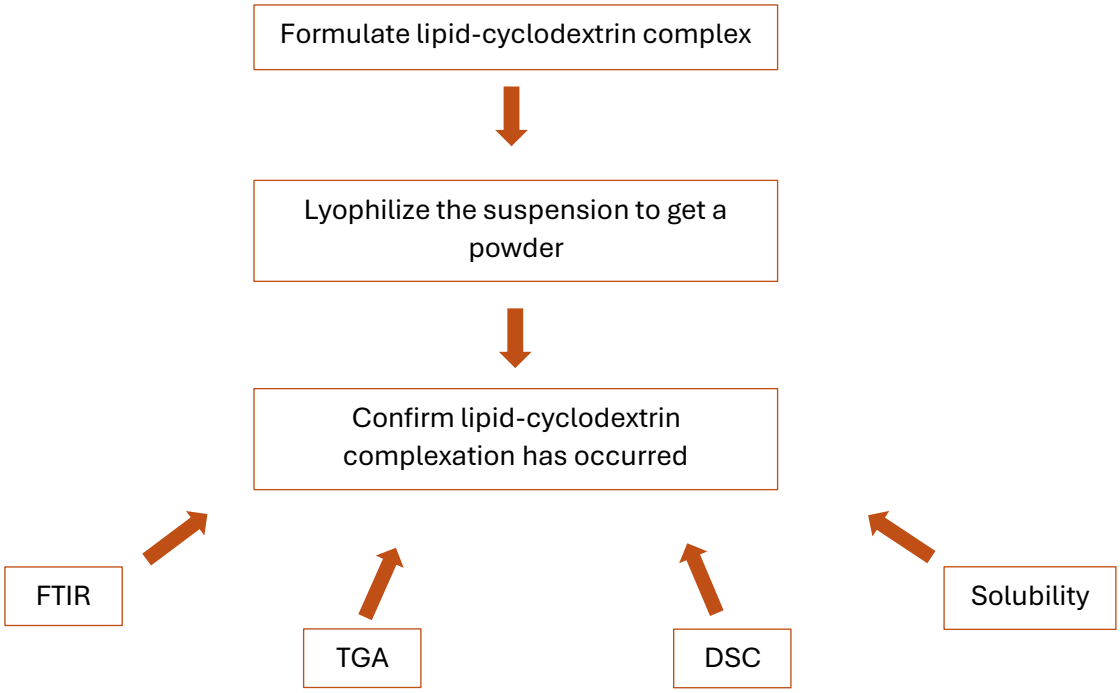

STEP 2:

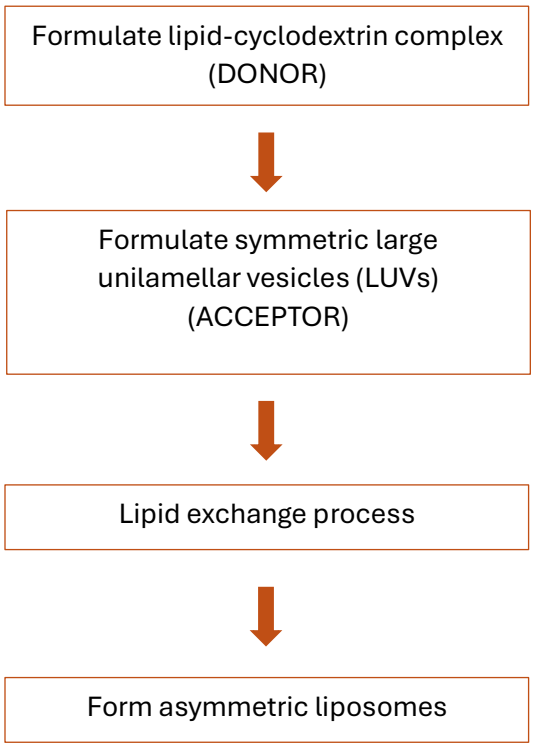

STEP 3:

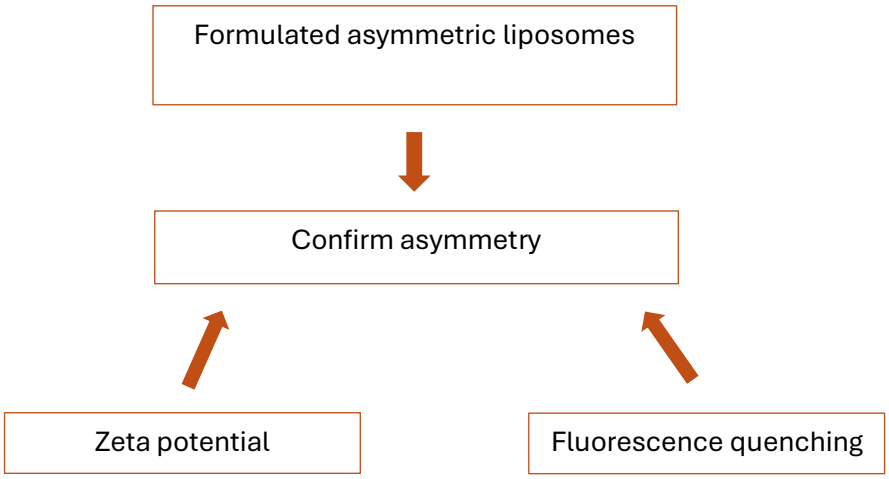
Formulated asymmetric liposomes
Confirm asymmetry
Zeta potential
Fluorescence quenching

FLOW CHART CHAPTER 4

STEP 1:

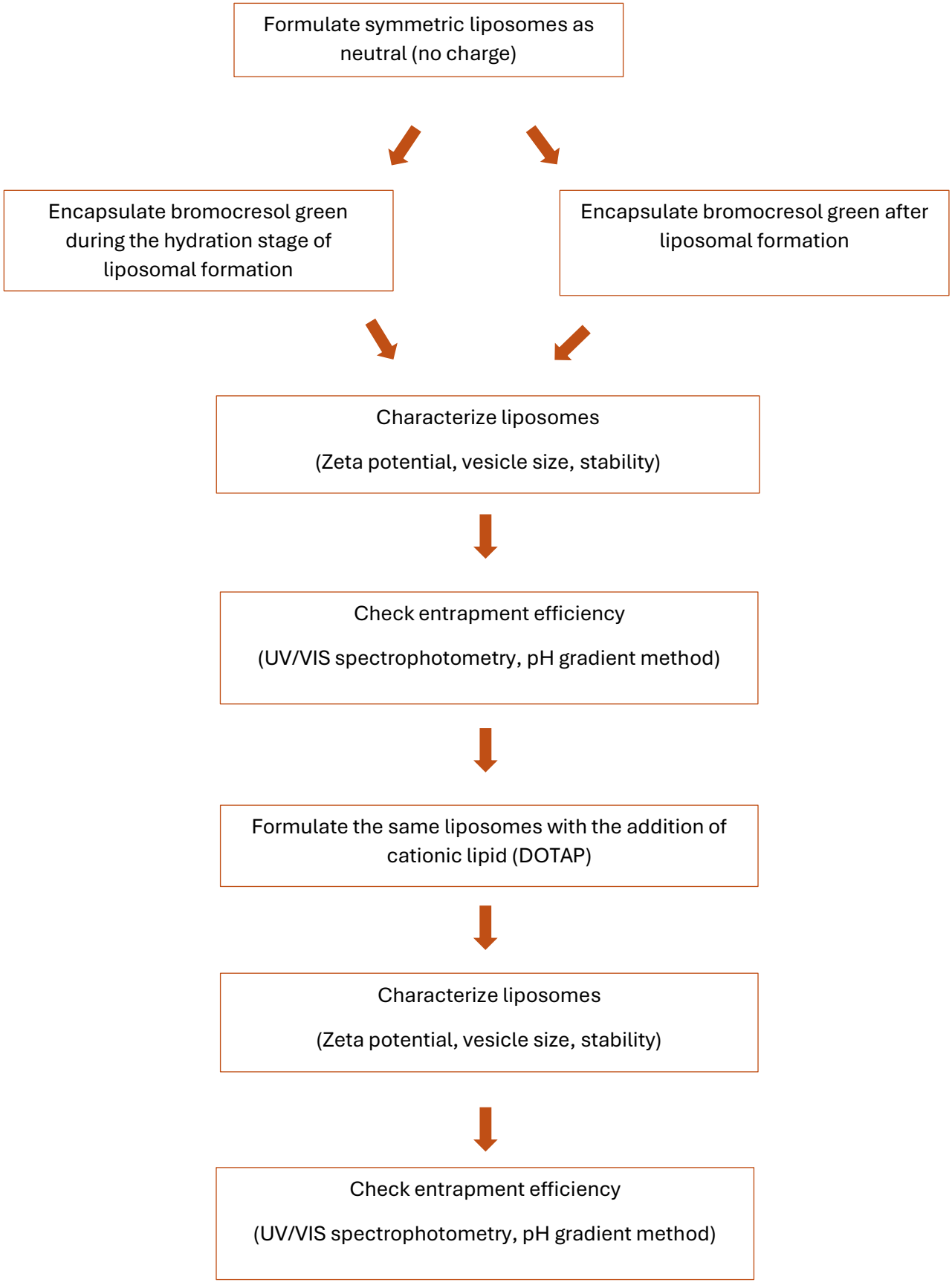

STEP 2:

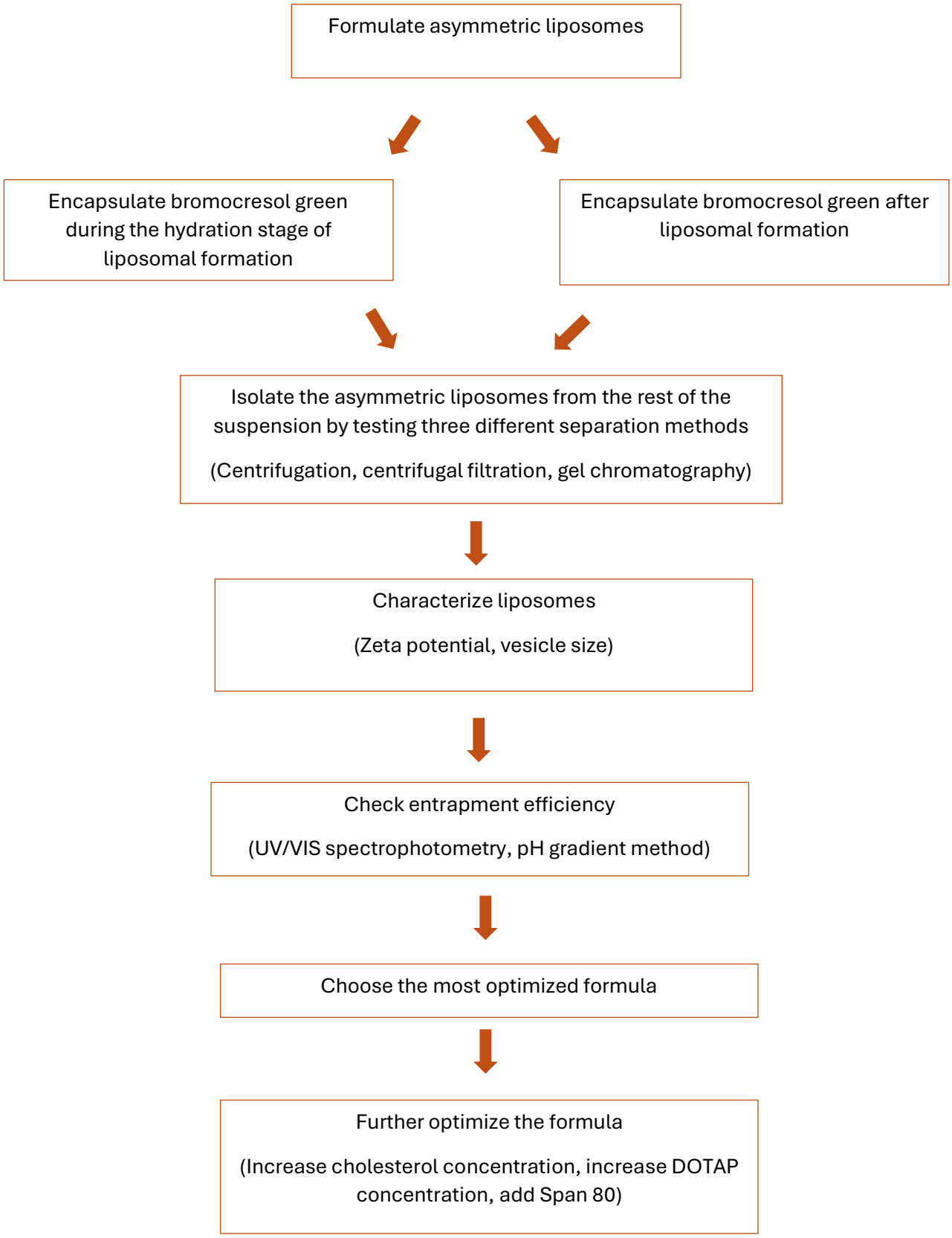
Formulate asymmetric liposomes
Encapsulate bromocresol green during the hydration stage of liposomal formation
Encapsulate bromocresol green after liposomal formation
Isolate the asymmetric liposomes from the rest of the suspension by testing three different separation methods
(Centrifugation, centrifugal filtration, gel chromatography)
Characterize liposomes
(Zeta potential, vesicle size)
Check entrapment efficiency
(UV/VIS spectrophotometry, pH gradient method)
Choose the most optimized formula
Further optimize the formula
(Increase cholesterol concentration, increase DOTAP concentration, add Span 80)

FLOW CHART CHAPTER 5

Formulate most optimized asymmetric liposomal formulation

↓

Test three different DNA amount

(3µl, 6µl,12µl)

↓

Choose the best liposomes to DNA ratio

Ratio→19.4:1 (6µl)

↓

Encapsulate DNA using 3 different encapsulation methods

1. Method A- Adding the DNA to symmetric acceptor vesicle
2. Method B- Adding the DNA during the lipid exchange stage
3. Method C- Adding the DNA to the asymmetric

↓

Choose the best encapsulation method

(Adding the DNA to symmetric acceptor vesicle)

(Entrapment efficiency checked using Nanodrop lite machine)

↓

Measure the stability of the asymmetric liposomes formed as empty vesicles and as DNA loaded vesicles

2. Further work

The potential for future work in this field remains enormous, as the field is still nascent. In this study, the highest concentrations tested were 2 mM for the acceptor vesicles and 4 mM for the donor complex. However, pushing these levels higher led to unexpected issues like aggregation, which disrupted complex formation and impacted the overall performance of the liposomes. This suggests that exceeding a certain threshold can introduce challenges. Future work should explore ways to boost lipid concentration without triggering these issues, possibly by tweaking formulation conditions or adding stabilising agents. Overcoming these hurdles could lead to more efficient and stable liposomes, paving the way for broader applications in drug delivery and related biomedical fields. Moreover, the exact percentage of complexation and asymmetry formation needs to be further explored as it will help in accurately studying the vesicles' properties.

To build on previous research, a deeper dive is required into the factors that influence liposomal asymmetry stability and ways to reduce lipid flip-flop within the liposomes. Keeping the asymmetry intact is vital, particularly for drug delivery purposes. One potential solution could be lyophilisation, which might help maintain the structural integrity of liposomes by limiting lipid movement. Conducting systematic studies on this technique could offer valuable insights. Another promising approach involves integrating specific proteins, which may help reinforce the bilayer and regulate lipid flip-flop. Investigating these protein-lipid interactions further could lead to more potent, more effective liposomal formulations with longer lasting asymmetry.

So far, no transfection studies have been conducted on asymmetric liposomes. Exploring this avenue in the future could provide crucial insights into the effectiveness and safety of asymmetric liposomes, helping to determine their potential for use in biomedical applications.

References

1. Zangi L, Lui KO, von Gise A, Ma Q, Ebina W, Ptaszek LM, et al. Modified mRNA directs the fate of heart progenitor cells and induces vascular regeneration after myocardial infarction. Nat Biotechnol. 2013 Oct;31(10):898–907.

2. Bhaskarwar A. Liposomes: Fundamentals, Properties and Applications for Targeted Drug Delivery [Internet]. New York, UNITED STATES: Momentum Press; 2018 [cited 2021 Dec 13]. Available from: http://ebookcentral.proquest.com/lib/sunderland/detail.action?docID=5848213

3. Li B, London E. Preparation and Drug Entrapment Properties of Asymmetric Liposomes Containing Cationic and Anionic Lipids. Langmuir. 2020 Oct 27;36(42):12521–31.

4. Mokhtarieh AA, Davarpanah SJ, Lee MK. Ethanol treatment a Non-extrusion method for asymmetric liposome size optimization. DARU J Pharm Sci. 2013 Apr 18;21(1):32.

5. Tseu GYW, Kamaruzaman KA. A Review of Different Types of Liposomes and Their Advancements as a Form of Gene Therapy Treatment for Breast Cancer. Molecules. 2023 Feb 3;28(3):1498.

6. Akbarzadeh A, Rezaei-Sadabady R, Davaran S, Joo SW, Zarghami N, Hanifehpour Y, et al. Liposome: classification, preparation, and applications. Nanoscale Res Lett. 2013 Feb 22;8(1):102.

7. Tenchov R, Bird R, Curtze AE, Zhou Q. Lipid Nanoparticles–From Liposomes to mRNA Vaccine Delivery, a Landscape of Research Diversity and Advancement. ACS Nano. 2021 Nov 23;15(11):16982–7015.

8. Attia MA, Essa EA, Elebyary TT, Faheem AM, Elkordy AA. Brief on Recent Application of Liposomal Vaccines for Lower Respiratory Tract Viral Infections: From Influenza to COVID-19 Vaccines. Pharmaceuticals. 2021 Nov;14(11):1173.

9. Lombardo D, Kiselev MA. Methods of Liposomes Preparation: Formation and Control Factors of Versatile Nanocarriers for Biomedical and Nanomedicine Application. Pharmaceutics. 2022 Mar;14(3):543.

10. Hamilton RL, Goerke J, Guo LS, Williams MC, Havel RJ. Unilamellar liposomes made with the French pressure cell: a simple preparative and semiquantitative technique. J Lipid Res. 1980 Nov;21(8):981–92.

11. Rieth MD, Lozano A. Preparation of DPPC liposomes using probe-tip sonication: Investigating intrinsic factors affecting temperature phase transitions. Biochem Biophys Rep. 2020 Jul 1;22:100764.

12. Andra VVSNL, Pammi SVN, Bhatraju LVKP, Ruddaraju LK. A Comprehensive Review on Novel Liposomal Methodologies, Commercial Formulations, Clinical Trials and Patents. Bionanoscience. 2022;12(1):274–91.

13. Gouda A, Sakr OS, Nasr M, Sammour O. Ethanol injection technique for liposomes formulation: An insight into development, influencing factors, challenges and applications. J Drug Deliv Sci Technol. 2021 Feb 1;61:102174.

14. Javia A, Misra A, Thakkar H. Liposomes encapsulating novel antimicrobial peptide Omiganan: Characterization and its pharmacodynamic evaluation in atopic dermatitis and psoriasis mice model. Int J Pharm. 2022 Aug 25;624:122045.

15. Kastner E, Verma V, Lowry D, Perrie Y. Microfluidic-controlled manufacture of liposomes for the solubilisation of a poorly water soluble drug. Int J Pharm. 2015 May 15;485(1):122–30.

16. Shah S, Dhawan V, Holm R, Nagarsenker MS, Perrie Y. Liposomes: Advancements and innovation in the manufacturing process. Adv Drug Deliv Rev. 2020 Jan 1;154–155:102–22.

17. London E. Membrane Structure–Function Insights from Asymmetric Lipid Vesicles. Acc Chem Res. 2019 Aug 20;52(8):2382–91.

18. Cheng HT, Megha, London E. Preparation and Properties of Asymmetric Vesicles That Mimic Cell Membranes. J Biol Chem. 2009 Mar;284(10):6079–92.

19. Watson H. Biological membranes. Essays Biochem. 2015;59:43–69.

20. Enoki TA, Wu J, Heberle FA, Feigenson GW. Investigation of the domain line tension in asymmetric vesicles prepared via hemifusion. Biochim Biophys Acta BBA - Biomembr. 2021 Jun;1863(6):183586.

21. Wood WG, Igbavboa U, Müller WE, Eckert GP. Cholesterol Asymmetry in Synaptic Plasma Membranes. J Neurochem. 2011 Mar;116(5):684–9.

22. Fujimoto T, Parmryd I. Interleaflet Coupling, Pinning, and Leaflet Asymmetry—Major Players in Plasma Membrane Nanodomain Formation. Front Cell Dev Biol [Internet]. 2017 [cited 2022 Jul 4];4. Available from: https://www.frontiersin.org/articles/10.3389/fcell.2016.00155

23. Bretscher MS. Asymmetrical Lipid Bilayer Structure for Biological Membranes. Nature New Biol. 1972 Mar;236(61):11–2.

24. Devaux PF. Static and dynamic lipid asymmetry in cell membranes. Biochemistry. 1991 Feb 5;30(5):1163–73.

25. Barsukov LI, Kulikov VI, Bergelson LD. Lipid transfer proteins as a tool in the study of membrane structure. Inside-outside distribution of the phospholipids in the protoplasmic membrane of Micrococcus<math><mtext>Micrococcus</mtext></math>lysodeikticus<math><mtext>lysodeikticus</mtext></math>. Biochem Biophys Res Commun. 1976 Aug 9;71(3):704–11.

26. Rothman JE, Kennedy EP. Symmetrical distribution of phospholipids in the membrane of *Bacillus megaterium*. J Mol Biol. 1977 Mar 5;110(3):603–18.

27. Kodigepalli KM, Bowers K, Sharp A, Nanjundan M. Roles and regulation of phospholipid scramblases. FEBS Lett. 2015 Jan 2;589(1):3–14.

28. Marquardt D, Geier B, Pabst G. Asymmetric lipid membranes: towards more realistic model systems. Membranes. 2015 May 6;5(2):180–96.

29. Callan-Jones A, Sorre B, Bassereau P. Curvature-Driven Lipid Sorting in Biomembranes. Cold Spring Harb Perspect Biol. 2011 Feb;3(2):a004648.

30. Verkleij AJ, Zwaal RF, Roelofsen B, Comfurius P, Kastelijn D, van Deenen LL. The asymmetric distribution of phospholipids in the human red cell membrane. A combined study using phospholipases and freeze-etch electron microscopy. Biochim Biophys Acta. 1973 Oct 11;323(2):178–93.

31. Kučerka N, Nieh MP, Katsaras J. Asymmetric Distribution of Cholesterol in Unilamellar Vesicles of Monounsaturated Phospholipids. Langmuir. 2009 Dec 1;25(23):13522–7.

32. Wang W, Yang L, Huang HW. Evidence of Cholesterol Accumulated in High Curvature Regions: Implication to the Curvature Elastic Energy for Lipid Mixtures. Biophys J. 2007 Apr 15;92(8):2819–30.

33. Ma Y, Poole K, Goyette J, Gaus K. Introducing Membrane Charge and Membrane Potential to T Cell Signaling. Front Immunol [Internet]. 2017 Nov 9 [cited 2025 Jun 17];8. Available from: https://www.frontiersin.org/journals/immunology/articles/10.3389/fimmu.2017.01513/full

34. Edgar JR. Q&A: What are exosomes, exactly? BMC Biol. 2016 Jun 13;14(1):46.

35. Raposo G, Stoorvogel W. Extracellular vesicles: Exosomes, microvesicles, and friends. J Cell Biol. 2013 Feb 18;200(4):373–83.

36. Théry C, Zitvogel L, Amigorena S. Exosomes: composition, biogenesis and function. Nat Rev Immunol. 2002 Aug;2(8):569–79.

37. Kamiya K, Osaki T, Takeuchi S. Formation of nano-sized lipid vesicles with asymmetric lipid components using a pulsed-jet flow method. Sens Actuators B Chem. 2021 Jan 15;327:128917.

38. Henson PM, Bratton DL, Fadok VA. Apoptotic cell removal. Curr Biol CB. 2001 Oct 2;11(19):R795-805.

39. Zwaal RFA, Comfurius P, Bevers EM. Surface exposure of phosphatidylserine in pathological cells. Cell Mol Life Sci CMLS. 2005 May;62(9):971–88.

40. Fadeel B, Xue D. The ins and outs of phospholipid asymmetry in the plasma membrane: roles in health and disease. Crit Rev Biochem Mol Biol. 2009;44(5):264–77.

41. Lingwood D, Simons K. Lipid rafts as a membrane-organizing principle. Science. 2010 Jan 1;327(5961):46–50.

42. Heberle FA, Feigenson GW. Phase Separation in Lipid Membranes. Cold Spring Harb Perspect Biol. 2011 Apr;3(4):a004630.

43. Brown DA, London E. Functions of lipid rafts in biological membranes. Annu Rev Cell Dev Biol. 1998;14:111–36.

44. Rietveld A, Simons K. The differential miscibility of lipids as the basis for the formation of functional membrane rafts. Biochim Biophys Acta. 1998 Nov 10;1376(3):467–79.

45. St. Clair JW, London E. Effect of sterol structure on ordered membrane domain (raft) stability in symmetric and asymmetric vesicles. Biochim Biophys Acta BBA - Biomembr. 2019 Jun;1861(6):1112–22.

46. Ahmed SN, Brown DA, London E. On the Origin of Sphingolipid/Cholesterol-Rich Detergent-Insoluble Cell Membranes: Physiological Concentrations of Cholesterol and Sphingolipid Induce Formation of a Detergent-Insoluble, Liquid-Ordered Lipid Phase in Model Membranes. Biochemistry. 1997 Sep 1;36(36):10944–53.

47. Wang TY, Silvius JR. Cholesterol does not induce segregation of liquid-ordered domains in bilayers modeling the inner leaflet of the plasma membrane. Biophys J. 2001 Nov;81(5):2762–73.

48. Cheng HT, London E. Preparation and Properties of Asymmetric Large Unilamellar Vesicles: Interleaflet Coupling in Asymmetric Vesicles Is Dependent on Temperature but Not Curvature. Biophys J. 2011 Jun 8;100(11):2671–8.

49. Kiessling V, Crane JM, Tamm LK. Transbilayer Effects of Raft-Like Lipid Domains in Asymmetric Planar Bilayers Measured by Single Molecule Tracking. Biophys J. 2006 Nov 1;91(9):3313–26.

50. Collins MD, Keller SL. Tuning lipid mixtures to induce or suppress domain formation across leaflets of unsupported asymmetric bilayers. Proc Natl Acad Sci. 2008 Jan 8;105(1):124–8.

51. Greco E, Quintiliani G, Santucci MB, Serafino A, Ciccaglione AR, Marcantonio C, et al. Janus-faced liposomes enhance antimicrobial innate immune response in Mycobacterium tuberculosis infection. Proc Natl Acad Sci U S A. 2012 May 22;109(21):E1360-1368.

52. Anderson CF, Grimmett ME, Domalewski CJ, Cui H. Inhalable nanotherapeutics to improve treatment efficacy for common lung diseases. Wiley Interdiscip Rev Nanomed Nanobiotechnol. 2020 Jan;12(1):e1586.

53. Whittenton J, Harendra S, Pitchumani R, Mohanty K, Vipulanandan C, Thevananther S. Evaluation of Asymmetric Liposomal Nanoparticles for Encapsulation of Polynucleotides. Langmuir. 2008 Aug 1;24(16):8533–40.

54. Son M, London E. The dependence of lipid asymmetry upon polar headgroup structure[S]. J Lipid Res. 2013 Dec 1;54(12):3385–93.

55. Son M, London E. The dependence of lipid asymmetry upon phosphatidylcholine acyl chain structure. J Lipid Res. 2013 Jan;54(1):223–31.

56. Li MH, Raleigh DP, London E. Preparation of Asymmetric Vesicles with Trapped CsCl Avoids Osmotic Imbalance, Non-Physiological External Solutions, and Minimizes Leakage. Langmuir ACS J Surf Colloids. 2021 Oct 5;37(39):11611–7.

57. Lin Q, London E. Preparation of Artificial Plasma Membrane Mimicking Vesicles with Lipid Asymmetry. PLOS ONE. 2014 Jan 28;9(1):e87903.

58. Davis ME, Brewster ME. Cyclodextrin-based pharmaceutics: past, present and future. Nat Rev Drug Discov. 2004 Dec;3(12):1023–35.

59. Scott HL, Kennison KB, Enoki TA, Doktorova M, Kinnun JJ, Heberle FA, et al. Model Membrane Systems Used to Study Plasma Membrane Lipid Asymmetry. Symmetry. 2021 Aug;13(8):1356.

60. Heberle FA, Marquardt D, Doktorova M, Geier B, Standaert RF, Heftberger P, et al. Subnanometer Structure of an Asymmetric Model Membrane: Interleaflet Coupling Influences Domain Properties. Langmuir. 2016 May 24;32(20):5195–200.

61. Markones M, Drechsler C, Kaiser M, Kalie L, Heerklotz H, Fiedler S. Engineering Asymmetric Lipid Vesicles: Accurate and Convenient Control of the Outer Leaflet Lipid Composition. Langmuir. 2018 Feb 6;34(5):1999–2005.

62. Markones M, Fippel A, Kaiser M, Drechsler C, Hunte C, Heerklotz H. Stairway to Asymmetry: Five Steps to Lipid-Asymmetric Proteoliposomes. Biophys J. 2020 Jan 21;118(2):294–302.

63. Doktorova M, Heberle FA, Marquardt D, Rusinova R, Sanford RL, Peyear TA, et al. Gramicidin Increases Lipid Flip-Flop in Symmetric and Asymmetric Lipid Vesicles. Biophys J. 2019 Mar 5;116(5):860–73.

64. Nguyen MHL, DiPasquale M, Rickeard BW, Doktorova M, Heberle FA, Scott HL, et al. Peptide-Induced Lipid Flip-Flop in Asymmetric Liposomes Measured by Small Angle Neutron Scattering. Langmuir. 2019 Sep 10;35(36):11735–44.

65. Mokhtarieh AA, Cheong S, Kim S, Chung BH, Lee MK. Asymmetric liposome particles with highly efficient encapsulation of siRNA and without nonspecific cell penetration suitable for target-specific delivery. Biochim Biophys Acta BBA - Biomembr. 2012 Jul;1818(7):1633–41.

66. Sun HY, Deng G, Jiang YW, Zhou Y, Xu J, Wu FG, et al. Controllable engineering of asymmetric phosphatidylserine-containing lipid vesicles using calcium cations. Chem Commun. 2017 Nov 28;53(95):12762–5.

67. Guo HY, Sun HY, Deng G, Xu J, Wu FG, Yu ZW. Fabrication of Asymmetric Phosphatidylserine-Containing Lipid Vesicles: A Study on the Effects of Size, Temperature, and Lipid Composition. Langmuir. 2020 Oct 27;36(42):12684–91.

68. Drechsler C, Markones M, Choi JY, Frieling N, Fiedler S, Voelker DR, et al. Preparation of Asymmetric Liposomes Using a Phosphatidylserine Decarboxylase. Biophys J. 2018 Oct 16;115(8):1509–17.

69. Takaoka R, Kurosaki H, Nakao H, Ikeda K, Nakano M. Formation of asymmetric vesicles via phospholipase D-mediated transphosphatidylation. Biochim Biophys Acta BBA - Biomembr. 2018 Feb 1;1860(2):245–9.

70. Pautot S, Frisken BJ, Weitz DA. Engineering asymmetric vesicles. Proc Natl Acad Sci. 2003 Sep 16;100(19):10718–21.

71. Karamdad K, V. Law R, M. Seddon J, J. Brooks N, Ces O. Preparation and mechanical characterisation of giant unilamellar vesicles by a microfluidic method. Lab Chip. 2015;15(2):557–62.

72. de Matos MBC, Miranda BS, Rizky Nuari Y, Storm G, Leneweit G, Schiffelers RM, et al. Liposomes with asymmetric bilayers produced from inverse emulsions for nucleic acid delivery. J Drug Target. 2019 Jul;27(5–6):681–9.

73. Hu PC, Li S, Malmstadt N. Microfluidic fabrication of asymmetric giant lipid vesicles. ACS Appl Mater Interfaces. 2011 May;3(5):1434–40.

74. Lu L, Schertzer JW, Chiarot PR. Continuous microfluidic fabrication of synthetic asymmetric vesicles. Lab Chip. 2015 Aug 11;15(17):3591–9.

75. Ghazal A, Gontsarik M, Kutter JP, Lafleur JP, Ahmadvand D, Labrador A, et al. Microfluidic Platform for the Continuous Production and Characterization of Multilamellar Vesicles: A Synchrotron Small-Angle X-ray Scattering (SAXS) Study. J Phys Chem Lett. 2017 Jan 5;8(1):73–9.

76. Enoki TA, Feigenson GW. Asymmetric Bilayers by Hemifusion: Method and Leaflet Behaviors. Biophys J. 2019 Sep;117(6):1037–50.

77. Kamiya K, Kawano R, Osaki T, Akiyoshi K, Takeuchi S. Cell-sized asymmetric lipid vesicles facilitate the investigation of asymmetric membranes. Nat Chem. 2016 Sep;8(9):881–9.

78. Kamiya K, Osaki T, Takeuchi S. Formation of vesicles-in-a-vesicle with asymmetric lipid components using a pulsed-jet flow method. RSC Adv. 2019;9(52):30071–5.

79. Doktorova M, Symons JL, Levental I. Structural and functional consequences of reversible lipid asymmetry in living membranes. Nat Chem Biol. 2020 Dec;16(12):1321–30.

80. Askal HF, Khedr AS, Darwish IA, Mahmoud RM. Quantitative Thin-Layer Chromatographic Method for Determination of Amantadine Hydrochloride. Int J Biomed Sci IJBS. 2008 Jun;4(2):155–60.

81. Marquardt D, Heberle FA, Pan J, Cheng X, Pabst G, Harroun TA, et al. The structures of polyunsaturated lipid bilayers by joint refinement of neutron and X-ray scattering data. Chem Phys Lipids. 2020 Jul;229:104892.

82. Kawakami S, Hashida M. Targeted delivery systems of small interfering RNA by systemic administration. Drug Metab Pharmacokinet. 2007 Jun;22(3):142–51.

83. Immordino ML, Dosio F, Cattel L. Stealth liposomes: review of the basic science, rationale, and clinical applications, existing and potential. Int J Nanomedicine. 2006 Sep;1(3):297–315.

84. Ramamoorth M, Narvekar A. Non Viral Vectors in Gene Therapy- An Overview. J Clin Diagn Res JCDR. 2015 Jan;9(1):GE01–6.

85. Schaffert D, Wagner E. Gene therapy progress and prospects: synthetic polymer-based systems. Gene Ther. 2008 Aug;15(16):1131–8.

86. Ren T, Song YK, Zhang G, Liu D. Structural basis of DOTMA for its high intravenous transfection activity in mouse. Gene Ther. 2000 May;7(9):764–8.

87. Opanasopit P, Nishikawa M, Hashida M. Factors affecting drug and gene delivery: effects of interaction with blood components. Crit Rev Ther Drug Carrier Syst. 2002;19(3):191–233.

88. Reagle T, Xie Y, Li Z, Carnero W, Baumgart T. Methyl-β-cyclodextrin asymmetrically extracts phospholipid from bilayers, granting tunable control over differential stress in lipid vesicles. Soft Matter. 2024 May 29;20(21):4291–307.

89. M. Machin J, A. Ranson N, E. Radford S. Protein-induced membrane asymmetry modulates OMP folding kinetics and stability. Faraday Discuss [Internet]. 2025 [cited 2025 Jun 27]; Available from: https://pubs.rsc.org/en/content/articlelanding/2025/fd/d4fd00180j

90. Matsuki Y, Iwamoto M, Oiki S. Asymmetric Lipid Bilayers and Potassium Channels Embedded Therein in the Contact Bubble Bilayer. In: Furini S, editor. Potassium Channels: Methods and Protocols [Internet]. New York, NY: Springer US; 2024 [cited 2025 Jun 27]. p. 1–21. Available from: https://doi.org/10.1007/978-1-0716-3818-7_1

91. Borges Fernandes B, Ghosh S, Williams I, Forth J, Ruiz-Perez L, Battaglia G. Investigating chemotaxis in asymmetric liposomes. APS March Meet Abstr. 2024 Mar;2024:OD01.005.

92. Pašalić L, Maleš P, Čikoš A, Pem B, Bakarić D. The rise of FTIR spectroscopy in the characterization of asymmetric lipid membranes. Spectrochim Acta A Mol Biomol Spectrosc. 2024 Jan;305:123488.

93. Merck | United Kingdom | Life Science Products & Service Solutions [Internet]. [cited 2025 Jul 2]. Available from: https://www.sigmaaldrich.com/GB/en?srsltid=AfmBOoov_Cy-P1weSudR0zw1YHdtL5TH38iUi6kg6aWAenzsmpj48VVV

94. Avanti Polar Lipids [Internet]. [cited 2022 Nov 9]. Phase Transition Temperatures for Glycerophospholipids. Available from: https://avantilipids.com/tech-support/physical-properties/phase-transition-temps

95. (PDF) An X-ray Diffraction study for isotactic polypropylene fibers produced with take-up speeds of 2500-4250 m/min. ResearchGate [Internet]. [cited 2025 Jul 2]; Available from: https://www.researchgate.net/publication/255843439_An_X-ray_Diffraction_study_for_isotactic_polypropylene_fibers_produced_with_take-up_speeds_of_2500-4250_mmin

96. A review on surfactants as edge activators in ultradeformable vesicles for enhanced skin delivery. ResearchGate [Internet]. [cited 2025 Jul 2]; Available from: https://www.researchgate.net/publication/286135388_A_review_on_surfactants_as_edge_activators_in_ultradeformable_vesicles_for_enhanced_skin_delivery

97. Odeh F, Nsairat H, Alshaer W, Alsotari S, Buqaien R, Ismail S, et al. Remote loading of curcumin-in-modified β-cyclodextrins into liposomes using a transmembrane pH gradient. RSC Adv. 2019 Nov 13;9(64):37148–61.

98. Balan V, Mihai CT, Cojocaru FD, Uritu CM, Dodi G, Botezat D, et al. Vibrational Spectroscopy Fingerprinting in Medicine: from Molecular to Clinical Practice. Materials. 2019 Sep 6;12(18):2884.

99. Infrared Spectroscopy [Internet]. [cited 2025 Jan 23]. Available from: https://www2.chemistry.msu.edu/faculty/reusch/virttxtjml/spectrpy/infrared/infrared.htm

100. de la Arada I, González-Ramírez EJ, Alonso A, Goñi FM, Arrondo JLR. Exploring polar headgroup interactions between sphingomyelin and ceramide with infrared spectroscopy. Sci Rep. 2020 Oct 19;10:17606.

101. (PDF) The chain order of binary unsaturated lipid bilayers modulated by aromatic-residue-containing peptides: An ATR-FTIR spectroscopy study. ResearchGate [Internet]. 2024 Dec 9 [cited 2025 Jan 23]; Available from:

https://www.researchgate.net/publication/317373387_The_chain_order_of_binary_unsaturated_lipid_bilayers_modulated_by_aromatic-residue-containing_peptides_An_ATR-FTIR_spectroscopy_study

102. Portaccio M, Faramarzi B, Lepore M. Probing Biochemical Differences in Lipid Components of Human Cells by Means of ATR-FTIR Spectroscopy. Biophysica. 2023 Sep;3(3):524–38.

103. Choosakoonkriang S, Wiethoff CM, Anchordoquy TJ, Koe GS, Smith JG, Middaugh CR. Infrared Spectroscopic Characterization of the Interaction of Cationic Lipids with Plasmid DNA*. J Biol Chem. 2001 Mar 1;276(11):8037–43.

104. (PDF) Microencapsulation of the Biocide Benzisothiazolinone (BIT) by Inclusion in Methyl-β-cyclodextrin and Screening of Its Antibacterial and Ecotoxicity Properties. ResearchGate [Internet]. 2024 Oct 22 [cited 2025 Jan 23]; Available from: https://www.researchgate.net/publication/384068681_Microencapsulation_of_the_Biocide_Benzisothiazolinone_BIT_by_Inclusion_in_Methyl-b-cyclodextrin_and_Screening_of_Its_Antibacterial_and_Ecotoxicity_Properties

105. (PDF) Encapsulation of Isoniazid-conjugated Phthalocyanine-In-Cyclodextrin-In-Liposomes Using Heating Method. ResearchGate [Internet]. 2024 Dec 9 [cited 2025 Jan 23]; Available from: https://www.researchgate.net/publication/335021720_Encapsulation_of_Isoniazid-conjugated_Phthalocyanine-In-Cyclodextrin-In-Liposomes_Using_Heating_Method

106. Coats AW, Redfern JP. Thermogravimetric analysis. A review. Analyst. 1963 Jan 1;88(1053):906–24.

107. Trotta F, Zanetti M, Camino G. Thermal degradation of cyclodextrins. Polym Degrad Stab. 2000 Sep 1;69(3):373–9.

108. Sambasevam K, Mohamad S, Muhamad Sarih N, Ismail N. Synthesis and Characterization of the Inclusion Complex of ??-cyclodextrin and Azomethine. Int J Mol Sci. 2013 Feb 1;14:3671–82.

109. Chen X, Li C, Zhao J, Wang Y, Xu Y, Xu B. Influence of phospholipid structures on volatile organic compounds generation in model systems. Food Res Int. 2024 Nov 1;196:115009.

110. Wei L. Thermal Properties of Some Lipid Components of Cell Membranes.

111. Kv K, Sr A, Pr Y, Ry P, Vu B. Differential Scanning Calorimetry: A Review. Res Rev J Pharm Anal. 2014 Dec 29;3(3):11–22.

112. ResearchGate [Internet]. [cited 2025 Jan 24]. Figure 4. DSC thermograms of (a) α-CD, (b) β-CD, (c) DHAB, (d)... Available from: https://www.researchgate.net/figure/DSC-thermograms-of-a-a-CD-b-b-CD-c-DHAB-d-DHAB-a-CD-e-DHAB-b-CD-f-HAB_fig1_257946742

113. Giordano F, Novak C, Moyano JR. Thermal analysis of cyclodextrins and their inclusion compounds. Thermochim Acta. 2001 Dec 14;380(2):123–51.

114. Garvey CJ, Bryant SJ, Elbourne A, Hunt T, Kent B, Kreuzer M, et al. Phase separation in a ternary DPPC/DOPC/POPC system with reducing hydration. J Colloid Interface Sci. 2023 May;638:719–32.

115. (PDF) Studies on Lactoferricin-derived Escherichia coli Membrane-active Peptides Reveal Differences in the Mechanism of N-Acylated Versus Nonacylated Peptides. ResearchGate [Internet]. 2024 Oct 22 [cited 2025 Jan 25]; Available from: https://www.researchgate.net/publication/51072722_Studies_on_Lactoferricin-derived_Escherichia_coli_Membrane-active_Peptides_Reveal_Differences_in_the_Mechanism_of_N-Acylated_Versus_Nonacylated_Peptides

116. (PDF) Effects of extrusion, lipid concentration and purity on physico-chemical and biological properties of cationic liposomes for gene vaccine applications. ResearchGate [Internet]. 2024 Dec 4 [cited 2025 Jan 25]; Available from: https://www.researchgate.net/publication/225051822_Effects_of_extrusion_lipid_concentration_and_purity_on_physico-chemical_and_biological_properties_of_cationic_liposomes_for_gene_vaccine_applications

117. (PDF) The role of sterol rings and side chain on the structure and phase behaviour of sphingomyelin bilayers. ResearchGate [Internet]. 2024 Oct 22 [cited 2025 Jan 25]; Available from: https://www.researchgate.net/publication/23288511_The_role_of_sterol_rings_and_side_chain_on_the_structure_and_phase_behaviour_of_sphingomyelin_bilayers

118. Pahwa M, Mp A, Agasti SS. Organic/inorganic hybrid nanostructures for biological imaging and delivery. In: Yin Y, Lu Y, Xia Y, editors. Encyclopedia of Nanomaterials (First Edition) [Internet]. Oxford: Elsevier; 2023 [cited 2024 Mar 23]. p. 478–95. Available from: https://www.sciencedirect.com/science/article/pii/B9780128224250000725

119. cambride isotope laboratories. NMR solvent chart [Internet]. Cambridge Isotope Laboratories, Inc.; Available from: https://chem.washington.edu/sites/chem/files/documents/facilities/nmrsolventschart_001.pdf

120. Cyclolab [Internet]. [cited 2025 Feb 8]. Available from: https://cyclolab.hu/products/nonionic_cyclodextrins-c11/random_methylalphacyclodextrin_ds_11-p65/

121. Avanti Research [Internet]. [cited 2025 Feb 8]. 18:1 TAP (DOTAP) | Avanti Chloroform, Powder Chloride Salt. Available from: https://avantiresearch.com/product/890890

122. 16:0-18:1 PC (POPC) | 26853-31-6 | Avanti [Internet]. [cited 2025 Feb 8]. Available from: https://avantiresearch.com/product/850457

123. Avanti Research [Internet]. [cited 2025 Feb 8]. Brain SM | Avanti. Available from: https://avantiresearch.com/product/860062

124. Avanti Research [Internet]. [cited 2025 Feb 8]. 16:0-18:1 PE | 26662-94-2 | Avanti. Available from: https://avantiresearch.com/product/850757

125. Malvern Instruments Limited. Zetapotentail introduction. 2015; Grovewood Road, Malvern, Worcestershire, UK. WR14 1XZ.

126. Shao XR, Wei XQ, Zhang S, Fu N, Lin YF, Cai XX, et al. Effects of Micro-environmental pH of Liposome on Chemical Stability of Loaded Drug. Nanoscale Res Lett [Internet]. 2017 [cited 2024 Mar 24];12. Available from: https://www.ncbi.nlm.nih.gov/pmc/articles/PMC6890883/

127. Stephan MS, Dunsing V, Pramanik S, Chiantia S, Barbirz S, Robinson T, et al. Biomimetic asymmetric bacterial membranes incorporating lipopolysaccharides. Biophys J. 2023 Jun 6;122(11):2147–61.

128. Romanov V, McCullough J, Gale BK, Frost A. A Tunable Microfluidic Device Enables Cargo Encapsulation by Cell- or Organelle-Sized Lipid Vesicles Comprising Asymmetric Lipid Bilayers. Adv Biosyst. 2019 Jul;3(7):1900010.

129. McIntyre JC, Sleight RG. Fluorescence assay for phospholipid membrane asymmetry. Biochemistry. 1991 Dec 1;30(51):11819–27.

130. Guimarães D, Noro J, Loureiro A, Lager F, Renault G, Cavaco-Paulo A, et al. Increased Encapsulation Efficiency of Methotrexate in Liposomes for Rheumatoid Arthritis Therapy. Biomedicines. 2020 Dec 18;8(12):630.

131. Bromocresol Green ACS reagent, Dye content 95 76-60-8 [Internet]. [cited 2024 Nov 11]. Available from: http://www.sigmaaldrich.com/

132. Li J, Wang X, Zhang T, Wang C, Huang Z, Luo X, et al. A review on phospholipids and their main applications in drug delivery systems. Asian J Pharm Sci. 2015 Apr 1;10(2):81–98.

133. Goodman SR, editor. Chapter 2 - Cell Membranes. In: Medical Cell Biology (Third Edition) [Internet]. San Diego: Academic Press; 2008 [cited 2024 Nov 12]. p. 27–57. Available from: https://www.sciencedirect.com/science/article/pii/B9780123704580500074

134. Montizaan D, Yang K, Reker-Smit C, Salvati A. Comparison of the uptake mechanisms of zwitterionic and negatively charged liposomes by HeLa cells. Nanomedicine Nanotechnol Biol Med. 2020 Nov 1;30:102300.

135. Wang DY, van der Mei HC, Ren Y, Busscher HJ, Shi L. Lipid-Based Antimicrobial Delivery-Systems for the Treatment of Bacterial Infections. Front Chem [Internet]. 2020 Jan 10 [cited 2024 Nov 12];7. Available from: https://www.frontiersin.org/journals/chemistry/articles/10.3389/fchem.2019.00872/full

136. Inglut CT, Sorrin AJ, Kuruppu T, Vig S, Cicalo J, Ahmad H, et al. Immunological and Toxicological Considerations for the Design of Liposomes. Nanomaterials. 2020 Feb;10(2):190.

137. Adams DH, Joyce G, Richardson VJ, Ryman BE, Wiśniewski HM. Liposome toxicity in the mouse central nervous system. J Neurol Sci. 1977 Mar 1;31(2):173–9.

138. Yamauchi M, Kusano H, Saito E, Iwata T, Nakakura M, Kato Y, et al. Development of wrapped liposomes: Novel liposomes comprised of polyanion drug and cationic lipid

complexes wrapped with neutral lipids. Biochim Biophys Acta BBA - Biomembr. 2006 Jan 1;1758(1):90–7.

139. Benita S, Poly PA, Puisieux F, Delattre J. Radiopaque Liposomes: Effect of Formulation Conditions on Encapsulation Efficiency. J Pharm Sci. 1984 Dec 1;73(12):1751–5.

140. Syama K, Jakubek ZJ, Chen S, Zaifman J, Tam YYC, Zou S. Development of lipid nanoparticles and liposomes reference materials (II): cytotoxic profiles. Sci Rep. 2022 Oct 27;12(1):18071.

141. Lapinski MM, Castro-Forero A, Greiner AJ, Ofoli RY, Blanchard GJ. Comparison of Liposomes Formed by Sonication and Extrusion: Rotational and Translational Diffusion of an Embedded Chromophore. Langmuir. 2007 Nov 1;23(23):11677–83.

142. Studies on the interactions of tiny amounts of common ionic surfactants with unsaturated phosphocholine lipid model membranes. Chem Phys Lipids. 2022 Oct 1;248:105236.

143. (PDF) Size Distribution of Spontaneously Formed Liposomes by the Alcohol Injection Method. ResearchGate [Internet]. 2024 Oct 22 [cited 2025 Feb 1]; Available from: https://www.researchgate.net/publication/10885186_Size_Distribution_of_Spontaneously_Formed_Liposomes_by_the_Alcohol_Injection_Method

144. Rehman AU, Omran Z, Anton H, Mély Y, Akram S, Vandamme TF, et al. Development of doxorubicin hydrochloride loaded pH-sensitive liposomes: Investigation on the impact of chemical nature of lipids and liposome composition on pH-sensitivity. Eur J Pharm Biopharm. 2018 Dec;133:331–8.

145. Tokudome Y, Jinno M, Todo H, Kon T, Sugibayashi K, Hashimoto F. Increase in Ceramide Level after Application of Various Sizes of Sphingomyelin Liposomes to a Cultured Human Skin Model. Skin Pharmacol Physiol. 2011;24(4):218–23.

146. Bulbake U, Doppalapudi S, Kommineni N, Khan W. Liposomal Formulations in Clinical Use: An Updated Review. Pharmaceutics. 2017 Mar 27;9(2):12.

147. Cao Y, Dong X, Chen X. Polymer-Modified Liposomes for Drug Delivery: From Fundamentals to Applications. Pharmaceutics. 2022 Apr 2;14(4):778.

148. Villasmil-Sánchez S, Rabasco AM, González-Rodríguez ML. Thermal and 31P-NMR studies to elucidate sumatriptan succinate entrapment behavior in phosphatidylcholine/cholesterol liposomes. Comparative 31P-NMR analysis on negatively and positively-charged liposomes. Colloids Surf B Biointerfaces. 2013 May 1;105:14–23.

149. Alhariri M, Majrashi MA, Bahkali AH, Almajed FS, Azghani AO, Khiyami MA, et al. Efficacy of neutral and negatively charged liposome-loaded gentamicin on planktonic bacteria and biofilm communities. Int J Nanomedicine. 2017 Sep 18;12:6949.

150. Brgles M, Jurašin D, Sikirić MD, Frkanec R, Tomašić J. Entrapment of Ovalbumin into Liposomes—Factors Affecting Entrapment Efficiency, Liposome Size, and Zeta Potential. J Liposome Res. 2008 Jan;18(3):235–48.

151. Smistad G, Jacobsen J, Sande SA. Multivariate toxicity screening of liposomal formulations on a human buccal cell line. Int J Pharm. 2007 Feb 7;330(1–2):14–22.

152. Avanti Research [Internet]. [cited 2024 Nov 15]. How Do I Concentrate A Liposome? Available from: https://avantiresearch.com/tech-support/faqs/concentrate-liposomes

153. Gonzalez Gomez A, Syed S, Marshall K, Hosseinidoust Z. Liposomal Nanovesicles for Efficient Encapsulation of Staphylococcal Antibiotics. ACS Omega. 2019 Jun 30;4(6):10866–76.

154. Centrifugation Separations [Internet]. [cited 2024 Nov 15]. Available from: https://www.sigmaaldrich.com/GB/en/technical-documents/technical-article/protein-biology/protein-pulldown/centrifugation-separations

155. Amicon Ultra-2 Centrifugal Filter 100 kDa MWCO Millipore [Internet]. [cited 2024 Nov 15]. Available from: http://www.sigmaaldrich.com/

156. Cipolla D, Wu H, Eastman S, Redelmeier T, Gonda I, Chan HK. Development and Characterization of an In Vitro Release Assay for Liposomal Ciprofloxacin for Inhalation. J Pharm Sci. 2014 Jan 31;

157. Hagel L. Gel-filtration chromatography. Curr Protoc Mol Biol. 2001 May;Chapter 10:Unit 10.9.

158. G5080, Sephadex G-50, Fine, filtration medium, 20-80 um [Internet]. [cited 2024 Nov 16]. Available from: http://www.sigmaaldrich.com/

159. Sur S, Fries AC, Kinzler KW, Zhou S, Vogelstein B. Remote loading of preencapsulated drugs into stealth liposomes. Proc Natl Acad Sci U S A. 2014 Jan 28;111(6):2283.

160. Shi NQ, Qi XR, Xiang B. Preparation and Characterization of Drug Liposomes by pH-Gradient Method. In: Lu WL, Qi XR, editors. Liposome-Based Drug Delivery Systems [Internet]. Berlin, Heidelberg: Springer; 2018 [cited 2024 Nov 19]. p. 1–12. Available from: https://doi.org/10.1007/978-3-662-49231-4_18-1

161. Zhang ZJ, Osmałek T, Michniak-Kohn B. Deformable Liposomal Hydrogel for Dermal and Transdermal Delivery of Meloxicam . Int J Nanomedicine. 2020 Nov 24;15:9319–35.

162. Nayak D, Tippavajhala VK. A Comprehensive Review on Preparation, Evaluation and Applications of Deformable Liposomes. Iran J Pharm Res IJPR. 2021;20(1):186–205.

163. Scilit [Internet]. [cited 2025 Jul 3]. Solubilization of phospholipids by detergents structural and kinetic aspects. Available from: https://www.scilit.com/publications/302487139ec6177f829ed4daf2f8d29c

164. Garcia-Manyes S, Redondo-Morata L, Oncins G, Sanz F. Nanomechanics of lipid bilayers: heads or tails? J Am Chem Soc. 2010 Sep 22;132(37):12874–86.

165. Lv H, Zhang S, Wang B, Cui S, Yan J. Toxicity of cationic lipids and cationic polymers in gene delivery. J Control Release Off J Control Release Soc. 2006 Aug 10;114(1):100–9.

166. Cevc G, Blume G. Lipid vesicles penetrate into intact skin owing to the transdermal osmotic gradients and hydration force. Biochim Biophys Acta BBA - Biomembr. 1992 Feb 17;1104(1):226–32.

167. Elsayed MMA, Abdallah OY, Naggar VF, Khalafallah NM. Deformable liposomes and ethosomes: mechanism of enhanced skin delivery. Int J Pharm. 2006 Sep 28;322(1–2):60–6.

168. Brgles M, Šantak M, Halassy B, Forcic D, Tomašić J. Influence of charge ratio of liposome/DNA complexes on their size after extrusion and transfection efficiency. Int J Nanomedicine. 2012;7:393–401.

169. Elsana H, Olusanya TOB, Carr-wilkinson J, Darby S, Faheem A, Elkordy AA. Evaluation of novel cationic gene based liposomes with cyclodextrin prepared by thin film hydration and microfluidic systems. Sci Rep. 2019 Oct 22;9(1):15120.

170. Digiacomo L, Giulimondi F, Capriotti AL, Piovesana S, Montone CM, Chiozzi RZ, et al. Optimal centrifugal isolating of liposome–protein complexes from human plasma. Nanoscale Adv. 2021 Jun 30;3(13):3824–34.

171. Rasmussen MK, Pedersen JN, Marie R. Label-Free Sensing of Biorecognition on Liposomes. ACS Sens. 2020 Dec 24;5(12):4057–63.

172. Gao Y, Yang K, Shelling AN, Wu Z. Nanotechnology-Enabled COVID-19 mRNA Vaccines. Encyclopedia. 2021 Sep;1(3):773–80.

173. US20100130588A1 - Novel lipid formulations for nucleic acid delivery - Google Patents [Internet]. [cited 2025 Jul 3]. Available from: https://patents.google.com/patent/US20100130588A1/en

174. Safinya CR, Ewert KK, Majzoub RN, Leal C. Cationic liposome–nucleic acid complexes for gene delivery and gene silencing. New J Chem. 2014 Oct 14;38(11):5164–72.

175. Strickley RG. Solubilizing Excipients in Oral and Injectable Formulations. Pharm Res. 2004 Feb;21(2):201–30.

176. Velagaleti R, Ku S. Solutol HS15 as a Novel Excipient. 2010 Nov 2 [cited 2025 Feb 3];34. Available from: https://www.pharmtech.com/view/solutol-hs15-novel-excipient

177. Effect of oil and co-surfactant on the formation of Solutol HS 15 based colloidal drug carrier by Box–Behnken statistical design. Colloids Surf Physicochem Eng Asp. 2014 Jul 5;453:68–77.

178. Yeo LK, Olusanya TOB, Chaw CS, Elkordy AA. Brief Effect of a Small Hydrophobic Drug (Cinnarizine) on the Physicochemical Characterisation of Niosomes Produced by Thin-Film Hydration and Microfluidic Methods. Pharmaceutics. 2018 Oct 13;10(4):185.

179. Alani AWG, Rao DA, Seidel R, Wang J, Jiao J, Kwon GS. The effect of novel surfactants and Solutol HS 15 on paclitaxel aqueous solubility and permeability across a Caco-2 monolayer. J Pharm Sci. 2010 Aug;99(8):3473–85.

180. Li B, London E. Inner leaflet cationic lipid increases nucleic acid loading independently of outer leaflet lipid charge in asymmetric liposomes. Methods. 2023 Nov 1;219:16–21.

181. Kriegseis S, Vogl AY, Aretz L, Tonnesen T, Telle R. Zeta potential and long-term stability correlation of carbon-based suspensions for material jetting. Open Ceram. 2020 Nov 1;4:100037.

182. ResearchGate [Internet]. [cited 2024 Nov 28]. (PDF) The relationship between pH and zeta potential of 30 nm metal oxide nanoparticle suspensions relevant to in vitro toxicological evaluations. Available from: https://www.researchgate.net/publication/232047273_The_relationship_between_pH_and_zeta_potential_of_30_nm_metal_oxide_nanoparticle_suspensions_relevant_to_in_vitro_toxicological_evaluations

183. Baylot V, Le TK, Taïeb D, Rocchi P, Colleaux L. Between hope and reality: treatment of genetic diseases through nucleic acid-based drugs. Commun Biol. 2024 Apr 23;7(1):1–17.